ics Lib.

VOLUME 37 SECOND SERIES NUMBER 11

THE PHYSICAL REVIEW

A JOURNAL OF EXPERIMENTAL AND THEORETICAL PHYSICS

CONDUCTED BY

THE AMERICAN PHYSICAL SOCIETY

BOARD OF EDITORS

Managing Editor, JOHN T. TATE, University of Minnesota, Minneapolis
Assistant Editor, J. W. BUCHTA, University of Minnesota, Minneapolis
E. U. CONDON, C. J. DAVISSON, F. K. RICHTMYER, K. F. HERZFELD, A. W. HULL,
F. W. LOOMIS, A. J. DEMPSTER, DAVID M. DENNISON, J. C. SLATER

JUNE 1, 1931

Albert A. Michelson, 1852–1931 – ROBERT A. MILLIKEN 1377
Application of Spinor Analysis to the Maxwell and Dirac Equations – OTTO LAPORTE AND GEORGE E. UHLENBECK 1380
Tensor Form of Dirac's Equation – BORIS PODOLSKY 1398
Repulsive Energy Levels in Band Spectra – JOSEPH KAPLAN 1406
Note on the Visible Halogen Bands with Special Reference to ICl – ROBERT S. MULLIKEN 1412
Pictorial Representations of the Electron Cloud for Hydrogen-Like Atoms – H. E. WHITE 1416
Note on the Calculation of van der Waals Forces – HENRY MARGENAU 1425
Experimental Study of the Natural Widths of the X-Ray Lines in the *L*-Series Spectrum of Uranium – JOHN H. WILLIAMS 1431
Breadth of the Compton Modified Line with the Double Crystal Spectrometer – ARCHER HOYT AND JESSE DUMOND 1443
Oscillating Arc: Elements of Group VI – E. Z. STOWELL 1452
High Frequency Behavior of a Plasma – LEWI TONKS 1458
Ultraviolet Absorption Spectrum of Sulfur Dioxide – WILLIAM W. WATSON AND ALLAN E. PARKER 1484
Further Study of the Absorption of Infrared Radiation by Water Vapor – E. K. PLYLER AND W. W. SLEATOR 1493
Diffusion Problem for a Solid in Contact with a Stirred Liquid – T. E. W. SCHUMANN 1508
Dielectric Constant of Formic, Acetic, and Propionic Acids, and the Electric Moment of Complex Molecules – C. T. ZAHN 1516
On Impurities in Metals – FRANCIS BITTER 1527
Letters to the Editor – 1548

OH Bands and the Ultraviolet Line Spectrum of the Wehnelt Interrupter, *R. William Shaw*—1548; An Infrared Band System of Iodine Bromide, *Richard M. Badger and Don M. Yost*—1548; Thermionic Emission in Caesium-Oxide Photo-cells at Room Temperatures, *E. F. Kingsbury and G. R. Stilwell*—1549; A Case of Abnormal Molecular Rotation, *O. Oldenberg*—1550; On the Effect of Resonance in the Exchange of Excitation Energy, *O. K. Rice*—1551; Continuous Spectrum of Hydrogen Molecular Ion (H_2^+), *Y. Hukumoto*—1552; New Covariant Relations Following from the Dirac Equations, *G. E. Uhlenbeck and Otto Laporte*—1552; On the Gas-Temperature in the Positive Column of an Arc, *Alfred von Engel and Max Steenbeck*—1554.

PUBLISHED BY THE AMERICAN PHYSICAL SOCIETY
EDITORIAL OFFICE: MINNEAPOLIS, MINN.

THE AMERICAN PHYSICAL SOCIETY

OFFICERS OF THE SOCIETY

President:	W. F. G. SWANN	Bartol Research Foundation, Philadelphia, Pa.
Vice-President:	PAUL D. FOOTE	The Gulf Companies, Pittsburgh, Pa.
Secretary:	W. L. SEVERINGHAUS	Columbia University, New York City
Treasurer:	G. B. PEGRAM	Columbia University, New York City
Editor:	JOHN T. TATE	University of Minnesota, Minneapolis, Minn.
Local Secretary for the Pacific Coast:	L. B. LOEB	University of California, Berkeley, Calif.

THE PHYSICAL REVIEW

Published by the American Physical Society. Executive office: University of Minnesota, Minneapolis, Minn. Two volumes annually, twelve issues per volume.

First series. From July 1, 1893, to January 1, 1913, the REVIEW was conducted by Edward L. Nicholas, Ernest Merritt and Frederick Bedell, with the financial support of Cornell University. The first four volumes were issued annually; subsequent volumes, semi-annually; thirty-five volumes in all.

Second series. On January 1, 1913, the REVIEW was transferred to the American Physical Society as announced on the first page of the new series which was then begun. Since then it has been conducted by a Board of Editors elected by the Society. Semi-annual volumes begin in January and July. Since July 1, 1929, the REVIEW has been issued twice a month.

Contributors are referred to page 2 of the advertisements for further information.

Annual subscription, throughout the Postal Union, $12.00 in advance.

General index, 1893-1920, $4.00, in advance.

Back Volumes, $9.00 per volume; Back Numbers, $1.50 per copy for issues prior to July 1, 1929 (Vols. 1-33), $.75 per copy for issues subsequent thereto. Postage is free if remittance accompanies order; otherwise postage is extra. No bound volumes can be supplied. The REVIEW offers to purchase a limited number of First Series, Vol. 1, No. 1 (at $2.00 each); Second Series, Vol. 7, No. 1, January 1916; Vol. 7, No. 2, February 1916; Vol. 7, No. 4, April 1916; and Vol. 7, No. 5, May 1916 (at $2.00 each).

Advertisements. Rates will be supplied by the Editor on request. Copy for each number must be received at Minneapolis two weeks prior to the dates of issue; old copy is used until new copy is received. Send electrotypes direct to the printers, George Banta Publishing Co., Menasha, Wis.

Discount of ten per cent is allowed to members of the American Physical Society on purchase of back numbers.

Changes of Address and Complaints of failure to receive the REVIEW, in the case of members of the Physical Society, should be addressed to the Treasurer; in the case of other subscribers, to the Editor. New copies can be sent free in response to complaint of non-delivery only if notice of non-delivery is received within three months of date of issue.

Editorial Correspondence should be addressed to the PHYSICAL REVIEW, University of Minnesota, Minneapolis, Minn.

Entered at the post office at Menasha, Wis., as second class matter.
Acceptance for mailing at special rate of postage provided for in section 1103, Act of October 3, 1917, authorized September 6, 1926.

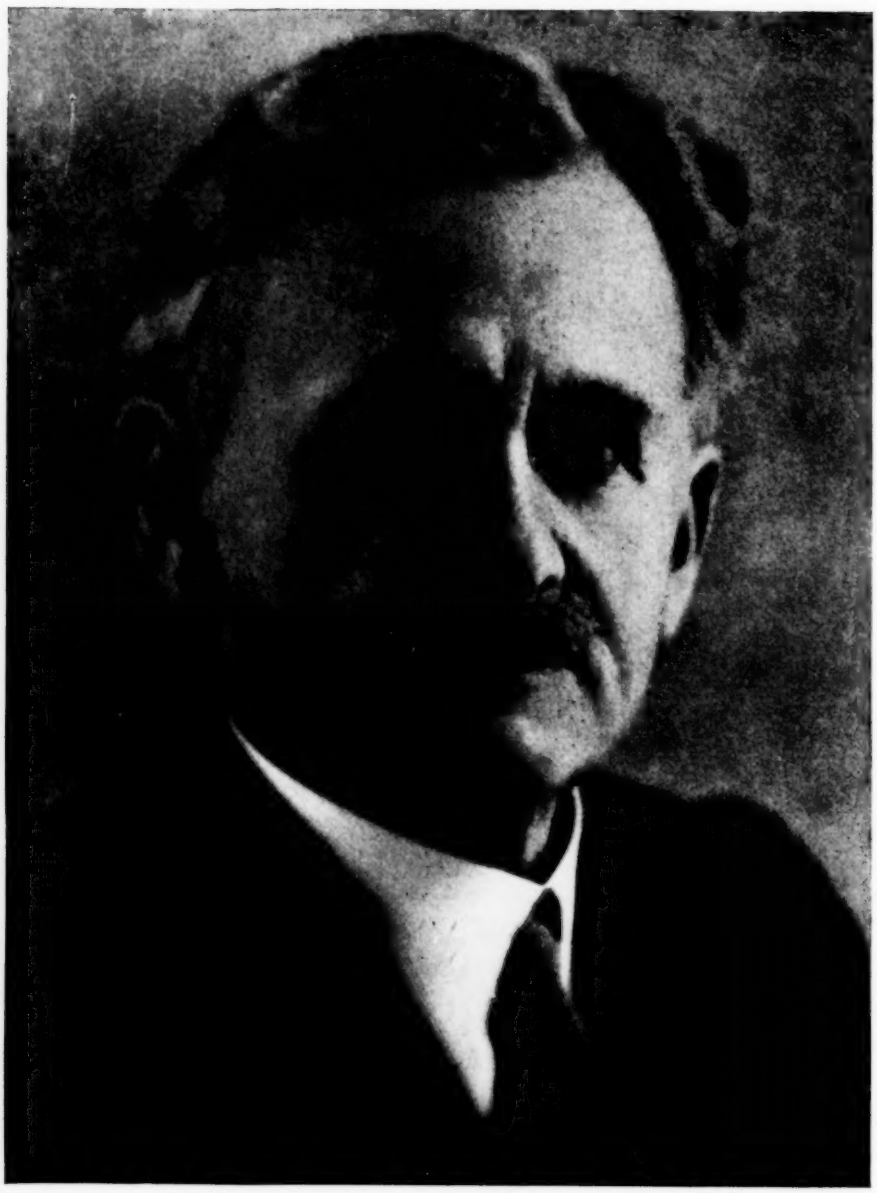

Albert A. Michelson

Second Series *June 1, 1931* *Vol. 37, No. 11*

THE

PHYSICAL REVIEW

ALBERT A. MICHELSON, 1852-1931

AT ONE o'clock on Saturday afternoon, May 9, 1931, death came very quietly in his home in Pasadena to the most illustrious of the American physicists of our generation, at the age of seventy-eight years and five months. Six weeks earlier he had taken to his bed, after having made with his associates, Messrs. Pease and Pearson, enough observations to assure himself that his last experiment on the speed of light as measured in an evacuated pipe a mile long and three feet in diameter buried in the earth on the Irvine ranch near Santa Ana, California, was going to yield results as satisfactory as he had anticipated. This experiment had been planned for the sake of obtaining a check by a method entirely free from atmospheric effects of all kinds upon the accuracy of his next preceding determination made over a twenty-one mile stretch between California mountain peaks. He did not expect by these new experiments to exceed the accuracy previously obtained, but rather to add something to the *reliability* of the previous determination.

More than a month before his death, Mr. Michelson had known that he would never get up again, for a creeping paralysis was coming over him of which he himself was altogether conscious. His mind was quite clear until two days before the end, when a lesion occurred which brought on unconsciousness within an hour, an unconsciousness from which he never again awoke.

As one of the men who has had the most enduring and most intimate association with Mr. Michelson and his work, I esteem it a privilege now to make a few additions to my former appreciation of him and his achievement.

Under the caption, "Michelson's Economic Value," now published as Chapter VII in a volume by Scribner's entitled "Science and the New Civilization," I have attempted to appraise in broad lines the significance for our times of measurements of the highest skill and accuracy of the sort which Michelson has done and for which his name stands the world over, and I should like to refer to that appraisal and merely supplement it here by adding some details both of a scientific and of a personal sort.

Practically all of Mr. Michelson's work in physics centered about determinations for increasing the precision of measurement. He has been called an extremely skillful and intelligent instrument designer, but while he was that

he was much more than that, for his attention was always on the problem to be solved, not primarily on the instrument for solving it, and he was always seeking for problems incapable of solution save by improvements in the accuracy of measurement. Ten different times in the fifty-one years of his activity, extending from 1880 when at the age of twenty-eight he became the best known American physicist by virtue of his new speed-of-light measurement up to 1931 when he died, still trying to prove the certainty of his determination and precision of that most fundamental constant, he made major outstanding advances, which I list as follows:

1. Measurements of the speed of light, 1880–1931.
2. Development of the Michelson interferometer, 1882 et seq.
3. Ether-drift experiments, 1887–1928.
4. The first analysis of the fine structure of spectral lines, 1894–1900.
5. Development of the Michelson-Stratton harmonic analyzer, 1897.
6. Development of the principle of the Echelon spectrograph, 1898.
7. Perfection and increase in resolution of the line grating, 1902–1917.
8. First accurate measurement of the rigidity of the earth, 1916.
9. Development of the U. S. Naval Range Finder, 1918.
10. Direct interferometer measurement of the diameter of stars, 1921.

Of these ten five, namely the second, third, fourth, and tenth, have to do primarily with the interferometer or its application to various sensitive measurements. It was in measurements relating to the interference of light and speed of light that he was by far the greatest expert that the world has yet seen. He spent his scientific life largely in these two fields. He was not an omnivorous reader of the literature of physics, and did not try to follow closely the developments of the theoretical fields of electronics and quantum theory. He was essentially a classical physicist, but any one who ever heard him conduct a Ph.D. examination in physics, and any one who ever attended his lectures or heard him speak knows that his grasp of classical physics was penetrating and precise. His lectures and his papers were masterpieces of elegance and conciseness. He used a few words, but they were just the ones he wanted. Indeed, the precision of his mind was its dominating characteristic, which showed even in his sports. I have played tennis with him all my life, and his calling of balls, for example, was never generous either to himself or to his opponent. It was simply exact and just. Closely allied to this characteristic was his altogether extraordinary honesty. Pretense of any kind was utterly foreign to his make up. Indeed, he was one of those very rare persons who would not even tolerate fooling himself with respect to his own motives, as so many of us do. If his conduct was ever ungenerous he knew it and frankly admitted it, whether he thought it wise to change it or not. Before I became intimately associated with him I had heard that he was considered by his pupils to be somewhat unapproachable, occasionally arbitrary, and at times dictatorial, if not unreasonable, but in the twenty-five years in which we worked together I could not have been treated with greater courtesy and consideration, even in the few cases in which we differed in judgment. His dignity and courtesy of bearing were altogether striking characteristics, and as the

years passed he grew to be a man of great mellowness, kindness, and affability.

Like many a scientist, Mr. Michelson was also an artist, with a keen feeling for form and color, as well as for music. He painted well, played the violin well, and did well at tennis, chess, and billiards.

American Science and the American nation have lost in his death one of their finest and greatest figures.

ROBERT A. MILLIKAN

May 11, 1931.

APPLICATION OF SPINOR ANALYSIS TO THE MAXWELL AND DIRAC EQUATIONS

By Otto Laporte and George E. Uhlenbeck
Department of Physics, University of Michigan

(Received February 24, 1931)

Abstract

With the spinor analysis developed by B. van der Waerden which comprises all representations of the Lorentz group, even those not contained in ordinary tensor calculus, one is able to write all derivations and equations in an *automatically covariant form*. For the convenient translation into spinor language of the Maxwell equations, it becomes important to introduce three self-dual tensors, one representing the electromagnetic field, one corresponding to the Hertzian vector, and one representing a kind of current potential. These correspond to symmetric spinors of the 2nd rank. Many spinor equations thus become simpler than the corresponding tensorial equations, especially the expression for the stress energy tensor. From the 1st order Dirac equations in spinor form, as given by v.d. Waerden, we derived the 2nd order equation, which agrees with the Gordon-Klein form but for a correction term which again contains the self-dual field tensor. Further the expression for the current was derived, and its decomposition into conduction and polarization currents, and both Maxwell and Dirac equations were derived from a spinorial variation principle, analogous to the results of Gordon and Darwin. In addition to the divergence condition for the current three new invariant relations between the wave functions which are independent of the potentials were obtained (Chapter III, Eqs. (11), (12) and (13)).

Introduction

THE Dirac equations of the electron have for the first time furnished an example of a system of equations, which show an invariance of form when subjected to a Lorentz transformation, but which only very artificially could be written with tensors. This difficulty was felt especially by Darwin[1] when he wrote: "The relativity theory is based on nothing but the idea of invariance, and develops from it the conception of tensors as a matter of necessity; and it is rather disconcerting to find that apparently something has slipped through the net, so that physical quantities exist, which it would be, to say the least, very artificial and inconvenient to express as tensors."

The Dirac equation is

$$[(\Gamma^k p_k) + mc]\psi = 0 \tag{1}$$

where p_k represents the 4-vector[2]

$$p_k = \frac{h}{i}\frac{\partial}{\partial x^k} + \phi_k \tag{2}$$

[1] C. G. Darwin, Proc. Roy. Soc. **118**, 657 (1928).

[2] We use the Dirac h, which is $1/2\pi$ times the Planck constant, and write here; and in Ch. III, ϕ_k for e/c times the ordinary four potential.

and Γ^k are four four-row matrices, given by:[3]

$$\Gamma^1 = \begin{pmatrix} 0 & 0 & 0 & -1 \\ 0 & 0 & -1 & 0 \\ 0 & 1 & 0 & 0 \\ 1 & 0 & 0 & 0 \end{pmatrix} \quad \Gamma^2 = \begin{pmatrix} 0 & 0 & 0 & i \\ 0 & 0 & -i & 0 \\ 0 & -i & 0 & 0 \\ i & 0 & 0 & 0 \end{pmatrix}$$

$$\Gamma^3 = \begin{pmatrix} 0 & 0 & -1 & 0 \\ 0 & 0 & 0 & 1 \\ 1 & 0 & 0 & 0 \\ 0 & -1 & 0 & 0 \end{pmatrix} \quad \Gamma^4 = \begin{pmatrix} 0 & 0 & 1 & 0 \\ 0 & 0 & 0 & 1 \\ 1 & 0 & 0 & 0 \\ 0 & 1 & 0 & 0 \end{pmatrix} \tag{3}$$

ψ is a function of two kinds of variables, of x^i and an inner variable, which can only assume four discrete values; the p_k act upon the x^k while the Γ^k operate on the inner variable. This way of describing Eq. (1) is of course equivalent to regarding Eq. (1) as *four* equations containing 4 ψ's, each of them a function of x^k only.

There are *two* points of view possible, with regard to the transformation properties of the Dirac equation: The *first* of these regards the Γ^k as a matrix four vector, and the ψ as constant. According to the *second* point of view, the Γ^k are constants and the ψ are being transformed.

One can easily show that these two methods are equivalent. For if we subject the coordinates x^k to a Lorentz transformation,

$$x = x'L$$

then the p_k will be transformed like

$$p = L^{-1}p'.$$

If we consider Γ^k as a four vector, it will transform like x^k, and the scalar product

$$(\Gamma p) = (\Gamma' L L^{-1} p') = (\Gamma' p')$$

will remain invariant. On the other hand, we can always find a matrix S such that

$$p = L^{-1}p' = S^{-1}p'S. \tag{4}$$

Now the Γ^k are kept constant, and since they act on the inner variable only, they are exchangeable with S, so that

$$(S^{-1}\Gamma p' S)\psi + mc\psi = 0$$

or

$$(\Gamma p')(S\psi) + mc(S\psi) = 0.$$

Putting

$$\psi' = S\psi \tag{5}$$

[3] When written out, Eq. (1) agrees with the form given by Weyl, Gruppentheorie and Quantenmechanik, Leipzig 1928, page 171, Eq. (45′). If the above given matrices for Γ^1, Γ^2, Γ^3 are divided by i, they become identical to Weyl's Γ_1, Γ_2, Γ_3; our Γ^4 is equal to his Γ_0.

we regain (1), now with transformed ψ. This point of view regards the Γ^k simply as determining the coefficients $0, \pm 1, \pm i$ in the four wave equations.

For special two dimensional Lorentz transformations, Darwin has written out the transformation (5). They have the peculiar character that the coefficients contain the angle $\theta/2$, when the coordinates are rotated by the angle θ. We can see already from (4) that S is something like a square root of L.[4] This shows that ψ cannot be a tensor, and that there are equations, which defy translation into tensor language and yet fulfill the relativity principle. Now it has been known to the mathematicians that the ordinary tensor language does not comprise all possible representations of the Lorentz group as had always been assumed tacitly by the physicists.[5] The necessary extension of the tensor calculus, the *spinor calculus*, was given by B. van der Waerden,[6] upon instigation of Ehrenfest, and indeed gives all possible representations.

These two points of view correspond in a certain way to the particle and wave description of the electron. The first may give additional information concerning the particle velocity,[7] the second, however, is necessary for the consideration of the Dirac equations as field equations. In this case the ψ must naturally be transformed to a new coordinate system just as E and H in Maxwell's equations. We shall restrict ourselves to this point of view.

Chapter I. The Mathematical Apparatus of the Spinor Analysis

§1. Since van der Waerden's article is not very easily accessible, and in order to make the spinor analysis more popular, we shall briefly develop the few necessary theorems and formulae here, following van der Waerden closely.

Consider the following binary transformation

$$\begin{aligned} \xi_1' &= \alpha_{11}\xi_1 + \alpha_{12}\xi_2 \\ \xi_2' &= \alpha_{21}\xi_1 + \alpha_{22}\xi_2 \end{aligned} \tag{1}$$

and its complex conjugate:

$$\begin{aligned} \bar{\xi}_1' &= \bar{\alpha}_{11}\bar{\xi}_1 + \bar{\alpha}_{12}\bar{\xi}_2 \\ \bar{\xi}_2' &= \bar{\alpha}_{21}\bar{\xi}_1 + \bar{\alpha}_{22}\bar{\xi}_2 \end{aligned} \tag{2}$$

with the determinant

$$\begin{vmatrix} \alpha_{11} & \alpha_{12} \\ \alpha_{21} & \alpha_{22} \end{vmatrix} = 1. \tag{3}$$

All these transformations form a group of $8-2=6$ parameters. Any two numbers transforming like the ξ_1, ξ_2 in (1), we shall call a spinor of the 1st rank, and denote by

[4] Landau therefore calls ψ a half vector.

[5] Compare especially Hermann Weyl, Gruppentheorie und Quantenmechanik, Leipzig, 1928. Kap. III.

[6] B. van der Waerden, Göttinger Nachrichten 1929, page 100. The spinor formalism is already implicitly contained in the book of Weyl, and in a paper by V. Fock, Zeits. f. Physik **57**, 261 (1929).

[7] V. Fock, Zeits. f. Physik **55**, 127 (1929); G. Breit, Proc. Natl. Acad. **14**, 553 (1928); E. Schrödinger, Sitzungsber. Berliner Akad. **24**, 418 (1930).

$$a_k \qquad k = 1, 2$$

whereas any two quantities transforming like (2) will be written

$$b_{\dot r} \qquad \dot r = \dot 1, \dot 2.$$

Any four quantities transforming like the products $\xi_1\xi_1$, $\xi_1\xi_2$, $\xi_2\xi_1$, $\xi_2\xi_2$ we call a spinor of the 2nd rank and write

$$a_{kl} \qquad k, l = 1, 2.$$

Correspondingly 4 quantities transforming like the products of $\bar\xi_1$ and $\bar\xi_2$ we denote by

$$b_{\dot r\dot s} \qquad \dot r, \dot s = \dot 1, \dot 2.$$

There are also "mixed" spinors of the 2nd rank transforming like a product of a barred ξ and an unbarred ξ, denoted by

$$c_{\dot r k} \qquad \dot r = \dot 1, \dot 2;\ k = 1, 2.$$

Analogously we can define spinors of higher rank, like $a_{\dot r\dot m l}$.

One can show easily, that because of (3) the area of the parallelogram formed by two spinors ξ_k and η_l

$$\xi_1\eta_2 - \xi_2\eta_1$$

is invariant under transformation (1). This enables us to introduce *contravariant* spinors a^k or $b^{\dot r}$, according to

$$\boxed{\begin{aligned} a^1 &= a_2 & b^{\dot 1} &= b_{\dot 2} \\ a^2 &= -a_1 & b^{\dot 2} &= -b_{\dot 1} \end{aligned}} \tag{4}$$

because in this way the scalar products

$$a_1c^1 + a_2c^2 = a_\lambda c^\lambda$$
$$b_{\dot 1}d^{\dot 1} + b_{\dot 2}d^{\dot 2} = b_{\dot\rho}d^{\dot\rho}$$

are invariant.[8] When we establish the usual connection between covariant and contravariant indices by means of a spinor ϵ^{kl} according to

$$a^k = \epsilon^{k\lambda}a_\lambda \tag{5}$$

we find

$$-\epsilon^{kl} = \begin{pmatrix} 0 & -1 \\ 1 & 0 \end{pmatrix} \qquad -\epsilon_{kl} = \begin{pmatrix} 0 & +1 \\ -1 & 0 \end{pmatrix}$$

and

$$\epsilon^{k\lambda}\epsilon_{l\lambda} = -\delta_l{}^k \tag{6}$$

where

[8] Summation signs are as usual suppressed; dummy indices are always given Greek letters, free indices Latin letters.

$$\delta_l{}^k = \begin{pmatrix} 1 & 0 \\ 0 & 1 \end{pmatrix}.$$

As in the usual tensor algebra, the only covariant operations are also here *multiplication* and *contraction*. For instance from the spinors $a_{\dot r\dot s}{}^l$ and $b^{\dot m}{}_{kt}$ we can form the spinor of the 6th rank

$$c_{\dot r\dot s}{}^{l\dot m}{}_{kt} = a_{\dot r\dot s}{}^l b^{\dot m}{}_{kt}$$

or the spinor of 4th rank

$$c_{\dot s}{}^l{}_{kt} = a_{\dot\mu\dot s}{}^l b^{\dot\mu}{}_{kt}$$

or the spinor of the 2nd rank

$$c_{\dot s t} = a_{\dot\mu\dot s}{}^\lambda b^{\dot\mu}{}_{\lambda t}.$$

The following two rules are essential in calculations. According to (6) we have

$$\boxed{a_\lambda b^\lambda = -\, a^\lambda b_\lambda} \tag{7}$$

An immediate consequence of this is that any spinor of odd rank has absolute value zero

$$a_\lambda a^\lambda = 0; \quad a^{\lambda\mu\nu} a_{\lambda\mu\nu} = 0. \tag{7a}$$

Similarly we have

$$\boxed{a^\lambda b_\lambda c_m + a_\lambda b_m c^\lambda + a_m b^\lambda c_\lambda = 0}. \tag{8}$$

Of course this rule may also be applied to the product $a^\lambda c_{\lambda m}$. It also holds for three dotted indices.

There are two more rules concerning the relations of dotted and undotted indices.

1° It is not necessary to fix the position of dotted and undotted indices belonging to the same spinor. Thus, for instance

$$a_{\dot r l t} = a_{l\dot r t} = a_{lt\dot r}.$$

On the other hand two dotted or two undotted indices are not necessarily interchangeable; if they are, the spinor in question has special symmetry properties.

2° The complex conjugate of any spinor equation is obtained by replacing all undotted indices by dotted ones and *vice versa*.

§2. We will now establish the connection between spinors and world tensors. We assert that the following combinations of components of a second rank spinor $a_{\dot s t}$ are to be associated with the components of a world vector A^1, A^2, A^3, A^4 as follows

$$\left.\begin{aligned} \tfrac{1}{2}(a_{\dot{2}1} + a_{\dot{1}2}) &= A^1 = A_1 \\ \frac{1}{2i}(a_{\dot{2}1} - a_{\dot{1}2}) &= A^2 = A_2 \\ \tfrac{1}{2}(a_{\dot{1}1} - a_{\dot{2}2}) &= A^3 = A_3 \\ \tfrac{1}{2}(a_{\dot{1}1} + a_{\dot{2}2}) &= A^4 = -A_4 \end{aligned}\right\} \tag{9}$$

These combinations are real, and after a transformation (1) and (2) they will still be real; thus their transformation coefficients are real also. To prove that it is a Lorentz transformation we solve (9) for the a_{it} and obtain using (4)

$$\left.\begin{aligned} a_{\dot{2}1} &= -a^{\dot{1}2} = A^1 + iA^2 = A_1 + iA_2 \\ a_{\dot{1}2} &= -a^{\dot{2}1} = A^1 - iA^2 = A_1 - iA_2 \\ a_{\dot{1}1} &= +a^{\dot{2}2} = A^3 + A^4 = A_3 - A_4 \\ -a_{\dot{2}2} &= -a^{\dot{1}1} = A^3 - A^4 = A_3 + A_4 \end{aligned}\right\}. \tag{10}$$

Now it is easily verified that

$$-\tfrac{1}{2}a_{\dot{\sigma}\tau}a^{\dot{\sigma}\tau} = A_\gamma A^\gamma. \tag{11}$$

To every transformation (1) there corresponds one Lorentz transformation; *vice versa*, since the connection formulae between the transformation coefficients of A and the α's of eq. (1) are quadratic, there are two transformations (1) differing in sign, corresponding to one Lorentz transformation.[9] Therefore (1) and (2) form a representation of the Lorentz group. It can be proved, and this is the fundamental theorem of the spinor analysis, that one obtains all representations of the Lorentz group by transforming all possible spinors according to (1) and (2). It follows that the true "quantities" belonging to the Lorentz group are spinors, of which tensors form only a special class. Analogous to (10) spinors of the fourth rank with two dotted and two un-

[9] For example using the transformation formulae (1) and (2) for a spinor $a_{\dot{i}l}$ we find that for a Lorentz transformation

$$\begin{aligned} ct' &= ct\cosh\theta + \sinh\theta \\ z' &= ct\sinh\theta + z\cosh\theta \end{aligned}$$

there correspond the two transformation matrices

$$\alpha_{kl} = \begin{pmatrix} \pm e^{\theta/2} & 0 \\ 0 & \pm e^{-\theta/2} \end{pmatrix}$$

and with a special rotation

$$\begin{aligned} x' &= x\cos\theta + y\sin\theta \\ y' &= -x\sin\theta + y\cos\theta \end{aligned}$$

there correspond the two matrices

$$\alpha_{kl} = \begin{pmatrix} \pm e^{-i\theta/2} & 0 \\ 0 & \pm e^{+i\theta/2} \end{pmatrix}.$$

For general spacial rotations we see that because of the invariance of t, that is to say of $\bar{\xi}_1\xi_1 + \bar{\xi}_2\xi_2$ the corresponding binary transformation (1) will be unitarian. For more information compare especially H. Weyl, Gruppentheorie und Quantentheorie, Leipzig 1928, p. 106–114.

dotted indices correspond to world tensors of the second rank. The formulae connecting them are obtained from (10) by multiplication. For instance

$$\left.\begin{aligned} a_{\dot{2}\dot{2}11} &= a^{\dot{1}\dot{1}22} = A^{11} - A^{22} + i(A^{12} + A^{21}) = A_{11} - A_{22} + i(A_{12} + A_{21}) \\ -a_{\dot{2}\dot{2}21} &= a^{\dot{1}\dot{1}12} = A^{31} - A^{41} + i(A^{32} - A^{42}) = A_{31} + A_{41} + i(A_{32} + A_{42}) \end{aligned}\right\} \quad (12)$$

In the following table all possible kinds of spinors of the 5 lowest ranks are written down and those corresponding to world tensors are underscored.

$$\underline{a}$$

$$a_k \qquad a_{\dot{m}}$$

$$a_{kl} \qquad \underline{a_{\dot{m}l}} \qquad a_{\dot{m}\dot{n}}$$

$$a_{kll} \qquad a_{\dot{m}ll} \qquad a_{\dot{m}\dot{n}l} \qquad a_{\dot{m}\dot{n}\dot{r}}$$

$$a_{klltv} \qquad a_{\dot{m}ltv} \qquad \underline{a_{\dot{m}\dot{n}tv}} \qquad a_{\dot{m}\dot{n}\dot{r}v} \qquad a_{\dot{m}\dot{n}\dot{r}\dot{s}}$$

§3. Although the underscored spinors correspond *directly* to tensors of half their rank, the *spinors of even rank* can be related to tensors of higher rank, which possess certain symmetry properties. Let us consider the simplest spinors of this kind a_{kl} and its complex conjugate $a_{\dot{m}\dot{n}}$. We decompose a_{kl} into a symmetric and antisymmetric spinor, according to

$$a_{kl} = \tfrac{1}{2}(a_{kl} + a_{lk}) + \tfrac{1}{2}(a_{kl} - a_{lk}) = \sigma_{kl} + \alpha_{kl}. \quad (13)$$

The antisymmetric part α_{kl} has only one "Kennzahl"

$$\alpha_{12} = -\alpha_{21} = \tfrac{1}{2}(a_{12} - a_{21}) = \tfrac{1}{2}(a_1^{\,1} + a_2^{\,2}) = \tfrac{1}{2}a_\rho^{\,\rho}$$

which is an invariant. The symmetric part σ_{kl} has three "Kennzahlen" and can be shown to correspond to an *antisymmetric self-dual tensor*. Consider a real antisymmetric world tensor F^{kl}. The dual tensor to this is obtained by means of

$$F^*_{kl} = \pm \frac{i}{2}\delta_{kl\alpha\beta}F^{\alpha\beta} \quad (14)$$

where $\delta_{klmn} = 0$ when any two indices are equal and $= \pm 1$ according to whether the indices form an even or odd permutation of the numbers 1234. Thus two dual tensors F^{*kl} are possible to an originally real tensor F^{kl}; they differ only by the sign, so that one is the complex conjugate of the other. Obviously the dual to F^{*kl} is again the original F^{kl} without asterisk. The self-dual tensor G^{kl} is the sum of the two[10]

$$\left.\begin{aligned} G^{kl} &= F^{kl} + F^{*kl} \\ \overline{G}^{kl} &= F^{kl} - F^{*kl}. \end{aligned}\right\} \quad (15)$$

Calling the three Kennzahlen k_1, k_2, k_3, G^{kl} may be written

[10] We note the theorem, that for any two self-dual tensors G^{kl} and H^{kl} the product

$$G^{k\lambda}\overline{H}_{k\lambda} \equiv 0$$

$$G^{kl} = \begin{pmatrix} 0 & k_3 & -k_2 & -ik_1 \\ -k_3 & 0 & k_1 & -ik_2 \\ k_2 & -k_1 & 0 & -ik_3 \\ ik_1 & ik_2 & ik_3 & 0 \end{pmatrix} \tag{15a}$$

or taking the lower sign in (14)

$$\overline{G}^{kl} = \begin{pmatrix} 0 & \bar{k}_3 & -\bar{k}_2 & i\bar{k}_1 \\ -\bar{k}_3 & 0 & \bar{k}_1 & i\bar{k}_2 \\ \bar{k}_2 & -\bar{k}_1 & 0 & i\bar{k}_3 \\ -i\bar{k}_1 & -i\bar{k}_2 & -i\bar{k}_3 & 0 \end{pmatrix}. \tag{15b}$$

Then we form the spinor of the fourth rank $g_{\dot{r}\dot{s}kl}$ according to (12) which using G^{kl} can be written

$$g_{\dot{r}\dot{s}k}{}^{l} = g_{\dot{r}\dot{s}}\delta_k{}^{l} \tag{16a}$$

and which using $\overline{G}^{kl}$ can be written

$$g_{\dot{r}}{}^{\dot{s}}{}_{kl} = \delta_{\dot{r}}{}^{\dot{s}}g_{kl}. \tag{16b}$$

Here the spinors $g_{\dot{r}\dot{s}}$ and g_{kl} are *symmetric*. Solving (16) and (16a) we obtain

$$\left.\begin{aligned} g_{\dot{r}\dot{s}} &= \tfrac{1}{2}g_{\dot{r}\dot{s}\lambda}{}^{\lambda} \\ g_{kl} &= \tfrac{1}{2}g_{\dot{\sigma}}{}^{\dot{\sigma}}{}_{kl} \end{aligned}\right\}. \tag{17}$$

The formulae connecting the components of the symmetric spinors with those of the antisymmetric, self-dual world-tensor are

$$\left.\begin{aligned} g_{\dot{1}\dot{1}} &= 2(k_2 + ik_1) \\ g_{\dot{2}\dot{2}} &= 2(k_2 - ik_1) \\ g_{\dot{1}\dot{2}} = g_{\dot{2}\dot{1}} &= -2ik_3 \end{aligned}\right\} \tag{18}$$

and using (16a) we simply obtain the complex conjugate

$$\left.\begin{aligned} g_{11} &= 2(\bar{k}_2 - i\bar{k}_1) \\ g_{22} &= 2(\bar{k}_2 + i\bar{k}_1) \\ g_{12} = g_{21} &= 2i\bar{k}_3 \end{aligned}\right\}. \tag{18a}$$

§4. Corresponding to the introduction of a covariant gradient vector we now define a gradient spinor $\partial_{\dot{r}\dot{s}}$ according to the connection formulae (10) as follows

$$\left.\begin{aligned} \partial^{\dot{1}}{}_{1} = \partial_{\dot{2}\dot{1}} &= \frac{\partial}{\partial x^1} + i\frac{\partial}{\partial x^2} \\ -\partial^{\dot{2}}{}_{2} = \partial_{\dot{1}\dot{2}} &= \frac{\partial}{\partial x^1} - i\frac{\partial}{\partial x^2} \\ -\partial^{\dot{2}}{}_{1} = \partial_{\dot{1}\dot{1}} &= \frac{\partial}{\partial x^3} - \frac{\partial}{\partial x^4} \\ -\partial^{\dot{1}}{}_{2} = -\partial_{\dot{2}\dot{2}} &= \frac{\partial}{\partial x^3} + \frac{\partial}{\partial x^4} \end{aligned}\right\} \tag{19}$$

where the contravariant vector (x^1, x^2, x^3, x^4) corresponds to (x, y, z, ct). Analogously to (11) we may now translate the familiar vector analytical operations like Div or $\Box$ into the spinor language. We have

$$\frac{\partial \phi^\alpha}{\partial x^\alpha} = -\frac{1}{2}\partial_{\dot\sigma\tau}\phi^{\dot\sigma\tau} \tag{20}$$

and

$$\frac{\partial^2 S}{\partial x_\alpha \partial x^\alpha} = -\frac{1}{2}\partial_{\dot\sigma\tau}\partial^{\dot\sigma\tau}S. \tag{21}$$

Chapter II. Maxwell Equations in Spinor Form

§5α. To facilitate the comparison, we shall briefly recapitulate the Maxwell equations in the ordinary tensor form. As usual we define the antisymmetric field tensor

$$F^{kl} = \begin{pmatrix} 0 & H_z & -H_y & -E_x \\ & 0 & H_x & -E_y \\ & & 0 & -E_z \\ & & & 0 \end{pmatrix} \tag{1}$$

then the dual tensor according to (14) is

$$F^{*kl} = -i\begin{pmatrix} 0 & E_x & -E_y & H_x \\ & 0 & E_x & H_y \\ & & 0 & H_z \\ & & & 0 \end{pmatrix} \tag{2}$$

The two Maxwell equations are

$$\frac{\partial F^{k\lambda}}{\partial x^\lambda} = S^k \tag{3}$$

$$\frac{\partial F^{*k\lambda}}{\partial x^\lambda} = 0$$

where S^k is the four-current $(\rho v_x/c, \rho v_y/c, \rho v_z/c, \rho)$ obeying the continuity equation

$$\frac{\partial S^\lambda}{\partial x^\lambda} = 0. \tag{5}$$

We can embody these two equations into one

$$\frac{\partial G^{k\lambda}}{\partial x^\lambda} = S^k \tag{6}$$

by using the self-dual tensor

$$G^{kl} = F^{kl} + F^{*kl} \tag{7}$$

which has the form (15), with[11]

$$\vec{k} = \vec{H} - i\vec{E}. \tag{8}$$

We can derive G^{kl} from the four-potential $\phi^k = (A_x, A_y, A_z, \phi)$ by means of

$$G^{kl} = \frac{\partial \phi^l}{\partial x_k} - \frac{\partial \phi^k}{\partial x_l}. \tag{9}$$

The ϕ^k are subjected to the accessory condition

$$\frac{\partial \phi^\lambda}{\partial x^\lambda} = 0. \tag{10}$$

Introducing (9) into (6), using (10) we get the wave equation for ϕ^k

$$\frac{\partial^2 \phi^k}{\partial x_\lambda \partial x^\lambda} = S^k. \tag{11}$$

§5β. To free ourselves from the condition (10) imposed on the potentials, we express ϕ^k in terms of a self-dual antisymmetric tensor Z^{kl}, the analogue to the Hertzian vector in three dimensions by means of[12]

$$\phi^k = \frac{\partial Z^{k\lambda}}{\partial x^\lambda}. \tag{12}$$

Introducing this in (11), we get for Z^{kl} a third order differential equation

$$\frac{\partial}{\partial x^\lambda} \frac{\partial^2 Z^{k\lambda}}{\partial x_\alpha \partial x^\alpha} = S^k.$$

In the three dimensional form one reduces this to a second order differential equation by an integration of the current $\rho v/c$ with respect to the time.[13] The analogue of this is the derivation of S^k from a stream potential Q^{kl}, which is again an antisymmetric self-dual tensor, according to

[11] Comp. Riemann-Weber, Die partiellen Differentialgleichungen der Physik, Braunschweig 1901, Vol. II, 348. L. Silberstein, Ann. d. Physik **22,** 579 (1907). See also F. Zerner, Handbuch der Physik vol. XII, p. 93.

[12] When we represent Z^{kl} by the scheme

$$Z^{kl} = i \begin{pmatrix} 0 & Z_z & -Z_y & iZ_x \\ & 0 & Z_x & iZ_y \\ & & 0 & iZ_z \\ & & & 0 \end{pmatrix}$$

then the three dimensional form of (12) is

$$A = i \operatorname{curl} Z - \frac{1}{c} \frac{\partial Z}{\partial t}$$

$$\phi = \operatorname{div} Z.$$

[13] See e.g. Madelung, Die mathematischen Hilfsmittel des Physikers, Berlin 1922, p. 196.

$$S^k = \frac{\partial Q^{k\lambda}}{\partial x^\lambda}. \tag{13}$$

This causes the continuity equation (5) to be identically satisfied. For Z^{kl} we then get the wave equation

$$\frac{\partial^2 Z^{kl}}{\partial x_\alpha \partial x^\alpha} = Q^{kl}. \tag{14}$$

§5γ. The stress-energy tensor $T_k{}^l$ whose divergence is equal to the components of the four force can be written

$$T_k{}^l = \tfrac{1}{2}(F_{k\alpha}F^{l\alpha} - F^*{}_{k\alpha}F^{*l\alpha}).$$

This can be written in terms of our tensor G_{kl}

$$T_k{}^l = \tfrac{1}{4}(G_{k\alpha}\overline{G}^{l\alpha} + \overline{G}_{k\alpha}G^{l\alpha}) \tag{15}$$

where the conjugate tensor is to be formed according to Eq. (15) of Chapter I. As is well known this tensor has a diagonal sum which is zero

$$T_\alpha{}^\alpha = 0 \tag{16}$$

as one sees using the theorem of footnote 10. Consequently $T_k{}^l$ has only nine linearly independent "Kennzahlen."

§5δ. It is important for the sequel briefly to discuss the phenomenological form of the Maxwell equations in matter. Since the dielectric displacment D and the magnetic induction B are connected with E and H through

$$\begin{aligned} D &= E + P \\ B &= H + I \end{aligned} \tag{17}$$

where P and I are the electric and magnetic polarization respectively, we can write the Maxwell equations

$$\left.\begin{aligned} \operatorname{div} E &= \rho' & \qquad \operatorname{div} B &= 0 \\ \operatorname{curl} B - \frac{1}{c}\frac{\partial E}{\partial t} &= \frac{J}{c} & \qquad \operatorname{curl} E + \frac{1}{c}\frac{\partial B}{\partial t} &= 0 \end{aligned}\right\} \tag{18}$$

where

$$\begin{aligned} \rho' &= \rho - \operatorname{div} P \\ \frac{J}{c} &= \frac{\rho v}{c} + \operatorname{curl} I + \frac{1}{c}\frac{\partial P}{\partial t}. \end{aligned} \tag{19}$$

If ρ, $(\rho v/c)$, P and I are given, the above system agrees formally with the equations in vacuo. To write (18) and (19) in four dimensional form we introduce the two self-dual tensors G'^{kl} and M^{kl}. They have the form (15a) where

$$\begin{aligned} \vec{k}_{G'} &= \vec{B} - i\vec{E} \\ \vec{k}_M &= \vec{I} + i\vec{P}. \end{aligned} \tag{20}$$

We then write (18) and (19)

$$\left.\begin{aligned} &\frac{\partial G'^{k\lambda}}{\partial x^\lambda} = J^k \\ \text{where}\quad &J^k = S^k + \frac{1}{2}\left(\frac{\partial M^{k\lambda}}{\partial x^\lambda} + \frac{\partial \overline{M}^{k\lambda}}{\partial x^\lambda}\right) \end{aligned}\right\} \tag{21}$$

§6α. Having been able to write the entire formalism of Maxwell equations with the help of the self-dual world tensor G^{kl} and its complex conjugate, we can now introduce by means of formulae (18) and (18a) two symmetric spinors $g_{\dot m\dot n}$ and g_{kl} of the second rank, and thus avoid the introduction of fourth-rank spinors altogether. It is obvious that the spinor g_{kl}, just like the tensor $\overline{G}^{kl}$, will only be needed in the formulation of the stress-energy tensor.

We know from Chapter II, that the four-current S^k becomes a spinor $s_{\dot m l}$, the gradient $\partial/\partial x^k$ according to (19) a spinor operator $\partial_{\dot m l}$; we see now that the simplest way of connecting $\partial_{\dot m l}$ and $s_{\dot m l}$ in a manner analogous to (6), is by letting $\partial_{\dot m l}$ act on a spinor with two dotted or two undotted indices. We choose the former and write Maxwell equations[14]

$$\partial^{\dot\rho}{}_l g_{\dot\rho\dot m} = 2 s_{\dot m l}. \tag{6a}$$

The continuity equation for the four current reads

$$\partial^{\dot\mu\lambda} s_{\dot\mu\lambda} = 0. \tag{5a}$$

The identity of this with (5) was already noted in Chapter I formula (20).

The analogue of the four potential ϕ^k will be the spinor $\phi_{\dot m l}$. It is connected with the field spinor $g_{\dot r\dot s}$ by the following curl-like operation, which, however, in this case is symmetrical:

$$g_{\dot r\dot s} = \partial_{\dot r\lambda}\phi_{\dot s}{}^\lambda + \partial_{\dot s\lambda}\phi_{\dot r}{}^\lambda \tag{9a}$$

The $\phi_{\dot m l}$ are subjected to the divergence condition

$$\partial^{\dot\mu\lambda}\phi_{\dot\mu\lambda} = 0. \tag{10a}$$

Introducing (9a) into (6a) we have

$$\partial^{\dot\rho}{}_l(\partial_{\dot\rho\alpha}\phi_{\dot m}{}^\alpha + \partial_{\dot m\alpha}\phi_{\dot\rho}{}^\alpha) = 2 s_{\dot m l}.$$

Using (8) Chapter I, we can transform each term according to

$$\partial^{\dot\rho}{}_l\partial_{\dot\rho\alpha}\phi_{\dot m}{}^\alpha = -\partial^{\dot\rho}{}_\alpha\partial_{\dot\rho}{}^\alpha\phi_{\dot m l} - \partial^{\dot\rho\alpha}\partial_{\dot\rho\alpha}\phi_{\dot m l}$$

$$\partial^{\dot\rho}{}_l\partial_{\dot m\alpha}\phi_{\dot\rho}{}^\alpha = -\partial_{\dot m l}\partial_{\dot\rho\alpha}\phi^{\dot\rho\alpha} - \partial_{\dot\rho l}\partial^{\dot\rho}{}_\alpha\phi_{\dot m}{}^\alpha.$$

[14] For $l=1$, $\dot m=\dot 1$ and for $l=2$, $\dot m=\dot 2$ we have

$$\partial^{\dot 1}{}_1 g_{\dot 1\dot 1} + \partial^{\dot 2}{}_1 g_{\dot 2\dot 1} = 2 s_{\dot 1 1}$$
$$\partial^{\dot 1}{}_2 g_{\dot 1\dot 2} + \partial^{\dot 2}{}_2 g_{\dot 2\dot 2} = 2 s_{\dot 2 2}$$

With (4), (10), (19), (18) of Ch. I, and (8) Chapter II, this becomes:

$$\left(\operatorname{curl}_s H - \frac{1}{c}\dot E_s + \operatorname{div} E\right) - i\left(\operatorname{curl}_s E + \frac{1}{c}\dot H_s - \operatorname{div} H\right) = \frac{\rho v_s}{c} + \rho$$

$$\left(-\operatorname{curl}_s H + \frac{1}{c}\dot E_s + \operatorname{div} E\right) + i\left(\operatorname{curl}_s E + \frac{1}{c}\dot H_s + \operatorname{div} H\right) = \frac{\rho v_s}{c} + \rho$$

from which follow four of the eight Maxwell equations.

Adding these, the last two terms cancel because of (7) Chapter I, and due to (10a), we get

$$\partial_{\rho\alpha}\partial^{\dot\rho\alpha}\phi_{\dot m l} = 2s_{\dot m l}. \tag{11a}$$

§6β. The analogue of the self-dual Hertzian tensor Z^{kl} is the symmetric Hertzian spinor $z_{\dot r\dot s}$. The potential spinor $\phi_{\dot m l}$ is derived from this according to

$$\phi_{\dot m l} = \partial^{\dot\sigma}{}_l z_{\dot m\dot\sigma}. \tag{12a}$$

By this operation the divergence condition (10a) is identically fulfilled, for we obtain, introducing (12a) into (10a)

$$\partial^{\dot\mu\lambda}\phi_{\dot\mu\lambda} = \partial^{\dot\mu\lambda}\partial^{\dot\sigma}{}_\lambda z_{\dot\mu\dot\sigma}$$

using the symmetry of $z_{\dot\mu\dot\sigma}$ we have

$$\partial^{\dot\mu\lambda}\phi_{\dot\mu\lambda} = \tfrac{1}{2}\left\{\partial^{\dot\mu\lambda}\partial^{\dot\sigma}{}_\lambda + \partial^{\dot\sigma\lambda}\partial^{\dot\mu}{}_\lambda\right\} z_{\dot\mu\dot\sigma} \equiv 0.$$

This vanishes applying (7) Chapter I to the index λ. Analogous to the stream potential Q_{kl}, a self-dual tensor we now derive the stream spinor $s_{\dot m l}$ from

$$s_{\dot m l} = \partial^{\dot\sigma}{}_l q_{\dot m\dot\sigma} \tag{13a}$$

where $q_{\dot m\dot s}$ is again a symmetric spinor of the second rank. Introducing (12a) and (13a) into (11a), and dropping a ∂ operator on both sides, we obtain the wave equation for $z_{\dot m\dot s}$

$$\partial_{\dot\rho\alpha}\partial^{\dot\rho\alpha} z_{\dot m\dot s} = 2q_{\dot m\dot s}. \tag{14a}$$

§6γ. The spinor analogue of the stress-energy tensor T_{kl} will be a spinor of the fourth rank with two dotted and two undotted indices. Its divergence will have to be equal to the spinor $f_{\dot m l}$ which corresponds to the four vector of the Lorentz force density and the action density. To derive this expression we write down the Maxwell equations and their conjugates according to (6a), using (7) Chapter I

$$\partial_{\dot\rho l} g^{\dot\rho\dot m} = -2s^{\dot m}{}_l$$
$$\partial_{\dot r\lambda} g^{\lambda k} = -2s_{\dot r}{}^k.$$

Then we multiply the upper equation with g^{lk} and the lower with $g^{\dot r\dot m}$ and contract with respect to r and l. After adding we can write this

$$\partial_{\dot\rho\lambda}\left\{g^{\dot\rho m} g^{\lambda k}\right\} = -2\left\{g^{\dot\rho\dot m} s_{\dot\rho}{}^k + g^{\lambda k} s^{\dot m}{}_\lambda\right\}.$$

Introducing

$$t^{\dot r\dot m l k} = \tfrac{1}{4} g^{\dot r\dot m} g^{l k} \tag{15a}$$

we have

$$\partial_{\dot\rho\lambda} t^{\dot\rho\dot m\lambda k} = 2f^{\dot m k} \tag{15b}$$

where the force spinor

$$f^{\dot m k} = -\tfrac{1}{4}\left\{g^{\dot\rho\dot m} s_{\dot\rho}{}^k + g^{\lambda k} s^{\dot m}{}_\lambda\right\}. \tag{15c}$$

It follows from the symmetry of the spinors $g^{\dot{r}\dot{m}}$ and g^{lk} that $t^{\dot{r}\dot{m}lk}$ has only nine "Kennzahlen." Thus relation (16) is already embodied in the structure of the stress-energy spinor.

§6δ. Analogous to the developments of §5δ we introduce two symmetric spinors $g'_{\dot{r}\dot{s}}$ and $m_{\dot{r}\dot{s}}$ which correspond to the self-dual tensors G'^{kl} and M^{kl}. We then write the spinor analogue of (21)

$$\partial^{\dot{s}}{}_l g'_{\dot{s}\dot{r}} = 2j_{\dot{r}l}$$

where

$$j_{\dot{r}l} = s_{\dot{r}l} + \tfrac{1}{4}(\partial^{\dot{s}}{}_l m_{\dot{s}\dot{r}} + \partial_{\dot{r}}{}^{\alpha} m_{\dot{s}\alpha}) \tag{21a}$$

where the first term on the right side is due to conduction and the second term to electric and magnetic polarization.

Chapter III. The Dirac Equations in Spinor Form

§7. Van der Waerden has shown how to write the Dirac equations in spinor form. The four wave functions ψ of Dirac correspond to two spinors of the first rank $\psi_{\dot{m}}$ and χ_l, and his equations become

$$mc\chi_l - \left(\frac{h}{i}\partial^{\dot{s}}{}_l + \phi^{\dot{s}}{}_l\right)\psi_{\dot{s}} = 0 \tag{1a}$$

$$mc\psi_{\dot{m}} + \left(\frac{h}{i}\partial_{\dot{m}}{}^{\lambda} + \phi_{\dot{m}}{}^{\lambda}\right)\chi_{\lambda} = 0 \tag{1b}$$

where $\phi^{\dot{s}}{}_l$ is the potential spinor as according to (9a) Chapter II. We shall also need the complex conjugate equations which read

$$mc\chi_{\dot{m}} - \left(-\frac{h}{i}\partial_{\dot{m}}{}^{\lambda} + \phi_{\dot{m}}{}^{\lambda}\right)\psi_{\lambda} = 0 \tag{2a}$$

$$mc\psi_l + \left(-\frac{h}{i}\partial^{\dot{s}}{}_l + \phi^{\dot{s}}{}_l\right)\chi_{\dot{s}} = 0. \tag{2b}$$

We now wish to obtain the second order Dirac equations. Introducing the abbreviation

$$p^{\dot{s}}{}_l = \frac{h}{i}\partial^{\dot{s}}{}_l + \phi^{\dot{s}}{}_l \tag{3}$$

we eliminate χ_l from (1) and get

$$m^2c^2\psi_{\dot{m}} + p_{\dot{m}}{}^{\lambda}p^{\dot{s}}{}_{\lambda}\psi_{\dot{s}} = 0.$$

We apply the identity (8) Chapter I to the second term and have, using also identity (7) Chapter I,

$$p_{\dot{m}}{}^{\lambda}p^{\dot{s}}{}_{\lambda}\psi_{\dot{s}} = -\tfrac{1}{2}p^{\dot{s}\lambda}p_{\dot{s}\lambda}\psi_{\dot{m}} + \tfrac{1}{2}p_{\dot{s}\lambda}p_{\dot{m}}{}^{\lambda}\psi^{\dot{s}} - \tfrac{1}{2}p_{\dot{m}}{}^{\lambda}p_{\dot{s}\lambda}\psi^{\dot{s}}.$$

Taking (3) into account we see that

$$p_{\dot{\sigma}\lambda}p_{\dot{m}}{}^{\lambda}\psi^{\dot{\sigma}} - p_{\dot{m}}{}^{\lambda}p_{\dot{\sigma}\lambda}\psi^{\dot{\sigma}} = \frac{h}{i}\psi^{\dot{\sigma}}(\partial_{\dot{\sigma}\lambda}\phi_{\dot{m}}{}^{\lambda} + \partial_{\dot{m}\lambda}\phi_{\dot{\sigma}}{}^{\lambda})$$

$$= \frac{h}{i}\psi^{\dot{\sigma}}g_{\dot{m}\dot{\sigma}},$$

the latter because of (9a) Chapter II. Thus the second-order wave equation becomes

$$-\frac{1}{2}\left(\frac{h}{i}\partial^{\dot{\sigma}\lambda} + \phi^{\dot{\sigma}\lambda}\right)\left(\frac{h}{i}\partial_{\sigma\lambda} + \phi_{\sigma\lambda}\right)\psi_{\dot{m}} + m^2c^2\psi_{\dot{m}} = -\frac{h}{2i}g_{\dot{m}\dot{\sigma}}\psi^{\dot{\sigma}}. \tag{4}$$

Correspondingly one obtains

$$-\frac{1}{2}\left(\frac{h}{i}\partial^{\dot{\sigma}\lambda} + \phi^{\dot{\sigma}\lambda}\right)\left(\frac{h}{i}\partial_{\dot{\sigma}\lambda} + \phi_{\dot{\sigma}\lambda}\right)\chi_k + m^2c^2\chi_k = \frac{h}{2i}g_{k\lambda}\chi^{\lambda}. \tag{5}$$

The left side is identical with the Gordon wave equation written in spinor form, whereas the right side represents the spin correction. It is satisfactory, that the field only occurs in the form of our symmetric spinor $g_{\dot{m}\dot{n}}$ resp. g_{kl}.

§8. To derive the expression for the current we multiply (1a) with ψ^l, (1b) with $-\chi^{\dot{m}}$, (2a) with $-\psi^{\dot{m}}$, (2b) with χ^l, and add all four equations. Using repeatedly identity (7) Chapter I all terms containing the mass and the potentials cancel and we can write the result

$$\partial^{\dot{\mu}\lambda}j_{\dot{\mu}\lambda} = 0 \tag{6}$$

where

$$j_{\dot{m}l} = \psi_{\dot{m}}\psi_l + \chi_{\dot{m}}\chi_l. \tag{7}$$

§9. We shall split up the above expression after the fashion of Eq. (1a) Chapter II. We replace $\psi_{\dot{m}}$ and χ_l in (7) by their expressions following from (1a) and (1b) and have, using identity (8) Chapter I

$$mcj_{\dot{m}l} = -\psi_l\left(\frac{h}{i}\partial_{\dot{m}}{}^{\alpha} + \phi_{\dot{m}}{}^{\alpha}\right)\chi_{\alpha} + \chi_{\dot{m}}\left(\frac{h}{i}\partial^{\dot{\sigma}}{}_l + \phi^{\dot{\sigma}}{}_l\right)\psi_{\dot{\sigma}}$$

$$= +\psi^{\alpha}\left(\frac{h}{i}\partial_{\dot{m}\alpha} + \phi_{\dot{m}\alpha}\right)\chi_l - \chi^{\dot{\sigma}}\left(\frac{h}{i}\partial_{\dot{\sigma}l} + \phi_{\dot{\sigma}l}\right)\psi_{\dot{m}}$$

$$+\psi_{\alpha}\left(\frac{h}{i}\partial_{\dot{m}l} + \phi_{\dot{m}l}\right)\chi^{\alpha} - \chi_{\dot{\sigma}}\left(\frac{h}{i}\partial_{\dot{m}l} + \phi_{\dot{m}l}\right)\psi^{\dot{\sigma}}.$$

We then replace in (7) ψ_l and $\chi_{\dot{m}}$ by the expressions following from (2a) and (2b) and transform the equations by means of (8) Chapter I in a completely analogous fashion. We thus obtain four expressions for $mcj_{\dot{m}l}$. Adding all of them we have after a few elementary transformations

$$j_{\dot{r}l} = s_{\dot{r}l} + \tfrac{1}{4}(\partial^{\dot{\sigma}}{}_l m_{\dot{\sigma}\dot{r}} + \partial_{\dot{r}}{}^{\alpha}m_{\alpha l}) \tag{8}$$

where

$$s_{\dot{r}l} = \frac{h}{4imc}(\psi_\alpha \partial_{\dot{r}l}\chi^\alpha + \chi_\alpha \partial_{\dot{r}l}\psi^\alpha + \psi^\dot{\sigma}\partial_{\dot{r}l}\chi_\dot{\sigma} + \chi^\dot{\sigma}\partial_{\dot{r}l}\psi_\dot{\sigma}) \tag{9}$$

$$+ \frac{1}{2mc}\phi_{\dot{r}l}(\psi_\alpha \chi^\alpha + \psi_\dot{\sigma}\chi^\dot{\sigma})$$

$$\left.\begin{aligned} m_{\dot{r}\dot{s}} &= \frac{h}{imc}(\psi_\dot{r}\chi_\dot{s} + \psi_\dot{s}\chi_\dot{r}) \\ m_{kl} &= \frac{-h}{imc}(\psi_k \chi_l + \psi_l \chi_k) \end{aligned}\right\} \tag{10}$$

Equations (8) (9) and (10) are the spinor form for the decomposition of the current first given independently by Gordon[15] and Darwin.[16] Similarly to the correction terms on the right side of (4), the spinor (10) expresses the existence of a spin.

§10. The multiplication process described in §8 is not the only process by means of which the potentials $\phi_{\dot{m}l}$ may be eliminated from the Dirac equations. In fact, besides the one leading to the continuity Eq. (6), it is possible in three more ways to eliminate the $\phi_{\dot{m}l}$ each of which lead to an invariant relation between the ψ and χ.

For the sake of convenience we write down the four Dirac equations, but using only covariant ∂-operators. In four columns at the right side of the equations, the various factors, with which we multiply are given.

	a	b	c	d
$mc\chi_l + \frac{h}{i}\partial_{\dot{\sigma}l}\psi^\dot{\sigma} + \phi_{\dot{\sigma}l}\psi^\dot{\sigma} = 0$	$+\psi^l$	$+\psi^l$	$+\chi^l$	$+\chi^l$
$mc\psi_\dot{m} - \frac{h}{i}\partial_{\dot{m}\lambda}\chi^\lambda - \phi_{\dot{m}\lambda}\chi^\lambda = 0$	$-\chi^\dot{m}$	$+\chi^\dot{m}$	$+\psi^\dot{m}$	$+\psi^\dot{m}$
$mc\chi_\dot{m} - \frac{h}{i}\partial_{\dot{m}\lambda}\psi^\lambda + \phi_{\dot{m}\lambda}\psi^\lambda = 0$	$-\psi^\dot{m}$	$-\psi^\dot{m}$	$+\chi^\dot{m}$	$-\chi^\dot{m}$
$mc\psi_l + \frac{h}{i}\partial_{\dot{\sigma}l}\chi^\dot{\sigma} - \phi_{\dot{\sigma}l}\chi^\dot{\sigma} = 0$	$+\chi^l$	$-\chi^l$	$+\psi^l$	$-\psi^l$

We obtain

(a) $$\partial_{\dot{\sigma}\lambda}(\psi^\dot{\sigma}\psi^\lambda + \chi^\dot{\sigma}\chi^\lambda) = 0. \tag{6}$$

This is Eq. (6) for the current.

(b) $$\partial_{\dot{\sigma}\lambda}(\psi^\dot{\sigma}\psi^\lambda - \chi^\dot{\sigma}\chi^\lambda) + 2i\frac{mc}{h}(\psi^\lambda \chi_\lambda + \psi_\dot{\sigma}\chi^\dot{\sigma}) = 0 \tag{11}$$

(c) (d) Adding and subtracting the results of process (c) and (d) we have, using (7) and (7a) Chapter I

[15] W. Gordon, Zeits. f. Physik **50**, 630 (1928).
[16] G. Darwin, Proc. Roy. Soc. **A120**, 621 (1928).

$$\chi^{\lambda}\partial_{\dot{\sigma}\lambda}\psi^{\dot{\sigma}} - \psi^{\dot{\sigma}}\partial_{\dot{\sigma}\lambda}\chi^{\lambda} = 0 \tag{12}$$

$$\chi^{\dot{\sigma}}\partial_{\dot{\sigma}\lambda}\psi^{\lambda} - \psi^{\lambda}\partial_{\dot{\sigma}\lambda}\chi^{\dot{\sigma}} = 0. \tag{13}$$

It is clear, that these are the only relations between the wave functions which are independent of the potentials $\phi_{\dot{m}l}$, because we have eight equations (the four Dirac equations and their complex conjugates) in which only four potentials $\phi_{\dot{m}l}$ occur.[17] It is curious, that three of these relations are also independent of the mass.

A few words may be added concerning the quadratic invariants which do not involve differentiation. Due to (7a) Chapter I the only two invariants are:

$$\left.\begin{aligned} \Delta &= \psi_{\lambda}\chi^{\lambda} \\ \bar{\Delta} &= \psi_{\dot{\sigma}}\chi^{\dot{\sigma}} \end{aligned}\right\}. \tag{14}$$

It is easily verified[18] that the square of the current

$$j_{\dot{\sigma}\lambda}j^{\dot{\sigma}\lambda} = 2\Delta\bar{\Delta} \tag{15}$$

and the square of the polarization spinor (10):

$$\left.\begin{aligned} m_{\dot{\rho}\dot{\sigma}}m^{\dot{\rho}\dot{\sigma}} &= 2\left(\frac{h}{mc}\right)^2\bar{\Delta}^2 \\ \text{and} \qquad m_{\alpha\beta}m^{\alpha\beta} &= 2\left(\frac{h}{mc}\right)^2\Delta^2 \end{aligned}\right\} \tag{16}$$

Introducing the abbreviation

$$k_{\dot{s}l} = \psi_{\dot{s}}\psi_{l} - \chi_{\dot{s}}\chi_{l}$$

for the spinor whose divergence occurred in (11), it is readily seen that

$$\left.\begin{aligned} k^{\dot{\rho}}{}_{l}m_{\dot{\rho}\dot{s}} &= -\frac{h}{imc}j_{\dot{s}l}\bar{\Delta} \\ j^{\dot{\rho}}{}_{l}m_{\dot{\rho}\dot{s}} &= -\frac{h}{imc}k_{\dot{s}l}\bar{\Delta}. \\ k_{\dot{\sigma}\lambda}j^{\dot{\sigma}\lambda} &= 0 \end{aligned}\right\} \tag{17}$$

§11. Darwin[19] has shown how to derive both the Maxwell and the Dirac equations from a variation principle. The analogous development using spinor analysis runs as follows. We start with the Lagrangian function

[17] Relations (11), (12) and (13) were found more or less accidentally by the authors. The point of view described in the text was supplied by Professor G. Y. Rainich, who found them independently. Professor Rainich further communicated to us a rigorous proof of the fact that the Dirac equations possess only two algebraic quadratic invariants, which are simply our Δ and $\bar{\Delta}$. Also relations (17) are due to him. The authors are greatly indebted to Professor Rainich for several discussions on the subject.

[18] Compare C. G. Darwin, Proc. Roy. Soc. **A120,** 621 (1928). See esp. p. 627.

[19] C. G. Darwin, Proc. Roy. Soc. **A118,** 654 (1928).

$$L = \frac{h}{i}\{\psi^{\dot\mu}\partial_{\dot\mu}{}^{\lambda}\psi_{\lambda} - \chi^{\dot\mu}\partial_{\dot\mu}{}^{\lambda}\chi_{\lambda} - \psi^{\lambda}\partial^{\dot\mu}{}_{\lambda}\psi_{\dot\mu} + \chi^{\lambda}\partial^{\dot\mu}{}_{\lambda}\chi_{\dot\mu}\} + 2mc(\Delta + \bar\Delta) + \phi^{\dot\mu\lambda}j_{\dot\mu\lambda} - \tfrac{1}{2}g^{\dot\mu\dot\rho}g_{\dot\mu\dot\rho} \qquad (18)$$

where the meaning of Δ, $\bar\Delta$, $j_{\dot m l}$ and $g_{\dot m\dot n}$ in terms of ψ, χ, and ϕ are given in Eq. (14) (7) Chapter III and (9a) Chapter II respectively. L is to be considered a function of ψ, χ, ϕ and their derivatives.

1°. Varying ψ_l we obtain as Euler-Lagrange equation

$$\partial_{\dot\mu}{}^{l}\left\{\frac{\partial L}{\partial(\partial_{\dot\mu}{}^{\alpha}\psi_{\alpha})}\right\} - \frac{\partial L}{\partial\psi_l} = 0$$

which is identical with (1a).

2°. Varying $\chi_{\dot m}$ we obtain

$$\partial^{\dot m}{}_{\lambda}\left\{\frac{\partial L}{\partial(\partial^{\dot\sigma}{}_{\lambda}\chi_{\dot\sigma})}\right\} - \frac{\partial L}{\partial\chi_{\dot m}} = 0$$

which is identical with (1b).

3°. Varying $\psi_{\dot m}$ we get (2a) and varying χ_l we get (2b).

4°. Varying $\phi_{\dot m l}$ we obtain

$$\partial_{\dot\sigma}{}^{l}\left\{\frac{\partial L}{\partial(\partial_{\dot\sigma\alpha}\phi_{\dot m}{}^{\alpha})}\right\} - \frac{\partial L}{\partial\phi_{\dot m l}} = 0$$

that is to say

$$\partial_{\dot\sigma}{}^{l}g^{\dot\sigma\dot m} = 2j^{\dot m l} = 2(\psi^{\dot m}\psi^{l} + \chi^{\dot m}\chi^{l})$$

which are the Maxwell equations with the Dirac current.

A TENSOR FORM OF DIRAC'S EQUATION

By Boris Podolsky*
California Institute of Technology

(Received April 8, 1931)

Abstract

In this paper a simple tensor form of Dirac's equation is obtained. This is accomplished by considering ψ_s and $\gamma^\alpha(rs)$ of the usual equations as being related to a set of n-beins as invariants corresponding to true tensors ψ_μ and $\Gamma^\alpha{}_\beta{}^\sigma$. The results are, however, independant of the choice of the n-beins. It is thus shown that the introduction of the idea of half-vectors in the quantum mechanics, while undoubtedly desirable when dealing exclusively with cartesian coordinates, is unnecessary.

1. MUCH work was done in attempting to find a generalization of Dirac's wave equation to general relativity. Of this the most important is probably the work of Fock.[1] In nearly all these, however, ψ is regarded as a half-vector. It is interesting, therefore, to see to what extent it is possible to achieve this generalization using only the ordinary tensors.

It became quite clear, as the result of other investigations, that the extension of Dirac's equations to general relativity necessitates the introduction of n-beins, i.e. a local cartesian coordinate system at each point. This, however, does not spoil the generality of equations obtained, as they turn out to be independent of the particular choice assumed.

2. For our purpose it is convenient to write Dirac's equation in the following form:

$$\sum_s e_s \left\{ \Gamma^\alpha{}_{rs} \left(p_\alpha + \frac{e}{c} \Phi_\alpha \right) + mc\Gamma_{rs} \right\} \psi_s = 0 \tag{1}$$

where all subscripts take the values 1, 2, 3, and 4. As is done in the work of Fock, summations with respect to doubled Greek indices are always implied, while summations with respect to Latin indices are explicitly indicated. The matrices are taken to be the following:

$$\Gamma^1 = \begin{pmatrix} 0 & 1 & 0 & 0 \\ 1 & 0 & 0 & 0 \\ 0 & 0 & 0 & 1 \\ 0 & 0 & 1 & 0 \end{pmatrix}; \quad \Gamma^2 = \begin{pmatrix} 0 & -i & 0 & 0 \\ i & 0 & 0 & 0 \\ 0 & 0 & 0 & i \\ 0 & 0 & -i & 0 \end{pmatrix}; \quad \Gamma^3 = \begin{pmatrix} 1 & 0 & 0 & 0 \\ 0 & -1 & 0 & 0 \\ 0 & 0 & 1 & 0 \\ 0 & 0 & 0 & -1 \end{pmatrix}$$

$$\Gamma^4 = I = \begin{pmatrix} 1 & 0 & 0 & 0 \\ 0 & 1 & 0 & 0 \\ 0 & 0 & 1 & 0 \\ 0 & 0 & 0 & 1 \end{pmatrix}; \quad \Gamma = \begin{pmatrix} 0 & 0 & 0 & -1 \\ 0 & 0 & 1 & 0 \\ 0 & 1 & 0 & 0 \\ -1 & 0 & 0 & 0 \end{pmatrix}. \tag{2}$$

* This work was started at the Leipzig Physikalisches Institut while the author was there on a National Research Fellowship.

[1] Fock, Journ. de Phys. **10**, 392 (1929) in which other references are given. See also Tetrode, Zeits. f. Physik **50**, 336 (1928), and Wigner, Zeits. f. Physik **53**, 592 (1929).

Here $p_\alpha = (h/2\pi i)\partial/\partial x^\alpha$; $x^\alpha = (x, y, z, ct)$; $\Phi_\alpha = (A_x, A_y, A_z, -\phi,)$, where ϕ is the scalar and (A_x, A_y, A_z) the vector potential. Also, the quantities $e_1 = e_2 = e_3 = -1$, $e_4 = 1$, are introduced for later convenience.

3. We now introduce a set of n-beins by means of sixteen parameters h_s^ν and their corresponding moments $h_{s\nu}$ as is done by Fock. Designating local components of vectors, i.e. ordinary cartesian projections on the vectors constituting the n-beins at each point, by Latin indices and their tensor components by Greek indices, we have the following relations:

$$\begin{aligned} A_\sigma &= \sum_k e_k A_k h_{k\sigma} \\ A^\sigma &= \sum_k e_k A_k h_k^\sigma . \end{aligned} \tag{3}$$

The quantities e_k are introduced to make the components A_4, A^4, and $h_{4\sigma}$ real and are $e_1 = e_2 = e_3 = -1$, $e_4 = 1$, as in Eq. (1).

With this notation[2] the h's satisfy the following relations:

$$\begin{aligned} e_k h_k^\sigma h_{l\sigma} &= e_l h_k^\sigma h_{l\sigma} = \delta_{kl} \\ \sum_k e_k h_{k\sigma} h_k^\rho &= \delta_\sigma^\rho . \end{aligned} \tag{4}$$

Equations (3) can be immediately generalized to any tensor. Thus, for example:

$$A^{\alpha\beta}{}_\gamma = \sum_{r,s,t} e_r e_s e_t A_{rst} h_r^\alpha h_s^\beta h_{t\gamma} \tag{5}$$

or, solving for A_{rst} with the help of (4)

$$A_{rst} = A^{\alpha\beta}{}_\gamma h_{r\alpha} h_{s\beta} h_t^\gamma .$$

The quantities A_{rst} are invariants, i.e. they do not change with the change of the coordinate system, although they, of course, change with the change of the set of n-beins.

We may also have quantities such as

$$A^\alpha{}_{st} = A^{\alpha\beta}{}_\gamma h_{s\beta} h_t^\gamma , \tag{6}$$

which are in part invariants of a set of n-beins and in part tensors.

4. We extend Dirac's equation to general relativity by regarding the Latin indices occurring in Eq. (1) as the n-bein system indices. Thus, Γ_{rs} and ψ_s are invariants, and $\Gamma^\alpha{}_{rs}$ are the mixed quantities of the type of Eq. (6).

We will now rewrite Eq. (1) in a tensor form. First we observe that

$$\sum_s e_s \Gamma_{rs} \psi_s = \sum_{s,t} e_s \Gamma_{rs} \delta_{st} \psi_t = \sum_{s,t} e_s e_t \Gamma_{rs} h_s^\sigma h_{t\sigma} \psi_t , \text{ by (4)}$$

thus, by (3)

$$\sum_s e_s \Gamma_{rs} \psi_s = \Gamma_r^\sigma \psi_\sigma . \tag{7}$$

[2] The notation throughout this paper is that of Fock.

Similarly

$$\sum_s e_s \Gamma^{\alpha}{}_{rs}\left(p_\alpha + \frac{e}{c}\,\Phi_\alpha\right)\psi_s = \left(p_\alpha + \frac{e}{c}\,\Phi_\alpha\right)\sum_s e_s \Gamma^{\alpha}{}_{rs}\psi_s = \left(p_\alpha + \frac{e}{c}\,\Phi_\alpha\right)\Gamma^{\alpha}{}_{r}{}^{\sigma}\psi_\sigma. \tag{8}$$

In place of the ordinary partial derivative in the interpretation of p_α as an operator we now use

$$p_\alpha = \frac{h}{2\pi i}(\cdots)_{;\alpha} \tag{9}$$

where; α is the covariant derivative in the sense of Einstein.[3] This operator acting on a tensor gives again a tensor of one rank higher in covariant indices. It is defined with the help of the quantities

$$\Delta^{\sigma}{}_{\alpha\beta} = \sum_s e_s h_s{}^{\sigma}\frac{\partial h_{s\alpha}}{\partial x^\beta}. \tag{10}$$

In constructing Einstein's covariant derivatives one uses $\Delta^{\sigma}{}_{\alpha\beta}$ like $\{\alpha\beta, \sigma\}$ in ordinary covariant differentiation. Thus, for example,

$$(A_\beta{}^{\alpha})_{;\gamma} = \frac{\partial A_\beta{}^{\alpha}}{\partial x^\gamma} + A_\beta{}^{\sigma}\Delta^{\alpha}{}_{\sigma\gamma} - A_\sigma{}^{\alpha}\Delta^{\sigma}{}_{\alpha\beta}.$$

For us the important property of; α is

$$(h_s{}^{\nu})_{;\alpha} = (h_{s\nu})_{;\alpha} = (g_{\mu\nu})_{;\alpha} = 0. \tag{11}$$

From this follows:

$$\begin{aligned} p_\alpha \Gamma^{\alpha}{}_{r}{}^{\sigma}\psi_\sigma &= \frac{h}{2\pi i}(\Gamma^{\alpha}{}_{r}{}^{\sigma}\psi_\sigma)_{;\alpha} \\ &= \frac{h}{2\pi i}\left(\sum_s \Gamma^{\alpha}{}_{rs}e_s h_s{}^{\sigma}\psi_\sigma\right)_{;\alpha} \\ &= \frac{h}{2\pi i}\sum_s \Gamma^{\alpha}{}_{rs}e_s h_s{}^{\sigma}(\psi_\sigma)_{;\alpha} \end{aligned}$$

since $\Gamma^{\alpha}{}_{rs}$ are constants and by Eq. (11). Hence

$$\begin{aligned} p_\alpha \Gamma^{\alpha}{}_{r}{}^{\sigma}\psi_\sigma &= \left(\sum_s \Gamma^{\alpha}{}_{rs}e_s h_s{}^{\sigma}\right)\cdot\frac{h}{2\pi i}(\psi_\sigma)_{;\alpha} \\ &= \Gamma^{\alpha}{}_{r}{}^{\sigma}p_\alpha\psi_\sigma \end{aligned} \tag{12}$$

i.e., p_α and the Γ's commute.

[3] Einstein, Math. Ann. **102,** 685 (1930).

Using Eqs. (7), (8), and (13) we can rewrite Eq. (1) in the form

$$\left\{\Gamma^{\alpha}{}_{r}{}^{\sigma}\left(p_{\alpha}+\frac{e}{c}\,\Phi_{\alpha}\right)+mc\Gamma_{r}{}^{\sigma}\right\}\psi_{\sigma}=0.$$

Multiplying by $e_r h_{r\beta}$ and summing with respect to r, we obtain the desired equation:

$$\left\{\Gamma^{\alpha}{}_{\beta}{}^{\sigma}\left(p_{\alpha}+\frac{e}{c}\,\Phi_{\alpha}\right)+mc\Gamma_{\beta}{}^{\sigma}\right\}\psi_{\sigma}=0. \tag{13}$$

5. The adjoint to Eq. (1) by a similar transformation becomes

$$\left\{\Gamma^{\alpha}{}_{\beta}{}^{\sigma}\left(p_{\alpha}-\frac{e}{c}\,\Phi_{\alpha}\right)-mc\Gamma_{\beta}{}^{\sigma}\right\}\psi\dagger^{\beta}=0. \tag{14}$$

Multiplying Eq. (13) by $\psi\dagger^{\beta}$, Eq. (14) by ψ_{α} and adding we obtain

$$\psi\dagger^{\beta}\Gamma^{\alpha}{}_{\beta}{}^{\sigma}p_{\alpha}\psi_{\sigma}+\psi_{\alpha}\Gamma^{\alpha}{}_{\beta}{}^{\sigma}p_{\alpha}\psi\dagger^{\beta}=0$$

or

$$(\psi\dagger^{\beta}\Gamma^{\alpha}{}_{\beta}{}^{\sigma}\psi_{\sigma})_{;\alpha}=0. \tag{15}$$

We may interpret the expression in parenthesis as the current-density vector

$$J^{\alpha}=\Gamma^{\alpha}{}_{\beta}{}^{\sigma}\psi\dagger^{\beta}\psi_{\sigma}; \tag{16}$$

then Eq. (15) becomes a generalization of the equation

$$div J^{\alpha}=0.$$

Using Eqs. (3) and (5), Eq. (16) may be also written as follows:

$$J^{\alpha}=\sum_{r,s}e_r e_s\psi_r\dagger\Gamma^{\alpha}{}_{rs}\psi_s, \tag{17}$$

which is what one obtains directly from Eq. (1) and its adjoint.

6. The energy is given by the relation

$$-\frac{E}{c}=p_4=\frac{h}{2\pi i}(\cdots)_{;4}. \tag{18}$$

Of course, we can speak of energy of an electron only in a flat space-time in which one of the coordinates is singled out as time. Thus, if $x_4=ct$, Eq. (18) reduces to the usual

$$E=-\frac{h}{2\pi i}\frac{\partial}{\partial t}$$

which must of course be interpreted to mean that the numerical value of the energy is given by

$$E'=-\frac{h}{2\pi i}\int\psi\dagger^{\alpha}\frac{\partial}{\partial t}\psi_{\alpha}dV.$$

In this case E' is $-c$ times the time component of a vector

$$p_{\beta'} = \frac{h}{2\pi i}\int \psi\dagger^{\alpha}(\psi_{\alpha})_{;\sigma}dV. \tag{20}$$

7. The angular momentum operator of Dirac

$$M^{\alpha} = m^{\alpha} + \frac{h}{4\pi}\sigma^{\alpha}, \tag{21}$$

where $m^1 = yp_z - zp_y$, etc. in our notation becomes

$$M^{\alpha}{}_{rs} = m^{\alpha}\delta_{rs} + \frac{h}{4\pi}\sigma^{\alpha}{}_{rs}. \tag{22}$$

The Hamiltonian of Dirac is also a four-rowed square matrix H_{rs}, and the fact that M^{α} and H commute means

$$\sum_{s,t} M^{\alpha}{}_{rs}H_{st}\psi_t = \sum_{s,t} H_{rs}M^{\alpha}{}_{st}\psi_t. \tag{23}$$

The operator (22) has a meaning only in flat space-time. In that case, however, our Eq. (13) can be written in the form

$$\sum_{s} e_s\left\{H_{rs} + \frac{h}{2\pi i}\delta_{rs}\frac{\partial}{\partial t}\right\}\psi_s = 0 \tag{24}$$

where H_{rs} is the Dirac Hamiltonian. The relation (23) then holds, so that operator (22) is still a constant of the motion.

8. The invariance of Eq. (13) with respect to Lorentz transformations does not follow immediately from the tensor form of the equation. In Eq. (2) $\Gamma^{\alpha}{}_{rs}$ are assumed constants associated with a particular coordinate system. By a Lorentz transformation they change to $\Gamma'^{\alpha}{}_{rs}$ given by

$$\Gamma'^{\alpha}{}_{rs} = \Gamma^{\beta}{}_{rs}a_{\beta\alpha}, \tag{25}$$

where $a_{\beta\alpha}$ is a set of coefficients satisfying the relation

$$\begin{aligned} a_{\mu\nu}a_{\mu\rho} &= \delta_{\nu\rho} \\ a_{\mu\rho}a_{\nu\rho} &= \delta_{\mu\nu}. \end{aligned} \tag{26}$$

Now, since the original and the new coordinate systems are physically indistinguishable, we may have started with the new Γ's and the old coordinate system; i.e. we have no way of knowing to which coordinate system the originally assumed Γ's belong. Thus, we may have written instead of Eq. (1)

$$\sum_{s} e_s\left\{\Gamma'^{\alpha}{}_{rs}\left(p_{\alpha} + \frac{e}{c}\Phi_{\alpha}\right) + mc\Gamma_{rs}\right\}\psi'_s = 0. \tag{27}$$

We must now show that Eq. (27) leads to the same physical results as Eq. (1). It has been shown[4] that Eq. (25) may be put in the form

[4] See for example Moglich, Zeits. f. Physik **48,** 852 (1928) and Neumann, Zeits. f. Physik **48,** 868 (1928).

$$\Gamma'^{\alpha}{}_{rs} = \sum_{t,u} S\dagger_{rt}\Gamma^{\alpha}{}_{tu}S_{us}, \tag{28}$$

where S and $S^{\dagger}$ are matrices of the form

$$S = \begin{pmatrix} \alpha & \beta & 0 & 0 \\ \gamma & \delta & 0 & 0 \\ 0 & 0 & \bar{\alpha} & \bar{\beta} \\ 0 & 0 & \bar{\gamma} & \bar{\delta} \end{pmatrix}, \quad S\dagger = \begin{pmatrix} \bar{\alpha} & \bar{\gamma} & 0 & 0 \\ \bar{\beta} & \bar{\delta} & 0 & 0 \\ 0 & 0 & \alpha & \gamma \\ 0 & 0 & \beta & \delta \end{pmatrix}$$

and $\alpha\delta - \beta\gamma = 1$. Furthermore

$$\Gamma_{rs} = \sum_{t,u} S\dagger_{rt}\Gamma_{tu}S_{us}. \tag{29}$$

Using Eqs. (28) and (29), Eq. (27) may be written as follows:

$$\sum_{s,t,u} e_s S_{rt}\dagger \left\{ \Gamma^{\alpha}{}_{tu}\left(p_\alpha + \frac{e}{c}\,\Phi_\alpha \right) + mc\Gamma_{tu} \right\} S_{us}\psi'_s = 0.$$

Thus, if ψ'_s satisfies Eq. (27), ψ_u given by

$$e_u\psi_u = \sum_s e_s S_{us}\psi'_s \tag{30}$$

will satisfy Eq. (1). Similarly

$$e_u\psi_u\dagger = \sum_s e_s\psi'\dagger_s S_{su}\dagger. \tag{30'}$$

Thus Eq. (17) becomes

$$\begin{aligned} J^{\alpha} &= \sum_{r,s} \left(\sum_t e_t\psi'\dagger_t S_{tr}\dagger \right) \Gamma^{\alpha}{}_{rs} \left(\sum_u e_u S_{su}\psi'_u \right) \\ &= \sum_{t,u} e_t e_u \psi'\dagger_t \Gamma'^{\alpha}{}_{tu}\psi'_u, \text{ by (28)} \end{aligned}$$

This is just what would have been obtained directly from Eq. (27).

9. Similarly, the invariance of Eq. (13) with respect to rotation of n-beins must be tested by investigating what would have happened if the original set of Γ's became associated with another set of n-beins. Our original equation would then be

$$\sum_s e_s \left\{ \Gamma''^{\alpha}{}_{rs}\left(p_\alpha + \frac{e}{c}\,\Phi_\alpha \right) + mc\Gamma''_{rs} \right\} \psi''_s = 0 \tag{31}$$

where $\Gamma''^{\alpha}{}_{rs}$ and Γ''_{rs} are obtained from the given Γ's by a rotation of n-beins.

We will now show that the physical consequences of Eq. (31) are the same as of Eq. (1). In order to show this we must first find the relation between Γ'' and Γ. This is given by the condition that tensors $\Gamma^{\alpha}{}_{\beta}{}^{\sigma}$ must be independent of the n-beins. Thus,

$$\Gamma^{\alpha}{}_{\beta}{}^{\sigma} = \sum_{r,s} e_r e_s h_{r\beta} h_s{}^{\sigma} \Gamma^{\alpha}{}_{rs} = \sum_{r,s} e_r e_s h''_{r\beta} h''_s{}^{\sigma} \Gamma''^{\alpha}{}_{rs}. \tag{32}$$

Using the laws of transformation of the n-beins

$$\begin{aligned} h_{r\beta} &= \sum_t a_{tr} h''_{t\beta} \\ h_s{}^{\sigma} &= \sum_t a_{ts} h''_t{}^{\sigma} \end{aligned} \tag{33}$$

where $\sum_t a_{rt} a_{st} = \sum_t a_{tr} a_{ts} = \delta_{rs}$, we obtain

$$e_r e_s \Gamma''^{\alpha}{}_{rs} = \sum_{t,u} e_t e_u a_{rt} \Gamma^{\alpha}{}_{tu} a_{su} \tag{34}$$

and a similar equation for Γ''_{rs}. With the help of Eq. (34) we may rewrite Eq. (31) as follows

$$\sum_{s,t,u} e_t e_u a_{rt} a_{su} \left\{ \Gamma^{\alpha}{}_{tu} \left(p_\alpha + \frac{e}{c} \Phi_\alpha \right) + mc\Gamma_{tu} \right\} \psi''_s = 0. \tag{35}$$

If the a's are constants, which is the case if we have distant parallelism, Eq. (35) becomes

$$\sum_r e_t a_{rt} \left[\sum_u e_u \left\{ \Gamma^{\alpha}{}_{tu} \left(p_\alpha + \frac{e}{c} \Phi_\alpha \right) + mc\Gamma_{tu} \right\} \sum_s a_{su} \psi''_s \right] = 0. \tag{36}$$

Thus, if ψ''_s satisfies Eq. (31),

$$\psi_u = \sum_s a_{su} \psi''_s \tag{37}$$

will satisfy Eq. (1). Similarly

$$\psi_t\dagger = \sum_r \psi''\dagger_r a_{rt}. \tag{38}$$

The current-density vector which we would have constructed using ψ''_s would be

$$\begin{aligned} J''^{\alpha} &= \sum_{r,s} e_r e_s \Gamma''^{\alpha}{}_{rs} \psi''_r \dagger \psi''_s \\ &= \sum_{r,s} \left(\sum_{t,u} e_t e_u a_{rt} \Gamma^{\alpha}{}_{tu} a_{su} \right) \psi''_r \dagger \psi''_s, \text{ by (34)} \\ &= \sum_{t,u} e_t e_u \Gamma^{\alpha}{}_{tu} \left(\sum_r \psi''_r \dagger a_{rt} \right) \left(\sum_s a_{su} \psi''_s \right) \\ &= \sum_{t,u} e_t e_u \Gamma^{\alpha}{}_{tu} \psi\dagger_t \psi_u, \text{ by (37) and (38)} \\ &= J^{\alpha}, \text{ by (17)}. \end{aligned}$$

10. Thus we were able to find a tensor equation, Eq. (13), which is invariant with respect to the Lorentz transformation and with respect to the

n-bein rotations. It satisfies all the conditions which a correct generalization of the Dirac equation should satisfy.

As for the physical or geometrical interpretation of the tensors $\Gamma^{\alpha}{}_{\beta}{}^{\sigma}$ and $\Gamma_{\beta}{}^{\sigma}$ we can only say that their introduction required the use of covariant differentiation in Einstein's sense and a true distant parallelism. In this we approach Einstein's unified field theory. However, a complete transition cannot be achieved as long as we are compelled to introduce potentials Φ_{α} in our equations as something externally given.

REPULSIVE ENERGY LEVELS IN BAND SPECTRA

By Joseph Kaplan
University of California at Los Angeles

(Received April 20, 1931)

Abstract

An explanation is given for many cases of anomalous intensity distribution in the band spectra of diatomic molecules. Use is made of an interaction between the known energy levels of molecules and energy levels which are produced by the repulsive interaction of pairs of atoms in their normal and metastable energy levels. The chief types of anomalies which are discussed are those corresponding to the sudden cutting off of a group of bands at some low value of v', the initial vibrational quantum number, and the failure of bands to agree with the Franck-Condon theory. Use is made of these ideas to explain the long life of active nitrogen.

WHILE there have been some very unusual cases of intensity distribution in the band spectra of diatomic molecules, they have been the exception rather than the rule and for that reason very little attention has been paid to them. The writer has made use of some of these cases to calculate the heats of dissociation of nitrogen[1] and of carbon monoxide[2] and until recently nothing more was done with them. Recent experiments on some very unusual band spectrum intensites in nitrogen-oxygen mixtures, combined with the increased interest in the purely repulsive potential energy levels of Heitler and London,[3] have led the writer to what is believed to be a satisfactory explanation of many of the unusual examples of band spectrum excitation which have arisen. The recent paper by Turner[4] on the effect of magnetic fields on the fluorescence radiation of iodine, suggested the direction in which an explanation was to be sought for the above-mentioned cases. In this note we will only mention these cases and make brief remarks about their explanations.

As a typical example we will consider the second positive group of nitrogen. These bands correspond to transitions from the C level to the B level. No bands of this system are known whose initial levels are higher than $v'=4$, in spite of the fact that the total energy of the "C" level is about 15 volts, corresponding to dissociation into a ^2D and a ^2P metastable atom.[5] The energy in the C_4 level is about 13.9 volts and this is exactly equal to the dissociation energy of nitrogen into two metastable ^2D atoms. Therefore, unless the products of dissociation are assumed to be two ^2D atoms rather than a ^2D and a ^2P atom, one cannot explain the non-appearance of the higher vibrational levels by saying the $v'=4$ is the highest vibrational quantum number that

[1] J. Kaplan, Proc. Nat. Acad. Sci. **15**, 226 (1929).
[2] J. Kaplan, Phys. Rev. **35**, 957 (1930).
[3] Heitler and London, Zeits. f. Physik **44**, 455 (1927).
[4] L. A. Turner, Zeits. f. Physik **65**, 464 (1930).
[5] Mulliken, Phys. Rev. **32**, 186 (1928).

can be associated with the C level. An alternative explanation presents itself if one assumes that all vibrational states above $v'=4$ are quenched by transitions from the C level to the Heitler and London level which corresponds to the coming together of two metastable ^2D atoms. The probability of transitions from the stable molecular level to a Heitler and London level is undoubtedly governed by the same rules as those which govern the usual molecular transitions e.g. by the Franck-Condon principle. Thus one can in general study the shape of the potential energy curve corresponding to a Heitler and London level, from the way it combines with known potential energy curves. The writer proposes to make a careful study of this in the future.

There are two possible explanations for the case which was just discussed, so that we propose now to discuss some more convincing examples of interaction between repulsive and attractive potential energy curves. The fourth positive bands of nitrogen are developed with but one initial vibrational state, corresponding to the transition D_0-B_v. The writer has used this fact as a means of calculating the heat of dissociation of nitrogen, making the postulate that the reason for the non-appearance of higher vibrational states was that the molecule spontaneously dissociated when an attempt was made to excite the higher vibrational states. At the time the calculation was made this was thought to indicate an extreme anharmonicity of the D level and consequently a very small heat of dissociation for this level. The value of $\omega_0 x$ necessary to yield the extremely small value of D^v that this explanation demanded was so large as to be without precedent among band spectra. The present explanation will be seen to be much more reasonable. A purely repulsive potential energy curve corresponding to the coming together of a ^2D and a ^2P atom would cross the potential energy curve of the D level at just about the energy corresponding to its first or second vibrational states. Even if the D level does possess some vibrational states, a strong intercombination with the Heitler and London level might either prevent the excitation of these higher vibrational states or if they were excited, it might quench them. Probably both of these effects must be considered, but once again it is seen that a Heitler and London level is useful in explaining an unusual spectroscopic phenomenon.

Similar considerations may be applied to the third positive group, the $3A$ bands and the $5B$ bands of carbon monoxide.[6] All three of these groups possess but one initial vibrational level and the writer has used the lowest one of these electronic levels, the b level, as a means of calculating the heat of dissociation of CO, making the same assumption as was made for the D level in nitrogen. The generally accepted value for the heat of dissociation of CO is around 10.3 volts and the energy values of the initial levels of the third positive and the $5B$ bands are 10.34 and 10.61 volts respectively. Thus it is gain highly probable that the repulsive energy level which corresponds to the coming together of a normal carbon atom and a normal oxygen atom, will so combine with these two electronic levels as to prevent the excitation of higher

[6] J. Kaplan, Phys. Rev. **36**, 784 (1930).

vibrational states. The repulsive interaction of a normal oxygen atom and a carbon atom in the $^1S_0$ state will yield an energy level in the vicinity of 11.5 volts, and this will account for the absence of vibrational states higher than $v'=0$ in the $3A$ bands of CO.

Returning to the consideration of the nitrogen molecule we call attention to several other cases of anomalous intensity distribution in band spectra, which seem to be examples of interaction between attractive and repulsive levels in the molecule. A system of nitrogen bands, discovered by Birge and Hopfield,[7] and having but a single initial vibrational state at 12.8 volts, shows a very unusual intensity distribution among the bands of the progression. Now 12.8 volts corresponds very closely to the energy of recombination of a normal nitrogen atom and a metastable atom in the ^2P level. Once again therefore we can blame the peculiar development of the bands on an interaction between an attractive and a repulsive energy state. In the same report, Birge and Hopfield call attention to many irregularities in the bands which make up the ultraviolet system $^1S-{}^1P$. Since the electronic energy of this system is 8.5 volts and most of the irregularities are connected with the progressions arising on $v'=4$, 5 and 6, the explanation is given that these irregularities arise from interactions between this level and the repulsive level which is formed when two normal nitrogen atoms come together. The heat of dissociation of nitrogen is about 9.1 volts[8] and the energy of the $v'=4$ level is 9.3 volts. By comparison with the previous examples it is certainly reasonable to assume that the above explanation is correct.

The experiments which first called the writer's attention to the possibilities of the ideas presented here, were designed to reproduce some of the peculiar intensity phenomena which arise in the first positive bands of nitrogen as produced in the aurora borealis. Without attempting a detailed discussion of the experiment, we can say that as far as the intensity distribution among the bands is concerned, especially when the relative intensities of the bands in a single v' progression are considered, the first positive bands are surprisingly sensitive to excitation conditions, more so in fact than any other band system with which the writer has had experience. Elsewhere[9] the present writer has called attention to the violent variation in intensities which arises when inert gases are mixed with active nitrogen. This variation in intensities, which is a variation of intensities in v' progressions, must be looked on as a variation in transition probabilities, because the relative intensities of bands within a v' progression are fixed by the relative transition probabilities, which can be determined by the Franck-Condon principle. In practically all discussions of band spectra it is assumed that the predictions of the above principle hold and in general they do apply. The anomalous cases presented here are those which arise either under unusual excitation conditions or in the case of energy levels which are very sensitive to excitation conditions and thus yield exceptional intensities even under normal dis-

[7] Birge and Hopfield, Astrophys. J. **68** 257 (1928).
[8] Birge, Trans. Faraday Soc. **25** 718 (1929).
[9] J. Kaplan, Phys. Rev. **36,** 778 (1930).

charge conditions. A few more remarks about the first positive bands will soon convince us that it is partly an example of the very sensitive energy state rather than that of unusual excitation conditions.

It is easy to see, from only a casual inspection of the spectrum, some of the unusual features of the first positive bands. One unusual feature is, that while most of the first positive bands possess four heads, the bands whose initial levels correspond to $v'=13$, 14, 15, 16 and sometimes $v'=17$, as well as those with $v'=19$, 20, 21, possess only strong single heads. In some discharges even $v'=3$, 4 and 5 showed this characteristic. Under some conditions there are remarkable variations in the relative intensities of the four heads and sometimes only one strong head appears where four appeared under normal conditions. Furthermore the intensities of the bands which possess these single-heads under normal conditions, are less than those originating on higher vibrational states, which is in itself an exceptional occurrence, and in agreement with the idea that the vibrational states corresponding to the single-headed bands are quenched by some mechanism in the molecule. In some of the experiments on the spectra of oxygen-nitrogen mixtures it was possible to produce the first positive bands with a sharp cut-off at $v'=12$. The vibrational states higher than $v'=12$ were almost completely missing thus giving here an excitation similar to some of the examples discussed above for NO, N_2 and CO.

A calculation of the energies corresponding to the range of vibrational states from which single-headed bands arise shows them to be in regions of the potential energy curve where one might quite reasonably postulate interaction with repulsive energy levels of the molecule. The vibrational levels associated with the initial electronic state of the first positive group lie between 9.35 and 13.9 volts. In this range there are four possible Heitler and London levels corresponding to the coming together of two normal atoms, or one normal and one ^2D metastable atom or one normal and one ^2P atom or two ^2D atoms. We therefore readily see why this group of bands should be so highly sensitive to changes in conditions of excitation. The energies of recombination corresponding to the above modes of interaction are 9.1, 11.47, 12.66 and 13.84 volts. The observation in some experiments of single headedness around $v'=3$ probably corresponds to the 9.1 volt level, the $v'=13$ to 17 correspond to both 11.47 and 12.66 since their energies lie just between these two values and finally the single headed bands around $v'=20$ or 21 can correspond to either 12.66 or 13.84.

The most interesting application of the idea of interaction between attractive and repulsive levels is to the problem of the afterglow of active nitrogen. Here the question has often been asked as to the reason why the afterglow persists for such a long time. What is the mechanism in the nitrogen molecule which regenerates metastable atoms, normal atoms and metastable molecules and keeps the afterglow visible for what is a very long time when one considers the degree of metastability of the energy states involved. If we postulate that many of the molecules in the initial states of the first positive bands interact with Heitler and London levels and dissociate

instead of radiating, then we have a direct mechanism for sustaining the afterglow. We literally allow the molecule to waste its time during the process of the decay of the afterglow. It may be that only a very small number of excited nitrogen molecules lose their energy by radiation, most of them simply redissociating due to interaction with one of the repulsive levels. Thus if the walls of the afterglow tube are such as to allow the persistence of atoms, and it is well known that the walls are of paramount importance here, then one can expect a very long duration for the glow. Until further investigation has been made, it is not possible to say which of the two factors governs the life of the glow. It will be an interesting problem to study the effect of this new factor on the life of the nitrogen afterglow.

One final example will be discussed because of the good numerical agreement with heats of dissociation to which it leads. It has been known for a long time to spectroscopists that the beta bands of nitric oxide possess a very exceptional intensity distribution.[10] These bands were first discovered in active nitrogen and the intensity distribution to which we refer is the one which is observed there. The writer has reported two experiments in which the beta bands were observed in the discharge but no careful study of intensity distribution has been made there. The two main anomalies in the intensity distribution in active nitrogen are the failure of the bands to fit the Franck-Condon theory and the absence of progressions higher than $v'=4$ even though $v'=5$ has been observed in absorption. The energy of the $v'=4$ level of the B band system is 6.15 volts and about three years ago the writer made some calculations of heats of dissociation of N_2 and O_2, using this as the heat of dissociation of NO. The success of this method in N_2 and CO was the reason for these calculations. The resulting value for O_2 was so low that it was not considered at the time. In view of the recent revisions of the heats of dissociation of N_2 and O_2, it is now possible to calculate a new value for NO,[11] using 9.1 volts for N_2 and 5.06 volts for O_2. The heat of dissociation of NO is found to be 6.15 volts so that the explanation is immediately apparent. We have here an example exactly like that of the second positive bands of nitrogen. The fact that in this case the phenomenon is observed in active nitrogen, where the interaction between attractive and repulsive levels is probably rather strong, makes the explanation more interesting. Here again we postulate an interaction between the excited states on which the beta bands arise and the Heitler and London level corresponding to the coming together of a normal oxygen and a normal nitrogen atom. The failure of the beta bands to obey the Franck-Condon rule for band intensities is added evidence that the proposed explanation is correct, since that also occurred in some other cases mentioned earlier in this paper.

We have seen that the interaction between a repulsive and an attractive level will account for the sudden curtailing of band systems and that many such examples are accompanied by a failure of the bands to obey the Franck-Condon rule. This latter phenomenon can be referred to as a variation of

[10] Barton, Jenkins and Mulliken, Phys. Rev. **30**, 175 (1927).

[11] Birge and Sponer, Phys. Rev. **28**, 259 (1926).

intensity within a progression, because a little consideration will show that the Franck-Condon rule predicts very definitely only the relative intensities within a single progression. Without going into much detail at this time it can be shown how the interactions which account for the curtailing of band systems will also account for a variation of intensities within a progression. The Franck-Condon theory is usually applied in a qualitative manner by drawing the two potential energy curves which are involved and noticing what lower states result when vertical lines are drawn through the two extreme values for the separation of the two atoms in the vibrating molecule. This procedure is correct provided the initial state radiates to, or in any other way goes to, only a single lower electronic state. The relative intensities of the bands which arise on a single initial vibrational state are then definitely fixed. If however the upper state finds itself in a position to interact with another lower state, the transition probabilities can be fixed now only by a consideration of both lower potential energy curves. It is obvious that one might readily expect large variations in the intensity distribution in progressions in this way. In the present paper we have shown how a third lower level, namely the Heitler and London level, may be brought in to the picture. From the nature of the observations it appears that this third level is sensitive to conditions and thus the intensity of interaction with normal levels will vary a great deal.

The present paper has been written mainly to bring out the one idea which is presented here. For that reason we have not published any spectra. This will be done in other publications which can be brought out with more leisure and in more detail, since this work is now being extended.

NOTE ON THE VISIBLE HALOGEN BANDS, WITH SPECIAL REFERENCE TO ICl

By Robert S. Mulliken
Ryerson Physical Laboratory, University of Chicago

(Received April 9, 1931)

Abstract

It is pointed out that the dissociation of excited ICl molecules, after absorption of light in the visible bands, into normal atoms is in harmony with theory. In analogy with the other halogens, these bands probably belong to a $^3\Pi \leftarrow {}^1\Sigma^+$ transition. The upper level of the bands is, however, doubtless not just the 0^+ part of the $^3\Pi_0$ as in the homonuclear halogen molecules, but is probably the whole $^3\Pi_0$, or else the $^3\Pi_1$. Detailed arguments against the possibility that the upper state of the halogen bands may be $^3\Sigma$ are given. Conclusions drawn in previous papers from the behavior of the I_2 bands in magnetic fields are revised.

IN TWO previous papers,[1,2] the writer has shown that the well-known visible absorption bands of the molecules Cl_2, Br_2, and I_2 probably correspond to the transition $0^+_u(^3\Pi) \leftarrow {}^1\Sigma^+_g$. The object of the present note is to supplement these papers by extending their application to such molecules as ICl, and by revising two or three doubtful or erroneous statements made in them.

Interpretation of ICl Bands

In molecules like ICl, relations between molecular and atomic electron states somewhat different from those in I_2 or Cl_2 are to be expected. This is obvious from the fact that we have four combinations $I(^2P_{1\frac{1}{2}})+Cl(^2P_{1\frac{1}{2}})$, $I(^2P_{1\frac{1}{2}})+Cl(^2P_{\frac{1}{2}})$, $I(^2P_{\frac{1}{2}})+Cl(^2P_{1\frac{1}{2}})$, and $I(^2P_{\frac{1}{2}})+Cl(^2P_{\frac{1}{2}})$, where with I_2 we have only three. Besides, it can hardly be taken for granted that the electronic states of the molecule ICl should show any close analogy to those of I_2 or Cl_2. Nevertheless, experience with other molecules shows that such an analogy may be expected (cf. analogies of SO to S_2 and O_2, CS and SiO to CO, AlO to BO, etc.).

A clearer understanding can be obtained by attempting to assign electron configurations. It has been assumed[2] that the normal and excited states of the visible absorption bands of chlorine are $\ldots 4d\sigma^2 3p\pi^4 4d\pi^4$, $^1\Sigma^+_g$ and $\ldots 4d\sigma^2 3p\pi^4 4d\pi^3 5f\sigma$, $^3\Pi_u$ (inverted) and that the corresponding states of I_2 are $\ldots 6d\sigma^2 5p\pi^4 6d\pi^4$, $^1\Sigma^+_g$ and $\ldots 6d\sigma^2 5p\pi^4 6d\pi^3 7f\sigma$, $^3\Pi_u$. It seems likely that the normal and excited states of the visible ICl bands have exactly the same configurations of outer electrons as I_2, the outer Cl electrons being promoted to equality with those of the I atom. Such a promotion appears necessary, since all the orbits which the outer electrons would occupy in Cl_2 are already filled in the I atom of ICl. This argument then supports the analogy already men-

[1] R. S. Mulliken, Phys. Rev. **36,** 699 (1930).
[2] R. S. Mulliken, Phys. Rev. **36,** 1440 (1930).

tioned. The $^3\Pi$ excited state of ICl, like those of the other halogens, should in view of its electron configuration be *inverted*. The triplet width should probably be about the same as in the $^3\Pi$ of Br_2, for which 2400 cm^{-1} seems a reasonable estimate.

It has been shown[1] that in I_2 the upper state of the visible bands is probably a 0^+_u state and that on theoretical grounds such a state cannot possibly be derived from $I(^2P_{1\frac{1}{2}})+I(^2P_{1\frac{1}{2}})$ or $^2P_{\frac{1}{2}}+^2P_{\frac{1}{2}}$, but that it can be derived from $^2P_{1\frac{1}{2}}+^2P_{\frac{1}{2}}$, as is observed. It was also shown to be likely that this 0^+_u belongs to a $^3\Pi$ state (mentioned in the preceding paragraph) of which the 0^-_u, 1_u, and 2_u components theoretically can and probably do dissociate into unexcited atoms. In the case of ICl, however, because of the absence of the property indicated by *g* or *u*, there is no theoretical reason why the 0^+ component of a $^3\Pi$ state analogous to that of I_2 should not dissociate, like the 0^-, 1, and 2 components, into normal atoms. In fact the theory makes this probable,—although it does not require it.

For according to the rules giving the relations between case *c* molecular and atomic states,[2] we may expect the following correlations : case *c* states 3, 0^+, 0^-, 2, 1, 2, 1, 1, 0^+, 0^- from $I(^2P_{1\frac{1}{2}})+Cl(^2P_{1\frac{1}{2}})$; 2, 1, 1, 0^+, 0^- from $I(^2P_{1\frac{1}{2}})+Cl(^2P_{\frac{1}{2}})$ and a similar set from $I(^2P_{\frac{1}{2}})+Cl(^2P_{1\frac{1}{2}})$; 1, 0^+, 0^- from $I(^2P_{\frac{1}{2}})+Cl(^2P_{\frac{1}{2}})$. These are the same sets of states that one gets from $2I(^2P_{1\frac{1}{2}})$; $I(^2P_{1\frac{1}{2}})+I(^2P_{\frac{1}{2}})$; and $2I(^2P_{\frac{1}{2}})$, respectively, except for the fact that no indices *g* or *u* are assigned here. It will be seen that all the case *c* states 2, 1, 0^+, and 0^- necessary to give a $^3\Pi$ state in case *a* can be obtained from two normal atoms I+Cl. Now there has been a good deal of discussion as to whether the upper state of the visible ICl bands gives two normal atoms on dissociation or whether it gives an excited chlorine atom.[3] The experimental evidence[3] strongly favors the latter alternative, which is here seen to be in harmony with theory. (It also negatives the possibility that an excited iodine atom is formed on dissociation.)

Assuming that the ordinary visible ICl bands give two normal atoms on dissociation, the question may still be raised as to whether their upper level is really the 0^+ component of a $^3\Pi_0$ as in I_2. First it should be noted that, if 0^+ is stable, it should be accompanied by 0^-, forming a complete $^3\Pi_0$, since if 0^+ dissociates into normal atoms, the corresponding 0^- almost certainly does too. Next comes the question whether this $^3\Pi_0$ should be a stable molecular state. If one examines Fig. 2 of Ref. 2, it will be seen that the fact that 0^+_u of I_2 is a reasonably stable molecular state (dissociation energy 0.55 volts) is due largely to the fact that it gives an excited atom on dissociation. Fig. 2 indicates that the 0^- and even the $^3\Pi_1$ and $^3\Pi_2$ components of the $^3\Pi_u$ should be much less stable in I_2 than the 0^+, or perhaps not be real molecular states at all. In view of these relations, one may question whether the $^3\Pi_0$ state of ICl should be stable, since it dissociates giving normal atoms. It therefore seems worth while,—although of course the quantitative relations may be considerably different than in Cl_2, Br_2, and I_2,—to consider the possibility that the upper level of the ICl bands may be $^3\Pi_1$ or even $^3\Pi_2$, and that the $^3\Pi_0$ state gives rise only to a continuum. [It is, however, also theoretically possible, although im-

probable, that both components of the $^3\Pi_0$ state might give excited atoms on dissociation, so that $^3\Pi_0$ would be a higher but stable state.] A possible indication that the upper level of the ICl bands is not $^3\Pi_0$ as in the other halogens is the fact that its energy (1.69 volts above the ground state)[3] is lower than that of any of the other halogens, while its dissociation energy (0.47 volts[3]) is nearly as large as that of I_2. If, however, it should turn out after all to be $^3\Pi_0$, then one should probably find at longer wave-lengths other bands leading to $^3\Pi_1$ and perhaps also to $^3\Pi_2$.

Additions and Corrections to Previous Papers

Possibility that the upper level of the halogen bands is $^3\Sigma$. A possible interpretation of the visible halogen bands which was not entirely disposed of in Refs. 1 and 2 was that they belong to a $^3\Sigma^+_u$ (case b), $^1\Sigma^+_g$ transition with $\Delta K = \pm 1$ in which only those combinations having $\Delta J = \Delta K = \pm 1$ are observed, the other possible combinations $\Delta J = 0$ being for some unknown reason very weak. This reason might possibly be found in the intersystem character of $^3\Sigma \leftarrow {}^1\Sigma$, for whose intensity relations we have no reliable guiding theory. [But as was mentioned in Ref. 1(p. 701), we know that in the $^1\Sigma \leftarrow {}^3\Sigma$ atmospheric oxygen bands, the transitions with $\Delta J = 0$ are as strong as those with $\Delta J = \pm 1$, and there seems no reason why the same should not be true here. Nevertheless since it is likely[4,5] that the atmospheric bands are $^1\Sigma^+_g \leftarrow {}^3\Sigma^-_g$, the argument may not hold, since this is a quadrupole transition.] A rather strong argument is that there is no theoretical necessity here for a $^3\Sigma^+_u$ state (which becomes 0^-_u plus 1_u in case *c*) to give $^2P_{1\frac{1}{2}} + {}^2P_{\frac{1}{2}}$ on dissociation, as the upper levels of the halogen bands are empirically known to do, whereas in the case of a 0^+_u state such a necessity does exist. [There is, to be sure, no theoretical proof that such a $^3\Sigma^+_u$ state could *not* give $^2P_{1\frac{1}{2}} + {}^2P_{\frac{1}{2}}$ here, although the theory strongly favors $^2P_{1\frac{1}{2}} + {}^2P_{1\frac{1}{2}}$ as dissociation products.[2]] A consideration of electron configurations also strongly favors a 0^+_u state (belonging to a $^3\Pi_0$) as against a $^3\Sigma^+_u$ state.[2]

Granting that the upper level of the halogen bands is 0^+_u, this might still conceivably be a 0^+_u which, together with a 1_u, would go over for small r into a case *b* $^3\Sigma^-_u$ state.[2] But a consideration of possible electron configurations makes this very improbable; at least two excited electrons would be required. Everything considered, it seems very probable that the identification of the upper state of the halogen bands as a 0^+_u belonging to a $^3\Pi_0$ is correct.

Magnetic behavior of iodine bands. In Ref. 1 the fact that a $^3\Pi_0$ molecular gas should be paramagnetic was taken as an explanation of the Faraday effect

[3] G. E. Gibson and H. C. Ramsperger, Phys. Rev. **30,** 598 (1927); E. D. Wilson, Phys. Rev. **32,** 611 (1928); G. E. Gibson and O. K. Rice, Nature, March 9, 1929; G. E. Gibson, Zeits. f. Physik **50,** 692 (1928); J. Patkowski and W. E. Curtis, Trans. Faraday Soc. **25,** 725 (1929); W. E. Curtis and O. Darbyshire, Trans. Faraday Soc. **27,** 77 (1931). G. K. Rollefson and F. F. Lindquist, J. Am. Chem. Soc. **52,** 2793 (1930); **53,** 1184 (1931).

[4] R. S. Mulliken, Phys. Rev. **32,** 880 (1928).

[5] R. S. Mulliken, Phys. Rev. 1931 (Abstract, Washington Meeting, Spring, 1931). Recent work of Childs and Mecke (Zeits. f. Physik **68,** 344, 1931) gives extremely low absorption coefficients in the atmospheric bands, and so favors $^1\Sigma^+_g$ rather than the possible alternative $^1\Sigma^-_u$ as the upper state of these bands.

observed in the iodine bands. Unfortunately, however, the fact was overlooked that the observed Faraday effect indicates that the normal state of iodine ($^1\Sigma^+_g$) is magnetically rather more sensitive than the upper (0^+_u) state.[6] The fact was also overlooked that, although a $^3\Pi_0$ molecular gas should be paramagnetic (less so, however, if the $^3\Pi_0$ is widely split into 0^+ and 0^-), this does not imply a first-order Zeeman effect. In fact, the 0^+ and 0^- states belonging to a $^3\Pi_0$ state should behave, if well-separated, very much like $^1\Sigma$ states in respect to the Zeeman or Faraday effect; but if the separation of the 0^+ and 0^- states should be small and if, as is the case for low K values in I_2, the separations of the rotational levels should be less than the spacing of the components of a normal Zeeman triplet, a magnetic field should produce a Paschen-Back effect in the $^3\Pi_0$ levels.[7]

But unless there is an error in Kemble's conclusion that the normal more than the excited state is responsible for the observed Faraday effect, we should probably return to Kemble's explanation[6] of this effect in the iodine bands, namely, that it is caused by the development of a small magnetic moment through the rotation of the molecule. Its existence would then really give no evidence either for or against the $^3\Pi_0$ nature of the upper electron level in the iodine bands. Nevertheless a renewed investigation of the matter would be of interest.

The quenching of the fluorescence of the iodine bands in a magnetic field, emphasized in Ref. 1, seems to indicate a special sensitiveness of the upper level to magnetic fields. The most promising suggestion as to the cause of the magnetic quenching of fluorescence seems to be Turner's idea[8] that it is due to a magnetically induced predissociation.

Indeed Van Vleck has now found, in a paper soon to be published, that a magnetic field may be expected to induce predissociation in the 0^+ state belonging to a $^3\Pi_0$ when the 0^+ and 0^- components dissociate as shown in Fig. 2 of Ref. 2. Thus the existence of magnetic quenching gives strong evidence in favor of the designation $0^+_u(^3\Pi_0)$.

[6] Cf. E. C. Kemble, Nat. Research Council Bulletin on Molecular Spectra, p. 347.

[7] The writer is indebted to Professor J. H. Van Vleck for the elucidation of these points. Cf. J. H. Van Vleck, Phys. Rev. **31,** 587 (1928).

[8] L. A. Turner, Zeits. f. Physik **65,** 477 (1930).

PICTORIAL REPRESENTATIONS OF THE ELECTRON CLOUD FOR HYDROGEN-LIKE ATOMS

By H. E. White
University of California, Berkeley

(Received April 21, 1931)

Abstract

It is well known that the solutions of the wave-equation for hydrogen-like atoms may be represented graphically by interpreting $\Psi\Psi^*$ as a *probability density*. The *probability density factors* $\Phi_m\Phi_m^* \cdot [\Theta_{m,l}]^2 \cdot [R_{n,l}]^2 = \Psi\Psi^*$ are represented graphically and briefly discussed and compared with the electron orbits of four classical models. Graphs for *s*, *p*, *d*, *f*, *g*, and *h* electrons are given. An attempt to combine the *probability density factors* and form some graphical representation of $\Psi\Psi^*$ has resulted in the construction of a mechanical device or model, see Fig. 5, which when photographed, gives very closely the desired result. Photographs for the magnetic states $m = 0, \pm 1, \pm 2, \pm 3, \cdots$ are given for $1s$, $2p$, $3d$, $4f$, $2s$, $3p$, $4d$, $5f$, $3s$, $4p$, and $5d$ electrons, see Fig. 6.

WITH all of the successes of the quantum mechanics one still hears on every hand, for want of an atomic model, the terms *electron orbits*, *penetrating orbits*, *non-penetrating orbits*, etc. This is of course due to the fact that in many cases one may think in terms of the simpler electron orbits and be led to a result which is the same or very nearly the same as that given by the quantum mechanics. In going over some of the correlations very often made between the two theories several interesting graphical comparisons have been forthcoming.

It is well known that for a non-relativistic, conservative dynamical system of one nucleus and one electron (that is a hydrogen-like atom) Schroedinger's wave-equation

$$\Delta^2\Psi + \frac{8\pi^2\mu}{h^2}(W - V)\Psi = 0 \tag{1}$$

expressed in polar coordinates ϕ, θ, and r, see Fig. 1 may be solved by replacing Ψ by the product of a function of ϕ alone, another of θ alone, and another of r alone,

$$\Psi = \Phi_m \cdot \Theta_{m,l} \cdot R_{n,l}. \tag{2}$$

With this substitution the equation is separated into three total differential equations the well-known solutions of which are,

$$\Phi_m = (2\pi)^{-1/2} e^{im\phi}, \quad m = 0, \pm 1, \pm 2, \pm 3, \cdots \pm l \tag{3}$$

$$\Theta_{m,l} = \left(\frac{(2l+1)(l-m)!}{2(l+m)!}\right)^{1/2} \sin^m\theta \cdot P_l^m(\cos\theta), \quad l = 0, 1, 2, 3, \cdots (n-1) \tag{4}$$

$$R_{n,l} = \left[\frac{4(n-l-1)!Z^3}{[(n+l)!]^3 n^4 a_1^3}\right]^{1/2} \left(\frac{2Zr}{na_1}\right)^l e^{-zr/na} L_{n+l}^{2l+1}\left(\frac{2Zr}{na_1}\right), \quad n = 1, 2, 3, \cdots \tag{5}$$

involving in addition to the *normalizing factors*, the complex exponentials $e^{im\phi}$, the "*associated Legendre polynomials*," and derivatives of the "*Laguerre polynomials*," where m, l, and n, are to be associated with the *magnetic*, *azimuthal*, and *total quantum numbers* respectively. It is also well known that $\Psi\Psi^* dv$, which is interpreted as the *probability* of the electrons being found in a given element of volume dv is very small outside the region occupied by the corresponding classical electron orbits.

For descriptive purposes it has been convenient to think of the *probability density* $\Psi\Psi^* = P$ in terms of the angles ϕ and θ and of the distance r independently. From Eqs. (2), (3), (4), and (5) the *probability density*

$$\Psi\Psi^* = \Phi_m\Phi_m^* \cdot [\Theta_{m,l}]^2 \cdot [R_{n,l}]^2. \tag{6}$$

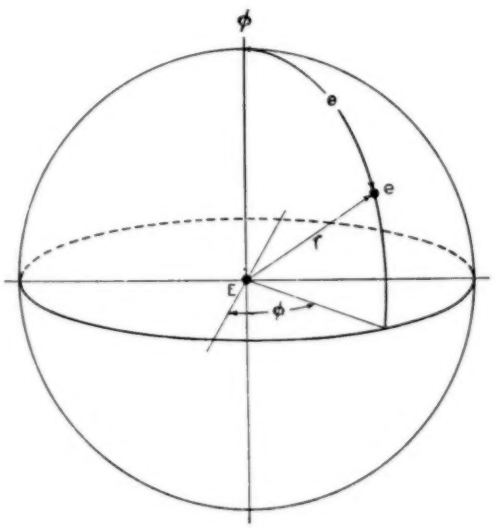

Fig. 1.

There are in general four classical models to be compared with these *probability density factors*. These four well-known models, which will here be called (a), (b), (c), and (d), have the same *total quantum number* n, and *azimuthal quantum numbers* as follows; (a) l (b) $[l(l+1)]^{1/2}$ (c) $l+\frac{1}{2}$, (d) $l+1=k$. It should be pointed out that none of these classical orbital models is correct and that, for want of an atomic model, any one of them may, with certain limitations, be used. In general (a) and (b) serve as vector models while (c) and (d) serve well as orbital models.

The $\Phi_m\Phi_m^*$ factor. For given m, Φ_m times its complex conjugate Φ_m^* is a constant, so that for any given state the probability of an electrons being found in any small element of angle $d\phi_1$ is the same as for any other equal angle $d\phi_2$. For all allowed electron states the *probability density* is therefore symmetrical about the ϕ (magnetic) axis. $\Phi_m\Phi_m^*$ plotted as a function of the angle ϕ (0 to 2π) would graphically be represented in rectangular coordinates by a straight line or in angular coordinates by a circle.

The $[\Theta_{m,l}]^2$ factor. For given m and l values the polynomials of Eq. 4 and consequently $[\Theta_{m,l}]^2$ are readily calculated from well known recursion formulas.[1]

Values of the *probability density factor* $[\Theta_{m,l}]^2$ are given in Table I and plotted in rectangular coordinates in Fig. 2.

Unsold[2] has shown that for given n and l, the *probability density* summed over the states $m=+l$ to $m=-l$ presents spherical symmetry about the nucleus. Since $\Phi_m\Phi_m^*$ is constant for any state one has simply to show that

$$\sum_{m=-l}^{m=+l} [\Theta_{m,l}]^2 = \text{constant}. \tag{7}$$

This well-known theorem is seen to be true from the last column of Table I or graphically from the curves of Fig. 2. For example, the sum of the three

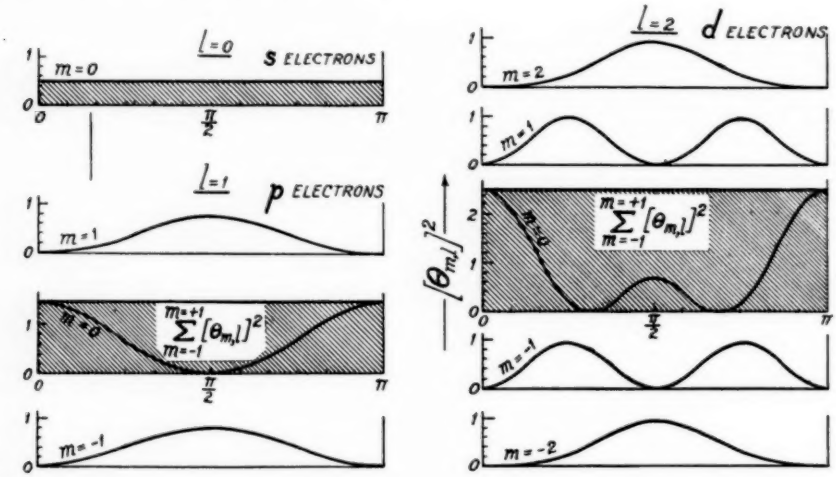

Fig. 2. The probability density factor $(\Theta_{m,l})^2$ as a function of θ for s, p, and d electrons. The straight lines and the shaded areas represent spherical symmetry, the result of the summation of the curves from $m=+l$ to $m=-l$.

curves for the three p states $m=1, 0, -1$ gives a straight line as indicated by The shaded area. Thus it is that in some of the complex spectra three similar p electrons five similar d electrons, or seven similar f electrons form spherical symmetry, that is an S term, as the most stable state.

If angular coordinates are used when plotting $[\Theta_{m,l}]^2$ a number of interesting correlations with the classical orbits may be made. Such curves are shown in Fig. 3 for s, p, d, f, g, and h electrons. Beneath each figure the corresponding classical orbit is given oriented in each case according to the vector model (a). In order to illustrate an orbit rather than its straight line projection the ϕ axis is tipped slightly out of the plane of the paper. It must be remembered that the electron is not confined to the shaded area in each

[1] See "Quantum Mechanics," by Condon and Morse, p. 63.

[2] Unsold, Ann. d. Physik **82,** 379 (1927).

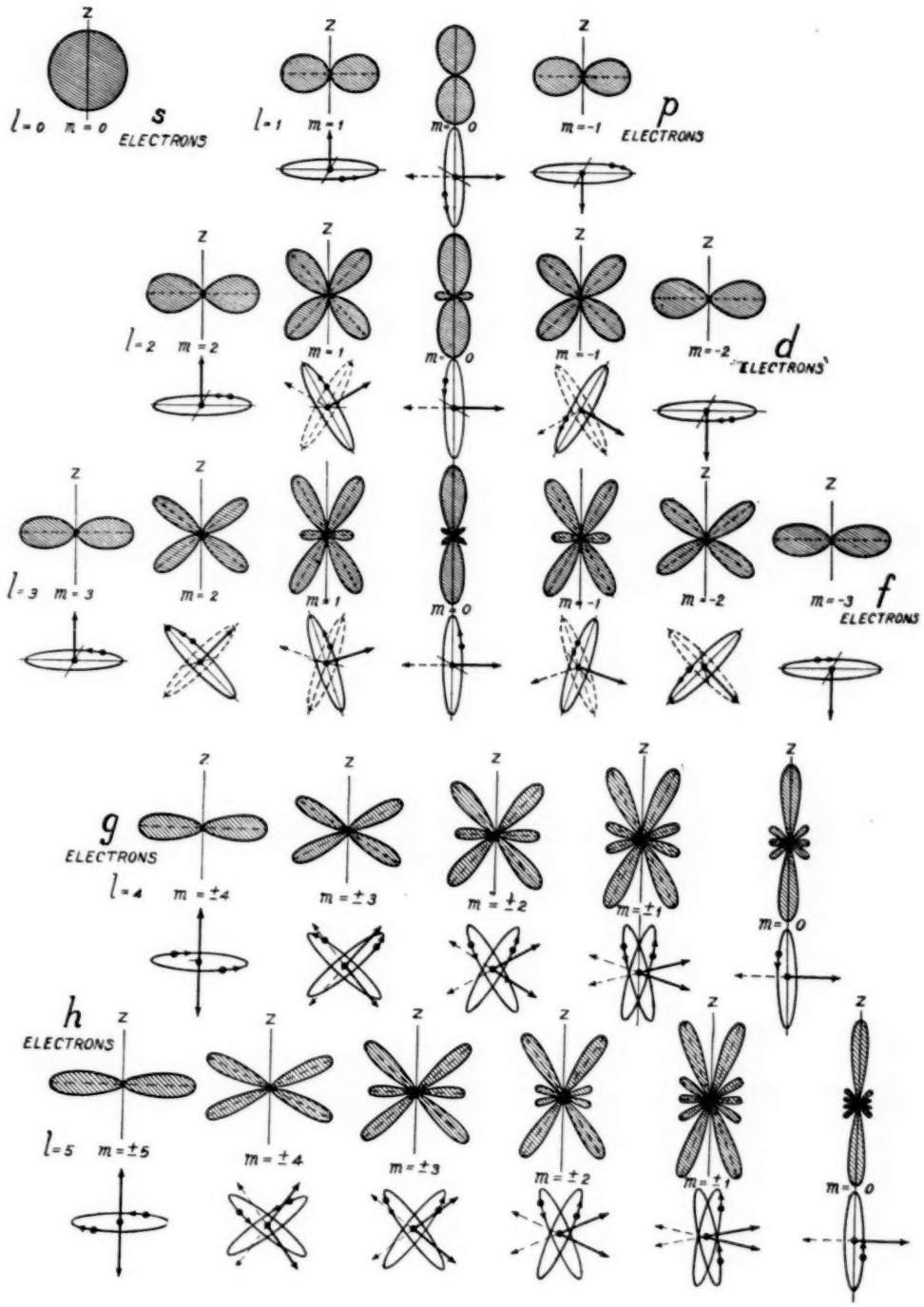

Fig. 3. The probability density factor $(\Theta_{m,l})^2$ plotted in angular coordinates for s, p, d, f, g, and h electrons. For states $m=0$ the scale is approximately $1/l+1$ times that of the other states of the same l value. The classical oriented orbit for each quantum state is given below each figure, tilted slightly out of the normal plane to show an orbit rather than a straight line.

TABLE I. *The probability density factor* $[\Theta_{m,l}]^2$.

Electron	l	m	$[\Theta_{m,l}]^2$	$\sum_{m=-l}^{m=+l} [\Theta_{m,l}]^2$
s	0	0	$1/2$	$1/2$
p	1	± 1	$3/4 \sin^2\theta$	$3/2$
		0	$3/2 \cos^2\theta$	
d	2	± 2	$15/16 \sin^4\theta$	$5/2$
		± 1	$15/4 \sin^2\theta \cos^2\theta$	
		0	$10/16 (3\cos^2\theta - 1)^2$	
f	3	± 3	$35/32 \sin^6\theta$	$7/2$
		± 2	$105/16 \sin^4\theta \cos^2\theta$	
		± 1	$21/32 \sin^2\theta(5\cos^2\theta - 1)^2$	
		0	$7/8 (5\cos^3\theta - 3\cos\theta)^2$	

probability figure but that the magnitude of a line joining the center and any point on the curve is a measure of the electrons probability of being found in the direction of that line.

Since the plane in which each curve is drawn represents any plane through the ϕ axis symmetry of $\Phi_m\Phi_m^*$ is obtained by rotating each curve about the ϕ (or *magnetic*) axis. Corresponding to this axial symmetry there is the classical precession of each orbit around the ϕ axis producing a somewhat similar figure. For each $m=0$ curve the scale used is about $1/l+1$ times that of the other curves of the same l value.

For all $m=0$ states, excluding the spherically symmetrical s states, the *probability density* is greatest in the direction of the poles. With the exponent of $e^{im\phi}$ zero this distribution has been interpreted to mean[3] that there is no motion in the ϕ coordinate and that correlated with this the motion of the electron (i.e. the orbital plane) is in some one meridian plane, all meridian planes being of equal probability. The end states $m=\pm l$ on the other hand take on their largest values in the direction of the equatorial plane. In this case one correlates the opposite signs in the exponents of $e^{\pm im\phi}$ with the opposite directions of rotation in the orbit. The way in which each classically oriented orbit follows the corresponding curves, from $m=+l$ to $m=-l$, especially for the states of higher l value, is quite remarkable. It should be mentioned that if the classical orbits are oriented according to models (b), (c), or (d) that their general agreement with the probability curves is not as good as with model (a), however, this may be a matter of personal opinion.

The $[R_{n,l}]^2$ factor. The factor $[R_{n,l}]^2$ which gives the *probability density* as a function of r alone has been discussed in detail by many investigators. For given values of n and l the Laguerre polynomials and hence $R_{n,l}$ (see Eq. (5)) and $[R_{n,l}]^2$ may be evaluated.[1] Plotting $[R_{n,l}]^2$ against r in units of the radius of the first Bohr circular orbit $a^1=0.528$ AU. give the heavy line curves of Fig. 4. Multiplying $[R_{n,l}]^2$ by $4\pi r^2$, the area of a sphere of radius r, one obtains the so called *probability density distribution* curves, D, indicated by the shaded areas in the figure. The classical orbits corresponding to each of these

[3] See, Condon and Morse, "Quantum Mechanics."

curves, using model (c), are also shown. In each curve the *density distribution* differs greatly from zero only within the electron-nuclear distance of the corresponding classical orbits.

A more satisfactory correlation has been made by Pauling[4] by comparing the average value of r as calculated on both theories. The method of evaluating r from the quantum mechanics has been given by Waller[5] and is identical with the value obtained for the classical orbits if the *azimuthal quantum number* is taken to be $[l(l+1)]^{1/2}$, model (b). This average value of r is indicated in

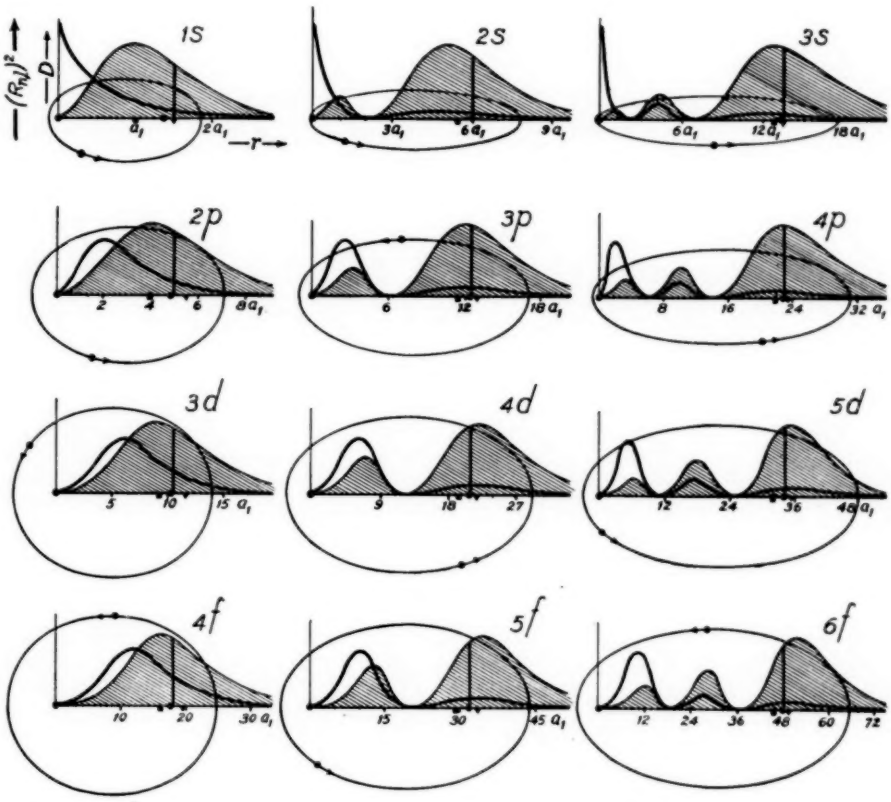

Fig. 4. The probability density factor $(R_{n,l})^2$ plotted as a function of the electron-nucleus distance r (r is measured in units of the first Bohr circular orbit). The density distribution curves $D=4\pi r^2\cdot(R_{n,l})^2$ the shaded areas, are to be compared with the electron-nucleus distance for the classical orbits, where the azimuthal quantum number is taken to be $l+\frac{1}{2}$.

each curve by a vertical line. The average value of r calculated for models (a), (c), and (d) are indicated on the r axis by triangular, circular, and square dots respectively.

For this radial comparison model (b) is to be preferred, however, a difficulty arises for the s states where the orbits reduce to straight lines with one

[4] Pauling, Proc. Roy. Soc. **114,** 181 (1927).
[5] Waller, Zeits. f. Physik **38,** 635 (1926).

end at the nucleus center. With model (c), the orbits shown in the figure, this difficulty does not arise and the agreement is practically the same.

The Probability Density $\Psi\Psi^*$

Attempts to bring together the *probability density factors* $\Phi_m\Phi_m^*$, $[\Theta_{m,l}]^2$, and $[R_{n,l}]^2$ into one single picture for $\Psi\Psi^*$, if we may call it a picture, have been somewhat successful. Langer and Walker[6] using a method which is as yet unpublished, have produced *probability density* photographs which represent the spherically symmetrical s states and the $2p$ states $m=+1$ and 0.

Preliminary attempts to produce a three dimensional model which will represent as closely as possible the *probability density* $\Psi\Psi^*$ has resulted in a mechanical device shown in Fig. 5. Spindles like the one shown in the center

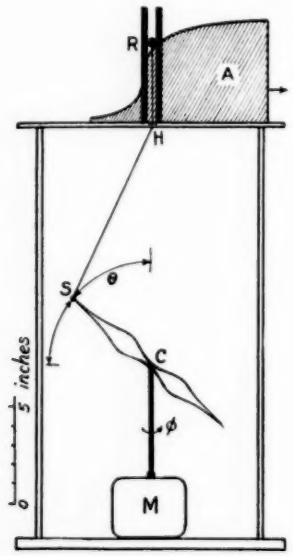

Fig. 5. A mechanical device which when set in motion and photographed represents the electron cloud for the various states of the hydrogen-like atoms. The model shown in the figure is for a $3d$ electron.

of the figure and in the last photograph of Fig. 6 are turned out on a lathe so that in projection they give the *density distribution* D curves of Fig. 4. Such a spindle is pivoted at its center by a small pin at C, and set in rotation about the vertical axis by means of a motor M. This motion gives the required symmetry about ϕ. At the same time that rotation about the ϕ axis is taking place, the angle θ is changed slowly from $\theta=0$ to $\theta=\pi/2$ by means of a swivel S and a double cord $SIIR$ which passes through a hole in the table top to a roller R, the motion of which is confined to the slot as shown. Curves of thin wood, e.g. A in Fig. 5, are cut so that when they are moved slowly but with uniform speed along the table top in the direction indicated by the arrow the angular

[6] See, "Atoms Molecules and Quanta," by Ruark and Urey, p. 565. Also Slater, Phys. Rev. **37**, 482 (1931).

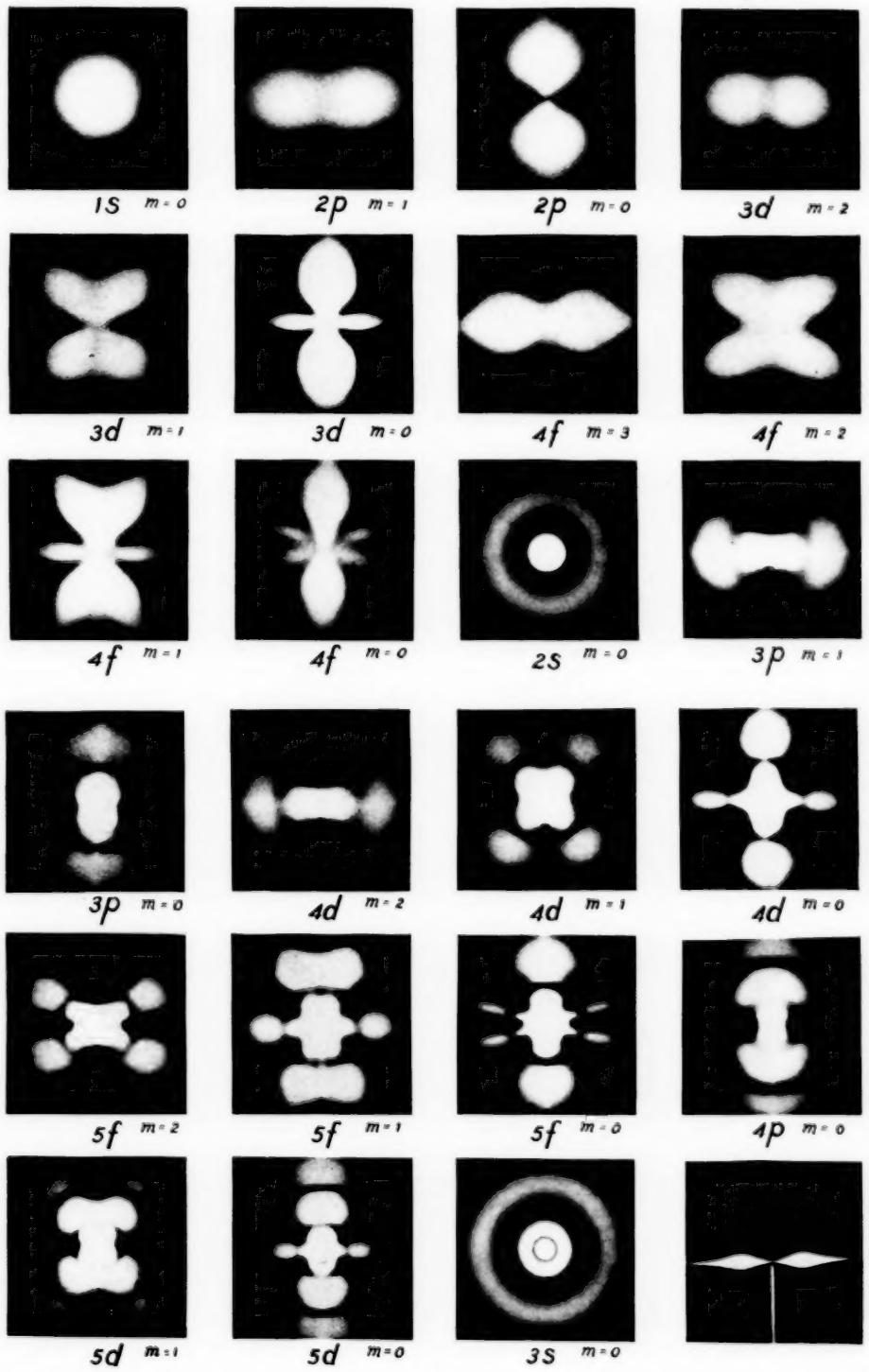

Fig. 6. Photographs of the electron cloud for various states of the hydrogen-like atoms as obtained from various models and the device shown in Fig. 5. The proability density $\Psi\Psi^*$ is symmetrical about the ϕ or magnetic axis which is vertical. The scale for each figure may be obtained from Fig. 4.

velocity $d\theta/dt$ is changed in the proper manner to give, as nearly as possible, the correct density when photographed. A time exposure started when $\theta=0$ and stopped when $\theta=\pi/2$ for the model shown yields the figure for the $3d$ state $m=0$. In constructing the various curves to be used at A, the changing angle of the cord IIR was taken into account and also the fact that as θ increases each point on the spindle moves in larger and larger circles and therefore faster. A small slot milled in the lower half of each spindle allows the angle $\theta=0$ to be reached. In projection each spindle should represent the *density distribution* curves, D of Fig. 5, in order that when rotating simultaneously about the ϕ and θ axes they give at each point in space the *density* $[R_{n,l}]^2$ curves of Fig. 5. It should be pointed out that there is a small amount of distortion due to the end on view of the spindle. This distortion is quite negligible, however, in that in this position the rapid motion as seen from the camera effects the photographic plates but little. Photographs for the states with negative m values are identical with those of positive m values. It may be seen by an examination of the figures that the addition of the $2p$ states $m=1, 0, -1$ or the sum of the $3d$ states $m=2, 1, 0, -1, -2$ will give spherical symmetry a figure like that of a $1s$ electron. Again the summation of the $4d$ states $m=2, 1, 0, -1, -2$ will give spherical symmetry resembling the $2s$ state. This may be considered as somewhat of a check on the figures in general and is quite as good as can be expected both from the standpoint of photographic reproduction of densities and the mechanical difficulties in the model.

The s states in Fig. 6 were made in a much simpler manner than the others and represent cross-sections only. Curves cut from white paper glued to the face of a blackened disk, and set rotating give the figures shown. Cross-section photographs have also been made for the nodal states by changing θ alone, ϕ remaining fixed. While these photographs are in general better, the more complete three dimensional reproductions are given in Fig. 6. The author wishes to take this opportunity to thank Professor Oppenheimer for his criticism of this paper.

NOTE ON THE CALCULATION OF VAN DER WAALS FORCES[1]

By Henry Margenau
Sloane Physics Laboratory, Yale University

(Received April 28, 1931)

Abstract

The general expression for the van der Waals energy arising from dipole interaction between atoms involves a summation over transition probabilities. These are in most cases difficult to calculate. It is here pointed out that since these transition probabilities obey the sum rule of Thomas and Kuhn, they may be evaluated in a manner which permits van der Waals' forces to be calculated with good approximation, provided that the polarizability is known. The method is outlined and illustrated by application to two examples: Na and He. The result in the case of He is in very good agreement with that obtained by the variational method.

THE methods proposed so far for a calculation of intermolecular forces depend on an (exact or approximate) knowledge either of the molecular wave functions[2] or of the oscillator strengths (dispersion f-values) associated with transitions from the ground state of the molecules in question.[3] Occasionally, useful approximations were obtained in terms of polarizabilities and other known characteristics. In this note we wish to suggest a method, semi-empirical in character and not involving the use of wave functions, which in general, enables a calculation of van der Waals forces between atoms with greater accuracy than others of equal simplicity permit. It consists in expressing the perturbational energy of the second order as a sum over f-values, as was first done by London, and then determining these f-values by means of the sum rule of Thomas and Kuhn, and the relative intensities of spectral lines.

Suppose that the two interacting atoms, A_1 and A_2, are similar and a distance R apart, R being so large that electron interchange does not take place. Let both A_1 and A_2 be in their lowest energy state which we take to be spherically symmetrical (s-state). α and β denumerate the various excited states of A_1 and A_2 respectively. If we restrict our consideration to the effects of the classical dipole interaction

$$V = \frac{e^2}{R^3}(y_1y_2 + z_1z_2 - 2x_1x_2) \tag{1}$$

[1] Part of the considerations here presented have been reported at the meeting of the Amer. Phys. Soc., Feb. 26–28. Hitherto we did not feel that they were of sufficient interest to be published more fully. Recently, however, Slater and Kirkwood (see ref. 2) have calculated a value for the attractive forces between He atoms differing widely from London's result. They attribute this discrepancy to the neglect of double electron jumps in London's theory. Aside from being applicable to many cases not of immediate interest at present, the method here outlined shows the correctness of the latter supposition.

[2] Eisenschitz and London, Zeits. f. Physik **60**, 491 (1930); Slater and Kirkwood, Phys. Rev. **37**, 682 (1931); Hassé, Proc. Camb. Phil. Soc. **27**, 66 (1931).

[3] F. London, Zeits. f. phys. Chemie, B, **11**, 222 (1930).

which is proper for large separations only, the second order perturbation energy of A_1+A_2 becomes

$$\Delta_2 E = -\sum_{\alpha\beta}{}' \frac{|V_{11,\alpha\beta}|^2}{E_\alpha + E_\beta - 2E_1}, \tag{2}$$

where

$$|V_{11,\alpha\beta}|^2 = \frac{e^4}{R^6}(y_{1\alpha}{}^2 y_{1\beta}{}^2 + z_{1\alpha}{}^2 z_{1\beta}{}^2 + 4x_{1\alpha}{}^2 x_{1\beta}{}^2 + 2y_{1\alpha}z_{1\alpha}y_{1\beta}z_{1\beta} - 4x_{1\alpha}y_{1\alpha}x_{1\beta}y_{1\beta} - 4x_{1\alpha}z_{1\alpha}x_{1\beta}z_{1\beta}) \tag{3}$$

$q_{1\alpha}$ is the coordinate matrix associated with a transition of A from the lowest state (1) to the state α, e.g. $x_{1\alpha}=\int R_{10}(r)xR_{nl}(r)P_l{}^m e^{im\phi}r^2\sin\theta dr d\theta d\phi$; n, l, and m being the quantum numbers with their usual significance. (We are writing R_{10} for the radial function of the lowest state without meaning to imply that $n=1$ for this state.) It follows directly that

$$\sum_m x_{1\alpha}y_{1\alpha} = \sum_m x_{1\alpha}z_{1\alpha} = \sum_m y_{1\alpha}z_{1\alpha} = 0,$$

and that

$$\sum_m x_{1\alpha}{}^2 = \sum_m y_{1\alpha}{}^2 = \sum_m z_{1\alpha}{}^2 = \tfrac{1}{3}\delta_1{}^l r_{1\alpha}{}^2.$$

Hence in summing (3) over the magnetic quantum numbers of both A_1 and A_2 we obtain $\frac{2}{3}\delta_1{}^{l_\alpha}\delta_1{}^{l_\beta}e^4/R^6\, r_{1\alpha}{}^2 r_{1\beta}{}^2$ so that (2) becomes

$$\Delta_2 E = -\frac{2}{3}\frac{e^4}{R^6}\sum_{\alpha\beta}{}' \frac{r_{1\alpha}{}^2 r_{1\beta}{}^2}{E_\alpha + E_\beta - 2E_1}, \tag{4}$$

where now the summation is no longer over magnetic quantum numbers and includes only states connected with the ground state by dipole radiation ($l_\alpha = l_\beta = 1$). But $r_{1\alpha}$ is related to the f-values appearing in the dispersion formula

$$n^2 - 1 = \frac{e^2 N}{\pi m}\sum_\alpha \frac{f_{1\alpha}}{\nu_\alpha{}^2 - \nu^2}$$

by the relation

$$r_{1\alpha}{}^2 = \frac{3}{2m}\left(\frac{h}{2\pi}\right)^2 \frac{f_{1\alpha}}{E_\alpha - E_1}. \tag{5}$$

Substituting this in (4) there results a formula meanwhile already obtained by London and used by him to compute intermolecular forces by means of a knowledge of a limited number of empirical f-values. We wish to propose a scheme permitting the f-values to be determined independently of spectroscopic dispersion formulae, which necessarily emphasize unduly the f's in the vicinity of the spectral region for which the formulae were calculated.

Combining (5) and (4) and realizing that $\Sigma_{\alpha\beta}{}'$ includes an integration over the continuous region of the spectrum we may write

$$\Delta_2 E = -F\Big\{ \sum_{\alpha\beta}{}' \frac{f_{1\alpha}f_{1\beta}}{v_\alpha v_\beta(v_\alpha + v_\beta)} + 2\sum_{\alpha}{}' \int_0^\infty \frac{f_{1\alpha}(df_{1E}/dE)dE}{v_\alpha(1+E)(v_\alpha+1+E)} + \int_0^\infty\int_0^\infty \frac{(df_{1E'}/dE')(df_{1E''}/dE'')dE'dE''}{(1+E')(1+E'')(2+E'+E'')}\Big\}. \tag{6}$$

We are here using the abbreviations:

$$\epsilon_\alpha = -E_\alpha;\ v_\alpha = 1 - \frac{\epsilon_\alpha}{\epsilon_1};\ F = \frac{1}{R^6}\,\frac{3}{2m^2\epsilon_1{}^3}\left(\frac{he}{2\pi}\right)^4$$

E is the energy of any state beyond the series limit, measured in units equal to the energy of the series limit, ϵ_1. (6) does not take explicit account of possible multiple electron transitions to discrete states beyond the series limit, the energy of which is frequently not known. They may be considered included in the integration, however, since the f-values will be adjusted in such a manner that their sum obeys the theorem of Kuhn and Reiche,[4] which postulates:

$$\sum_{\alpha}{}' f_{1\alpha} + \int_0^\infty \frac{df_{1E}}{dE}\,dE = Z_0 \tag{7}$$

Z_0 being the number of dispersion electrons.

It becomes necessary to make some assumption about the distribution of the f_{1E}'s. Fortunately, the calculation of $\Delta_2 E$ is not very sensitive to this choice, provided that (7) is satisfied. We shall suppose, in conformity with what is known about H and x-ray spectra, that

$$\frac{df_{1E}}{dE} = \frac{\gamma}{(1+E)^3}, \tag{8}$$

γ being at present undetermined. Moreover, we shall consider that the relative intensities of the first few emission lines of the principal series are known. The accuracy of the calculation is not seriously impaired if this is not the case. Suppose these relative intensities to be J_α. Then one may easily verify that

$$f_{1\alpha} = \frac{\beta J_\alpha}{v_\alpha{}^3} \equiv \beta\phi_\alpha, \tag{9}$$

since $J_\alpha = \text{const.}\ (E_\alpha - E_1)^4 r_{1\alpha}{}^2$. β is another undetermined constant. To determine β and γ we have first (7), which may be written on account of (8) and (9):

$$\beta\sum_{\alpha}{}'\phi_\alpha + \frac{\gamma}{2} = Z_0 \tag{10}$$

and second the expression for the polarizability in a static field:

[4] For complex structures, this sum rule is merely an approximation.

$$\alpha = \frac{1}{m}\left(\frac{eh}{2\pi}\right)^2 \sum_\alpha{}' \frac{f_{1\alpha}}{(E_\alpha - E_1)^2},$$

or, explicitly,

$$\alpha = \frac{1}{m\epsilon_1{}^2}\left(\frac{eh}{2\pi}\right)^2 \left\{ \sum_\alpha{}' \frac{f_{1\alpha}}{v_\alpha{}^2} + \int_0^\infty \frac{(df_{1E}/dE)dE}{(1+E)^2} \right\} \tag{11a}$$

whence

$$\beta \sum_\alpha{}' \frac{\phi_\alpha}{v_\alpha^2} + \frac{\gamma}{4} = m\epsilon_1{}^2\left(\frac{2\pi}{eh}\right)^2 \alpha. \tag{11}$$

(10) and (11) supply the required numerical values of β and γ. If line intensities are not known, we may put the first $\phi = 1$ and all others equal to 0. The evaluation of (6) is now an easy matter.

In cases where $Z_0 = 1$ (no multiple jumps) the contribution of the region beyond the series limit is usually small. It may then be advisable to write (6)

$$\Delta_1 E = -\frac{F}{2}\left\{ \sum_{\alpha\beta}{}'(1 + P_{\alpha\beta}) f_{1\alpha} f_{1\beta} + 2 \sum_\alpha{}' \int_0^\infty (1 + P_{\alpha E}) f_{1\alpha} \frac{df_{1E}}{dE}\, dE \right.$$
$$\left. + \int_0^\infty \int_0^\infty (1 + P_{E'E''}) \frac{df_{1E'}}{dE'} \frac{df_{1E''}}{dE''}\, dE' dE'' \right\},$$

with the abbreviations

$$P_{\lambda\mu} = \frac{1 - v_\lambda v_\mu (v_\lambda + v_\mu)/2)}{v_\lambda v_\mu (v_\lambda + v_\mu)/2)},$$

v_E being $1+E$.
Using (7), this goes over into

$$\Delta_2 E = -\frac{F}{2}\left\{ Z_0{}^2 + \sum_{\alpha\beta}{}' P_{\alpha\beta} f_{1\alpha} f_{1\beta} + 2 \sum_\alpha{}' P_{\alpha E} f_{1\alpha} \frac{df_{1E}}{dE}\, dE \right.$$
$$\left. + \int_0^\infty \int_0^\infty P_{E'E''} \frac{df_{1E'}}{dE'} \frac{df_{1E''}}{dE''}\, dE' dE'' \right\}. \tag{12}$$

Recalling the definition of the v's we see that in some cases where the energy of all excited states is small compared with that of the lowest state they do not differ greatly from 1, which makes the P's small. Then one may expect to attain a fair approximation to the polarization forces by retaining in the $\{\}$ of (12) only the term $Z_0{}^2$. For hydrogen, the last 3 terms contribute about 8 percent of the total. If we make use of (8), (9), (10), and (11) expression (12) becomes:

$$\Delta_2 E = -\frac{F}{2}\left\{ Z_0{}^2 + \beta^2 \sum_{\alpha\beta}{}' P_{\alpha\beta}\phi_\alpha\phi_\beta + \beta\gamma \sum_\alpha{}' R_\alpha \phi_\alpha - 10.170\gamma^2 \right\}, \tag{13}$$

where

$$R_\alpha = \frac{4}{v_\alpha^2}\left[\frac{1}{3} - \frac{1}{2v_\alpha} + \frac{1}{v_\alpha^2} - \frac{1}{v_\alpha^3}\log(1+v_\alpha)\right] - 1.$$

For hydrogen, this expression gives $\Delta_2 E$ to within 1 percent if only 4ϕ's are used.

As an illustration, let us compute the polarization energy of two Na-atoms by the method here outlined. α can here be calculated since the f-values happen to be known.[5] They will also afford a check on our β and γ. α turns out to be 24.2×10^{-24}. (We omit the details of the calculation, which is made with the aid of Eq. (11.) We shall use only ϕ_2, corresponding to the resonance transition, and put it equal to 1. v_2 is then 0.409; $\epsilon_1 = 8.145\times10^{-12}$ ergs. Eqs. (10) and (11) give

$$\beta + \frac{\gamma}{2} = 1; \quad \frac{\beta}{0.409^2} + \frac{\gamma}{4} = 5.88,$$

so that $\beta = 0.888$ and $\gamma = 0.224$. From (13) one then obtains

$$\Delta_2 E = \frac{12.5}{R^6} \times 10^{-58} \text{ ergs} = \frac{790}{r^6} \text{ volts},$$

if r is measured in $\mathring{A}$. The correct value, which may be calculated from Sugiura's work, is

$$\Delta_2 E = \frac{14.5}{R^6} \times 10^{-58} \text{ ergs}.$$

It may be approximated as closely as desired, of course, by taking a greater number of ϕ's into account. We note in passing that these results suggest the existence of very strong polarization forces and the formation of polarization molecules, such as were observed in K_2 by Kuhn.[6]

Another more interesting application is to He, where our calculations can be no longer controlled by a sufficiently accurate knowledge of the f-values. There exist intensity measurements on the emission lines of the "principal" series[7] from which the ϕ_α's may be obtained by (9). We have considered 10 of them, but it turns out that very few of them would have been sufficient, because the main contribution to the f's seems to come from the region beyond the series limit. Taking α as 0.206×10^{-24}, Eqs. (10) and (11) become

$$\beta \sum_\alpha{}' \phi_\alpha + \tfrac{1}{2}\gamma = 2$$

$$\beta \sum_\alpha{}' \frac{\phi_\alpha}{v_\alpha^2} + \frac{1}{4}\gamma = 1.122.$$

If now we use the relative intensity data in Hopfield's arbitrary units $\Sigma_\alpha{}'\phi_\alpha =$

[5] Y. Sugiura, Phil. Mag. **4**, 495 (1927).

[6] Kuhn, Naturwissenschaften **18**, 332 (1930). See also Oldenberg, Zeits. f. Physik **47**, 184 (1928) and **55**, 1 (1929).

[7] Hopfield, Astrophys. J. **72**, 133 (1930).

293.7, and $\Sigma_\alpha' \phi_\alpha / v_\alpha^2 = 351.1$, whence $\beta = 5.97 \times 10^{-4}$ and $\gamma = 3.64$. The surprising magnitude of γ shows clearly, and probably over-emphasizes, the important rôle of the transitions to states beyond the ionization limit of one electron. That these states need not belong to the continuous spectrum, and that our integration (instead of summation) is dictated by convenience and lack of data to handle them more properly has already been pointed out. Substituting β and γ in (6), or more conveniently in (13) (where now, of course, on account of the size of γ only the second term in $\{\}$ may be neglected) we find

$$\Delta_2 E = \frac{9.68}{R^6} \times 10^{-61}(1.49)\ \text{ergs} = \frac{14.4}{R^6} \times 10^{-61}\ \text{ergs} = \frac{0.91}{r^6}\ \text{volts, if } r \text{ is in } \mathring{A}. \quad (14)$$

(The somewhat smaller value reported previously[8] was obtained by considering only transitions of one electron, putting $Z_0 = 1$, which is not legitimate.) (14) agrees very well indeed with the result of Slater and Kirkwood, calculated with a variational method, namely

$$\Delta_2 E = \frac{14.9}{R^6} \times 10^{-61}\ \text{ergs}.$$

The latter authors suggest that the large difference between their result and the one obtained by applying London's simple approximation, which yields an upper limit $\Delta_2 E_{\max} = 12.4 \times 10^{-61}$ ergs, is occasioned by the neglect of double jumps in London's expression. The calculations presented here make this evident.

[8] See ref. 1.

AN EXPERIMENTAL STUDY OF THE NATURAL WIDTHS OF THE X-RAY LINES IN THE *L*-SERIES SPECTRUM OF URANIUM

By John H. Williams
Department of Physics, University of California

(Received April 21, 1931)

Abstract

The half widths at half maximum of the rocking curves in parallel positions of the double x-ray spectrometer with calcite crystals reflecting in the first order have been investigated as a function of wave-length and this function is shown to be linear.

The rocking curves of U $L\alpha_1$ in three different antiparallel positions of the instrument give a natural width which is practically independent of the dispersion. The natural widths of U $L\alpha_1$ and U $L\beta_1$ have been observed as a function of voltage and no significant dependence was noted.

The half widths at half maximum of twelve lines in the uranium *L*-series spectrum were studied and the results are:

Line U *L*	α_1	α_2	β_1	β_2	β_3	β_4	β_5	β_6	γ_1	γ_2	γ_3	γ_4
$\Delta\lambda$ in X.U.	0.439	0.494	0.299	0.369	0.382	0.726	0.252	0.487	0.242	0.57	0.47	0.233
ΔV in volts	6.56	7.20	7.17	8.04	9.40	16.1	5.94	9.71	7.96	19.7	16.2	8.18

Possible correlations with the electron transitions are suggested and the predominance of nuclear effects are evident from the greater widths of lines involving the elliptical orbit L_I.

The observed widths are compared to the classical and quantum theory widths and the size of the nucleus necessary to explain the discrepancy is given. The possibility of observing the splitting of the energy levels due to nuclear spin as suggested by Breit is rejected. The actual shape of the line U $L\alpha_1$ has been investigated and found to approximate that predicted by the classical theory.

THE natural widths of x-ray lines in the *K*-series of molybdenum have been measured by Ehrenberg and Mark,[1] Ehrenberg and von Susich,[2] Davis and Purks,[3] Allison and Williams,[4] and Mark and von Susich[5] with the double x-ray spectrometer. Experiments on the relative widths of some x-ray lines in the *L*-series of lead and thallium have been carried out by Allison.[6] This paper is a report of experiments performed on the natural widths of the x-ray lines in the *L*-series spectrum of uranium. The accurate measurement of a greater number of lines in the *L*-series offers an opportunity to study any dependence on the transitions involved.

[1] Ehrenberg and Mark, Zeits. f. Physik **42,** 807 (1927).

[2] Ehrenberg and von Susich, Zeits. f. Physik **42,** 823 (1927).

[3] Davis and Purks, Proc. Nat. Acad. Sci. **13,** 419 (1927); **14,** 172 (1928); Phys. Rev. **34,** 181 (1929).

[4] Allison and Williams, Phys. Rev. **35,** 1476 (1930).

[5] Mark and von Susich, Zeits. f. Physik **65,** 253 (1930).

[6] Allison, Phys. Rev. **34,** 176 (1929).

Apparatus

The double x-ray spectrometer used in these experiments has been previously described.[7] The following changes have been made. The vertical slits, limiting the divergence of the beam in a plane perpendicular to the axes of rotation of crystals A and B, were 2 mm in width. The horizontal slits, limiting the divergence of the beam in a vertical plane including the axes of rotation, were of various widths which will be given later.

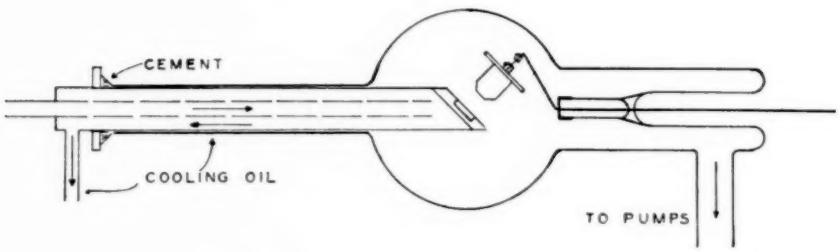

Fig. 1. Diagram of uranium target x-ray tube.

The x-ray tube used in these experiments is illustrated in Fig. 1. The tube was designed to give a large focal spot which would remain fixed on the target. These two properties of the tube are highly essential in the measurement of line widths as will be discussed later. The focal spot was at a distance of 50 cm from crystal A. The filament holder was designed from the type used by Professors Ross and Clark at Stanford University. It enabled the filament to be placed within one cm of the target and allowed the x-rays to be observed at an angle of 135° from the electron beam. The uranium was obtained from the Westinghouse Electric and Manufacturing Company. Many attempts were made to obtain good thermal contact between the uranium or some other metal but without success until finally the method used by S. K. Allison[8] was adopted. A piece of uranium was hydraulically pressed below the surface of a large copper block and the edges of the copper were peaned over while the uranium was under pressure. This served satisfactorily as a target up to a maximum power input of 0.4 kw. The tube was cooled by pumping cold kerosene through the hollow target holder.

The power for operating the tube was developed by a 5 kw. 550 cycle motor generator and the high potential supplied by a transformer was rectified by kenetrons and smoothed by condensers. The calculated voltage fluctuations were 0.6 percent at 48 kv and 6 milliamperes.

The calcite crystals used were those investigated in a previous experiment.[4] These crystals were preserved in a dessicator over dehydrated calcium chloride and sodium hydroxide, and it has been found that they have deteriorated only very slightly in the course of a year.

[7] Williams and Allison, J.O.S.A. and R.S.I. **18,** 473 (1929). For a further description see reference 4.

[8] Allison, Phys. Rev. **32,** 1 (1928).

Operation of the Instrument

The technique of measuring line widths has been previously developed. The degree of accuracy obtained with the double spectrometer can be seen by comparing the values of 0.144 and 0.163 X.U. for the half width at half maximum of Mo$K\alpha_1$ obtained by Mark and von Susich[5] and the value of 0.147 X.U. obtained by Allison and Williams.[4] The method of operation used in these experiments was that previously described.[4] The method of setting the crystal faces vertical was retained. Frequent readings of the temperature were taken while observations were being made and no significant changes were noted.

Reduction of Observed Results

The majority of the results have been obtained in the (1,1) position following a notation given in a previous paper.[9] The dispersion D of the double spectrometer is given by

$$D \equiv \frac{d\theta_B}{d\lambda} = \frac{n_A}{2d \cos \theta_A} + \frac{n_B}{2d \cos \theta_B} \tag{1}$$

n_A and n_B are the orders in which crystals A and B are reflecting respectively and θ_A and θ_B are the corresponding glancing angles. The sign of n_A is always taken positive. n_B is negative when the first incident and last reflected rays are on opposite sides of the first reflected ray,[10] otherwise it is taken positive. The dispersion D is therefore finite in all anti-parallel positions.

The first correction to be applied to the observed widths in anti-parallel positions is the geometric width due to the vertical spread of the beam. Schwarzschild's[10] equation for the "geometric breadth," $\delta\theta_B$, may be written

$$\delta\theta_B = \tfrac{1}{2} D\lambda\phi^2. \tag{2}$$

In this equation, $\delta\theta_B$ is the total angular range through which crystal B may be turned while reflecting the wave-length λ. If the widths of the slits limiting the divergence of the beam in a vertical plane are h_1 and h_2 ($h_2 \geqq h_1$), and the distance between them is L,

$$\phi = \frac{h_1 + h_2}{2L}. \tag{3}$$

The correction to be applied to the observed widths has been previously deduced[4] from Eqs. (2) and (3). Let ξ be the angular deviation of crystal B from the position of reflection for the central ray, (that ray passing through the geometrical centers of the slit apertures). Then the value of ξ at which the geometrical rocking curve drops to half maximum is given by[4]

$$\xi_{1/2} = \tfrac{1}{2} D\lambda\phi^2 \left\{ \frac{h_2}{h_1 + h_2} \right\}^2. \tag{4}$$

The values of $\xi_{1/2}$, in seconds of arc, calculated from Eq. (4) are arbitrarily subtracted from the observed full widths at half maximum.

[9] Allison and Williams, Phys. Rev. **35,** 149 (1930).
[10] Schwarzschild, Phys. Rev. **32,** 162 (1928).

The second correction to be applied to the resultant widths in anti-parallel positions is that due to the finite resolving power of calcite crystals. If it is assumed that the line has a Gaussian error curve distribution of intensity we have[11]

$$W = (W_A^2 + W_B^2 + D^2 W_\lambda^2)^{1/2} \tag{5}$$

In the above equation, W represents the half width at half maximum in angular measure of the observed rocking curve after the geometric correction has been applied, W_A the half width at half maximum in angular measure of the curve representing the intensity of reflection from crystal A as a function of the deviations from the Bragg angle, W_B is the same quantity for crystal B, D is the dispersion given by Eq. (1), and W_λ is the half width at half maximum in linear measure of the line. The quantities W_A and W_B are observed in positions of zero dispersion (i.e. $n_B = -n_A$) and will be discussed under the next heading. These two corrections are the only ones applied to the observed widths if the deviation of the crystal faces from verticality has been reduced to zero.

Study of Parallel Positions

In the positions of zero dispersion the observed width W is from Eq. (5)

$$W = (W_A^2 + W_B^2)^{1/2}. \tag{6}$$

Assuming the crystals to be the same, $W_A = W_B = W_C$

$$W = 2^{1/2} W_C. \tag{7}$$

The values of W_C have been studied as a function of λ for the first order of reflection from calcite. There is no geometric correction to be applied to the observed widths in parallel positions if the deviation of the crystal faces from verticality is reduced to zero. The method of imposing this condition has been previously described.[4] The crystals were first adjusted as accurately as possible by the cathetometer method and a rocking curve was taken. Crystal B was then rotated through a minute of arc about an axis lying in a horizontal plane and a second rocking curve taken. This procedure was repeated until a position of crystal B was found which gave a rocking curve of minimum width. From this observed value of W the interference pattern width of a single crystal, W_C, was obtained by the use of Eq. (7).

The values of W_C have been obtained with the crystals reflecting the wave-lengths 908, 718, and 613 X.U. in the first order. These are plotted in Fig. 2. W_C is seen to be a linear function of the wave-length.

Darwin[12] and Ewald[13] have considered the problem of reflection of plane monochromatic waves from an ideal crystal. The extent of 100 percent reflection is given by

$$\Delta\theta = 4\delta \operatorname{cosec} 2\theta \tag{8}$$

[11] Schwarzschild, reference 10. Obtained by combining Eqs. (43) and (45) of his paper.
[12] Darwin, Phil. Mag. **27,** 325 and 675 (1914).

where θ is the glancing angle and δ is the deviation of the index of refraction from unity. Since [14]

$$\delta = 1 - \mu = Ne^2\lambda^2/2\pi mc^2 \tag{9}$$

where N is the number of electrons per cm^3, e is the electronic change in e.s.u., m is the mass of the electron, and c is the velocity of light, and from the Bragg law

$$\operatorname{cosec}\theta = 2d/n\lambda$$

we have

$$\operatorname{cosec} 2\theta = d \sec\theta/n\lambda. \tag{10}$$

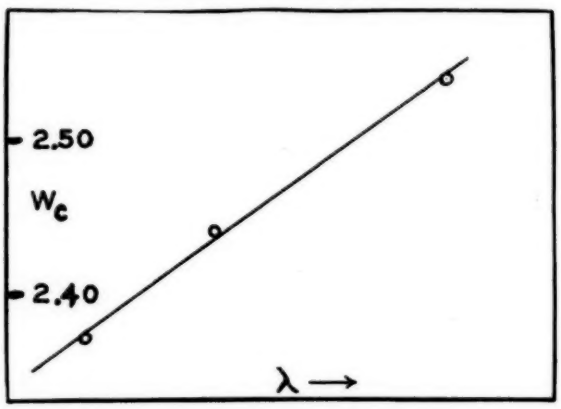

Fig. 2. The interference pattern width of a single crystal, W_C, as a function of the wave-length.

Substituting from Eqs. (9) and (10) in Eq. (8)

$$\Delta\theta = k\lambda \sec\theta \tag{11}$$

where

$$k = 2Ne^2d/\pi mnc^2.$$

Thus $\Delta\theta$ is an approximately linear function of λ as may be shown from the Bragg law and expansion in powers of λ.

$$\Delta\theta = k\lambda[1 + \tfrac{1}{2}(n\lambda/2d)^2 + 3/8(n\lambda/2d)^4 + 5/16(n\lambda/2d)^6 + \cdots]. \tag{12}$$

This series is rapidly convergent for first order reflection from calcite in the region examined.

The experimental value of W_C was found to be 1.6 times as large as that calculated for a perfect calcite crystal by a method given in a previous paper.[15] The value of W_C for the calcite crystals reflecting the wave-length 908 X.U. in the second order was 0.90 seconds of arc. This decrease of W_C for calcite with reflection in the second order is in agreement with the results of Davis and Purks[16] and Allison and Williams.[17]

[13] Ewald, Phys. Zeits. **26,** 29 (1925).
[14] A. H. Compton, X-Rays and Electrons, page 205.
[15] See reference 4. Eqs. (10) and Tables III and IV.
[16] Davis and Purks, Phys. Rev. **34,** 181 (1929).
[17] See reference 4, page 1489.

Study of U $L\alpha_1$ in Different Orders

It has been pointed out that a systematic change in the observed natural widths when measured in positions of different dispersion may be due to the finite size of the focal spot. During the observation of a curve crystal B is rotated through small angles while crystal A is left fixed. Under the previous adjustments when crystal B is reflecting the peak of the line the radiation comes from the most intense part of the focal spot. As crystal B is rotated up to and through this central position, the radiation comes from slightly different parts of the focal spot, and hence will have a different initial intensity. In positions of higher dispersion greater errors would arise from this cause, and the magnitude of the effect can be calculated. In order to overcome this difficulty the broad focus tube was used and the radiation was taken at an angle of 45° from the target. To obtain a measure of the intensity distribution of the focal spot the following experiment was performed. The double spectrometer was adjusted to reflect the peak of a given line and was left fixed in this position. The x-ray tube, which was mounted on a moveable carriage driven by a screw, was advanced by small steps in a horizontal direction perpendicular to the line of the slits. Thus the radiation reflected by the crystals at different steps came from successive parts of the focal spot, and the intensity could be examined directly. It was found that at a distance of 1.5 mm from the center the intensity had fallen to half of the maximum value. It is thus felt that the error arising from this source has been greatly reduced. Any further enlargement of the focal spot would decrease the intensity to a degree causing uncertainty in the observations.

The half widths at half maximum of the line U $L\alpha_1$ were investigated in three different positions of the double spectrometer. The results are given in Table I.

Table I. *Half widths at half maximum for U $L\alpha_1$ at 48 kv.*

Position (n_A,n_B)	D in ″/X.U.	h_1 cm	h_2 cm	$\xi_{\frac{1}{2}}$	W	$(W_A^2+W_B^2)$	W_λ in X.U.	Weighted average of W_λ in X.U.
(1,−2)	36.942	0.3	0.5	1.1″	16.9″	7.3″	0.453	
"	"	"	"	"	16.2	"	0.433	0.442
"	"	"	0.4	0.7	16.6	"	0.445	
(1,1)	68.877	0.3	0.3	0.7	27.6	12.9	0.398	
"	"	"	"	"	30.6	"	0.442	
"	"	"	"	"	30.9	"	0.445	
"	"	"	"	"	30.9	"	0.445	0.439
"	"	"	"	"	30.6	"	0.442	
"	"	0.2	0.2	0.3	29.8	"	0.430	
(1,2)	105.81	0.3	0.8	8.5	45.0	7.3	0.425	
"	"	0.5	0.5	3.1	46.0	"	0.433	
"	"	"	"	"	47.9	"	0.452	0.437
"	"	"	"	"	46.4	"	0.438	

The weighted averages have been secured by a personal estimate of the quality of the data.

For these observations D varies from 36.942 to 105.81 seconds per X.U. and the half width at half maximum, W_λ, varies from 0.442 to 0.437 X.U.

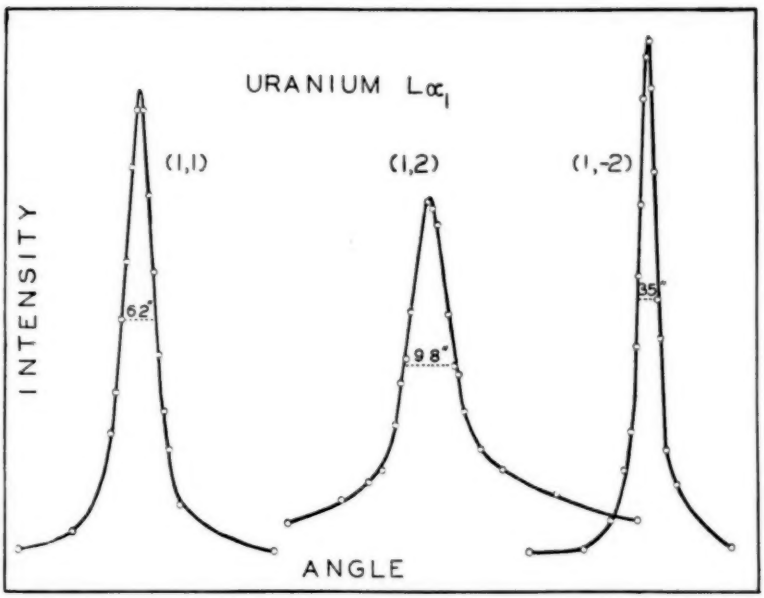

Fig. 3. Observed rocking curves of uranium $L\alpha_1$ at 48 kv. Ordinates are proportional to ionization currents, abscissae to angular settings of crystal B. The vertical scale is different for each curve.

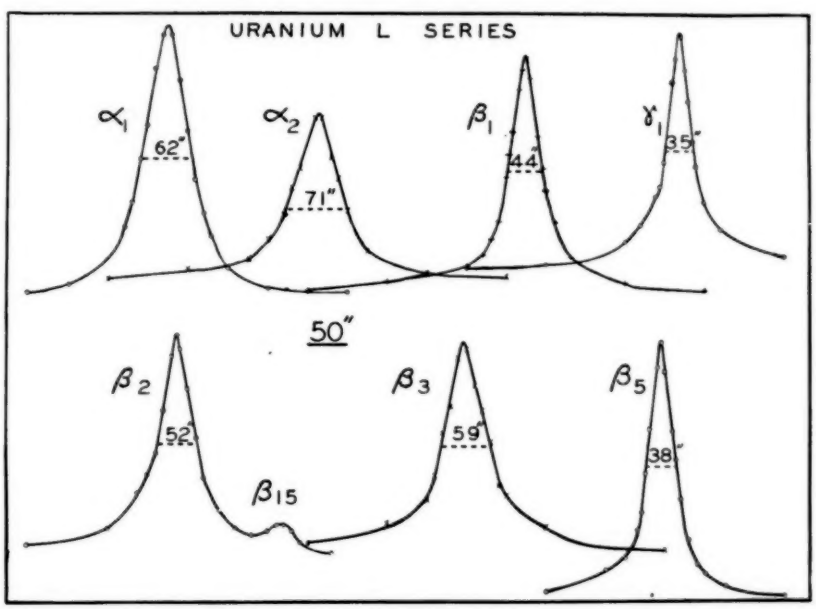

Fig. 4. Observed rocking curves in the (1, 1) position for seven lines in the uranium L spectrum at 48 kv. Ordinates are proportional to ionization currents, abscissae to angular settings of crystal B. The vertical scale is not the same for all the curves.

There is a trend towards narrower widths at positions of higher dispersion but this decrease is well within the experimental error, and the magnitude of this effect is less than formerly noted.[4] Typical curves of the line U $L\alpha_1$ in three different positions of the instrument are shown in Fig. 3.

The Natural Widths of the *L*-Series Lines of Uranium

Twelve lines of the *L*-series spectrum of uranium have been observed in the (1,1) position of the double x-ray spectrometer. Seven of these are shown in Fig. 4.

The half widths at half maximum of these lines have been calculated from the observed rocking curves in the (1,1,) position at 48 kv and are given in Table II. The details given in Table I are partially omitted but all corrections have been applied. The weighted averages of W_λ are obtained from a personal estimate of the quality of the data and the probable errors were calculated from the least squares formula.

The natural widths of U $L\alpha_1$ and U $L\beta_1$ have been examined as a function of voltage. Rocking curves in the (1,1) position were taken at different voltages under identical geometric conditions. The experimental error is greater at lower voltages due to the decrease in intensity as the excitation voltage is approached. The results are given in Table III where again the details of the calculation are omitted though all corrections were applied. An estimate of the experimental error of W_λ is also given.

Table II. *Half widths at half maximum for the L-series lines of uranium at 48 kv.*

Line	D in $''$/X.U.	$(W_A^2+W_B^2)$	Number of observations	Weighted average of W_λ in X.U.
U$L\alpha_1$	68.877	12.9$''$	6	0.439±0.004
α_2	68.895	13.0	5	0.494± .006
β_1	68.580	11.9	8	0.299± .002
β_2	68.628	12.1	8	0.369± .003
β_3	68.568	11.8	5	0.382± .009
β_4	68.618	12.0	5	0.726± .010
β_5	68.590	11.9	6	0.252± .006
β_6	68.680	12.3	4	0.487± .009
γ_1	68.448	11.2	7	0.242± .003
γ_2	68.438	11.2	4	0.57 ± .02
γ_3	68.430	11.1	4	0.47 ± .01
γ_6	68.426	11.1	5	0.233± .005

Table III. *Half widths at half maximum of $UL\alpha_1$ and $UL\beta_1$ as a function of voltage.*

Voltage in kv.	W_λ of U$L\alpha_1$ in X.U.	W_λ of U$L\beta_1$ in X.U.
48	0.440±.005	0.295±0.005
39	0.445±.005	0.294± .005
30	0.439±.010	0.287± .010
24	0.435±.015	0.30 ± .02

Table III shows that there is no significant change of width with voltage for U $L\alpha_1$ and U $L\beta_1$ in the voltage region studied. Thus the part of the width of these lines due to satellites arising from multiply ionized states of the atom

is negligible. These lines involve the final orbits L_{III} and L_{II} and it is reasonable to assume that their behaviour is representative of lines arising from transitions to these levels. The lines involving the orbit L_I have such a relatively weak intensity that it is not practicable to measure their widths at voltages less than 48 kv.

Discussion of the Natural Widths

In order to facilitate the discussion of the natural widths and to make possible any correlations with the electron transitions involved the results are shown in Table IV.

In the third column the energy breadth ΔV in volts is calculated from

$$\Delta V = 12336\Delta\lambda/\lambda^2 \tag{13}$$

where $\Delta\lambda$ and λ are in Angstroms.

The fourth column of Table IV gives the initial and final quantum states of the atom for the transition involved. The fifth column gives the eccentricity of the initial and final orbits on the classical quantum theory measured by k/n.[18]

The $\Delta\lambda$s of the lines vary from 0.233 to 0.726 X.U. and the range of wave-lengths from 592.6 to 920.14 X.U. The half width at half maximum predicted by the classical theory[19] is 0.059 X.U. and is independent of the wave-length in question.

A study of Table IV has suggested the following possible correlations. U $L\beta_3$, U $L\beta_4$, U $L\gamma_2$, and U $L\gamma_3$ involving the highly elliptical orbit L_I have the greatest energy widths observed. U $L\alpha_2$ and U $L\beta_1$ involve transitions from the same initial orbit and the eccentricities of the orbits involved are the same; the energy widths agree. U $L\beta_2$ and U $L\gamma_1$ involve transitions from similar initial orbits and the eccentricities of the orbits are the same as well as the changes in quantum numbers; the energy widths agree. For the lines U $L\beta_5$ and U $L\gamma_6$ the changes in the quantum numbers and the eccentricities of the orbits involved are the same but the energy widths are very different. There is however an agreement between their $\Delta\lambda$s. U $L\gamma_2$ and U $L\gamma_3$ involve orbits of the same eccentricity and there is a rough agreement between their energy widths; however the changes in quantum numbers are different.

These correlations are by no means complete but the wave-length region involved is so relatively great that the validity of a direct comparison between the energy widths or $\Delta\lambda$s and the transitions involved is doubtful. It is felt that no simple complete empirical correlation can be given. Coster[20] has qualitatively considered the question of the width of x-ray lines on the classical quantum theory. He concludes that the width of lines involving transitions between elliptical orbits is greater than those involving circular orbits. If ΔV is considered to be a measure of the width of the line these predictions are born out in general by the results shown in Table IV. The great

[18] Sommerfeld, Atombau und Spektrallinien, 4th edition, p. 125, Eq. 14.

[19] See reference 4, Eq. (20).

[20] Coster, Zeits. f. Physik **45**, 797 (1927).

TABLE IV. *Collected results on the half widths at half maximum of the observed rocking curves in the (1,1) position of the L-spectrum of uranium at 48 kv.*

Line	$\Delta\lambda$ in X.U.	ΔV in volts	Initial / Final	n	l	j	ϵ	Δn	Δl	Δj
$UL\alpha_1$	0.439	6.56		3	2	5/2	1	1	1	1
				2	1	3/2	1			
α_2	0.494	7.20		3	2	3/2	1	1	1	0
				2	1	3/2	1			
β_1	0.299	7.17		3	2	3/2	1	1	1	1
				2	1	1/2	1			
β_2	0.369	8.04		4	2	5/2	3/4	2	1	1
				2	1	3/2	1			
β_3	0.382	9.40		3	1	3/2	2/3	1	1	1
				2	0	1/2	1/2			
β_4	0.726	16.1		3	1	1/2	2/3	1	1	0
				2	0	1/2	1/2			
β_5	0.252	5.94		5	2	5/2	3/5	3	1	1
				2	1	3/2	1			
β_6	0.487	9.71		4	0	1/2	1/4	2	1	−1
				2	1	3/2	1			
γ_1	0.242	7.96		4	2	3/2	3/4	2	1	1
				2	1	1/2	1			
γ_2	0.57	19.7		4	1	1/2	1/2	2	1	0
				2	0	1/2	1/2			
γ_3	0.47	16.2		4	1	3/2	1/2	2	1	1
				2	0	1/2	1/2			
γ_4	0.233	8.18		5	2	3/2	3/5	3	1	1
				2	1	1/2	1			

width of U $L\gamma_2$, U $L\gamma_3$, and U $L\beta_4$, the last as previously observed by Allison[6] in lead and thallium, are the best illustrations of the effect of an elliptical final orbit. The lines U $L\alpha_1$, U $L\alpha_2$, U $L\beta_1$ involving both initial and final circular orbits have the smallest ΔVs observed with the exception of U $L\beta_5$.

Professor J. R. Oppenheimer[21] has calculated the width of U $L\alpha_1$ to be expected on the quantum mechanics from the Einstein probability coefficients of the states involved. He gives

$$\begin{aligned} \frac{\Delta\nu}{\nu} &= \frac{\sum A_n}{\nu} \\ &\sim 3^3 2^{14} \alpha^3 Z^2 / 5^{12} \\ &\sim 6 \times 10^{-6} \end{aligned} \tag{14}$$

where ν is the frequency of the line considered. A_n is the Einstein probability coefficients of spontaneous emission from the levels n to the L level in ques-

[21] From private conversation with Professor Oppenheimer. I am greatly indebted to him for his interest in these results.

tion, and the summation if taken over all filled levels of the atom lying higher than the L levels, and α is the fine structure constant. On the basis of this reasoning $\Delta\nu/\nu < 10^{-5}$ whereas exprimentally $\Delta\nu/\nu \sim 5 \times 10^{-4}$.

Thus the observed width must be due to other phenomena decreasing the life time of the excited state and consequently increasing the line breadth. Some possible causes may be the changes of the energy levels due to Hund coupling with the valence electrons in the atom; interactions with the neighboring atoms in the metal; or the effects of nuclear spin suggested by Breit.[22] Since the L levels of uranium are so deeply buried in the atom it seems that the nuclear effects must predominate in broadening the line. Professor Oppenheimer has suggested the following possibilities due to coupling with the nucleus.

$$\begin{aligned} &(1) \quad \text{Electron interchange} \quad \Delta\nu/\nu \sim \left(\frac{a_n}{a_0}\right)^2 \frac{1}{Z} \\ &(2) \quad \text{Induced dipole} \quad \Delta\nu/\nu \sim \left(\frac{a_n}{a_0}\right)^3 \\ &(3) \quad \text{Quadrapole moment} \quad \Delta\nu/\nu \sim \left(\frac{a_n}{a_0}\right)^2 \frac{1}{Z}. \end{aligned} \tag{15}$$

In these equations a_n is the effective radius of the nucleus, a_0 is the mean radius of the orbit, and Z is the atomic number. The first of these arises from energy considerations of electron interchange between the orbital and nuclear electrons.

If a_0 is calculated from the Bohr formula

$$a_0 = \tau^2 h^2 / 4\pi^2 m e^2 Z \tag{16}$$

where τ is the total quantum number and the experimental value of $\Delta\nu/\nu$ is assumed then the following values are obtained for the radius of the nucleus.

$$\begin{aligned} &(1) \quad a_n \sim 4.5 \times 10^{-11} \text{ cm} \\ &(2) \quad a_n \sim 1.8 \times 10^{-11} \text{ cm} \\ &(3) \quad a_n \sim 4.5 \times 10^{-11} \text{ cm} \end{aligned}$$

From this reasoning alone the probability of finding a nuclear electron at these distances from the center of the nucleus is large whereas from the Rutherford scattering experiments the Coulomb law of force holds down to 10^{-13} cm. The possibility of an unexpected penetration of the orbits is thus suggested.

In Fig. 4 the line U $L\beta_{15}$, first resolved by Allison,[6] is almost completely resolved but no reliable estimate of its width could be given. It is of the order of magnitude of 0.3 X.U. Its separation from U $L\beta_2$ was found to be 1.89 X.U. as the average of three measurements.

The line $L\beta_5$ on the energy level diagram is a doublet O_V, O_{IV} to L_{III} with a relative intensity of 9 to 1 on the Burger-Dorgelo rules. Although the line is relatively narrow no evidence of the weaker component could be found.

[22] Breit, Phys. Rev. **35**, 1447 (1930).

U $L\beta_3$ and Mo $K\alpha_1$ have nearly identical wave-lengths, 708.4 and 707.768 X.U., but their widths are greatly different, 0.382 and 0.147 X.U. respectively. The width of an x-ray line is therefore not a function of wave-length alone, but depends on the atom and transition involved. The half widths at half maximum of the L-series lines of uranium are from 1.6 to 5 times as great as that of Mo $K\alpha_1$. This is in agreement with the work of Allison[6] on thallium and lead but in his work the crystals used were relatively poor and the adjustments of the instrument imperfect thus causing higher values of the widths.

The actual shape of the line U $L\alpha_1$ was investigated by taking many points on a rocking curve when the value of $\xi_{1/2}$ was reduced to negligible proportions. The classical theory gives for the shape of a line[23]

$$I_\nu = I_0 / \{ k^2 + [(2\pi\nu)^2 - (2\pi\nu_0)^2] \}. \tag{17}$$

In the derivation of Eq. (5) Schwarzschild[10] has assumed a Gaussian error curve distribution of intensity,

$$I'_\nu = I_0 e^{-k^2(\nu-\nu_0)^2} \tag{18}$$

The values of k and I_0 were selected so as to make the theoretical curves fit the actual curve at the maximum and half maximum ordinates. It was found that Eq. (17) gave a much better fit than Eq. (18). However the tails of the observed curve and the classical curve did not agree, the observed curve falling off more steeply than that given by Eq. (17).

Breit[22] has considered the effects of nuclear spin on x-ray terms and has predicted the splitting of the L_{II} level of uranium to be of the order of magnitude of 4.0 volts. This prediction is based upon the assumptions that the uranium nucleus has a spin 9/2 and a magnetic moment 9/2 proton units and that screening effects are neglected. If one attempts to apply this prediction to the line U $L\beta_1$ for example, it is found that the natural breadth of the line is so great that no appreciable evidence of splitting would be expected.

In conclusion, I should like to express my thanks to Professor S. K. Allison for the suggestion of this problem and his helpful correspondence during the course of the investigation. My thanks are also due Professor R.B. Brode for his kindly criticism and interest in this research.

[23] W. C. Mandersloot, Jahrbuch der Rad. und Elek. **13**, 1 (1916).

BREADTH OF THE COMPTON MODIFIED LINE WITH THE DOUBLE CRYSTAL SPECTROMETER

By Archer Hoyt and Jesse DuMond
California Institute of Technology, Pasadena

(Received April 20, 1931)

Abstract

Three experimenters using the double crystal spectrometer have recently reported very much narrower structure for the Compton modified line than the structure observed photographically by DuMond and Kirkpatrick with the multicrystal spectrograph whose resolution was entirely adequate to reveal such a narrow structure. We have repeated the experiment using a double crystal spectrometer similar to theirs. The results obtained are in satisfactory agreement with the previous observations of Compton line breadth by DuMond and Kirkpatrick with the multicrystal spectrograph and in disagreement with the experimenters who used double crystal spectrometers. The conclusions drawn are: (1) The Compton modified line due to Mo $K\alpha$ radiation scattered by graphite at angles of $165° \pm 10°$ and examined with the double crystal spectrometer has a breadth of from 21 to 22 XU at half-maximum height; (2) Under the above conditions there is no appreciable separation of the $K\alpha$ doublet in the shifted position; (3) No fine structure exists in the scattered spectrum of intensity greater than one-fifth the modified line intensity; (4) The ratio of modified to unmodified line intensity is estimated at (7.3:1); (5) There appears to be no essential difference between the results obtained with the single crystal, multicrystal and double crystal spectrometers in the study of this problem.

Purpose of Investigation

VERY early in the study of the Compton effect it was suspected that the modified line might be broader than either the primary line or the unmodified line. Ross[1] was apparently the first to attribute this breadth to the momenta of the scattering electrons. An experiment by Sharp[2] using a single crystal photographic spectrometer at large scattering angle established the fact that the modified line has greater breadth than the primary line or than the unmodified lines.

In the early experiments resolution and homogeneity of scattering angle were sacrificed more or less in order to obtain sufficient intensity for ionization spectrometers or to give photographic spectra in reasonable times. It was therefore difficult to arrive at more than qualitative conclusions as to the breadth and structure of the Compton line. One such qualitative test is to observe whether the $K\alpha$ doublet present in the primary radiation can or cannot be resolved in the modified radiation. In one of the early photographic spectra published by Ross the modified line did appear to be faintly resolved. The resolution of the spectrograph was however barely sufficient to separate the unmodified scattered doublet and the conclusion to be drawn from this

[1] Ross, Proc. Natl. Acad. **9**, 246 (1923).
[2] Sharp, Phys. Rev. **26**, 691 (1925).

photograph as to the breadth of the modified line remains consequently quite uncertain. Indeed the apparent resolution of the modified doublet might even be attributed to an accident of the photographic emulsion as Compton suggests in "X-Rays and Electrons," page 293.

More recently one of us in collaboration with H. A. Kirkpatrick has shown[3] by means of the multicrystal spectrograph that the breadth of the Compton modified line obeys, as a function of the scattering angle, the law to be expected on the hypothesis that the broadening is a Doppler effect of the moving electrons that scatter the radiation. This law is given roughly by the approximate equation for the breadth

$$\Delta\lambda = \beta\lambda \sin \tfrac{1}{2}\theta.$$

Thus for small scattering angles and hard primary radiation the modified line should be narrower than for larger scattering angles and soft primary radiation. Less marked differences in the breadths of the modified lines for different scattering materials might also be expected. *In comparing experimental results on the breadth of the modified line it is therefore essential to be sure that the conditions of the experiment are essentially the same.*

In a previous article one of us[4] has shown that the breadth and structure of the modified line for scattering of Mo$K\alpha$ radiation at large angles by beryllium was consistent with the assumption of two electrons per atom of beryllium dissociated to form a free electron gas of the type postulated by Fermi and Sommerfeld. The observed shape of the modified line from beryllium could be quite consistently accounted for as a Doppler broadening caused by electrons having the statistical velocity distribution quantitatively predicted by Sommerfeld's theory. (The correctness of the assumption of two free electrons per atom in beryllium has recently received support in the study of BeK lines from the work of Martin Söderman.)[5] The modified Compton line from beryllium for Mo$K\alpha$ primary radiation scattered at large angles was observed to be about 22 XU broad at half-maximum, a value much too great to permit resolution of the α doublet which has a separation of only 4 XU.

Measurements of the breadth of the modified Mo$K\alpha$ line scattered at large angles by graphite made with the multicrystal spectrograph show also breadths of the same order of magnitude at half-maximum, again about 22 XU. The resolution was entirely adequate to separate the unmodified $K\alpha$ doublet and the inhomogeneity of scattering angle less than one degree. This breadth is in agreement with the electron velocities to be expected in graphite.

In view of the foregoing the authors of this paper were much astonished to read reports of three other investigators[6] each using a double crystal spectrometer who found much narrower Compton modified lines in quite violent

[3] DuMond and Kirkpatrick, Phys. Rev. **37,** 136 (1931).

[4] J. W. DuMond, Phys. Rev. **33,** 643 (1929).

[5] Martin Söderman, Zeits. f. Physik **65B,** 656 (1930).

[6] Davis and Mitchell, Phys. Rev. **32,** 331 (1928); J. A. Bearden, Phys. Rev. **36,** 791 (1930); M. A. Gingrich, Phys. Rev. **36,** 1050 (1930).

disagreement with the above results. In one case the $K\alpha$ doublet of molybdenum scattered at large angles by graphite appeared as two extremely sharp peaksin the modified position almost completely resolved.

Some essential and hitherto unsuspected difference might exist between the methods of studying the Compton line with the double spectrometer and with the single spectrometer. The purpose of the present research was therefore to reveal any such effect as well as to check the work of the above mentioned investigators.

METHOD

Spectrometer. The double crystal calcite spectrometer with internal grid ion chamber and Hoffman type electrometer have been extensively described in another article[7] and need therefore no further space.

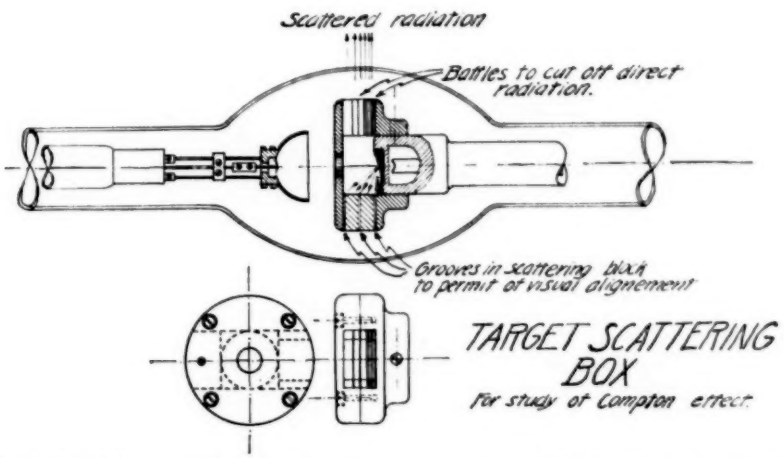
Scattered radiation
Baffles to cut off direct radiation.
Grooves in scattering block to permit of visual alignement
TARGET SCATTERING BOX
for study of Compton effect

Fig. 1. Special x-ray tube for the study of x-rays scattered at large angles provided with scatterer in vacuum in close proximity to target.

Special x-ray tubes. Two types of tube were tried. These are shown in Figs. 1 and 2. The tube shown in Fig. 1 is provided with a cylindrical copper housing carried on the front end of the target. This housing contains on one side the scatterer and on the opposite side an opening filled with thin steel sheets whose planes are parallel to the face of the target.

These sheets are so spaced that the direct radiation from the focal spot cannot issue between them due to its obliquity. They however permit the scattered radiation from the scatterer to issue freely. The scatterer is traversed by three fine slits parallel to the face of the target, one at the center, one at the side nearest the target and one at the side nearest the cathode. The tube was aligned with the spectrometer by sighting at the crystals through these slits and between the steel sheets. Without this precaution the tube might have been so positioned that the parallel rays demanded by the bicrystalline reflection would be oblique to the steel sheets and considerable loss of scattered intensity would have resulted.

[7] DuMond and Hoyt, Phys. Rev. **36**, 1702 (1930).

The scatterer was wide enough so that the selective reflection could take place over nearly the entire area of the two calcite crystals.

Considerable difficulty was encountered from gas given off by the graphite scatterer during the operation of the tube. After a gas discharge occurred in the tube it became difficult to reproduce conditions of voltage, current and x-ray intensity accurately. A large number of observations must be made in order to distinguish between accidental fluctuations in the readings and real characteristics of the spectrum and the chance that a gas discharge might occur before a sufficient number of readings could be made was deplorably high. The best of a number of curves taken with this tube is shown in Fig. 3. In the others the accidental fluctuations were even more pronounced. That such fluctuations are accidental is evident from the fact that they are not in the least reproducible.

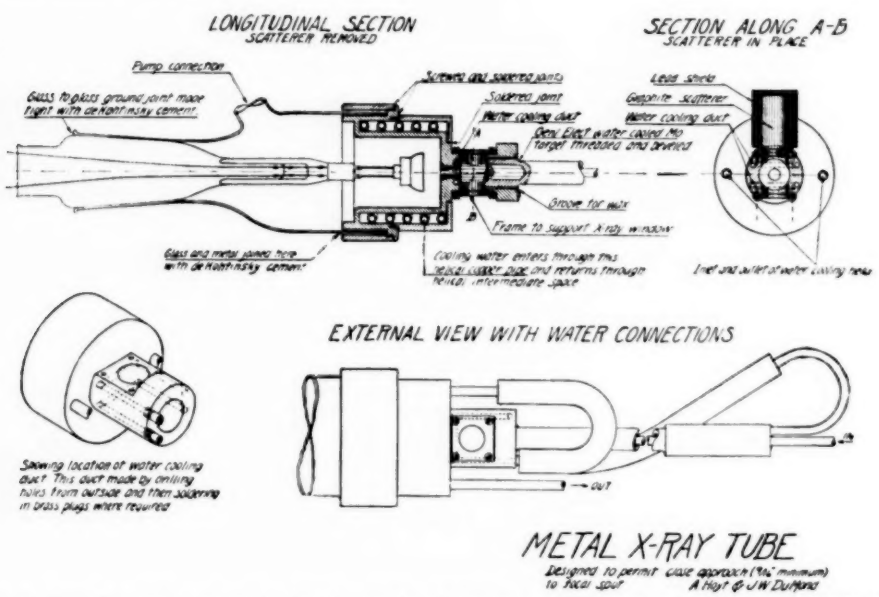
LONGITUDINAL SECTION
SCATTERER REMOVED
SECTION ALONG A-B
SCATTERER IN PLACE
Pump connection
Glass to glass ground joint made tight with de Khotinsky cement
Soldered joint
Water cooling duct
Lead shield
Graphite scatterer
Water cooling duct
Groove for mica
Frame to support X ray window
Glass and metal joined here with de Khotinsky cement
EXTERNAL VIEW WITH WATER CONNECTIONS
out
Showing location of water cooling duct. This duct made by drilling holes from outside and then soldering in brass plugs where required
METAL X-RAY TUBE
Designed to permit close approach (¼" minimum) to focal spot
A Hoyt & J W DuMond

Fig. 2. Special metal x-ray tube for the study of x-rays scattered at large angles provided with windows in close proximity to target to permit placing the scatterer outside vacuum.

On account of these difficulties the tube illustrated in Fig. 2 was constructed to permit a close approach of the scatterer to the focal spot while having the scatterer outside the tube. The windows in this tube are $\frac{1}{2}$ inch inch away from the center of the target. At first mica windows were used on this tube but these were several times destroyed by puncture, probably by fast electrons rediffusing from the focal spot. A thin mirror surface of beryllium deposited on the mica window by evaporation and placed on the inward side to conduct away such fast electrons did not suffice to prevent puncture. Finally aluminum windows 0.003 in. thick were resorted to. The direct radiation has to pass once through the window nearest the scatterer and the scattered radiation passed through both windows. These three passages had the effect of reducing the intensity by about 30 percent.

The graphite scatterer is cylindrical in form, 25 mm in diameter and 48 mm in length. It is completely enclosed in a lead housing 3 mm thick fitting closely about it. The front end of the graphite cylinder is turned down to such a diameter (18 mm) as to fit in direct contact with the entire x-ray window. The effect of the graphite alone could be ascertained by taking control readings with the graphite block removed.

The face of the molybdenum target was bevelled at an angle of 13° with the axis of the tube to reduce the absorption of the characteristic radiation excited in the deeper parts of the target and also to prevent the direct radiation from falling on the spectrometer.

The glass parts of the tube were jointed to each other and to the metal parts with de Khotinsky cement. The target was screwed into place and made tight with the same cement as were also the windows. For this reason the rather elaborate system of water cooling ducts shown in the drawing was provided. It was found entirely adequate to maintain all the joints cold enough to operate very satisfactorily.

Vacuum was maintained in this tube by a two stage mercury diffusion pump hanging under the spectrometer table. This pump was supported from the same rotating false table top[7] to which the x-ray tube was attached so that the pump and x-ray tube moved together as the spectrum was explored, and no flexible vacuum joints were necessary. An internal liquid air trap in a right angle bend in the vacuum line between the pumps and the tube was used instead of the more common type so as to minimize the obstruction offered to the issuance of gas from the tube.

The two curves obtained with this tube are shown in Figs. 4 and 5. It should be noted that much less power was used in this work than was used by two of the above mentioned experimenters. The x-ray tube ran at about 60 K.V. c.p.d.c. and 10.6 and 14.6 ma. in the two cases.

Results

All three curves shown here exhibit deplorably large accidental fluctuations in the readings relative to the faint effects studied. For this reason as large a number of readings as possible were taken. *In every case we have indicated the actual value of every single reading taken by plotting it as one point. No readings taken have been omitted.* In work of this kind there is grave danger of arriving at wrong conclusions by unintentional biased weighting of the observations due to omissions. It was felt to be too misleading to publish only the averages of several readings as this gives no idea of the order of accuracy or reproducibility involved.

Taken alone we do not feel that the curve in Fig. 3 made with the scatterer in the vacuum has enough points to be conclusive.

The other two curves seem to us to definitely indicate a broad diffuse structure for the Compton modified line from Mo$K\alpha$ scattered at large angles by graphite in very satisfactory agreement with the curves obtained at large angles with the multicrystal spectrograph. The smooth curve which we have drawn is intended to guide the eye over the observed points on the steep

sides of the intense unmodified lines. We hope the reader will pardon our continuation of these smooth curves through the modified region where they can only be taken as suggesting the general trend of the observations.

A few points were taken with the graphite scatterer removed, the tube running at the same voltage and current as before removal. The modified scattering disappears as would be expected but the unmodified lines are only partly diminished. The amount of this diminution indicated in Figs. 4 and 5 is to be taken as a measure of the unmodified scattering of the graphite. The line intensity remaining in the unmodified position after removal of the graphite is due principally to (1) unmodified scattering of primary radiation at small angles (where it is strong) at the window nearest the spectrometer and

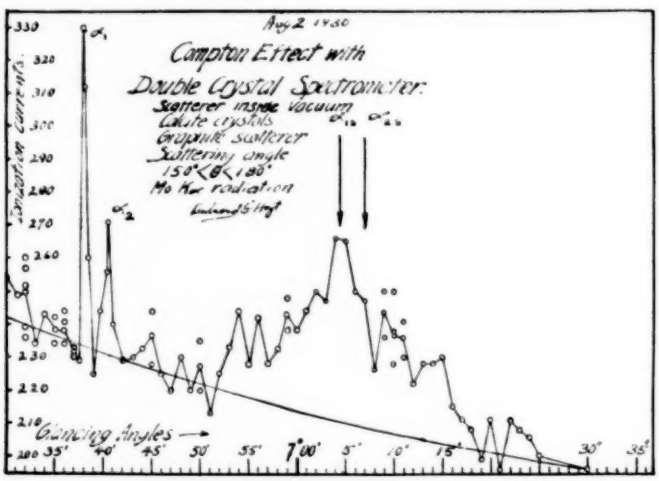

Fig. 3. Spectrum of x-radiation (Mo $K\alpha$) scattered at large angles by graphite with scatterer inside vacuum. The tube shown in Fig. 1 was used.

(2) fluorescence of the molybdenum films unavoidably deposited on both windows by vaporization from the target.

The unmodified lines have been plotted in Fig. 6 to a scale one fifth as high and five times as broad as in Fig. 4 to facilitate measuring their areas for the purpose of estimating the ratio of modified to unmodified intensity. The area thus obtained was multiplied by the ratio of the diminution in peak value of α_1 on removal of the graphite to the peak value with graphite in place in order to obtain the contribution of the graphite scattering alone. These curves in Fig. 6 give a clearer idea of the shape of the unmodified lines given by the double spectrometer here used and its resolving power. The vertical divergence or maximum obliquity of the rays with a plane normal to the dihedral angle formed by the two crystal faces did not exceed two degrees.

The maximum false broadening of the shifted radiation due to the inhomogeneity of scattering angle in these experiments is only 2 X.U.

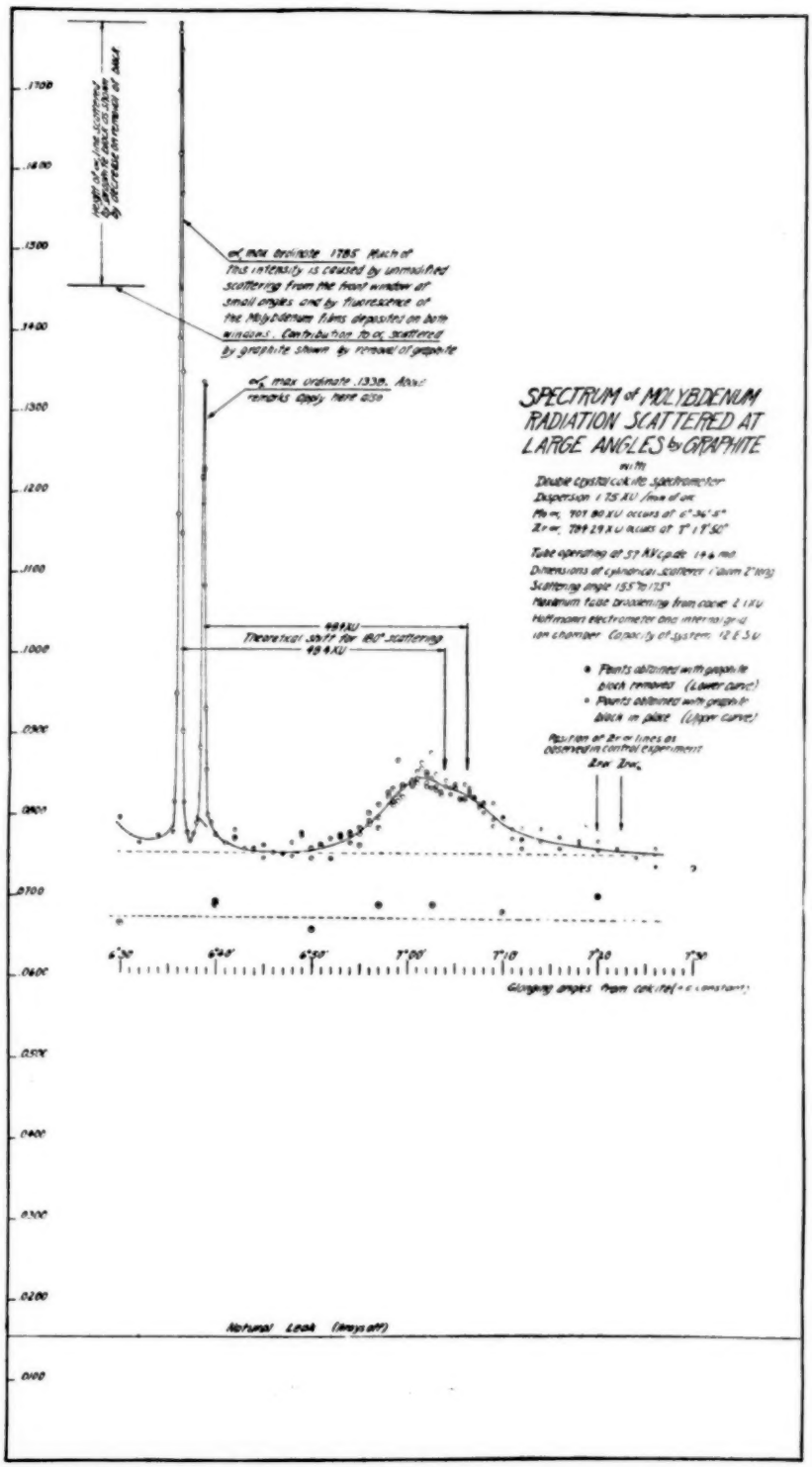
SPECTRUM of MOLYBDENUM RADIATION SCATTERED AT LARGE ANGLES by GRAPHITE
with
Double crystal calcite spectrometer
Dispersion 1.75 X.U. /mm of arc
Mo $K\alpha_1$ 707.80 X.U. occurs at 6°36'.5"
Zr $K\alpha_1$ 784.29 X.U. occurs at 7°1'.50"
Tube operating at 57 KV crest 19 ma.
Dimensions of cylindrical scatterer 1 diam 2" long
Scattering angle 135° to 135°
Maximum tube broadening from focus 2.1 X.U.
Hoffmann electrometer and ionization chamber. Capacity of system 12 E.S.U.
Points obtained with graphite block removed (Lower curve)
Points obtained with graphite block in place (Upper curve)
Position of Zr $K\alpha$ lines as observed in control experiment
Zr $K\alpha_2$ Zr $K\alpha_1$
of max ordinate 1785. Much of this intensity is caused by unmodified scattering from the front window at small angles and by fluorescence of the Molybdenum films deposited on both windows. Contribution to σ_s scattered by graphite shown by removal of graphite
σ_s max ordinate 1338. Above remarks apply here also
Theoretical shift for 180° scattering
49.9 X.U.
49.1 X.U.
Natural Leak (arrows off)
Glancing angles from calcite (+ c constant)

Fig. 4. Spectrum of x-radiation (Mo$K\alpha$) scattered at large angles by graphite with scatterer outside vacuum. The tube shown in Fig. 2 was used.

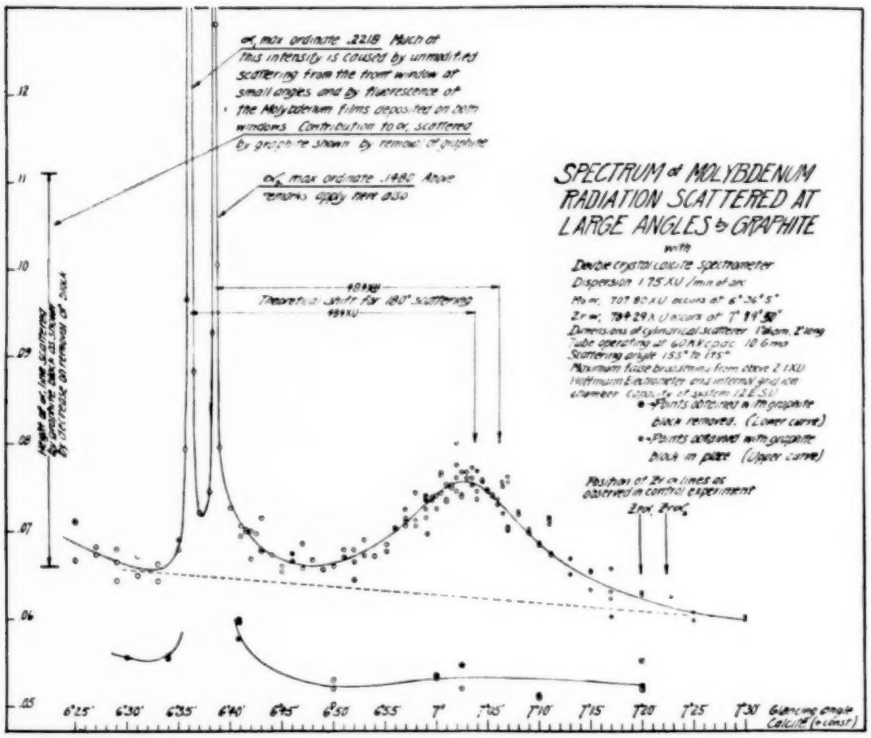

Fig. 5. Spectrum of x-radiation (Mo$K\alpha$) scattered at large angles by graphite with scatterer outside vacuum. The tube shown in Fig. 2 was used.

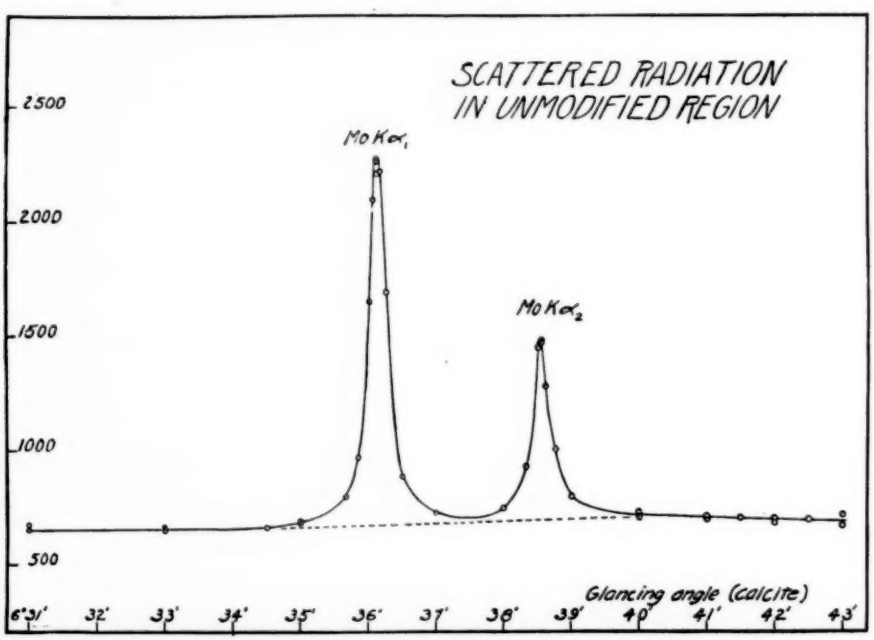

Fig. 6. Unmodified lines of Fig. 4 replotted to one-fifth the scale of ordinates and five times the scale of abscissae.

Conclusions

1. The Compton modified line due to Mo$K\alpha$ radiation scattered by graphite at angles of $165° \pm 10°$ and examined with the double crystal spectrometer has a breadth of from 21 to 22 XU at half-maximum height.

2. Under the above conditions there is no appreciable separation of the $K\alpha$ doublet in the shifted position.

3. No fine structure exists in the scattered spectrum of intensity greater than one fifth the modified line intensity.

4. The ratio of modified to unmodified intensity is estimated at 7.3:1.

5. There appears to be no essential difference between the results obtained with the single crystal, multicrystal and double crystal spectrometers in the study of this problem.

No explanation has been found for the discrepancy between the results of the three observers above referred to and the results here reported. Of the three the one who obtained the sharpest lines used far greater absolute x-ray intensities incident on his scatterer than were used in the present work. It seems quite out of the question however to suppose that his incident energy was sufficient so profoundly to modify the statistics of electron motion in the scatterer as to give a modified line so much sharper than those reported here.

THE OSCILLATING ARC: ELEMENTS OF GROUP VI

By E. Z. Stowell
University of Michigan, Ann Arbor

(Received April 21, 1931)

Abstract

A study of the behavior of sulphur, selenium, tellurium, chromium, molybdenum, tungsten and uranium as cathodes in an arc in hydrogen reveals that all of them permit radio-frequency oscillations to occur in a tuned circuit across the arc. No magnetic field is required for these oscillations. The elements of the sulphur group give unsteady oscillations, disintegrate rapidly and form hydrides with the arc atmosphere. The other elements yield steadier oscillations with no chemical action, and allow the arc to operate at a high temperature. The character of the spectra of these arcs in both the oscillating and the non-oscillating states is described and comparisons made. A mechanism is suggested whereby some elements will permit oscillations to occur and some will not.

I. Introduction

THE mechanism of the oscillating arc in hydrogen is sufficiently obscure so that much more data are necessary before possible explanations may be intelligently discussed. For this reason, a detailed study of the individual groups of the periodic table seems of value, not only to verify previous work with different equipment and different samples, but to obtain additional information regarding the character of the excitation when oscillating. In order to avoid duplication of work in progress in other laboratories, a study has been made of the behavior of the elements in the sixth group of the periodic table as cathodes in the arc in hydrogen. Group six was chosen because (1) no spectrograms have ever been taken of the elements of the sulphur group in such an arc, and (2) to check former results on the elements Mo, W, and U, which are of exceptional interest.

II. Apparatus

The arc was that used in previous experiments[1] and consists of a vertical lower electrode, used as the cathode, surrounded at its base by a coil to furnish a steady magnetic field when necessary; a detachable vertical upper electrode, used as anode; both being enclosed in a removable glass cylinder which permits the maintenance of an atmosphere of hydrogen around the arc flame. The upper electrode, or anode, is usually of copper; its composition has little or no effect upon the behavior of the arc. The lower electrode or cathode, is of copper, and cup-shaped, in order to hold various specimens of other elements under investigation. It should be stated that an arc cannot be struck between the anode and the unfilled cathode, in a hydrogen atmosphere. Both electrodes may be water-cooled if desired. Hydrogen is fed in from a standby

[1] Stowell and Huxford, Phys. Rev. **36**, 1348 (1930).

tank, and the exhaust disposed of either by combustion or escape to the outer air. The supply voltage is 220 d.c. A 20 ohm resistance and a large choke coil are in series with the arc; a radio-frequency circuit adjusted to about 300 k.c. is connected across the arc, with a current indicator in series. Striking is effected by a thumb screw which raises and lowers the anode.

The spectral region from 5500–3700A was covered with a double-prism glass spectrograph. This spectrum is about 3.5 inches long, and since usually but one element is worked with at a time, there is little ambiguity in line identification. Exposures intended to be comparable with one another were taken on the same plate with identical exposure times, and as nearly the same arc currents as it was possible to obtain.

III. Behavior of the Elements of the Sulphur Group

In accordance with results expressed in former papers[1,2] which indicated that elements of even atomic number when used as cathodes permitted the generation of radio-frequency oscillations, sulphur, selenium and tellurium all allow these oscillations to occur. These arcs are characterized by extensive formation of hydrogen sulphide, hydrogen selenide and hydrogen telluride, as the case may be; and also by rapid disintegration of the cathodes. The latter phenomenon doubtless arises from the porous nature of the solid element, and the fact that some of it is continually being removed through the exhaust in the form of hydride. None of these arcs require a magnetic field for the production of oscillations.

From the spectral standpoint this group is interesting because the degree of excitation of the cathode vapor seems to increase with atomic number. This will appear in the discussion of the individual elements.

(1) Sulphur. Sulphur is decidedly the worst of the arcs from the standpoint of electrode disintegration; it is difficult to obtain a long enough exposure for spectrographic purposes. An additional difficulty is the settling of the sulphur on the walls of the glass cylinder, thus greatly reducing the light intensity and lengthening the exposure time. It was found necessary to fill the cathode cup with fresh material and to clean the glass in the optical path several times in order to get a single satisfactory exposure.

In the non-oscillating condition (obtained by opening the tuned circuit across the arc) no trace of sulphur was observed in the spectral region covered. Copper lines only were obtained, and the arc was to all intents and purposes a copper arc. Upon closing the oscillating circuit and allowing current to flow therein, the copper spectrum remained, with the addition of one Balmer line, H_β, and one band of sulphur with head at λ4285, degraded to the red. No sulphur lines appeared. A trace of Al in the original copper electrodes indicated by the pair at λ3944–3961, was greatly intensified in this oscillating arc.

(2) Selenium. Selenium does not disintegrate as rapidly as sulphur, and one filling of the hollow cathode is generally sufficient for an exposure. The settling of selenium upon the glass walls is not objectionable. The radio-fre-

[2] Stowell and Redeker, Phys. Rev. **34**, 978 (1929).

quency current is maintained at a somewhat steadier value than in the case of sulphur.

The spectral differences between the oscillating and the non-oscillating conditions are not great. Both spectra show copper, H_β and H_γ, and most of the Exner and Haschek lines of Se. Using the identification given by the Blochs,[3] these lines belong to Se I. In addition, two bands of Se were obtained, with heads at λ4285 and λ4006, both degraded to the red. The Al impurity previously referred to as existing in the copper was again intensified in the spectrum of the oscillating arc. An interesting feature is that the Ca II doublet at nearly the same wave-lengths, λ3933–3968, was *not* intensified.

(3) Tellurium. Tellurium behaves electrically in a similar manner to selenium. The spectrum however shows a higher order of excitation than selenium, just as the latter is excited more strongly than sulphur. In both the oscillating and non-oscillating condition the copper background, with H_β and H_γ are obtained, together with a multitude of lines due to Te I[3] and the following lines due to Te II: λλ4725, 4352 and 4120. These last three are the most intense lines in the spectrum, and are more intense when the arc is permitted to oscillate. No Te bands are found. The same phenomena concerning the doublets of Al I and Ca II that were mentioned in the case of Se are reproduced here.

IV. Behavior of Cr, Mo, W and U

(1) Chromium. Metallic chromium, inserted into the cup-shaped cathode, will not permit an arc to be drawn out in an atmosphere of hydrogen. There are however transients in the radio-frequency circuit at the moment the direct current circuit breaks. Evidently if an arc could be drawn, there would also be oscillations.

(2) Molybdenum. Molybdenum, in the form of a spiral of the wire inserted into the cup and projecting a trifle beyond, gives an unsteady arc, intensely white. No magnetic field is necessary for current to flow in the tuned circuit. Electrode disintegration is slow.

A continuous spectrum is obtained with both the oscillating and non-oscillating arcs, with lines of copper, Mo I, Mo II,[4] H_β and H_γ, as well as lines of Cr and Fe, superimposed. The latter are present as impurities in the Mo. Certain of the Cr lines appear to be reduced in intensity in the oscillating arc. They are:

4698.49
4652.16 (Cr I)
4530.74
4289.72 (sensitive line of Cr I)
4274.81 (sensitive line of Cr I)
4254.34 (sensitive line of Cr I).

The iron lines are about the same intensity in both spectra. Both the Ca II and Al I doublets previously mentioned are intensified in the oscillating state.

[3] L. and E. Bloch, Ann. de Physique **13,** 233 (1930).
[4] Meggers and Kiess, Jour. Opt. Soc. **12,** 417 (1926).

(3) Tungsten. Tungsten furnishes probably the most interesting arc in the sixth group. A spiral of wire (10 mil) placed inside the cup and projecting beyond, gives oscillations of extreme steadiness and reproducibility. No magnetic field or cooling are necessary. The arc is an intense white; since it runs at a high temperature, the electron emission from the cathode is high, the arc length and current are quite constant, and there is little to cause frequency fluctuations. With the arc running properly, its heterodyned note cannot be distinguished from that given by an electron tube oscillator. Electrode disintegration is extremely slow. The arc has the peculiarity that the radio-frequency output is increased, if, after the oscillations have started, the electrodes are made to approach one another slightly.

The non-oscillating arc shows a very simple spectrum: a heavy continuous background, with H_β, the Ca II pair λ3933–3968, and λ5006.17 of tungsten superimposed. No copper appears.

The oscillating arc likewise produces a heavy continuous background with H_β superimposed; but the Ca II pair is lacking, and instead there appear the following lines of tungsten: λλ4294.62, 4074.37, 4008.76, and 5006.17. The last two, at least, are known to arise from W I.

(4) Uranium. The uranium arc in hydrogen resembles the tungsten arc, but is not as steady, since the electrode is no longer a homogeneous piece of wire, but crushed metal placed in the copper cup. The arc is much brighter in the oscillating state, and is intensely white.

The spectra obtained are exceedingly rich in lines. The majority of the uranium lines in Vol. 6 of Kayser's Handbuch are found, together with many lines due to the iron impurity. Continuous spectra are obtained with the arc in both the oscillating and the non-oscillating condition; this continuous spectrum is more intense in the former case. There are other marked differences between the two conditions, namely:

(a) the uranium lines in general are intensified in the "oscillating" spectrum.

(b) a small amount of potassium impurity, indicated by the doublet at λ4044–47, is slightly intensified in the "oscillating" spectrum.

(c) iron impurity, especially those lines due to Fe I, is much reduced in the "oscillating" spectrum.

(d) Ca impurity, as indicated by lines of Ca I and Ca II, is reduced in intensity by the oscillations.

(e) the trace of Al I impurity in the original copper is reduced in intensity by the oscillations.

Suppression of the iron impurity as in (c) is characteristic of these arcs, and may possibly be of service to spectroscopists, when chemical removal of such impurity in samples to be investigated would be unduly difficult or expensive.

V. Discussion

All of the elements in Group VI. thus permit the generation of radio-frequency oscillations. The elements in the sulphur group have been seen to be-

have somewhat differently from the other elements studied. They are characterized by comparatively rapid electrode disintegration with compound formation, and low excitation. The remaining elements of Group VI. when used as cathodes disintegrate much more slowly, do not form hydrides, and operate the arc at a high temperature, resulting in the emission of a continuous spectrum.

A mechanism whereby some elements will allow current to flow in a tuned circuit across the arc, and others will not, is suggested from fundamental considerations of such arcs. Provided certain secondary conditions as to circuit constants are satisfied, those arcs will permit oscillation which have a negative slope to their dynamic characteristic. For those arcs with no accompanying oscillations, as with the alkali metals when used as cathodes, one may assume that the dynamic characteristic has become excessively flattened, to the extent of losing its negative curvature.

Steinmetz[5] has shown how this may come about if there is a time lag in the reaction of the arc stream to the amount of current passing through it. Consider the static characteristic of an arc, for direct current, to be represented by

$$e = a + \frac{b}{i^{1/2}},$$

where a is the potential drop at the electrodes, and the second term gives the potential drop across the arc stream. The slope of this characteristic, at any current i_1, is

$$\left(\frac{de}{di}\right)_{i=i_1} = -\frac{b}{2i_1^{3/2}}.$$

The fluctuation in potential, made available for the tuned circuit, by a small flutuation in current, Δi_1, about the mean current i_1, is

$$\Delta e_1 = -\frac{b}{2i_1^{3/2}}\Delta i_1.$$

If now Δi_1 were periodic and equal to $\Delta I\epsilon^{j\omega t}$, Δe_1 would likewise be periodic, and current would flow in the attached circuit.

Suppose however that the volume, and therefore the resistance $(e-a)/i$ of the arc stream, cannot adjust itself immediately to new values of current. Such might occur, for example, if the atoms of the cathode vapor remained in their excited or ionized states for a length of time comparable with the period of the attached tuned circuit. In this case let the potential fluctuation Δe_1 lag behind the current fluctuation by an angle α; that is,

$$\Delta e_1 = -\frac{b}{2i_1^{3/2}}\Delta I\epsilon^{j(\omega t+\alpha)}.$$

[5] Steinmetz, "Theory and Calculation of Electric Circuits," p. 194.

Elimination of the time gives the shape of the new characteristic; its equation is evidently

$$\Delta e_1 = -\frac{b}{2i_1^{3/2}}\Delta i_1 \cdot \cos\alpha.$$

The potential fluctuation is thus reduced due to the time lag, and less current will flow in the tuned circuit. With α equal to $\pi/2$, the potential fluctuation will be 90° out of phase with the current fluctuation, and no power will be available for oscillations. For large angles of lag, the potential fluctuation, in this picture, would vanish, and no oscillations would appear.

This hypothesis is defective in that it does not introduce the all-important hydrogen atmosphere. The latter may enter the discussion either by determining the excitation and ionization times, or, as arc engineers have supposed, by furnishing a much steeper dynamic characteristic than other gases.

THE HIGH FREQUENCY BEHAVIOR OF A PLASMA

By Lewi Tonks
Research Laboratory, General Electric Company

(Received April 20, 1931)

Abstract

An analogue for a uniformly ionized gas on the basis of the known formula $K_p=1-\omega_0^2/\omega^2$ for its specific inductive capacity is found in a shunt-tuned circuit. In that formula $\omega_0^2=4\pi Ne^2/m$ and ω is the impressed angular frequency. This formula is extended to two simple cases of non-uniform ionization, with the conclusion that non-uniformity may be indistinguishable from large energy dissipation, insofar as reactive effects are concerned. Formulas have been derived for calculating the *conductivity and specific inductive capacity of a cylindrical plasma* (positive column of an arc) between parallel condenser plates from the measured impedance of this condenser by using a modification of Mossotti's Theory. The natural period of such a condenser occurs very nearly when $K_p=-1$. For a fixed frequency the reactance of such a composite condenser was followed for varying arc current by observing the length of Lecher System connected to the condenser plates which was required to cause circuit resonance. Two and sometimes three resonances were found. They occurred in the neighborhood of the calculated plasma-electron resonance as determined from electron density measurements, and varied with impressed frequency according to theory.

The theoretical variation of K_p was checked in the range $\omega_0^2>2\omega^2$ by the hyperbolic relation between change in condenser reactance and arc current there. Resistance measurements on the Lecher system, used in connection with a more detailed analysis, allowed *calculation of relative electron density* in the range from one-half to five times that giving resonance, checking the actual values. In the same range, the *resistance to electron motion* varied considerably. The maximum value occurred near resonance and checked, roughly, the value calculated from free path considerations. The alternating fields in the plasma varied from 0.17 to 1.2 $v\cdot cm^{-1}$ and the maximum amplitude of electron motion was 2.1×10^{-3} cm.

A transverse magnetic field was found to double the resonance as H. Gutton has found. The separation of resonances accords with theory.

I. Introduction

THE reaction of an ionized gas to very high frequency electric waves has been the subject of several investigations. Spontaneous oscillations in the neighborhood of 10^9 herz originally found by Penning[1] have been further investigated by Tonks and Langmuir[2] using the low pressure mercury arc. They found that the observed high frequency oscillations corresponded to the theoretical value for plasma-electron oscillations[3]

$$\nu = (Ne^2/\pi m)^{1/2} = 8980 \times N^{1/2} \qquad (1)$$

[1] Penning, Nature **118,** 301 (1926) and Physica **6,** 241 (1926).

[2] L. Tonks and I. Langmuir, Phys. Rev. **33,** 195 and 990 (1929).

[3] This frequency appears so often in investigations of the high frequency behavior of ionized gases that it will be given a definite name in this paper, namely, "plasma-electron frequency."

where ν is the oscillation frequency, m is the electronic mass, and N is the ionization density. This frequency, looked upon as the limiting frequency at which radio waves can be propagated in an ionized medium, has been discussed at some length by T. L. Eckersley.[4] Since an ionized gas exhibits a resonant frequency, it is of interest to know the behavior of such a gas toward forced oscillations. W. H. Eccles[5] has derived formulae which have been interpreted by Bergmann and Düring[6] as attributing a dielectric constant

$$K = K_0 - 4\pi Ne^2 m/(m^2\omega^2 + f^2) \tag{2}$$

and conductivity

$$\rho^{-1} = fNe^2/(m^2\omega^2 + f^2) \tag{3}$$

to the medium, where f is a dissipation factor appearing in the equation of motion of the electron.

H. Gutton and J. Clement[7] have made a rather thorough investigation of the dielectric properties of ionized hydrogen extending through the plasma resonance.[7.5] It was found that the natural period varied with the intensity of ionization roughly in the way that was theoretically expected, and they were able to obtain a fair numerical check between the ionization density calculated from Eq. (1) and that calculated rather indirectly from their results. More recently, C. Gutton[8] has confirmed the existence of a natural resonance period in an ionized gas by measuring the change in conductivity of ionized mercury vapor when a 2.76 meter wave was impressed on it. In his theoretical treatment of the gas reaction, however, H. Gutton introduces an elastic restoring force of unknown origin which seems to be not only unnecessary but somewhat in contradiction with the actual experimental results, as has been pointed out by J. Rybner.[9] Still more recently, Bergmann and Düring[6] have measured the change in dielectric constant of a small condenser in high vacuum arising from the introduction of electrons between the condenser plates. They have been able to check the theoretical value as given by Eq. (2) roughly, but the electron densities used were so small (in the neighborhood of 10^7 cm^{-3}) that K was but little different from K_0, that is, unity. Their measurements give an apparent conductivity which is of the order of magnitude given by Salpeter's[10] interpretation of f as arising from the momentum lost in electron collisions with gas molecules.

[4] T. L. Eckersley, Phil. Mag. **4,** 147 (1927).

[5] W. H. Eccles, Proc. Roy. Soc. **A87,** 79 (1912).

[6] L. Bergmann and W. Düring, Ann. d. Physik **1,** 1041 (1929).

[7] H. Gutton and J. Clement, L'Onde d'Electrique **6,** 137 (1927); H. Gutton, preliminary reports, Comptes Rendus **184,** 441 (1927); complete report, Ann. d. Physique **13,** 62 (1930).

[7.5] The term "plasma resonance" denotes the actual resonance of the system comprising the plasma and the condenser of which it forms part of the dielectric. This resonance occurs, in general, at a different ionization density from plasma-electron resonance. See the paragraph following Eq. (27) and the theoretical treatment in Section IX.

[8] C. Gutton, Ann. d. Physique **14,** 5 (1930).

[9] J. Rybner, L'Onde d'Electrique **7,** 428 (1928).

[10] J. Salpeter, Jahrb. der drahtl. Telegr. **8,** 252 (1914). But see the criticism of S. Benner, Annalen der Physik **3,** 993 (1929) regarding the application of Salpeter's results to this experiment. Salpeter treats the case in which the free time of an electron is variable, whereas in the Bergmann-Düring experiment, the effective free time of every electron is the same.

The present investigation extends the work of H. Gutton with the aim of making direct measurements of electron density so as to be able to check theoretical formulas more directly.

II. The Specific Inductive Capacity of a Plasma

The use of an ionized gas is necessary if high densities of electrons are to be obtained, but in a plasma the density of ionization is not uniform throughout the whole cross section. It therefore becomes of interest to know how non-uniformity in electron density affects plasma-resonance behavior.

The complex specific inductive capacity of a plasma can be found by direct substitution in the partial differential equation

$$\partial^2 Z/\partial x^2 = \mu K \partial^2 Z/\partial t^2 + [4\pi\mu N e^2/(f + jm\omega)]\partial Z/\partial t \tag{4}$$

as given by Eccles.[11] Substituting

$$Z = \exp\{j\omega[t - (\mu K_p)^{1/2}x]\}$$

where K_p denotes the complex specific inductive capacity and writing

$$4\pi\mu N e^2/m = \omega_x^2 \tag{5}$$

where ω_x is the local plasma-electron angular frequency and writing also

$$S = f/m \tag{6}$$

we find that

$$K_p = \frac{\omega_x^2 - \omega^2 + j\omega S}{-\omega^2 + j\omega S}. \tag{7}$$

This is the specific inductive capacity at each point of the ionized medium looked upon as a function of the electron density, since that enters ω_x and possibly S.

The response of the medium as a whole may be extremely complicated. The simplest case is the one in which the electron density is a function of one coordinate only and the impressed electric field lies in that same direction. In that case we may write

$$dV = (4\pi Q_0/K_p)dx$$

where V is the impressed voltage and Q_0 is the polarization of the medium. This may be integrated to the form

$$V = 4\pi Q_0 \overline{K_p^{-1}} x_p \tag{8}$$

for a plasma of thickness x_p where

$$\overline{K_p^{-1}} = (1/x_p)(-\omega^2 + j\omega S)\int_{\text{over } x_p} (\omega_x^2 - \omega^2 + j\omega S)^{-1} dx. \tag{9}$$

[11] Reference 5, page 87.

It is instructive to apply this formula to a hypothetical case. Neglecting the dissipation factor S, let us assume a simple linear law of variation of N in the plasma, as for instance,

$$N = N_0(1 - x/2a) \tag{10}$$

from $x=0$ to $x=a$. This leads to

$$\overline{K_p^{-1}} = -\frac{\omega^2}{\omega_0^2} \ln \left[\frac{\omega_0^2 - \omega^2}{\omega_0^2/2 - \omega^2}\right]^2 \tag{11}$$

where $\omega_0 = (4\pi N_0 e^2/m)^{1/2}$ is 2π times the plasma-electron frequency where the the ionization is densest.

The value of $\overline{K_p^{-1}}$ as a function of N_0 is shown as Curve 1 in Fig. 1.

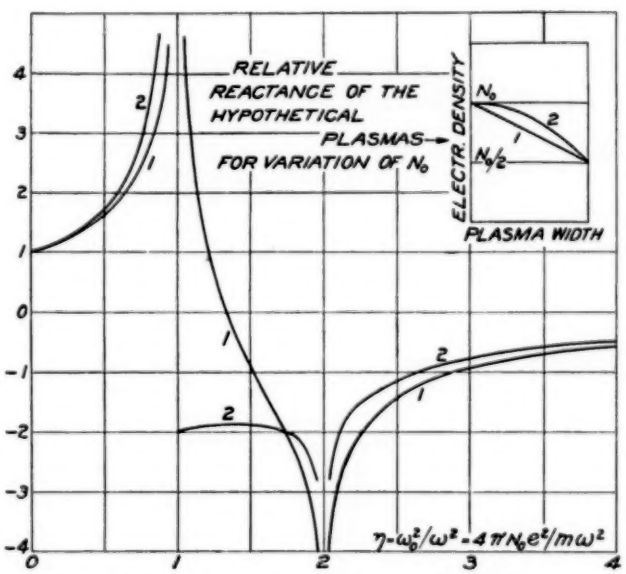

Fig. 1. Theoretical reactance of non-uniform plasmas.

Throughout the range $1 < \omega_0^2/\omega^2 < 2$ there is always a place in the plasma where local resonance occurs, giving rise to the middle section of the characteristic. The presence of resistance eliminates the infinities and leaves a curve resembling a resonance broadened by high dissipation, with the result that the width of the resonance region may only depend slightly upon the dissipative forces and may rather be a measure of the nonhomogeneity of the plasma. It was thought possible that a parabolic distribution of electron density

$$V = N_0(1 - x^2/2a^2) \tag{12}$$

might more nearly reproduce the assymmetry found in the actual resonance characteristics. Curve 2 was calculated with this in mind and although failing of its purpose, it may be useful in the appropriate case. Its equation is

$$\begin{aligned}\overline{K_p^{-1}} &= 2\eta^{-1}[2(\eta^{-1}-1)]^{-1/2}\tan^{-1}[2(\eta^{-1}-1)]^{-1/2} \\ &= \eta^{-1}[8(1-\eta^{-1})]^{-1/2}\ln\left\{\frac{[2(1\ \eta^{-1})]^{1/2}+1}{[2(1\ \eta^{-1})]^{1/2}-1}\right\}^2\end{aligned} \tag{13}$$

according as $\eta<1$ or $\eta>1$.

With the dissipative factor omitted, Eq. (7) takes the form

$$K_p = 1 - \omega_x^2/\omega^2 \tag{14}$$

which shows that each element of the plasma has a simple circuit analogue in a fixed condenser C shunted by a variable inductor L. The shunt admittance of such a circuit is

$$Z^{-1} = j\omega KC = j\omega C + (j\omega L)^{-1}$$

where K is the apparent specific inductive capacity of the condenser. Putting $LC=\omega_0^{-2}$ we obtain

$$K = 1 - \omega_0^2/\omega^2.$$

Each elementary volume ($dx\ dy\ dz$, x being parallel to the electric field) in even a non-uniform plasma is thus equivalent to a vacuum parallel-plate condenser of capacity

$$C = dydz/4\pi dx$$

shunted by an inductor of inductance

$$L = mdx/Ne^2dydz.$$

If, for example, a plasma contains two layers, each of which is uniform in electron density, it can be represented by two shunt circuits in series. Such a system shows double resonance provided that the separation of the two natural periods relative to the damping of the individual circuits is great enough. This double resonance could be observed either by increasing the electron densities proportionally (decreasing inductances in the circuit analogue) while the impressed frequency was maintained constant, or by varying the impressed frequency the keeping ionization densities unchanged. Extension of this reasoning makes it possible to understand how even a continuous variation in electron density, such as found in an actual plasma, may give rise to multiple resonance.

Digressing slightly, it may be remarked that H. Guttonn arrives at a relation essentially different from Eq. (14), namely,

$$K = 1 + (4\pi Ne^2/m)/(\omega_0^2 - \omega^2)$$

In this equation, $w_0/2\pi$ is the resonant frequency of the electrons and ω_0 is related to N by the empirical equation

$$\omega_0^2 = AN^{3/4}.$$

These equations make K decrease initially from unity as N is increased from zero, which is qualitatively the same as Eq. (14). When N is infinite, however,

these equations give K a weak positive infinity, whereas the strong negative infinity of Eq. (14) is qualitatively checked by H. Gutton's curves (Fig. 9 of Annales de Physique article) and by the measurements to be described below.

Turning now to the case of uniform ionization, it is evident that an analysis of the response of the medium reduces to an analysis of the electrostatic field between condenser plates in the presence of a dielectric of specific inductive capacity K_p. The simplest case is, of course, that of the plane parallel condenser, but that form is not suited to the positive column of an arc. The shape that has been adopted is that of a cylindrical plasma parallel to and midway between two plane condenser plates. This form has the experimental advantage that it is a natural form for a positive column, and that the electric lines of force in a uniform cylindrical plasma are straight and parallel so that there are no strong local fields at any point.

III. The Effective Specific Inductive Capacity of a Plane Parallel Condenser Containing a Cylindrical Plasma

Theoretically, a modification of Mossotti's theory of dielectrics makes the arrangement just outlined quantitative.[12] Mossotti's theory in its usual form contemplates a vacuum containing suspended conducting spheres. The response of such a configuration to an electric field can be treated quantitatively.[13] For present purposes the conducting spheres must be replaced by dielectric cylinders.

We consider then a large volume of dielectric (specific inductive capacity $=K$) made up of matter-free space in which are suspended infinitely long cylinders of specific inductive capacity K_p with their axes perpendicular to the uniform electric field E_e. The electric field tending to polarize any cylinder is

$$E_i = E_e + (4\pi/2)P \tag{15}$$

where P is the polarization of the composite dielectric, and the coefficient $4\pi/2$ applies to cylinders as $4\pi/3$ does to spheres. Within the polarized cylinder the field is

$$E_p = 2E_i/(K_p + 1) \tag{16}$$

analogous to $E_p = 3E_1/(K+2)$ in the case of spheres. The polarization of the cylinders is then

$$P_p = (K_p - 1)E_p/4\pi = (K_p - 1)E_i/2\pi(K_p + 1). \tag{17}$$

If θ denotes the fraction of the composite dielectric volume occupied by the cylinders,

$$P = \theta P_p = \theta(K_p - 1)E_i/2\pi(K_p + 1). \tag{18}$$

[12] H. Gutton's analysis based on Fig. 12 of his Ann. de Physique article cannot be justified theoretically. See J. Rybner, reference 9.

[13] Livens, Theory of Electricity, p. 228; Jeans, Electricity and Magnetism, Fifth Edition, p. 131 arrives at a formula which is not valid for sufficiently high values of dielectric constant.

Also

$$P = (K - 1)E_e/4\pi = (K - 1)E_i/2\pi(K + 1) \tag{19}$$

by using Eq. (15). Combining these two equations we find

$$(K - 1)/(K + 1) = \theta(K_p - 1)/(K_p + 1) \tag{20}$$

relating the dielectric constant, K_p, of the cylinders to that of the composite parallel-plate condenser, K. When K is not very different from unity, we can write

$$\delta K = 2\theta(K_p - 1)/(K_p + 1). \tag{21}$$

This formula was checked by the method H. Gutton used to determine the capacity values in the "equivalent" system shown in his Fig. 12. The arc tube, of 3.0 cm internal diameter, projecting well beyond and centered between two 7×7 cm condenser plates 7 cm apart was replaced by an open glass tube of the same size. With this tube empty, the Lecher System and condenser resonated with the thermocouple bridge at 17.9 cm, filled with mercury ($K_{Hg} = \infty$) at 16.3 cm, and filled with benzol ($K_B = 2.26$) at 17.35 cm. From Eq. (21)

$$\delta K_\infty = 2\theta$$

$$\delta K_B = 2\theta(2.26 - 1)/(2.26 + 1) = 0.386 \times 2\theta$$

whence

$$\delta K_B/\delta K_\infty = 0.386.$$

Since the changes in Lecher System length were small, they were proportional to capacity changes, whence

$$\delta K_B/\delta K_\infty = \delta L_B/\delta L_\infty = (17.9 - 17.35)/(17.9 - 16.3) = 0.34.$$

This is a satisfactory check considering that the experimental arrangement was only a rough approximation to that assumed mathematically. Since θ has been eliminated in the course of this calculation, the question naturally arises as to whether its value might not constitute an independent verification. The geometric capacity, C_0, terminating a resonant length, s, of Lecher system is given by

$$1/\omega C_0 K = Z_0 \tan (2\pi s/\lambda) \tag{22}$$

where Z_0 is the surge impedance of the system. It follows that the change in s required to retune after a slight change in K obeys the relation

$$\delta K/K = -2\pi\delta s/\lambda \sin (2\pi s_0/\lambda) \cos (2\pi s_0/\lambda)$$

and using Eq. (21)

$$\theta = -2\pi\delta s/\lambda \sin (4\pi s_0/\lambda) \tag{23}$$

since $K = 1$.

In the present case $s_0 = 27.2$ cm (for the bridge at 17.9 cm) and $\lambda = 187$ cm whence $\theta = 0.056$. The tube cross-section is $(\pi/4) \times 3.0^2 = 7.07$ cm^2, while the condenser cross-section is $7 \times 7 = 49$ cm^2 giving $\theta = 0.14$. This large discrepancy is easily accounted for both by the large edge effect in a condenser of the proportions used and also by the individual capacity of each plate to ground. Under these circumstances it is permissable to treat θ as an empirical constant in Eqs. (20) and (21).

It is fairly obvious that Eq. (21) may not be applicable to plasma resonance since δK becomes very large when $K_p K_c$ nears -1. In addition, a dissipative term must be included if the analysis is to be complete. From Eq. (7) (treating the plasma as if uniform by using ω_0 instead of ω_x)

$$K_p = \frac{\omega_0^2 - \omega^2 + j\omega S}{-\omega^2 + j\omega S} = \frac{\eta - 1 + jS/\omega}{-1 + jS/\omega} \tag{24}$$

if we put $\omega_0^2/\omega^2 = N/N_\omega = \eta$, N_ω being the electron density for which the plasma-electron angular frequency is ω, that is, $N_\omega = [\omega/(2\pi \times 8980)]^2$. From Eq. (20),

$$K^{-1} = 1 - 2\theta(K_p - 1)/[K_p + 1 + \theta(K_p - 1)] \tag{25}$$

Combining, we have

$$K^{-1} = 1 + \theta\eta/[1 - (1 + \theta)\eta/2 - 2jS/\omega] \tag{26}$$

for calculating the complex dielectric "constant" of the condenser when dissipation is included.

IV. Characteristics of a Tuned Circuit Made up of a Condenser Containing a Plasma and a Variable Inductor

If we suppose the condenser containing the plasma to be connected in series with an inductance, L, and denote its capacity when $N = 0$ by C_0, the series impedance of the combination is

$$Z = j[\omega L - (\omega C_0 K)^{-1}]$$

Putting

$$L = L_0 + \delta L$$

where L_0 is the inductance which tunes C_0, that is, $L_0 = (\omega^2 C_0)^{-1}$, this equation becomes

$$Z = j[\omega \delta L - \omega L_0 (K^{-1} - 1)].$$

Substituting from Eq. (26) and separating into real and imaginary parts we find

$$Z = j\omega \left[\delta L - L_0 \frac{(\theta/\phi)\eta'(1 - \eta'/2)}{(1 - \eta'/2)^2 + S^2/\omega^2} \right] + 4 \frac{\omega L_0 \theta \eta S/\omega}{(1 - \eta'/2)^2 + S^2/\omega^2}$$

where $\phi = 1 + \theta$ and $\eta' = \phi\eta$. When L is adjusted so that the circuit is in resonance, the reactance is zero and δL_r, the value of δL at resonance, is given by

$$\delta L_r = L_0 \frac{\theta\eta(1 - \eta'/2)}{(1 - \eta'/2)^2 + S^2/\omega^2} \tag{27}$$

As N is increased from zero, η and η' increase proportionally and δL_r increases from zero, at first proportionally to N but later more rapidly. If S were zero, δL_r would approach $+\infty$ as $\eta' = 2$, to reappear at $-\infty$, but the finite value of S causes δL_r to vary rapidly from a positive maximum to a negative minimum as η' passes through 2. As N becomes still larger, δL_r increases once more approaching $\delta L_\infty = -2\theta L_0/\phi$ as $\eta \to \infty$. This is just the type of behavior approximated to by the curve in H. Gutton's Fig. 9.

Obviously, the plasma resonance occurs at $\eta' = 2$. The qualitative circuit equivalent of the plasma between its condenser plates, as shown in Fig. 2, makes it evident that the shunt resonance does not occur when the plasma

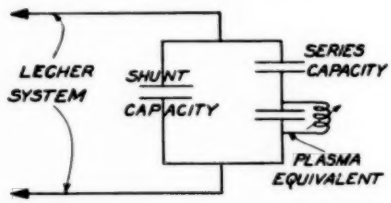

Fig. 2. Qualitative circuit equivalent of a plasma between condenser plates.

itself is tuned to the impressed frequency. This would be true only when the shunt capacity is zero. For example, the infinite plane parallel plasma is a (rather ideal) case in which plasma resonance would lie at $\eta = 1$. For a spherical plasma between parallel plates, resonance would occur near $\eta = 3$.

In the range where η' is different enough from 2 for S/ω to be neglected, Eq. (27) can be written

$$(1 - \eta'/2)\delta L_r = -(\eta'/2)\delta L_\infty(\theta\phi_\infty/\theta_\infty\phi)$$

the ratio in the right member being introduced to allow for changes in θ with N. It follows that

$$(\theta\phi_\infty/\theta_\infty\phi)\delta L_r^{-1} + \delta L_\infty^{-1}(2/\eta' - 1) = 0$$

and noting that $\eta' = \phi\eta = \phi N/N_\omega$ we have

$$(\theta\phi_\infty/\theta_\infty\phi)\delta L_r^{-1} = (2N_\omega/\delta L_\infty)(\phi N)^{-1} - \delta L_\infty^{-1}. \tag{28}$$

Now, changes in ϕ can be neglected since the actual value of θ is so small. It is thus justifiable to put $\phi/\phi_\infty = 1$, whence Eq. (28) becomes

$$(\theta/\theta_\infty)\delta L_r^{-1} = (2N_\omega/\delta L_\infty)(\phi_\infty N)^{-1} - \delta L_\infty^{-1}. \tag{29}$$

In the range of larger values of N (experimentally when $\eta' > 2$), the variation of θ with N was appreciable, but small, and the values of θ/θ_∞ could be calcu-

lated from the thickness of the wall sheath in the arc tube. For the smaller values of N, however, the variation of θ was not calculable and Eq. (29) could not be quantitatively tested in that range.

V. Preliminary Experiments

The plasma used in this investigation was the positive column of a mercury arc because the electrical methods for measuring ionization intensities have been applied most extensively to these arcs.[14] At first a tube containing an oxide-coated cathode was tried, but was found unsuitable on account of a conducting film which forms on the tube walls. This film appeared as a slight blackening, and its conductivity was made evident by the decrease in reson-

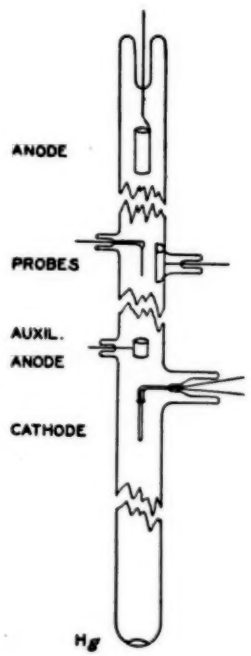

Fig. 3. Experimental arc tube.

ance current in the tuned circuit when the unexcited tube was placed between the condenser plates. That this film comes from the oxide cathode was proved by its absence in the next tube which had a hot tungsten filament. This tube, illustrated in Fig. 3, was a long cylinder of uniform internal diameter, 3.0 cm. The lower portion, containing a small quantity of mercury, was immersed in a water vath for pressure control. A short distance above the cathode was a ring electrode intended to be used as an auxiliary anode but soon abandoned. Thirty cm above this were two probes. One was a tungsten wire of 0.0127 cm diameter and 1.87 cm long placed in the axis of the tube. The other

[14] I. Langmuir and H. Mott-Smith, Jr., Gen. Elec. Rev., **27,** 449, 538, 616, 762 (1924); H. Mott-Smith, Jr. and I. Langmuir, Phys. Rev. **28,** 727 (1926); L. Tonks and I. Langmuir, Phys. Rev. **34,** 876 (1930).

was a square molybdenum plate, 1.95 cm on a side, on the tube wall opposite the probe and bent to fit the wall. These probes were intended to measure the intensity of ionization in the arc by well-known methods.[14] The main anode, a hollow cylinder, was 8 cm above these probes. The high frequency field was applied to the uniform column midway between the probes and the auxiliary anode by external electrodes of various shapes and sizes.

Initially a parallel wire system was connected with the external electrodes, later a small single loop inductance with variable condenser in series was employed, but finally a Lecher system consisting of two brass rods each 0.422 cm in diameter, spaced 3.90 cm on centers, and 180 cm long, was used for most of the measurements. The complete arrangement is shown schematically in Fig. 4. The Lecher system was tuned with a moveable bridge which consisted essentially of a low-resistance vacuum thermocouple of 2.6 ohms d.c. resistance. To prevent reflection effects from the free end of the Lecher sys-

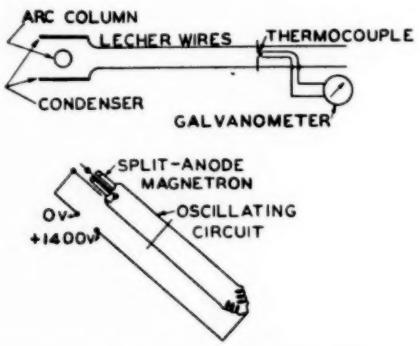

Fig. 4. Apparatus for observing ionized-mercury resonance.

tem, a short-circuiting bridge was attached to the thermocouple bridge and some 16 cm back of it, so that the two moved together. This 16 cm of conductor acts as a high impedance shunt to the thermocouple at all wave lengths used and effectively prevents any free-end oscillations without affecting the thermocouple calibration.[15] Stray effects arising from bringing the hand near to the free end of the Lecher system were minimized by by-passing the capacity currents along the thermocouple-to-galvanometer leads direct to the shorting bridge through small condensers.

A split-anode magnetron of Type FH-11 which can generate powerful oscillations up to 4×10^8 herz[16] was used as oscillation source. It was found more convenient to vary the arc current than to vary the frequency of the oscillator, since the e.m.f. in the Lecher system circuit then does not vary.

The earliest experiments showed two resonance frequencies in the plasma. In view of H. Gutton's single resonance, it was thought that this might arise in some way from the distributed excitation of the Lecher system together with its distributed inductance and capacity. With this in mind, a circuit with

[15] Paper to be submitted to I.R.E. Proc.
[16] W. C. White, Electronics **1**, 34 (1930).

lumped impedances was tried and as the same effect was observed, it was concluded that the double resonance was a property of the plasma itself.

Too high an excitation of the plasma circuit-resulted, as pointed out by C. Gutton, in additional ionization in the vicinity of plasma resonance which was often evident visibly by increased light from the region of the arc between the external electrodes. Such effects made measurements erratic and difficult of interpretation so that is was found best to work with very low excitation.

For the higher arc currents the tungsten wire cathode had to be run very hot. When it happened occasionally that it was too cool, the arc changed its appearance and the oscillation readings were erratic and quite different from the other condition. Too cool a cathode gives temperature-limited instead of space-charge-limited emission, the cathode drop increases, and the primary electrons, instead of ionizing the gas and causing glow on the anode side of the cathode only, penetrate down the tube and cause glow there also. With a plentiful supply of primary electrons, the cathode drop exceeds the ionizing potential only slightly so that although the electron at the cathode sheath edge has sufficient energy to ionize, the normal decrease in plasma potential as the electron moves away from the cathode is sufficient to bring its energy below the ionizing value. Of course, toward the anode, the gradient in the arc speeds up the electrons, but in the opposite direction ionization will be prevented. If, however, the electrons have several volts excess energy, as they have with temperature-limited currents, they are able to maintain a plasma even in the absence of an accelerating field in it. The change in oscillation readings undoubtedly arises from the change in arc conditions, and the fluctuations may be caused by line voltage variations which here appear as a variable cathode drop of about the same magnitude as the voltage variation itself, whereas with a hot enough cathode they cause only a small fractional change in arc current.

IV. Resonance Characteristic Measurements

In taking a resonance characteristic, the oscillation frequency of the magnetron oscillator was first fixed by adjusting the position of the bridge on the parallel conductors which, connected to the two anode sections of the magnetron, form the resonant circuit of the oscillator. The oscillation amplitude was fixed at a suitable value by adjusting the anode voltage, anode current (through filament current) and magnetic field of the magnetron. These three quantities were carefully maintained constant. The half wave-length was found from the separation of two successive nodes on a second Lecher system which could be coupled to the oscillator. This value agreed within 2 percent with the value found on the measuring system itself. The difference, which arises from the presence of the wood support in the measuring system, is small enough to be negligible in the present work.

The appendix of the arc tube was then immersed in a Dewar flask containing water at a temperature to give the desired mercury pressure.

With no arc in the tube, the resonance position of the bridge on the meas-

uring system and the thermocouple galvanometer reading were recorded. The arc was then started and the same readings were made at arc currents increasing roughly in a geometric ratio.

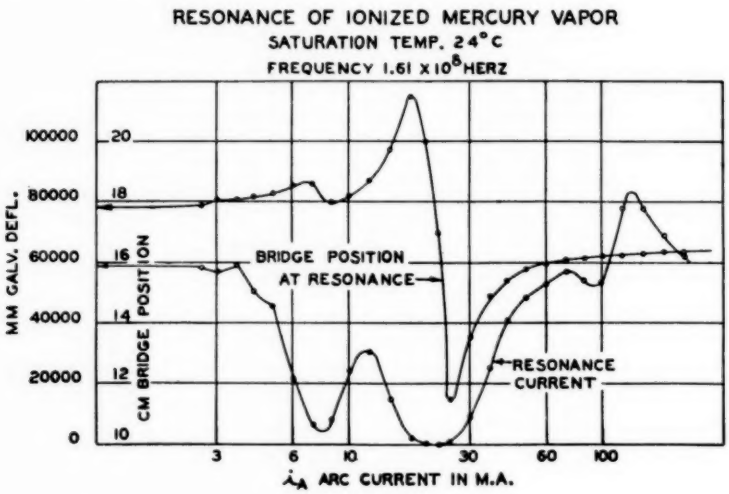

Fig. 5. Resonance characteristic of ionized mercury vapor.

The results of such a series of measurements are shown in Fig. 5. The two resonance points at 7.5 and 21.5 m.a., to be denoted as a- and b-resonances, respectively, are accompanied by the current minima expected at a shunt

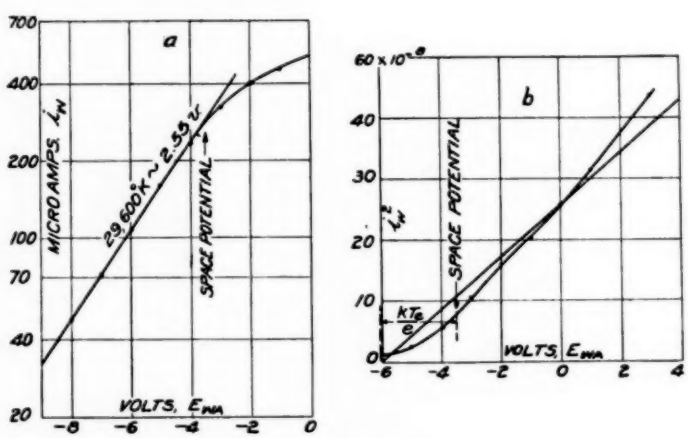

Fig. 6. Electrode volt-ampere characteristics for determining the electron density in the arc.

resonance. Excluding the immediate neighborhood of a resonance, the continual increase in s with increasing ionization intensity gives qualitative confirmation of the continual decrease in K_p with increase in N as required by Eq. (14). The variation in resonance current above 80 m.a. is not understood.

In order to compare the experimental results with the theoretical, it was necessary to determine the ionization intensity as a function of arc current. It developed that the wall electrode, Fig. 3, was unsuited to this purpose since the wall sheaths were too thick over the greater range of arc current. Accordingly, the cylindrical electrode w was employed for this purpose. Fig. 6 exhibits two plots of a typical volt-ampere characteristic. Fig. 6a is the semi-log plot which yields electron temperature and space potential. Fig. 6b is the $i^2 - V$ plot, the "slope" of which gives the electron density. Bearing in mind the ideal shape of this curve as shown by f^2 Fig. 7,[17] it is possible to make a

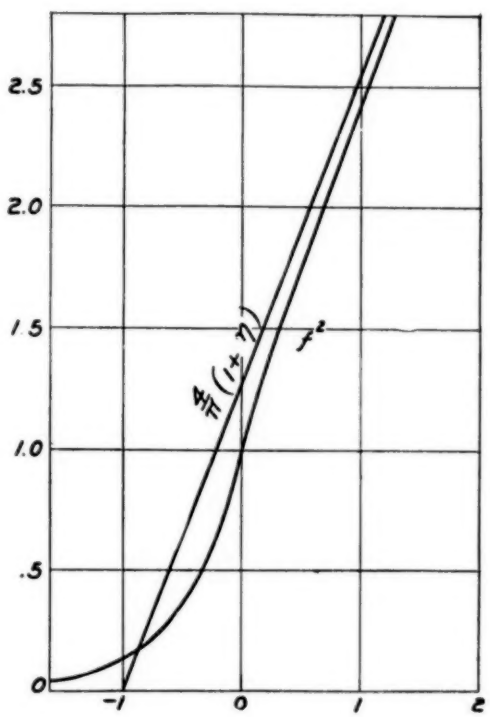

Fig. 7. Theoretical (f^2) volt-ampere characteristic and its approximation $[4(1+\eta)/\pi]$.

very good guess at the straight line whose slope is significant in the following way. This line intercepts the V-axis at the space potential less kT_e/e, the potential corresponding to the electron temperature. The space potential is -3.5 v, $kT/e = 2.5$ v, whence the intersection is at -6 v. The upward bend above zero volts is obviously due to ionization in the sheath. Very little latitude is thus left for drawing the asymptote of the ideal characteristic. As drawn, the slope is 4.3×10^{-8} amps$^2 \cdot$ v^{-1} which gives[18]

[17] Reproduction of Fig. 7 from I. Langmuir and H. M. Mott-Smith, Jr., G. E. Review, p. 617, Sept. (1924).

[18] Eq. (45) I. Langmuir and H. M. Mott-Smith, Jr., G. E. Rev. **27**, 455 (1924) or L. Tonks and I. Langmuir, Phys. Rev. **34**, 913 (1929).

$$n_e = 3.32 \times 10^{11} S^{1/2}/A = 3.32 \times 10^{11} \times 2.07 \times 10^{-4}/0.080$$
$$= 8.6 \times 10^{8} \text{ electrons} \cdot \text{cm}^{-3}$$

Like measurements at other arc currents and mercury pressures gave additional points on the curves of Fig. 8. Of course, at the higher pressures, special care was taken that the tube temperature at all points never fell below the appendix temperature.

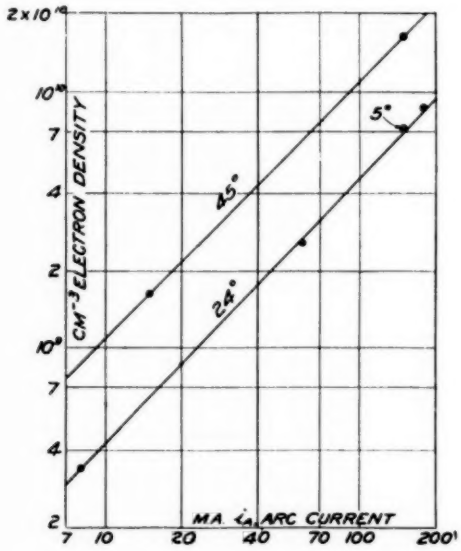

Fig. 8. Electron density in the arc as a function of arc current for different appendix temperatures.

With these data it became possible to correlate the frequency impressed on an ionized gas with the ionization density. The results of several resonance characteristics have been incorporated in Table I and Fig. 9. The "Theoretical Curve—Plane Plasma" is a plot of the equation $\nu = 8980\ N^{1/2}$, ($\omega_0 = \omega$ or

TABLE I. *Relation between plasma-resonance frequency and ionization density.*

Condenser plate size (cm^2)	Temp. (°C)	Frequency ($\times 10^{-6}$)	a-resonance i_a (ma) $N_e \times 159$	b-resonance i_a (ma) $N_e \times 159$	aa-resonance i_a (ma) $N_e \times 159$	Plasma-resonance density, calculated $2\nu^2/(8980)^2$
2.5×2.5	13±	1.59	7.2 0.27	22 0.86		0.63×10^9
2.5×2.5	24	1.59	8.0 0.34	26± 1.12	4.1?	.63
1×1 approx.	24.5	3.66	60. 2.54	145± 6.7	30 1.28	3.30
1×1 "	24	1.60	7.7 0.32	24 1.03	4.3 0.18	.63
1×1 "	24	2.35	21. 0.91	54± 2.28	12. 0.51	1.36
7×7	24	1.60	7.5 0.31	22 0.95		.63
7×7	45	1.60	5.5 0.60	15.5 1.66		.63

$\eta = 1$ in other forms). It gives the theoretical relation between ionization and plasma-resonance frequency for a plane plasma. The "Theoretical Curve—Cylindrical Plasma" is a plot of $\eta = 2$ and gives the same relation for the cylindrical plasma. The *a*-resonance and *b*-resonance curves show the observed behavior of the *a*- and *b*-resonance conditions in a 2.2-bar arc. It is

to be noted that the actual resonance frequency lies within 30 percent of the theoretical and that the slope of the straight lines is 0.42 and 0.45 compared to a theoretical 0.50. The *aa*-resonance is one which appeared at lower ionization densities in cases where the applied field was decidedly non-uniform. While it is possible to imagine that the *b*-resonance may arise primarily from the response of the outer portions of the plasma, and the *a*-resonance from the axial portion, it is rather difficult to account for a third resonance corresponding either to a still higher electron density or to a configuration approaching more nearly to the plane case.

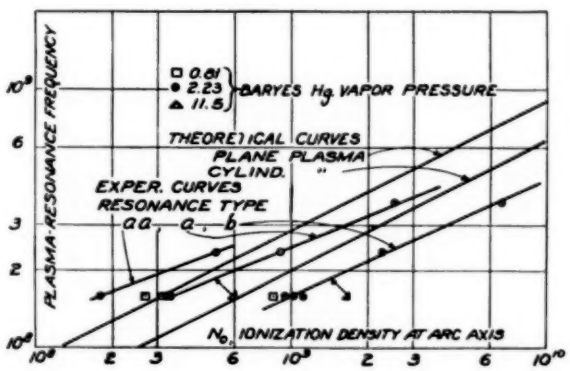

Fig. 9. Comparison of experimental and theoretical plasma-resonance frequencies.

The plasma resonance was found to be somewhat dependent on the gas pressure in the arc. Fig. 9 shows that a 14-fold pressure change caused a 2.2-fold change in resonant density. The resonance density thus varies roughly as the 0.3 power of the pressure. Compared to its variation with the square of the frequency, this is seen to be a small change which may arise from second order effects. It is probably significant that both *a*- and *b*-resonances were affected in the same ratio.

Although exact agreement of theory with experiment is lacking, it seems possible that the method used here may be useful in investigating electron concentration in cases where other methods fail. In recent unpublished work with Ne discharges, for instance, C. G. Found in this laboratory was found that the simple interpretation of probe characteristics fail, probably on account of the specific action of metastable atoms, whereas the present method appears to be directly applicable.

VII. Demonstration That $K_p \propto 1-\omega_0^2/\omega^2$ in the Range $\omega_0^2 > 2\omega^2$

It has been remarked that Eq. (29) can give a direct test of the specific inductive capacity formula. The δL's refer to inductance changes but, in connection with the Lecher system, they may just as well apply to the small changes in tuning length which have been found. Again, since tests have shown that N is very nearly proportional to i_A, we may interpret Eq. (29) as requiring that the reciprocal change in Lecher system tuning length caused by

increasing the arc current from zero to i_A shall be a linear function of the reciprocal of i_A, insofar as θ/θ_∞ is constant. The solid dots of Fig. 10 are plotted in this way from the same data as Fig. 5. At 40 amp^{-1} the imaginary part of K_p is no longer negligible so that Eq. (29) no longer applies, and at the lower values of i_A^{-1}, the curvature of the plot indicates that a correction for variation of θ is necessary.

This correction has been made in the following manner. If the plasma occupies a radius $a-x$ in the tube of radius a, then $\theta/\theta_\infty=(a-x)^2/a^2$ since x, the sheath thickness, approaches zero as i_A approaches infinity. Thus, to a first approximation,

$$\Delta\theta/\theta_\infty = (\theta - \theta_\infty)/\theta_\infty = -2x/a.$$

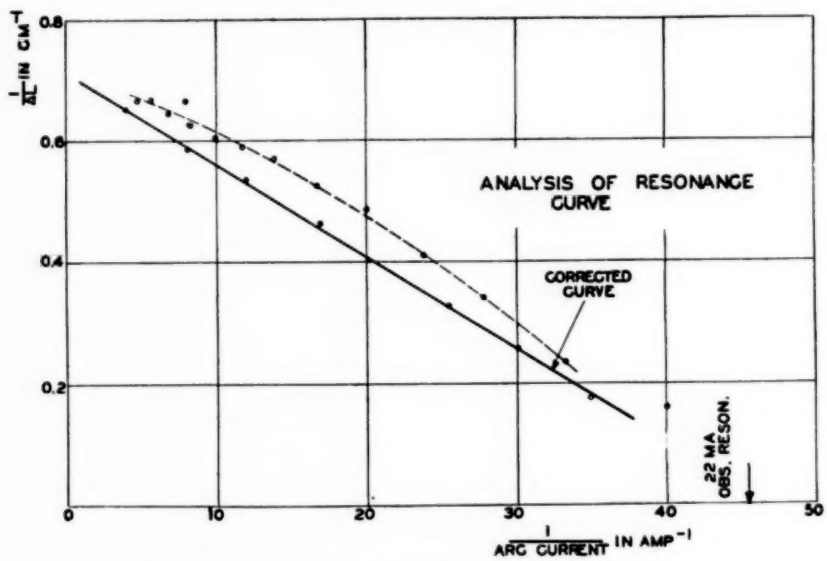

Fig. 10. Analysis of the resonance characteristic in Fig. 5.

Now x is related to I_p the positive ion current density to the wall through the space charge equation

$$I_p = 2.34 \times 10^{-6} V^{3/2}/600x^2$$

or

$$x = 6.25 \times 10^{-5} V^{3/4} I_p^{-1/2}$$

where V is the potential drop in the wall sheath and 600 is $(m_p/m_e)^{1/2}$. Now I. Langmuir and H. M. Mott-Smith, Jr., have found[19] that $I_p \propto i_A^{1.2 \text{ to } 1.3}$ and in the present tube I have found the relation to approximate

$$I_p = 1.08 \times 10^{-3} i_A^{1.4}$$

With $i_A = 0.060$ amp, it was found that $T_e = 28{,}600°$ whence[20]

[19] I. Langmuir and H. M. Mott-Smith, Jr., G. E. Rev. **27,** 764 (1924).
[20] L. Tonks and I. Langmuir, Phys. Rev. **34,** 898 (1929).

$$V = 6kT_e/e = 6 \times 28{,}600/11{,}600 = 14.8v$$

Assuming that V changes but little with i_A (T_e changes but slowly) these equations lead to

$$\Delta\theta/\theta_\infty = -0.0191 i_A^{-0.7}.$$

Substituting $1+\Delta\theta/\theta_\infty$ for θ/θ_∞ in Eq. (29) we have

$$(1 - 0.0191 i_A^{-0.7})\delta L_r^{-1} = (2N_\omega/\delta L_\infty)(\phi N)^{-1} - \delta L_\infty^{-1}.$$

Thus the δL_r^{-1} coordinate of each point should be decreased by an amount directly calculable from i_A. The fractional corrections were tabulated for a series of values of i_A^{-1} and these were applied in several cases to the smooth curve through the experimental points. As in Fig. 10, the resulting curve is always a straight line, the continuation of which intercepts the δL_r^{-1} axis very near to the actual b-resonance, thus confirming Eq. (14). Later Fig. 11, showing θ/θ_∞ as a function of i_A, was plotted and was found useful in subsequent calculations.

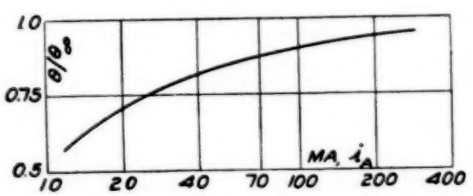

Fig. 11. Fraction of tube cross-section occupied by plasma.

The method here employed, by not requiring that the plasma fill the whole dielectric space, avoids the difficulties of interpretation encountered by Appleton and Childs[21] because of the formation of positive ion sheaths.

VIII. Detailed Analysis of Hg Resonance Characteristics

The resonant Lecher system length as a function of arc current and the thermocouple current as a function of arc current are the two characteristics so far mentioned. Another characteristic which can be obtained is the equivalent series resistance of the composite condenser.

It can be shown[15] that the resonance curve of a Lecher system readily lends itself to determinations of resistance. Let I_0 be the maximum (resonance) current in the thermocouple on the movable bridge and let I be the current at any nearby position s. The values of $[I^{-2} - I_0^{-2}]^{1/2}$ plotted against s give a straight line whose slope S_l in amp.$^{-1}\cdot$cm^{-1} is a measure of the resistance in the circuit. The relation is

$$R\cos^2(2\pi s_r/\lambda) = 2\pi Z_0/S_l I_0 \lambda - R_t \qquad (30)$$

where s_r is the effective length of Lecher system at resonance, R is the equivalent series resistance of the composite condenser, and R_t is the thermocouple resistance, the distributed resistance of the system being neglected.

[21] Appleton and Childs, Phil. Mag. **10**, 969 (1930).

R_t was determined with no current in the arc. The resonance curve at the first resonance, together with $(I^{-2}-I_0^{-2})^{1/2}$ are shown in Fig. 12. Resonance occurred at 11.77 cm. The next resonance occurred at 89.39 cm, giving a wave-length, λ, of 155.2 cm. This compares with 158 cm measured on a sys-

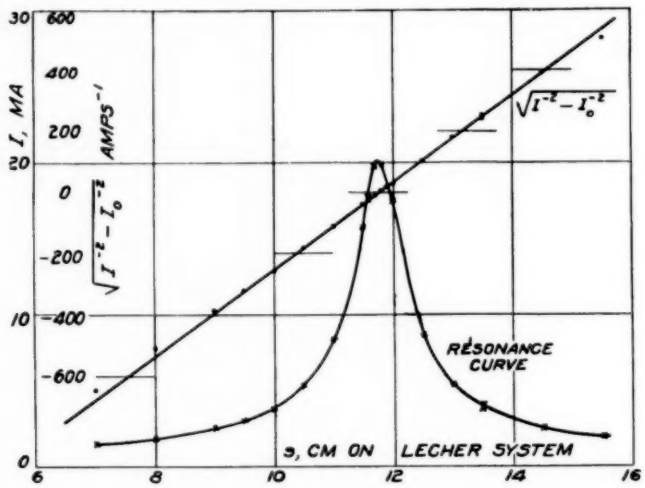

Fig. 12. Lecher system resonance curve and its analysis.

tem almost completely free of excess distributed capacity. The difference is too small to warrant detailed corrections, but in each case where λ appears the value which seems to be the more appropriate will be used.

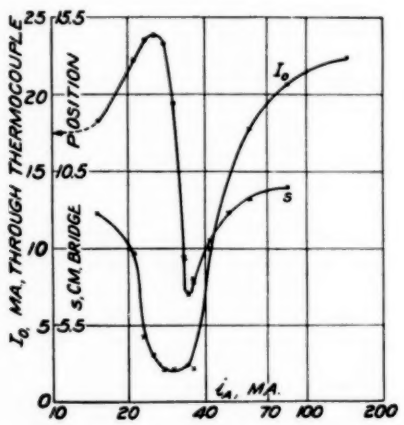

Fig. 13. Resonance characteristic for $\lambda = 158$ cm.

From the figure $S_l = 143$, $I_0 = 0.020$ amp., using $Z_0 = 353$, and $\lambda = 155.3$ we have $R_t = 4.98$ ω. At 89.39 cm the resonance curve yields $R_t = 6.81$ ω. The differences arises from the distributed resistance of the system, but as long as measurements are confined to the neighborhood of the first resonance, it will doubtless be accurate enough to include this resistance in R_t.

Fig. 13 shows the resonance characteristic at this same frequency. For each value of arc current sufficient points (not less than 5) on the resonance curve were taken to permit the slope S_l to be determined. The bridge shortening had been determined by the double-hump resonance method[15] so that s_r could be found from the bridge position. Zero correction and bridge shortening together amounted to +9.2 cm. R was then calculated from Eq. (30), and the values obtained appear in Fig. 14.

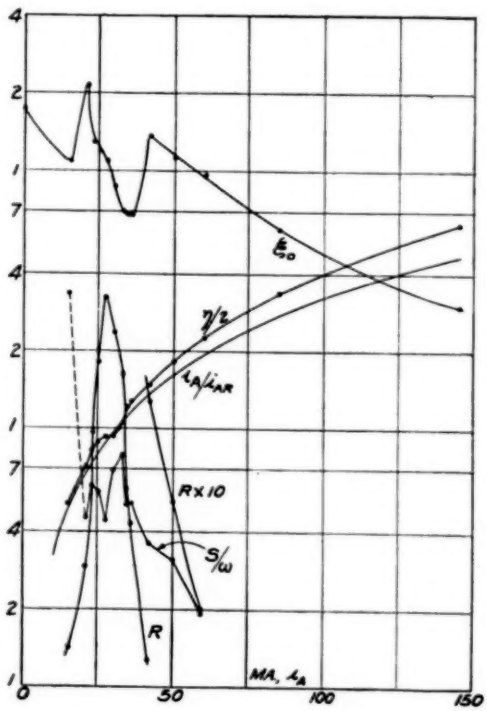

Fig. 14. Analysis of resonance and resistance characteristics.

Ranges: $\xi 0$ from 3.0×10^{-4} to 2.1×10^{-3} cm. $\eta/2$ from 0.51 to 6.2. i_A/i_{AR} is on the same scale. R from 14 to 320 ohms. S/w from 0.02 to 0.33.

It remains to interpret R and s_r in terms of the damping coefficient of the electron oscillations and the density of ionization. The specific inductive capacity K_0 of the composite condenser can be found from s_r readily since

$$\begin{aligned}(\omega K_0 C_0)^{-1} &= Z_0 \tan l \\ (\omega C_0)^{-1} &= Z_0 \tan l_0\end{aligned} \tag{31}$$

where $l = 2\pi s_r/\lambda$ and l_0 is the value of l for $N = 0 (K_0 = 1)$. It follows that

$$K_0 = \tan l_0 / \tan l \tag{32}$$

Thus the problem becomes that of a condenser of a complex capacity C_0K (Eq. (26)) equivalent to the combination, C_0K_0 in series with R;

$$(j\omega KC_0)^{-1} = R + (j\omega K_0 C_0)^{-1}. \tag{33}$$

Substituting from Eq. (26) and separating into real and imaginary parts we have

$$(2S/\omega)(1 - K_0^{-1}) - (\eta/2)\omega C_0 R(1 + \theta) = -\omega C_0 R$$
$$(2S/\omega)\omega C_0 R + (\eta/2)[1 - \theta - K_0^{-1}(1 + \theta)] = 1 - K_0^{-1}$$

whence

$$S/\omega = \theta\omega C_0 R/D \tag{34}$$

$$\eta/2 = [(1 - K_0^{-1})^2 + \omega^2 C_0^2 R^2/D] \tag{35}$$

where

$$D = (1 - K_0^{-1})[1 - K_0^{-1} - \theta(1 + K_0^{-1})] \tag{36}$$

The necessary data are all available. The calculations of R and K_0 have been discussed, $\theta_\infty = 0.056$, and $\omega C_0 = 0.00250$ by Eq. (31). The values of S/ω and $\eta/2$ calculated in this way are shown in Fig. 14. Since theory requires that

$$\eta/2 = N/N_{\text{resonance}} = i_A/0.031$$

very nearly, $i_A/0.031$ has been plotted for comparison. The higher values of $\eta/2$ for the larger values of i_A may well be due to an error in θ_∞. This failed to appear in Fig. 10 since there only relative values of θ were involved. A change to $\theta_\infty = 0.053$ would make $\eta/2$ coincide with $i_A/0.031$ at $i_A = 145$ m.a. and would not spoil the present agreement near resonance. It thus appears that the experimental results confirm the oscillation theory, not only to one side of the resonance region, but even through this region. The check is surprisingly good in view of the non-uniformity of the plasma.

It may be that this factor has more influence on the value of S/ω. Salpeter[10] has shown that collisions of electrons with gas atoms introduce a damping factor in the electron equation of motion and S is then the number of collisions per electron per second. In the present experiment with an electron mean free path of about 3 cm[22] and a speed of 1.22×10^8 cm/sec ($T_e\sim30{,}000°$) $S = 4.1\times10^7$. For a 158 cm wave, $\omega = 1.19\times10^9$, whence $S/\omega = 3.4\times10^{-2}$. On the other hand the electrons are reflected much more frequently from the sheath on the tube wall. Such reflections should, on the average, destroy the directed momentum just as collisions with gas atoms do. In the tube of 3.0 cm diameter, the mean free path for wall collisions may be estimated at 1.5 cm, and the effective speed at $[1.22/(1.5)^{1/2}]\times10^8$ cm sec, whence, due to this cause, $S/\omega = 0.056$. Adding the two dissipation factors we obtain, finally, $S/\omega = 0.090$, a value of the same order as found experimentally. Since the gas density and the electron temperatures change but little with a change in arc current, S/ω should, theoretically, be constant. Aside from experimental errors, which undoubtedly affect the values when R becomes comparable with R_t, that is, above $i_A = 50$ m.a., the non-homogeneity of the plasma may possibly account for a large part of the variation. The high 15-m.a. value may arise from the proximity to the a-type resonance.

[22] T. J. Killian, Phys. Rev. **35**, 1238 (1930), Table I.

Expressed as a decrement, δ,

$$\delta = \pi S/\omega$$

whence, theoretically, $\delta = 0.28$ and the amplitude of a free oscillation would decrease by 24 percent per cycle.

The analysis we have made makes it possible to calculate the electric field in the plasma and the amplitude of the electron motions. From Eqs. (16) and (19)

$$E_p/E_e = (K + 1)/(K_p + 1)$$

from which, using Eq. (20), we find

$$E_p/E_e = \frac{K - 1 - \theta(K + 1)}{-2\theta} = \frac{1 - K^{-1} - \theta(1 + K^{-1})}{-2\theta K^{-1}}$$

for the ratio of the field strength in the plasma to that in the composite condenser. Substituting for K from Eq. (33) we have

$$E_p/E_e = \frac{1 - K_0^{-1} - \theta(1 + K_0^{-1}) - j\omega C_0 R(1 + \theta)}{-2\theta(K_0^{-1} + j\omega C_0 R)} \tag{37}$$

or, in absolute magnitude

$$E_p/E_e = \frac{1}{2\theta}\left\{\frac{[1 - K_0^{-1} - \theta(1 + K_0^{-1})]^2 + [\omega C_0 R(1 + \theta)]^2}{K_0^{-2} + (\omega C_0 R)^2}\right\}^{1/2} \tag{38}$$

Now

$$E_e = V/d$$

where V is the condenser voltage and $d(=7$ cm) is the plate separation. Also

$$v = i_c Z_0 \tan l \tag{39}$$

where i_c is the condenser current, and

$$i_c = i_t \cos l \tag{40}$$

where i_t is the thermocouple current, whence it follows that,

$$E_e = (i_t Z_0/d) \sin l \tag{41}$$

The equation of motion of an electron on which Eq. (4) was based is

$$\ddot{\xi} + S\dot{\xi} = (eZ/m)\epsilon^{j\omega t}$$

whence the amplitude of motion is

$$\xi_0 = 2^{1/2} eE_p/m\omega^2(1 + S^2/\omega^2)^{1/2}$$

on the understanding that E_p is the r.m.s. value. In practical units

$$\xi_0 = 2.50 \times 10^{15} E_p/\omega^2(1 + S^2/\omega^2)^{1/2}$$

and for the present case ($\omega = 1.194 \times 10^9$)

$$\xi_0 = 1.75 \times 10^{-3}(1 + S^2/\omega^2)^{-1/2} E_p.$$

Only at $i_A = 15$ m.a. does S/ω make an appreciable contribution to the radical so that throughout most of the range ξ_0 is proportional to E_p. ξ_0 is plotted in Fig. 14 and it is interesting to note that the greatest amplitude was 1/500 cm. For this amplitude the maximum velocity is $\omega/500 = 0.6 \times 10^6$ cm/sec corresponding to a voltage of $10^{-4}v$.

The valley in the ξ_0 curve between 21 and 42 m.a. certainly arises from the effect of the increased resistance near plasma resonance in decreasing the resonant current in the Lecher System.

The values of S/ω given in Fig. 14 are based on simultaneous measurements of tuning length and resistance. But on the assumption of a uniform plasma, the Lecher System characteristic is, by itself, capable of giving a value of S/ω by using either the maximum variation in L_r (Lecher System tuning length) or the change in i_A accompanying this variation. By setting the derivative of Eq. (27) with respect to η (assuming that variations in θ and ϕ are negligible) equal to zero, we obtain the condition for the extreme values of L_r:

$$\eta' = 2\{1 + S^2/\omega^2 \pm [(1 + S^2/\omega^2)^2 - (1 + S^2/\omega^2)]^{1/2}\}. \tag{42}$$

The difference between the values of η' at the extremes of L_r is, therefore,

$$\Delta\eta' = \phi(N_2 - N_1)/N_\omega = 4[(1 + S^2/\omega^2)^2 - (1 + S^2/\omega^2)]^{1/2} \tag{43}$$

Solving for S/ω, noting that $\Delta\eta'^2/4 \ll 1$,

$$S/\omega = \Delta\eta'/4. \tag{44}$$

At plasma resonance, theory (Eq. (17)) requires that

$$\eta' = 2 = \phi N_r/N_\omega \tag{45}$$

where N_r is the electron density at plasma resonance [7.5]. Combining Eqs. (43), (44), and (45) we have

$$S/\omega = (N_2 - N_1)/2N_r \tag{46}$$

or, in terms of arc current

$$S/\omega = (i_{A2} - i_{A1})/2i_{AR} \tag{47}$$

where i_{AR} is the arc current at plasma resonance. The other relation mentioned is

$$S/\omega = [\delta L_\infty/(L_1 - L_2)]\theta\phi_\infty/\theta_\infty\phi \tag{48}$$

and is deduced by eliminating η' between Eqs. (27) and (42).

Applying these to the present case, Fig. 13 gives,

$$S/\omega = (34.5 - 25.)/2 \times 31 = 0.15$$

in the one case and

$$S/\omega = [1.3/(15 - 6.5)] \times 0.79 = 0.12,$$

in the other. These values are roughly twice as large as the maximum values shown in Fig. 14. This fact together with the asymmetry of the resonance characteristic indicates that other factors may be important here. The analysis of Section II shows, for instance, that if frictional factors were absent, the whole spread $\Delta\eta'$ could be due to a 30 percent variation in electron density.

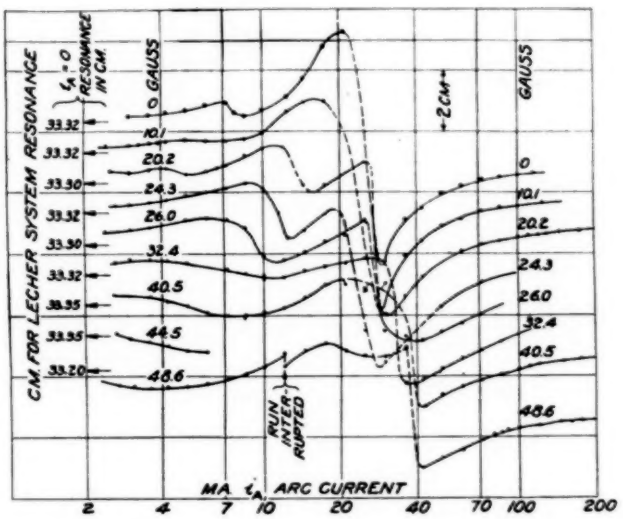

Fig. 15. Effect of transverse magnetic field on plasma-resonance.

IX. The Effect of a Magnetic Field

Appleton and Childs[21] have observed an absorption maximum arising from a constant magnetic field at right angles to the impressed electric field and Benner[23] has observed an accompanying change in dielectric constant. In neither of these cases was the electron density involved as a vital factor. Gutton,[7] however, observed a doubling of the resonance when he applied such a magnetic field to the ionized gas.

Resonance characteristics have been made of the mercury vapor plasma at a succession of magnetic fields. The field used was that from a pair of Helmholtz coils so placed that the oscillating portion of the positive column was in the uniform part of the field. The field was calculated from the coil dimensions as 8.1 gauss·amp.$^{-1}$. The characteristics obtained for a frequency of 1.605×10^9 herz are shown in Fig. 15. The dashed portions of the curves

[23] S. Benner, Die Naturwissenschaften, **17**, 120 (1929).

are those which are doubtful, either because experimental points were not obtained or because the points which were obtained were very uncertain on account of the flatness of the resonance curve. The splitting of the *b*-type resonance is clearly seen for magnetic field strengths from 20.2 gauss up, until at 48.6 gauss the curve begins to take on a more complicated form, due perhaps to the approach to the purely magnetic resonance of Appleton and Childs and Benner. For the frequency used this would occur with a magnetic field of $H = 2\pi mc\nu/e = 56.8$ gauss.

The expectation is that the two resonances will lie one to either side of the original. In the figure only the lower current resonance shows displacement for the smaller magnetic fields. This arises from the concentration of the arc by the magnetic field, which results in higher electron densities for the same arc current when the magnetic field is present.

In analyzing these curves we might proceed along the lines already developed, but more insight into the processes involved can be gained by examining the whole phenomena from a less formal point of view.[24]

Consider a uniform plasma bounded by the sheaths on two plane parallel non-conducting boundary walls. A uniform displacement of the electrons by an amount, ξ, throughout the plasma will develop a surface charge density of

$$\sigma_e = Ne\xi$$

at the sheath edge which exerts the restoring force

$$F_p = -4\pi Ne^2\xi$$

on each electron throughout the plasma. The electrons in the plasma are thus capable of free simple harmonic oscillations in accordance with the equation of motion

$$4\pi Ne^2\xi + m\ddot{\xi} = 0$$

whence the natural frequency is that found for plasma-electron oscillations, Eq. (1).

If the plasma is bounded by a cylinder, and the uniform parallel electron displacements are perpendicular to the axis, the restoring force is only

$$F_c = F_p/2 = -4\pi Ne^2\xi/2$$

and if the boundary is spherical

$$F_s = F_p/3.$$

The natural frequency is lowered in these cases, as has already been seen in the analysis of Section IV.

In proceeding to the case of superposed magnetic field, we may denote this shape factor by ϕ,

$$F = -4\pi Ne^2\phi.$$

[24] J. J. Thomson, Phil. Mag., **11**, 697 (1931) develops the same viewpoint along somewhat different lines.

This factor may be different in the ξ-direction from what it is at right angles to both this direction and the magnetic field. For instance, taking ξ perpendicular to infinite parallel plane boundaries, $\phi_\xi = 1$, while, introducing ζ for the electron displacement perpendicular to both ξ and H, $\phi_\zeta = 0$. In general, then, both shape factors must be included in the treatment. We have,

$$F_\xi = -4\pi N e^2 \phi_\xi \xi - (eH/c)\dot{\zeta} = m\ddot{\xi}$$

$$F_\zeta = -4\pi N e^2 \phi_\zeta \zeta + (eH/c)\dot{\xi} = m\ddot{\zeta}.$$

Putting $\xi = \xi_0 \epsilon^{j\omega}$, $\zeta = \zeta_0 \epsilon^{j\omega t}$, $\omega_H = eH/mc = 1.767 \times 10^7 H$, $\omega_0^2 = 4\pi N e^2/m = 3.18 \times 10^9 N$ and eliminating ζ_0 and ξ_0, we have

$$(\omega^2 - \phi_\xi \omega_0^2)(\omega^2 - \phi_\zeta \omega_0^2) = \omega^2 \omega_H^2,$$

as the condition for resonance. For a circular cylinder with axial magnetic field, $\phi_\xi = \phi_\zeta$ from symmetry, so that we may write

$$(\omega^2 - \phi\omega_0^2)^2 = \omega^2 \omega_H^2.$$

Since N was varied in the experiment to obtain resonance, we solve for the two values of ω_0^2, say ω_1^2 and ω_2^2, which satisfy this equation. It is readily found that

$$(\omega_2^2 - \omega_1^2)/(\omega_2^2 + \omega_1^2) = \omega_H/\omega$$

so that, in terms of arc currents at resonance, i_{A1} and i_{A2},

$$(i_{A2} - i_{A1})/(i_{A1} + i_{A2}) = \omega_H/\omega.$$

Table II based on Fig. 15 shows the agreement between calculated and observed resonance behavior. Columns 4 and 5 should agree. The bad discrep-

TABLE II. *Analysis of magnetic effect.*

H, (gauss)	0	10.1	20.2	24.3	26.0	32.4	40.5	44.5	48.6
i_{A1}, (m.a.)	25	22?	13	11	9	7?	4.5?	3.5?	2.
i_{A2}, (m.a.)			27	22	27	32	37		37?
$\frac{i_{A2}-i_{A1}}{i_{A2}+i_{A1}}$			0.35	0.33	0.50	0.64	0.78		0.90
ω_H/ω			0.35	0.43	0.46	0.57	0.71		0.85

ancy at 24.3 gauss is doubtless due to an erroneous determination of the 25-m.a. resonance on that curve, since this curve fails to fall in line with thetrend of all the others here. Otherwise the agreement is reasonably good.

THE ULTRAVIOLET ABSORPTION SPECTRUM OF SULFUR DIOXIDE

By William W. Watson and Allan E. Parker
Sloane Physics Laboratory, Yale University

(Received April 27, 1931)

Abstract

Measurements of spectrograms of the ultraviolet SO_2 absorption bands taken at different pressures, tube lengths and temperatures together with known infrared and Raman frequencies serve to locate the three fundamental vibrational series. Tables giving the band assignments to these sequences are included. The three lower state frequencies for infinitesimal amplitude are 1369, 1164 and 610 cm^{-1}, while for the excited state the corresponding frequencies are 341, 387 and 290 cm^{-1}. The types of addition series are discussed.

The excited state $\Delta\nu_v$:v curves for $v<4$ have a positive slope, while for $v>4$ there is a sudden reversal to the usual negative anharmonic coefficient. The three ground state frequencies indicate a value of 34° for the half-angle at the apex of the SO_2 triangular model. Comparisons of the heats of dissociation estimated from the extended areas under the $\Delta\nu_v$:v curves with thermal and spectroscopic data suggest the process $SO_2 \rightarrow S+O_2$ for the two symmetrical vibrations and $SO_2 \rightarrow SO+O$ for the asymmetrical vibration. The dissociation products appear to be the same in the two electronic states.

Introduction

UP TO the present time there has been but very little investigation of the details of the ultra-violet band systems of triatomic molecules. Great advances have been made in the study of diatomic molecular spectra with the aid of the quantum theory, but owing to their quite evident complexity, the spectra of polyatomic molecules have been avoided. Many of the ideas of molecular dynamics developed for diatomic molecules should be applicable to more complex molecules, however, and in addition there is now available much information on the fundamental vibrational frequencies of these molecules from their infrared and Raman spectra. Without this previous knowledge of the three fundamental frequencies of the ground state for molecules such as SO_2 and CS_2, the vibrational quantum analysis of their complex electronic band systems would be all but impossible.

The infrared vibration-rotation absorption bands of sulfur dioxide have recently been measured by Bailey, Cassie, and Angus.[1] Their work shows that the three fundamental bands are at 1361 cm^{-1}, 1152 cm^{-1}, and 606 cm^{-1}, but since a sufficient number of harmonic bands were not observed, the fundamental frequencies for infinitesimal amplitude of vibration could not be computed. The first and third of these frequencies correspond to a vibrating electric doublet lying along the bisector of the vertical angle of the triangular structure, while the middle frequency corresponds to an effective electric

[1] C. R. Bailey, A. B. D. Cassie, and W. R. Angus, Proc. Roy. Soc. **A130**, 142 (1930).

doublet in a direction perpendicular to this bisector and in the plane of the triangle. Both the existence of a rather large permanent dipole moment and the indicated structure and intensity of these infrared bands lead to the conclusion that the SO_2 molecule is definitely triangular in shape with an acute angle at the apex. The Raman spectrum of gaseous SO_2 has been investigated by Bhagavantam[2] who found but one line at 1154 cm^{-1}, whereas for liquid SO_2 Dickinson and West[3] find the three lines 1145.9 cm^{-1} (strong), 1340.1 cm^{-1} (medium, diffuse) and 524.3 cm^{-1} (weak, diffuse). The last line is explained by Bailey, Cassie, and Angus as the difference 1152–606.

The ultraviolet absorption bands of sulfur dioxide have been referred to by Henri[4] and others. The apparent predissociation limit at about λ 2525 (112,000 cal.) has been assumed by Henri[5] to correspond to $SO_2 \rightarrow SO + O$, and on this basis he develops an energy equation with other known data to give the heat of dissociation of O_2 as 126,400 cal. (5.5 volts). This calculation has been discussed by Herzberg[6]; and we return to the question in our discussion below.

Description of Spectrum

The ultraviolet absorption band systems of sulfur dioxide have been photographed with a Hilger E_1 quartz spectrograph, the gas being contained in a glass absorption tube 111 cm long, closed at the ends with quartz windows. The SO_2 was prepared by dropping HCl on to $NaHSO_3$, and was dried by passing through a long P_2O_5 tube. The source of continuous radiation for the background was the usual hydrogen discharge tube. The spectrograms with this 111 cm absorption cell were all taken with the gas at room temperature and at pressures varying from 80 cm to less than 1 mm Hg. Spectrograms were also obtained with a 27 cm absorption cell with the SO_2 at 1 cm Hg pressure and at the temperature of a solid CO_2-acetone mixture.

Fig. 1 is a reproduction of a series of spectrograms taken at various gas pressures with the longer absorption tube. To be noted are the evident strong series of band groups in the main absorption region, and the appearance of new bands at the long wave-length end at the higher pressures. These latter bands do not form a separate band system, as has been suggested by Henri[5]; but are associated with the main absorption system and represent transitions from vibrational levels with $v = 1$, 2 and 3 of the ground electronic state. At the lower temperature the very weak band at 30961 cm^{-1} is clearly the band of longest wave-length, suggesting that it is a 0,0 band, and there is considerable simplification in the region of strongest absorption. At the high frequency end of this system, absorption ceases at the lower pressures at about λ2500, the last bands being rather diffuse but with no continuous absorption in evidence. Another SO_2 band system which we have not investigated extends from about λ2350 farther into the ultraviolet. At pressures greater than

[2] S. Bhagavantam, Nature **126,** 995 (1930).
[3] R. G. Dickinson and S. S. West, Phys. Rev. **35,** 1126 (1930).
[4] V. Henri, Structure des Molecules.
[5] V. Henri, Nature **125,** 272 (1930).
[6] G. Herzberg, Zeitz. f. Physikal. Chemie **B10,** 189 (1930).

1 cm these two band systems are fused together, the absorption being continuous from the limit of the discrete bands to be seen in Fig. 1 to some point in the vacuum ultraviolet region.

Some of the stronger and more isolated bands at about λ3300 were photographed at high dispersion with a 21-foot concave grating, but these spectrograms fail to resolve any of the rotational structure. Furthermore these SO_2 bands do not have a sharp head, but rather seem to fade out on both sides. In the measurement of the lower dispersion spectrograms, then, we could only set the cross-hair on the estimated center of the band or, in the case of broad bands produced by overlapping, the overall width was measured. This of

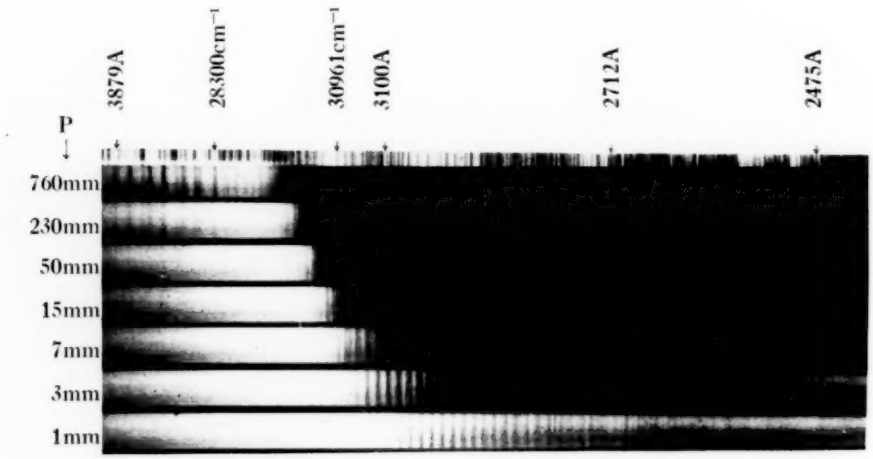

Fig. 1. Spectrograms of the ultraviolet SO_2 absorption bands taken with the Hilger E_3 spectrograph. The absorption path was 1 m, and the pressures were as indicated. To be noted are the group of bands at the red end of the high pressure spectrograms and the evident excited state sequences proceeding towards higher frequencies from 30961 at the lower pressures. Higher dispersion plates show that many of these apparently single bands are in reality groups of bands.

course limits the accuracy of the measurements, and entails a possible error in the interval between any two successive bands in the series referred to below, of say, 9 or 10 cm^{-1}.

Vibrational Analysis

The regular and intense series of bands observable in the region from λ3200 to λ2900 on the spectrograms for the lowest SO_2 pressures can only be vibrational sequences in the excited electronic state. These and other series terminate on the long wave-length end at about λ3230 in a region of bands of very low intensity, suggesting that the origin of the system is at about this frequency. Now in the high-pressure group to the red of this point the first strong band to appear with increasing gas pressure is at 28300 cm^{-1}. Assuming that this represents a transition from a lower vibrational level other than 0 of the symmetrical mode of vibration, another band is found at 29621, 1321 cm^{-1} to the high frequency side, from which the interval to 30961, which is the

long wave-length end of the strongest excited state sequence, is 1340 cm^{-1}. From these regularities as a starting point, the double array of bands originating in this (v_1', v_1'') mode of vibration as presented in Table I were found. Measurement towards the violet from the 28,300 band with differences characteristic of the asymmetric mode of vibration (1150 cm^{-1}), however, does not produce any correlation.

TABLE I. *Fundamental series corresponding to the 1369 cm^{-1} vibration.*

v_1' \ v_1''	0	1	2	3	Average $\Delta\nu$
0	30961	29621	28300	27002	
					360
1	31327	29979		27359	
					389
2	31719	30365	29043		
					430
3	32145	30801	29472		
					471
4	32619	31270	29942		
					487
5	33103	31757	30432		
					468
6	33571	32230	30895		
					458
7	34026	32683	31361		
					434
8	34461	33118	31793		
					424
9	34888	33539	32218		
					423
10	35318	33969	32638		
					420
11	35738	34390	33058		
					390
12	36130	34774	33451		
					384
13	36514	35156	33836		
					362
14	36876	35522	34193		
					354
15	37230				
					344
16	37574				
					329
17	37903				
Average $\Delta\nu$		1348	1326		

It was then to be assumed that the next strongest series of bands proceeding to the high frequency side of the origin is the $v_2''=0$ sequence belonging to the asymmetrical (1150 cm^{-1}) vibrational frequency. There is indeed a band at about this interval on the red side of each of these bands of the $v_2''=0$ sequence, and in this way the fundamental sequences given in Table II were developed. Now it is impossible to have these two double arrays of bands proceed from the same 0,0 band, although they must correspond to the same electronic energy change in the molecule. But if the two sets of frequencies are represented by an equation such as (1) with half-integral vibrational quantum numbers, they both yield the same electronic frequency $\nu_e=31468$.

TABLE II. *Fundamental series for the* 1164 cm^{-1} *vibration.*

v_2' \ v_2''	0	1	2	Average $\Delta\nu$
0	31074	29932	28802	
				413
1	31498	30343	29208	
				435
2	31928	30779	29648	
				462
3	32393	31241	30108	
				475
4	32865	31719	30584	
				454
5	33324	32169	31036	
				456
6	33771	32628	31498	
				433
7	34210	33058	31929	
				432
8	34634	33491	32367	
				413
9	35048	33901	32781	
				401
10	35438	34312	33183	
Average $\Delta\nu$	1148	1130		

TABLE III. *Fundamental series for the* 606 cm^{-1} *vibration.*

v_3' \ v_3''	0	1	2	3	Average $\Delta\nu$
0	31308	30700	30103	29499	
					298
1	31607	30999	30394	29798	
					303
2	31910	31298	30700	30103	
					308
3	32218	31607	31008	30412	
					298
4	32513	31907	31308		
					285
5	32797	32193	31592	30999	
					272
6	33071	32463	31864	31270	
					254
7	33328	32719	32116	31521	
					253
8	33578	32977	32367		
					228
9	33802	33204	32601		
					221
10	34026	33423	32820		
					215
11	34242	33640	33037		
					207
12	34449	33846	33246		
					181
13	34634	34026	33423		
					169
14	34805	34193	33591		
					170
15	34971	34367	33759		
Average $\Delta\nu$	605.5	601	596		

This affords experimental proof of the existence of zero-point vibrational energy. It is therefore not possible to represent these SO_2 bands by a double vibrational formula such as found by Henri and Howell[7] for the ultraviolet absorption bands of phosgene.

Knowing the ν_e frequency and the third fundamental vibration frequency 606 cm^{-1}, for the lowest electronic state, it was possible to predict the 0,0 band frequency for this mode of vibration to within about 100 cm^{-1} by assuming that the corresponding excited state frequency must lie within the limits 150 to 350 cm^{-1}. Investigation showed that for but one band, 31308, in this predicted interval did another band lie 606 cm^{-1} to the red with still another spaced 600 cm^{-1} further to the red. Placing this 31308 in Eq. (1) with $v_3'=v_3''=0$ the excited state vibrational interval was computed to be very closely 300 cm^{-1}. This proved to be correct, and the other bands in this third double array as given in Table III were easily arranged. This $v_3''=0$ sequence is not obvious from inspection of the spectrograms as for the other two $v''=0$ sequences. However, this is in agreement with the fact that the 606 cm^{-1} fundamental absorption band in the infrared is much weaker than the other two.[1]

These three sets of fundamental vibration progressions can be represented by an equation of the type

$$\nu = \nu_e + [a'(v'+\tfrac{1}{2}) + b'(v'+\tfrac{1}{2})^2] - [a''(v''+\tfrac{1}{2}) + b''(v''+\tfrac{1}{2})^2] \quad (1)$$

with $\nu_e=31468$. For all three sets of progressions, however, the excited state differences first increase to a maximum at about $v'=4$, after which they decrease in the regular manner (see discussion below). It is therefore necessary to use different a' and b' constants for the low and high values of v'. The mean values of the a and b constants which fit the three sets of band progressions are given in Table IV.

TABLE IV. *Fundamental vibrational constants for SO_2 (cm^{-1} units).*

	ν_1	ν_2	ν_3
a''	1369	1164	610
b''	−11	−9	−2.3
a'	+341	+387	+290
b'	+14 $\}\nu_1 \leqq 4$	+12 $\}\nu_2 \leqq 3$	+3 $\}\nu_3 \leqq 3$
a'	+556	+524	+350
b'	−7 $\}\nu_1 > 4$	−6 $\}\nu_2 > 3$	−7 $\}\nu_3 > 3$

All of the sequences in Tables I to III could be extended farther towards higher frequencies, but our accurate measurements do not extend into this region. However, it is obvious that these series account for only some 20 percent of the observed bands of which there are well over six hundred. Now only three fundamental frequencies are possible for a triatomic molecule, but we know from the study of the infrared bands of polyatomic molecules that addition frequencies occur. We have made plausible assignments of most of the

[7] V. Henri and O. R. Howell, Proc. Roy. Soc. **A128,** 192 (1930).

remaining bands to various forms of addition series based on the three fundamental series, but these assignments are not unambiguous in many cases because of the density of bands and because of the lack of any guide such as the greater intensity of the $v''=0$ sequences of the main series. Our analysis shows however that there are addition bands present of the type for which addition of one or two quanta of any one of the three modes of vibration happens simultaneously in both electronic states to either of the other two main series. Some of the weaker bands are probably also due to an S isotope effect, but we have not been able to make any assignments on this basis.

Discussion of Results

Fig. 2 is a plot of the course of the vibrational energy level differences in the three sets of excited state levels as a function of v. The unusual feature of these curves is the initial positive slope. During the accretion of these first

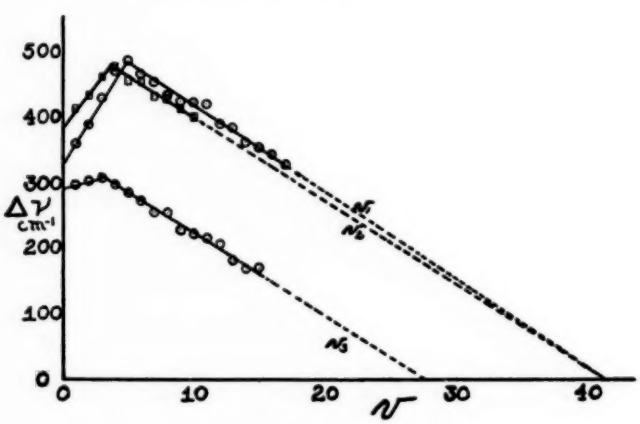

Fig. 2. Diagrams of the spacings of the excited state vibrational levels for the three fundamental modes of vibration. The interesting feature is the initial positive slope for each of the curves.

quanta of vibrational energy, the molecule, as it were, increases in stability, and then some rearrangement occurs after which the usual negative anharmonic term is operative. This phenomenon has been noted in only one instance for diatomic molecules, in the LiH spectrum[8]; but it is possibly of rather common occurrence for polyatomic molecules.[9]

In the ground electronic state of SO_2 the vibrational frequencies decrease in the usual manner with increasing v''. But since this spectrum originates in absorption by a cold gas, only the levels $v''=0$, 1 and 2 are represented. The anharmonic coefficients b can therefore not be determined with great accuracy, but they do allow an approximate determination of the vibrational

[8] G. Nakamura, Zeits. f. Physik **59**, 218 (1930)

[9] Positive slopes of the $\Delta\nu$:v curves, but without the maximum and subsequent negative slope, have been reported by H. D. Smyth and T. C. Chow (Abstract, Phys. Rev. **37**, 1023 (1931)) for CO_2 and by G. B. Kistiakowsky (Phys. Rev. **37**, 276, 1931) for C_2H_2.

frequencies for infinitesimal amplitude (the a'' constant in Eq. (1)) which could not be computed from the infrared absorption data.[1] Substitution of these three a'' frequencies in the determinant equation for the vibrational energy of a symmetrical triatomic molecule as given by Dennison[10], yields for α the half-angle at the apex of the isosceles triangle (cf. Fig. 3), the approximate values of 34° and 51°. Owing to the intensity relations in the infrared bands requiring an acute angle,[1] the lower of these two values is to be chosen. The vibrational frequencies a' of the excited state, however, give only imaginary solutions for this angle when placed in this equation.

Some conception of the values of the heats of dissociation for the SO_2 molecule can be obtained from the determination of the areas under the $\Delta\nu_v : v$ curves extrapolated to the convergence limit. The areas under the extrapolations are a rather large part of the whole energy, thereby limiting the accuracy of the calculation. This is particularly true of the lower electronic

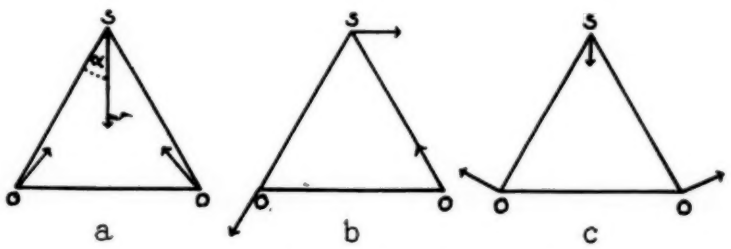

Fig. 3. Representation of the three fundamental SO_2 vibrations. *a*, the symmetrical 1369 cm^{-1} frequency; *b*, the asymmetrical 1164 cm^{-1} frequency; *c*, the symmetrical 610 cm^{-1} frequency. These three frequencies indicate α to be approximately 34°.

state values, but nevertheless the results of the computation are of some interest. One obtains the following heats of dissociation (excited state values are the sum of the areas under the curves of Fig. 2 and $\nu_e = 3.9$ volts):

Lower state:	$H_{v_1} = 5.3$	volts	(121,000 cal.)
	$H_{v_2} = 4.7$	"	(107,000 cal.)
	$H_{v_3} = 5.1$	"	(118,000 cal.)
Excited state:	$H_{v_1} = 5.2$	"	(120,000 cal.)
	$H_{v_2} = 5.3$	"	(121,000 cal.)
	$H_{v_3} = 4.3$	"	(99,000 cal.)

We picture the vibrations occurring after the manner of Fig. 3. For the two symmetric modes of vibration the dissociation products would be an S atom plus an O_2 molecule. One might expect a measure of agreement between these values and that obtained from thermal data. The heat of formation of SO_2 from sulfur vapor S_2 and O_2 is given as 69,260 calories. The heat of dissociations of S_2 is known from spectroscopic data to be 102,200 calories.[5] Hence

[10] D. M. Dennison, Phil. Mag. **1**, 203 (1926).

$$SO_2 \rightarrow \tfrac{1}{2}(S_2) + O_2 - \frac{102200}{2} - 69260 = \tfrac{1}{2}(S_2) + O_2 - 120360.$$

The agreement with our lower state H_{v_1} and H_{v_3} values is better than could be expected.

For the asymmetric mode of vibration the dissociation is probably into SO+O. Now the heat of dissociation of SO has been determined for the normal state of the ultraviolet SO band system by Henri and Wolff[11] as 148,000 cal. The value for O_2 should be approximately 5.1 volts.[6] Therefore one can write the energy equation

$$SO_2 \rightarrow SO + O - H_{v_2} = S + O + O - 148{,}000 - H_{v_2}$$
$$= \tfrac{1}{2}(S_2) + O_2 - 69260 - \frac{102200}{2} - 117300.$$

This requires H_{v_2} to be about 90,000 cal. as against our value of 107,000 cal. The discrepancy may be in part due to the fact that the SO radical after the dissociation has a considerable amount of vibrational energy. In fact, the distortion in the dissociation process should most certainly produce some vibration of the SO, the energy of which should be subtracted from our extrapolated H_{v_2} value to give the true heat of dissociation.[12]

Judging from the relative values of the computed heats of dissociation for the two electronic states of SO_2 involved, apparently the dissociation products are in both states the same. But because of the possibility of a considerable error in these values due to the large extrapolation, this statement should be made with reservations.

A considerable amount of information may be expected from the study of the ultraviolet band systems of the simpler polyatomic molecules. When the bands have sharp heads, as for example in the CS_2 system on the analysis of which we are now engaged, the accuracy of the measurements can be considerably improved. For absorption bands the rotational fine structure may not be resolvable even at the highest dispersion. But if obtained as emission bands, the theoretical resolving power of a large grating can be more nearly approached, and the rotational line pattern of some of the simpler polyatomic bands may be obtained. In that event the needed test of the theoretical treatment of the rotator with three different moments of inertia as given by Kramers and Ittmann[13] and others may be made.

[11] V. Henri and F. Wolff, Jour. de Phys. et Rad. **10,** 81 (1929).

[12] R. M. Badger and J. L. Binder, Phys. Rev. **37,** 800 (1931) have suggested this explanation for a similar discrepancy in the case of the HCN infrared bands.

[13] H. A. Kramers and G. P. Ittmann, Zeits. f. Physik **58,** 217 (1929).

FURTHER STUDY OF THE ABSORPTION OF INFRARED RADIATION BY WATER VAPOR

By E. K. Plyler and W. W. Sleator
University of Michigan

(Received April 8, 1931)

Abstract[1]

Making use of a spectrometer with a salt prism and echelette gratings, and a Moll thermal relay, the authors have reexamined with increased resolution the four absorption bands of water vapor whose centers lie near 1.87μ, 2.66μ, 3.15μ and 6.26μ. The new study has greatly increased the number of measured lines. Near 6.26μ and 3.17μ the number has been more than doubled. The new lines are mostly weak ones, but the work has resulted in a better determination of the wave-lengths of many strong lines, which now appear as sharp single effects freed from the former confusion in which several lines were taken for one. The center of the harmonic of the band at 6.26μ is seen to be better placed at 3.168μ than it was formerly at 3.11μ. It also appears that this band has no absorption at the center, and is of the same type as the fundamental.

Introduction

THE work to be described in this paper was done at the University of Michigan during the summers of 1928, and 1929, and the fall of 1930. It was found, after working over the atmospheric absorption near 2.66μ, that the apparatus now available, because of the higher resolution of which it is capable, permitted a more precise and complete analysis of the absorption spectrum of water than had been given in the papers by Sleator[2] and Sleator and Phelps.[3] A real advance may be claimed when what was formerly considered to be, and measured as, a single line, proves, as the present work in many cases shows, to consist of three or four. Furthermore many of the lines now given in the charts and tables are very sharp, and many more lines show in these figures quite the same shape, and this indicates that they are single effects, and not likely to break up on more refined analysis. On account of this better identification, and on account of more accurate calibration now employed, there is reason to think that the wave-lengths here given are more precise than the earlier numbers, which they should supplant.

Of the bands here studied, those near 6.26μ and 2.66μ have been classified as fundamentals, with vibration frequencies ν_1 and ν_2 respectively, the latter having a zero branch, the former being double. The frequency at 1.87μ represents the combination $\nu_1+\nu_2$ and that at 3.16μ is $2\nu_1$, so that this band is the first harmonic of that at 6.26μ. A classification of the known absorption bands of water has been given by Hettner.[4]

[1] This abstract appeared in the Bulletin of the American Physical Society of November 15, 1930, announcing the Chicago Meeting.

[2] W. W. Sleator, Astrophys. J. **48,** 125 (1918). References to earlier work are given in this paper.

[3] W. W. Sleator and E. R. Phelps, Astrophys. J. **62,** 28 (1925).

[4] G. Hettner, Zeits. f. Physik **1,** 345 (1920).

Experimental Procedure

The apparatus used was the compound spectrometer with sodium chloride prism and grating in series, of the type commonly used for work in the infrared, constructed and described by Meyer.[5] The grating used for the band at 6.26μ had 2,880 lines per inch, that employed for the others had 7,200. They were ruled by Barker. The thermopile was constructed and has been described by Firestone.[6] By adjusting the lamp which illuminates the thermocouple in the Moll relay the amplification factor could be controlled, and could be brought up to 300 by using a current of 3.5 amperes. At this amplification Brownian motion could be observed, so that four or six, sometimes eight, independent deflections of the galvanometer were taken at each setting of the grating. Small vibrations of the building due to the wind and other things affected the galvanometer. It was necessary to take most of the readings at night.

The spectrometer circle was set at a certain angle, then the deflections were read, then the circle was turned 15 seconds, and deflections taken again. This was continued through the region—that at 6.26μ extended over about 6 degrees. The graph which revealed the absorption lines was plotted with average deflection as ordinate, and angle or wave number as abscissa. The determination of the wave-length of a line depends in most cases upon three independent energy curves—in some cases more.

The step by which the circle was advanced between successive galvanometer readings was less than the angular value of the slit itself. In Table I, the data of which are given separately with the different figures, the degree of resolution used in the different bands is shown by giving the wave-length interval included in the second slit. Values used by Sleator and Phelps are shown for comparison.

Table I. *Effective resolving power.*

Region	Slit width (A.U.)	Slit width (cm^{-1})	Slit width (Sleator and Phelps) (A.U.)
1.87μ	4.1	1.16	8
2.66μ	3.1	0.44	
3.15μ	4.5	0.45	32
6.26μ	17.	0.45	80

The observations in this work were made upon the absorption by the water vapor in the air of the room. For the bands at 1.87μ and 3.16μ the absorption did not anywhere exceed forty percent, and it was not necessary to remove any moisture. In the other bands, however, there were very strong lines which could not be separated. In order to reduce the amount of water present a rough box was built around the spectrometer and phosphorus pentoxide was exposed inside. The effect of such drying is shown, for example, by the

[5] Aaron Levin and Charles F. Meyer, J.O.S.A. and R.S.I. **16,** 137 (1928).

[6] F. A. Firestone, Rev. Sci. Inst. **1,** 630 (1930).

inserted sections near line No. 177 in the curve of Fig. 5. Drying the air made it possible to separate and identify the lines. The pressure of water vapor in the undried air was 20 to 30 mm. In the dried air it was 2 to 3 mm. Fig. 3 also represents the energy curve near 2.66μ with dried air. Lines nos. 22, 23 and 24, for example, are better defined in this figure than in Fig. 2, which refers to the normal indoor atmosphere.

Results and Discussion

The measurements made during this work appear in the curves of the following figures, and in the tables. The tables show an arbitrary number for each line, and its relative intensity, wave-length, and wave-number. The relative intensities represent estimates only, based upon the depth of the lines. In many cases this estimate has been difficult and uncertain, because a certain line may represent only a weak absorption upon the side, so to speak, of a deeper and wider line, or it may represent a stronger effect if its neighbor is in fact a weaker one. Line number 35 in Figure 3, for example, has been assigned a relative intensity of 50 percent. But if it is really only a nick in the curve which shows No. 36 it ought to be marked, perhaps, 15 percent. In all cases where two lines over-lap there is doubt about the intensity of each. This composite effect, which partly disappeared when the air was dried, made it impossible to use the criterion of the area of the notch for estimating intensity. Improvement of the present analysis of the water spectrum demands first of all an enclosed spectrometer and absolute control of the amount of the absorbing medium. Second, it demands a resolution even higher than we could command.

When the amount of moisture was reduced by the means described, many lines in all the bands were made more narrow and sharp. On advancing the circle 15 seconds, the galvanometer deflection changed in may cases by 40 mm—say from 100 to 60. An error of 5 seconds in setting might affect the deflection by 15 mm. This unavoidable uncertainty of perhaps 5 seconds in setting may account for the difference in relative intensities of two lines as they appear in different curves, so that in one graph *a* is stronger than *b*, in another not so strong.

Figure 1 and Table II represent our study of the band at 1.87μ. Many new lines have appeared, for example line No. 48 in Fig. 5 of the paper of 1925 seems now to be a composite effect of those numbered 81, 82, and 83. There is no way of deciding what wave length, with the amount of water uncontrolled, such a combination ought to have. Accordingly there is no satisfactory basis for comparison of wave-lengths. In general, however, the new values are larger.

It may be remarked here that the numbers assigned to the lines are arbitrary. Also we have omitted numbers from all the tables at places where there are faint lines of uncertain positions, to which we cannot assign definite wave lengths.

In work done at Johns Hopkins University by Barnes[7] the energy of a

[7] R. Bowling Barnes, Phys. Rev. **36,** 296 (1930).

source of radiation was mapped in the region between 3 and 4μ. It shows two bands of atmospheric absorption, one of them with center near 3.73μ. With

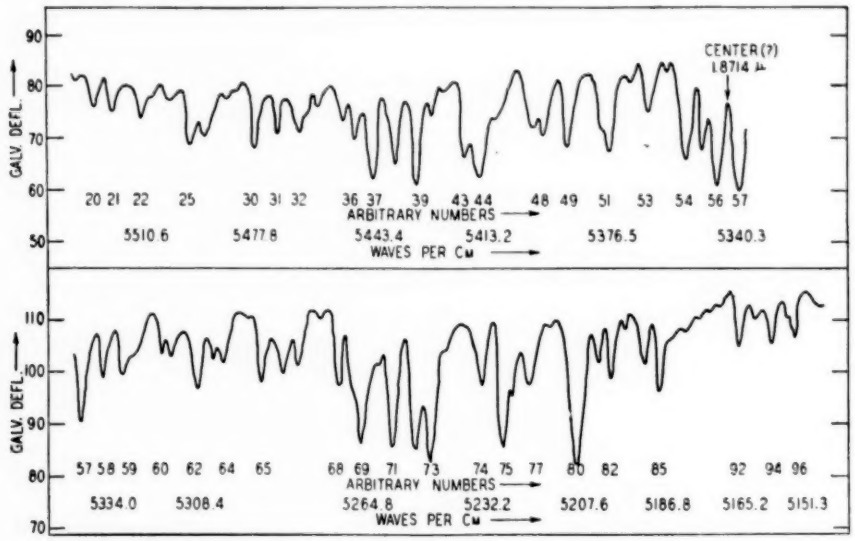

Fig. 1. Energy curve, region of 1.87μ, middle part. Echelette grating, 7200 lines per inch. Slits 0.12 mm, 12.4 secs, 1.16 waves per cm, 4.1A.

TABLE II. *Region of* 1.87μ.
Arbitrary numbers, relative intensities, wave-lengths, and wave-numbers of the stronger lines.

Line No.	Rel. int.	Wave-length	Wave-number	Line No.	Rel. int.	Wave-length	Wave-number
20	10	18100	5524.9	57	35	18725	5340.5
21	10	18117	5519.7	58	20	18747	5334.2
22	10	18146	5510.8	59	20	18769	5327.9
24	5	18174	5502.4	60	10	18801	5318.9
25	15	18194	5496.3	61	10	18811	5316.0
26	15	18209	5491.8	62	15	18837	5308.7
28	5	18229	5485.8	63	10	18851	5304.8
30	15	18255	5477.9	64	10	18865	5300.8
31	10	18278	5471.1	65	15	18900	5291.0
32	10	18300	5464.5	66	15	18920	5285.4
34	5	18318	5459.1	67	15	18934	5281.5
35	10	18342	5452.0	68	15	18974	5270.4
36	10	18352	5449.0	69	25	18994	5264.8
37	25	18370	5443.7	71	25	19025	5256.2
38	20	18392	5437.1	72	25	19048	5249.9
39	25	18412	5431.2	73	30	19063	5245.8
40	5	18428	5426.5	74	15	19112	5232.3
43	15	18459	5417.4	75	25	19132	5226.8
44	25	18473	5413.3	77	15	19158	5219.8
47	10	18525	5398.1	80	30	19202	5207.8
48	15	18535	5395.2	81	10	19225	5201.5
49	20	18557	5388.8	82	15	19235	5198.9
51	25	18599	5376.6	84	10	19269	5189.7
53	15	18636	5366.0	85	15	19279	5187.0
54	30	18672	5355.6	92	10	19360	5165.3
55	25	18688	5351.0	94	10	19391	5157.0
56	30	18703	5346.7	96	10	19412	5151.5

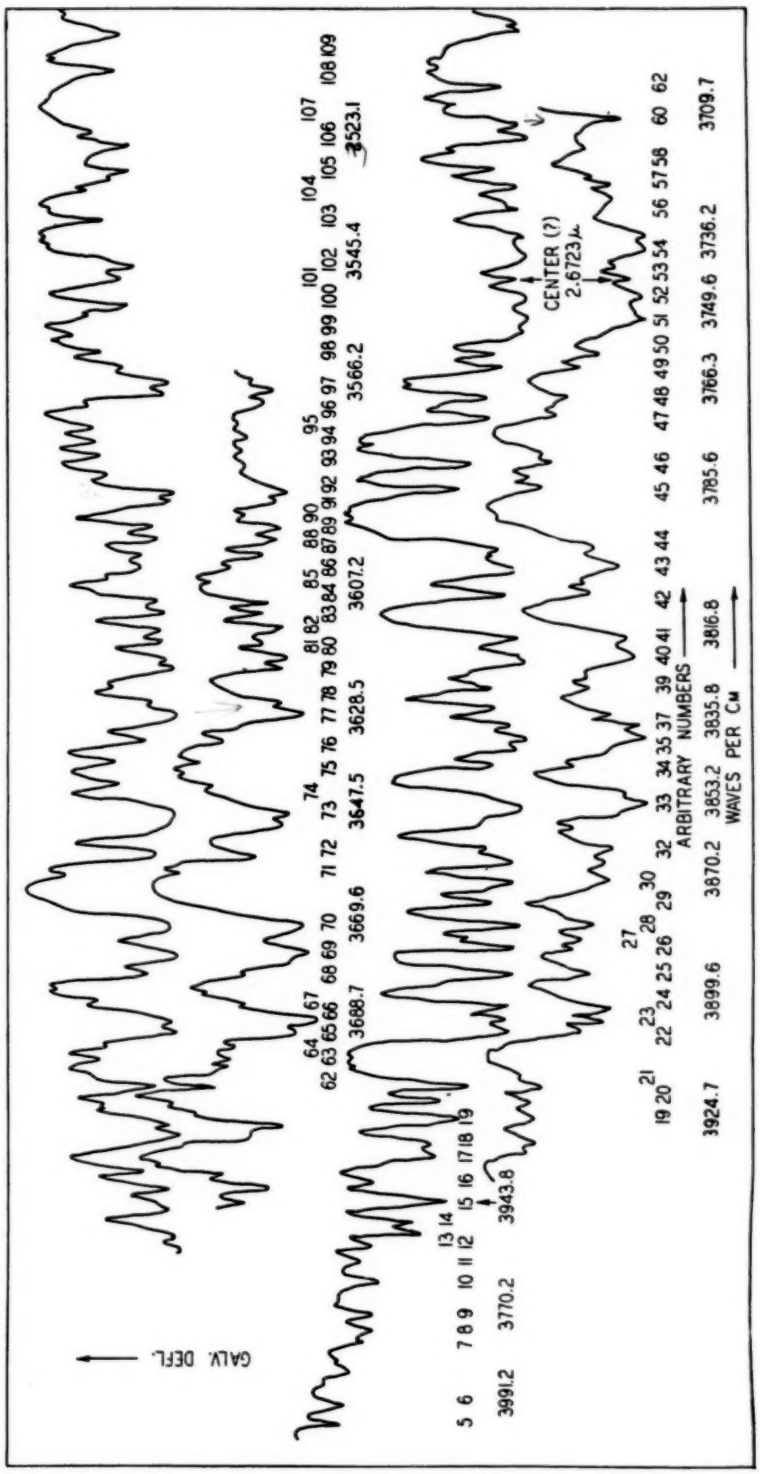

Fig. 2. Part of the energy curve, region of 2.66μ, two independent series. Echelette grating, 7200 lines per inch. Slits 0.1 mm, 10 secs, 0.44 waves per cm, 3.1A.

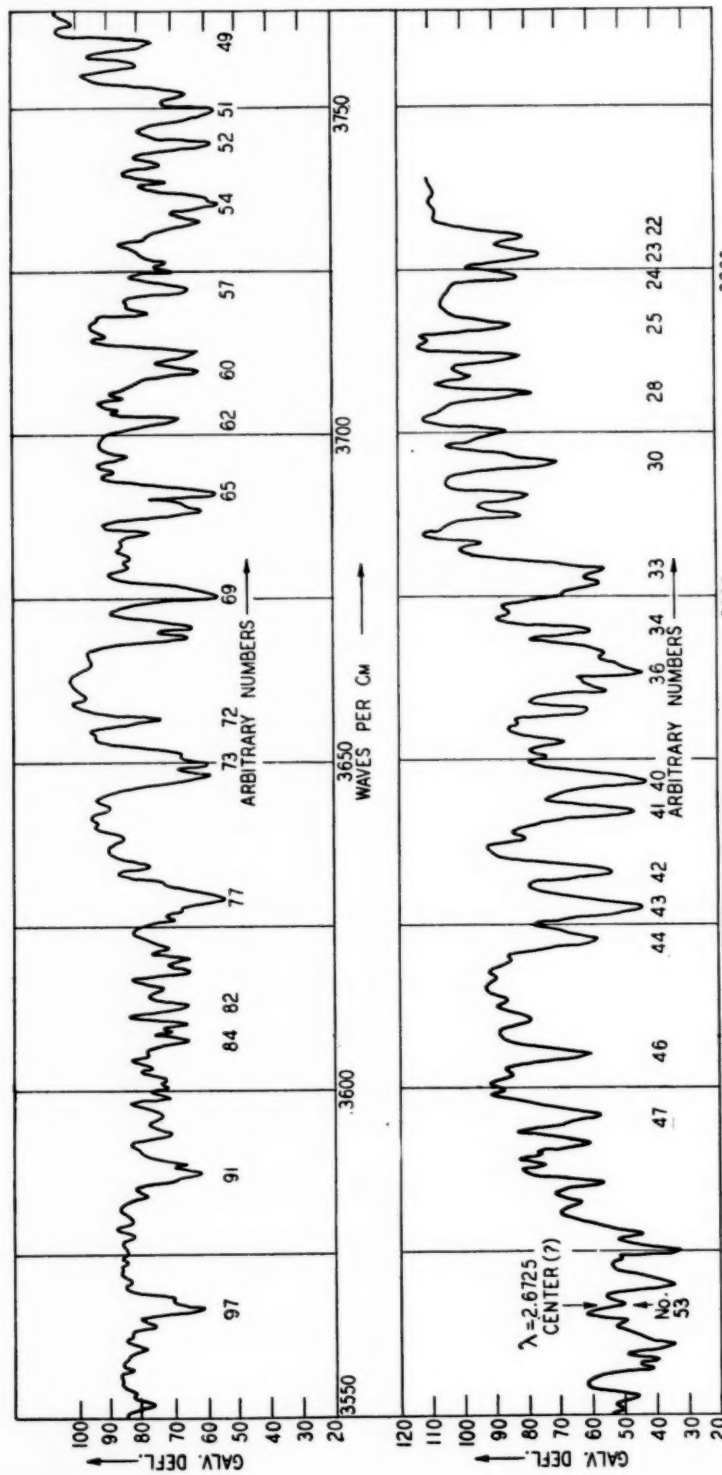

Fig. 3. Energy curve, part of the region of 2.67μ, on frequency scale. Air partly dried. Echelette grating, as in Fig. 2.

the prism-grating spectrograph we have carefully gone over part of this region, having the prism so placed that there was no deflection when the grating was set for 1.9μ. No absorption lines were to be found, though the slits were certainly narrow enough to show them. If certain wave-lengths given in Table II, beginning with No. 26, are multiplied by 2, the products agree remarkably well with many of the wave-lengths given by Barnes. Some of his numbers represent a good mean of adjacent wave-lengths, doubled. For example for line No. 26, 2λ is 3.6418μ. Barnes lists 3.642. Also if one compares the graph under consideration with that for the region near 1.87μ given in Fig. 4 of the paper of 1918 (reference 2) they appear very much alike. The work of Barnes was done with a grating and an infrared filter. It may be that the atmospheric absorption appearing at 3.75μ in Figs. 4 and 5 of that paper is a second order effect due to an overlapping of spectra.

In Figs. 2 and 3 and Table III are given our results for the region of 2.67μ, a fundamental band having a zero branch—showing at any rate strong absorption in the middle portion. Of the two curves in Figure 2 there is less moisture represented in the lower. For Fig. 3 there is less vapor still, and there is less overlapping and general confusion of the lines. For example, line No. 70

TABLE III. *Region of* 2.67μ.

Arbitrary numbers, relative intensities, wave-lengths and wave-numbers of the stronger lines.

Line No.	Rel. int.	Wave-length	Wave-number	Line No.	Rel. int.	Wave-length	Wave-number
1	15	24714	4046.3	29	60	25806	3875.1
1a	5	24795	4033.1	30	80	25838	3870.3
2	10	24834	4026.7	31	70	25869	3865.6
3	6	24871	4020.7	32	20	25892	3862.2
3a	5	24924	4012.2	33	80	25948	3853.9
4	10	24942	4009.3	33a	80	25959	3852.2
5	12	25027	3995.7	34	40	26010	3844.7
6	12	25055	3991.2	35	50	26031	3841.6
7	8	25103	3983.6	36	80	26049	3838.9
7a	6	25147	3976.6	37	20	26070	3835.8
8	12	25155	3975.4	38	50	26090	3832.9
9	12	25187	3970.3	39	40	26124	3827.9
10	15	25235	3962.8	40	85	26166	3821.8
11	6	25256	3959.5	41	80	26198	3817.1
12	10	25289	3954.3	42	75	26261	3807.9
13	30	25309	3951.2	43	85	26298	3802.6
14	20	25327	3948.4	44	55	26332	3797.7
15	40	25356	3943.8	45	55	26415	3785.7
16	12	25379	3940.3	46	60	26454	3780.1
17	40	25427	3932.8	46a	5	26493	3774.6
18	20	25442	3930.5	47	70	26521	3770.6
19	5	25479	3924.8	48	70	26550	3766.5
20	40	25506	3920.7	48a	10	26570	3763.6
21	55	25527	3917.4	49	75	26594	3760.2
22	50	25610	3904.7	50	50	26612	3757.7
23	65	25624	3902.6	50a	20	26647	3752.8
24	65	25644	3899.5	51	85	26667	3749.9
25	70	25694	3892.0	52	85	26700	3745.3
26	60	25731	3886.4	53	60	26724	3742.0
27	10	25746	3884.1	53a	20	26746	3738.9
28	70	25766	3881.1	54	85	26762	3736.6

TABLE III. (*Cont'd.*)

Line No.	Rel. int.	Wave-length	Wave-number	Line No.	Rel. int.	Wave-length	Wave-number
55	85	26790	3732.7	81	50	27660	3615.3
56	80	26825	3727.9	82	60	27679	3612.8
57	80	26863	3722.6	83	40	27700	3610.1
58	50	26889	3719.0	84	40	27720	3607.5
58a	20	26915	3715.4	85	10	27757	3602.7
59	80	26936	3712.5	86	30	27771	3600.9
60	80	26954	3710.0	87	30	27789	3598.6
61	30	26982	3706.2	88	40	27810	3595.8
62	60	27011	3702.2	89	30	27828	3593.5
63	25	27051	3696.7	90	30	27867	3588.5
64	15	27068	3694.4	91	65	27875	3587.4
65	80	27092	3691.1	92	20	27902	3584.0
66	85	27109	3688.8	93	20	27932	3580.1
67	10	27135	3685.3	94	20	27951	3577.7
68	10	27175	3679.9	95	20	27977	3574.4
69	80	27208	3675.4	96	10	28003	3571.0
70	80	27241	3670.9	97	70	28036	3566.8
70a	40	27251	3669.6	97a	20	28056	3564.3
71	10	27320	3660.3	98	20	28085	3560.6
72	70	27349	3656.4	99	15	28110	3557.5
72a	80	27398	3649.9	100	30	28151	3552.3
73	60	27415	3647.6	101	30	28188	3547.6
74	20	27452	3642.7	102	30	28204	3545.6
75	30	27486	3638.2	103	25	28276	3536.6
76	50	27517	3634.1	104	10	28320	3531.1
77	80	27557	3628.8	105	30	28348	3527.6
78	20	27575	3626.5	106	30	28384	3523.1
78a	30	27608	3622.1	107	10	28406	3520.4
79	60	27626	3619.8	108	30	28493	3509.6
80	40	27640	3618.0	109	30	28546	3503.1

is separated in Fig. 3, into two lines some 10A apart. Further comparison shows that the intensity of all the strong lines increases with the amount of water present. This change in intensity indicates that at least the strong lines in this region are due to water vapor, and not to carbon dioxide. The carbon dioxide band in the region of 2.73μ would probably not have strong lines below 2.69μ, corresponding to line No. 59. The effect of carbon dioxide in this region was studied by Sleator[2] and it was found that the strong lines throughout the region were enhanced by the use of steam (giving much more absorbing material) and reduced by drying the air. Figure 3 has been plotted with deflections on a scale of frequencies and is the reverse of the curves of Figure 2. Lines 22, 23 and 24 may be compared with the unresolved group shown as numbers 8 and 9 in Figure 5 of the paper of 1918, and this comparison fairly indicates the advance represented in the present work.

In Fig. 4 and Table IV are represented the results for the region of 3.16μ. It is perhaps here that previously published results are most inadequate. The table presents lines between 2.85 and 3.33μ, and the lines at the beginning of the table probably belong to the series shown in the previous figures. All the lines are weak in this region, whose center we have placed at 3.168μ, and which is probably the first harmonic of the band at 6.26μ. However, the separation of the two strong lines next the center on either side (Nos. 81 and 82) is 45.3 waves per cm, while the corresponding difference at the fundamental

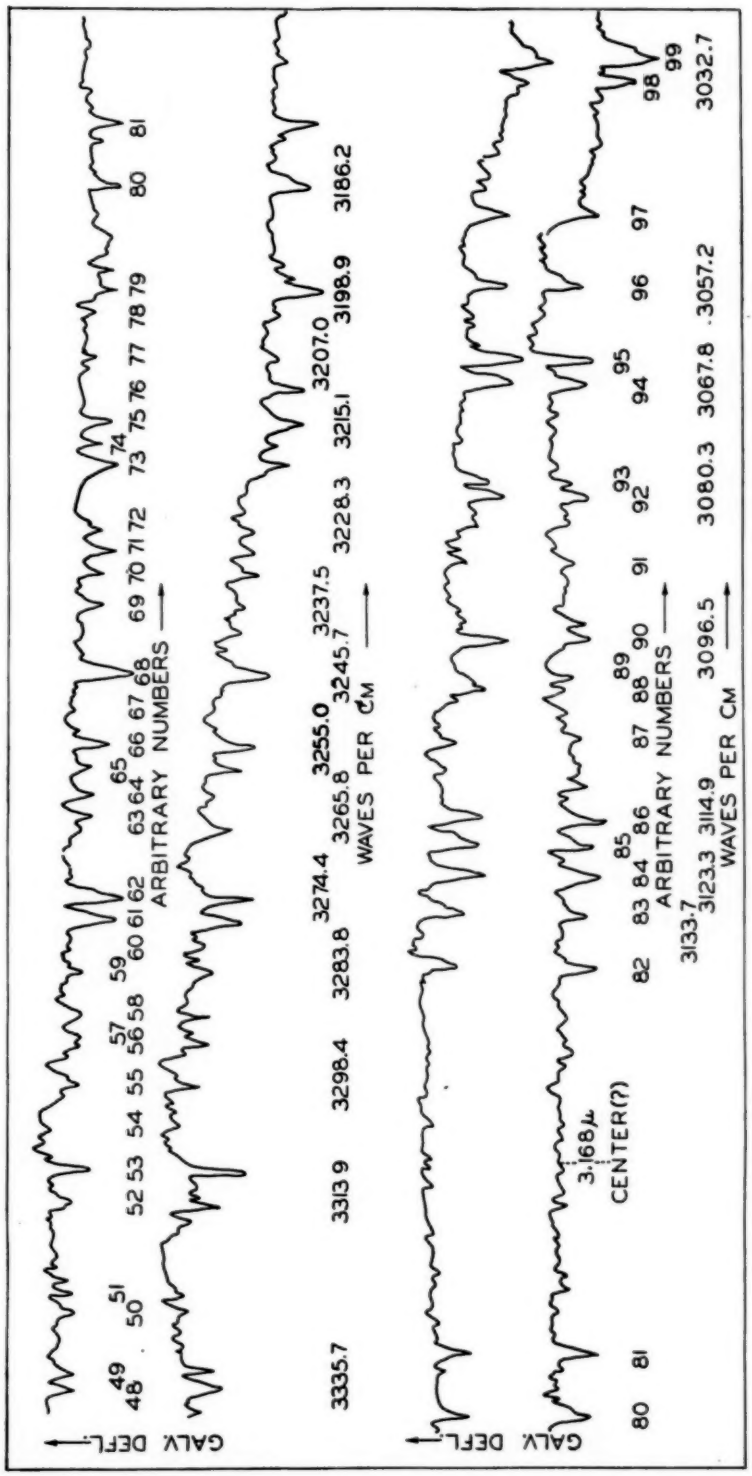

Fig. 4. Part of the energy curve, region of 3.16μ. Two independent series. Echelette grating, 7200 lines per inch. Slits 0.15 mm, 15 secs, 0.45 waves per cm, 4.5A.

TABLE IV. *Region of* 3.15μ
Arbitrary numbers, relative intensities, wave-lengths and wave-numbers of the stronger lines.

Line No.	Rel. int.	Wave-length	Wave-number	Line No.	Rel. int.	Wave-length	Wave-number
1	40	28546	3503.1	59	12	30452	3283.9
2	5	28561	3501.3	60	5	30489	3279.9
3	15	28588	3498.0	61	25	30515	3277.1
4	25	28655	3489.8	62	25	30540	3274.4
5	12	28672	3487.7	63	8	30620	3265.8
6	25	28702	3484.1	64	8	30663	3261.3
7	25	28714	3482.6	65	8	30693	3258.1
8	15	28762	3476.8	66	12	30721	3255.1
9	5	28801	3472.1	67	5	30762	3250.8
10	15	28828	3468.9	68	20	30809	3245.8
11	5	28844	3466.9	69	12	30887	3237.6
12	15	28861	3464.9	70	10	30923	3233.8
13	15	28873	3463.4	71	15	30949	3231.1
14	5	28901	3460.1	72	15	30976	3228.3
15	5	28919	3457.9	73	25	31053	3220.3
18	35	28992	3449.2	74	8	31077	3217.9
19	5	29013	3446.7	75	25	31102	3215.2
20	20	29032	3444.5	76	20	31144	3210.9
22	8	29066	3440.4	77	5	31181	3207.1
26	15	29128	3433.1	78	5	31237	3201.3
27	5	29161	3429.2	79	20	31261	3198.9
28	8	29176	3427.5	80	15	31384	3186.3
29	5	29194	3425.4	81	20	31456	3179.0
30	12	29206	3424.0	82	20	31911	3133.7
31	30	29219	3422.4	83	20	31972	3127.7
32	5	29265	3417.1	84	25	32017	3123.3
33	10	29318	3410.9	85	12	32054	3119.7
34	12	29366	3405.3	86	25	32103	3115.0
37	12	29437	3397.1	87	10	32176	3107.9
39	15	29457	3394.8	88	15	32239	3101.8
42	12	29528	3386.6	89	12	32256	3100.2
43	5	29687	3368.5	90	20	32294	3096.5
44	12	29703	3366.7	91	5	32385	3087.8
45	8	29736	3362.9	92	12	32463	3080.4
46	12	29789	3356.9	93	8	32480	3078.8
47	5	29880	3346.7	94	25	32596	3067.9
48	15	29961	3337.6	95	25	32623	3065.3
49	12	29979	3335.7	96	20	32710	3057.2
50	8	30050	3327.8	97	25	32791	3049.6
52	12	30175	3314.0	98	20	32948	3035.1
53	15	30218	3309.3	99	25	32973	3032.8
54	4	30269	3303.7	100	5	32984	3031.8
55	15	30317	3298.5	101	5	33039	3026.7
56	12	30366	3293.2	102	12	33135	3018.0
57	15	30377	3292.0	103	12	33192	3012.8
58	15	30401	3289.4				

is 40. The wave-lengths of certain lines listed in Table IV are in good agreement with values given by Barnes in the work cited (reference 7) for this region. In some cases his numbers represent averages of the wave-lengths of adjacent lines.

The results for the fundamental at 6.26μ are shown in part in Figs. 5 and 6, and completely in Table V. Hettner shows this band to extend from 4.5μ to 8.5μ, but we have studied only the central part. In Fig. 6 are represented the most important lines of this region on a scale of wave-numbers, showing by the length of the lines the intensities of absorption. The advancement lately

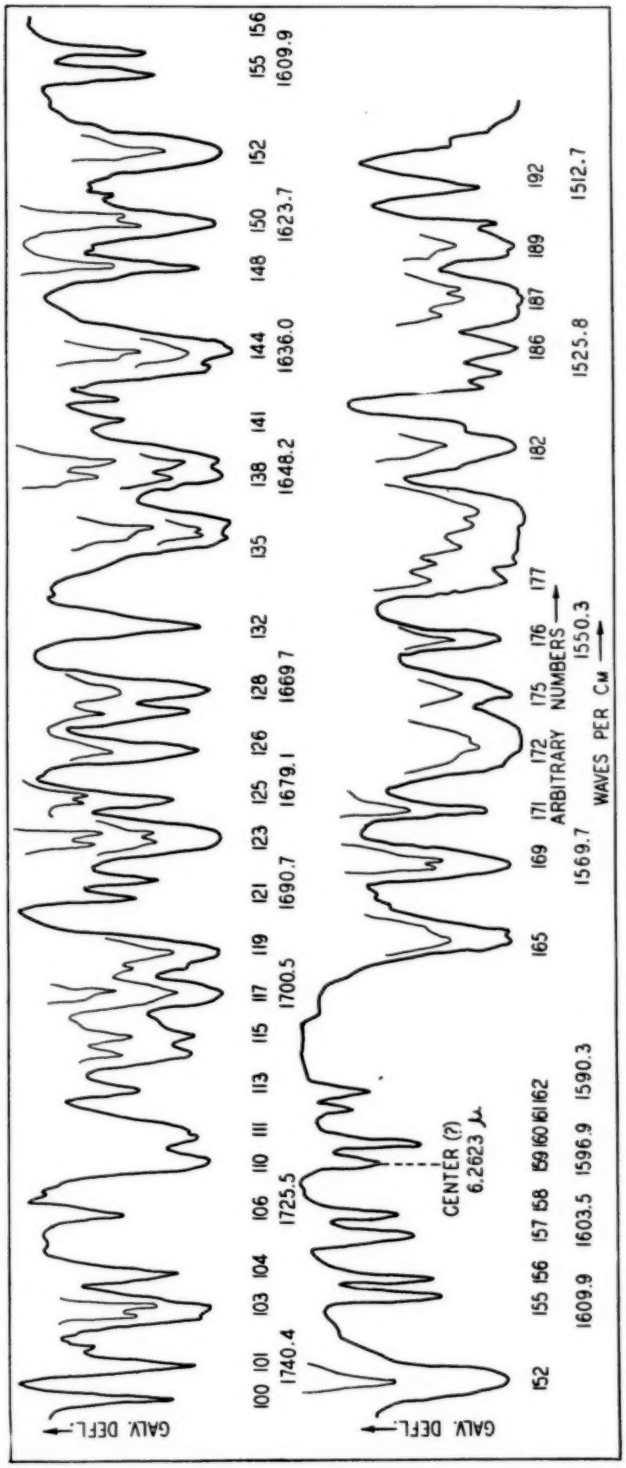

Fig. 5. Energy curve, region of 6.26μ, middle part. Echelette grating, 2880 lines per inch. Slits 0.2 mm, 21 secs, 0.45 waves per cm, 17A.

TABLE V. *Region of* 6.26μ.

Arbitrary numbers, relative intensities, wave-lengths, and wave-numbers of the stronger lines.

Line No.	Rel. int.	Wave-length	Wave-number	Line No.	Rel. int.	Wave-length	Wave-number
58	20	54413	1837.8	144	90	61128	1635.9
63	60	54644	1830.0	148	70	61414	1628.3
65	10	54673	1829.1	149	80	61570	1624.2
66	40	54774	1825.7	150	40	61602	1623.3
67	10	54839	1823.5	152	90	61841	1617.0
69	10	55005	1818.0	155	50	62117	1609.9
70	10	55159	1812.9	156	40	62202	1607.7
71	30	55211	1811.2	157	40	62358	1603.6
72	15	55288	1808.7	158	35	62435	1601.7
73	5	55385	1805.5	159	30	62625	1596.8
76	10	55487	1802.2	160	45	62693	1595.1
77	50	55541	1800.5	161	20	62804	1592.3
78	30	55661	1796.6	162	30	62880	1590.3
79	65	55762	1793.3	165	90	63425	1576.7
80	65	55814	1791.7	168	75	63693	1570.0
81	25	56004	1785.6	169	80	63706	1569.7
82	60	56142	1781.2	171	60	63884	1565.3
83	15	56184	1779.9	172	90	64115	1559.7
84	30	56295	1776.4	173	80	64142	1559.0
85	20	56396	1773.2	175	80	64321	1554.7
86	70	56439	1771.8	176	80	64500	1550.4
87	50	56533	1768.9	177	70	64706	1545.5
89	50	56739	1762.4	178	70	64765	1544.0
90	5	56832	1759.6	179	80	64833	1542.4
91	50	56898	1757.5	180	80	64916	1540.5
93	70	57082	1751.9	181	85	64960	1539.4
95	75	57169	1749.2	182	90	65193	1533.9
97	25	57219	1747.7	183	30	65261	1532.3
98	20	57250	1746.7	184	20	65396	1529.1
100	50	57338	1744.0	185	70	65451	1527.9
101	70	57457	1740.4	186	85	65537	1525.9
102	12	57526	1738.3	187	60	65656	1523.1
103	70	57663	1734.2	188	80	65718	1521.7
104	60	57784	1730.6	189	70	65755	1520.8
106	35	57999	1724.2	192	60	65913	1517.1
110	90	58204	1718.1	193	30	65977	1515.7
111	80	58287	1715.6	194	80	66107	1512.7
113	35	58452	1710.8	196	20	66226	1510.0
114	70	58588	1706.8	197	90	66344	1507.3
115	70	58653	1704.9	198	80	66385	1506.4
117	90	58813	1700.3	200	20	66575	1502.1
118	15	58894	1698.0	202	60	66711	1499.0
119	90	58958	1696.1	203	65	66829	1496.4
120	30	59151	1690.6	204	80	67119	1489.9
121	50	59216	1688.7	205	60	67220	1487.7
122	30	59356	1684.8	207	30	67499	1481.5
123	90	59400	1683.5	208	60	67736	1476.3
124	40	59504	1680.6	209	20	67866	1473.5
125	50	59524	1680.0	210	80	67928	1472.1
126	70	59683	1675.5	211	10	68070	1469.1
127	60	59817	1671.8	213	65	68259	1465.0
128	75	59886	1669.8	216	20	68559	1458.6
129	20	59918	1668.9	217	90	68631	1457.1
132	75	60131	1663.0	218	10	68693	1455.8
133	20	60162	1662.2	219	50	68848	1452.5
135	70	60444	1654.4	221	65	69052	1448.2
136	90	60496	1653.0	224	10	69318	1442.6
138	30	60682	1647.9	227	90	69595	1436.9
139	90	60738	1646.4	228	15	69753	1433.6
141	20	60864	1643.0	229	10	69816	1432.3
142	20	60942	1640.9	230	50	69911	1430.4
143	30	61046	1638.1	234	50	70219	1424.1

made is shown definitely in this region. For what appeared in Fig. 2 of the paper of 1925 as uncertain ripples in the level plateau of the center has now become eight very definite lines, numbers 155 to 162, arranged in pairs. The old lines Nos. 69 and 80, the second from the middle region on either side, now appear as two close lines each, Nos. 149 and 150 and Nos. 168 and 169 of Fig. 5. Line 159 which we have marked the center, because it is a geographic mid point, is not a particularly significant line. Some lines separated here, for example, numbers 172 and 173 and 168 and 169, are less than one wave per cm apart.

It may be well to compare some of the wave-lengths with those given in the previous papers from this laboratory. In many cases no basis for comparison exists, for one of the former "lines" now appears as several. However, there are many lines in the region of 2.67μ as it appeared in 1918 which have persisted as single effects, and there are several lines near 1.87μ and 6.26μ

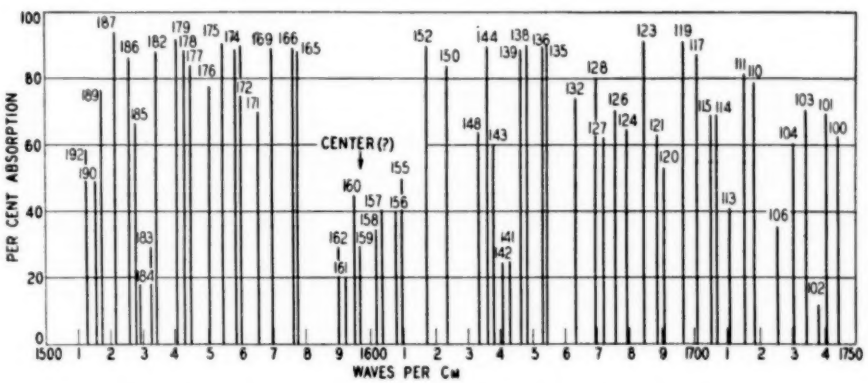

Fig. 6. Region of 6.26μ, middle part. Intensities of the absorption lines shown on a scale of waves per cm.

which may be compared in the paper of 1925 and the present one. The comparison shows that single lines in the band at 2.66μ are now assigned wave lengths from 3 to 7A greater than those of 1918. Perhaps the visual calibration formerly necessary accounts for the systematic difference. Similar differences appear at 1.87μ. At 6.26μ the difference is more irregular and somewhat larger. In many cases, however, no comparison is possible. For example, lines 114 and 115 were formerly given as one, No. 54, and Nos. 120 and 121 as number 58.

Some estimate of the precision attained in the wave lengths listed here is necessary and may be made as follows. The calibration of the 7,200 line grating, used in all the work except for the band at 6.26μ, was based on the mercury line whose wave-length was taken to be 10139.8A in air. This calibration has been done by Meyer, and charts have been made from which wave length and wave number can be read directly in terms of angles. This calibration is believed to involve no error greater than 1 part in 50,000. There exists always some uncertainty in setting the circle. If this amounts to 5 seconds, then the

location of an absorption line which depends at the tip upon perhaps four plotted points is also uncertain. Independently measured values of typical lines in two of the regions are shown in Table VI.

TABLE VI. *Typical values for the different angles and wave-lengths found for a single line.*

Line No.	Angle	Wave-length
31	24°31′55″	29219A
	31′55″	29219
	31′55″	29219
	32′0″	29221
33	24°37′25″	29322
	15″	29319
	10″	29317
	15″	29319
39	24°44′42″	29457
	50	29460
	40	29457
	45	29458
128	19°54′22″	59891
	30″	59897
	15″	59885
138	20°10′37″	60672
	45″	60678
	45″	60678
	50″	60682
148	20°26′ 7″	61416
	10″	61418
	5″	61418

When there are extreme differences of 20″ we have taken more than four independent energy curves. It seems fair to affect the values of wave-length in these regions with a probable error of ± 2A. It is perhaps an even chance that the true value of the wave-length in air, based upon the value used here for the mercury line, is within 2A on either side of the values given here. In order to guard against mistakes in reading the calibration charts, values of wave-length and values of wave-number were taken off independently, and afterward checked by looking up all the wave numbers in a table of reciprocals. These considerations and this estimate of precision refer to the regions 1.87μ, 2.66μ and 3.15μ.

The band at 6.26μ was studied with a grating having 2,880 lines per inch. Its calibration was based on the same value of the wave-length of the mercury line at 1μ, and also on work with visual lines. The spectrometer constant was 175,900A. There was no chart available, and our procedure was to compute independent values of λ, one from each plotted curve, by the equation $\lambda = \kappa \sin \theta$. First the wave numbers were looked up in the reciprocal tables, and then the wave numbers were independently computed by using cologs. Typical values in this region are given in Table VI. It does not seem that the spectrometer constant for this assembly is responsible for an error of 1A in our results, and perhaps the wave-lengths in Table V should be written ± 3A. To

reduce this uncertainty requires more observations, and more independent curves. The systematic difference between the wave-lengths given here, and those published in the paper of 1925, for such lines as may properly be compared, must arise from differences in calibration constant. The circle used in all this work, as well as in many other investigations made in this laboratory, has no appreciably eccentricity.

The advance over previous work represented here lies, first, in more reliable determinations of individual wave-lengths. Second, more lines have been measured, and this work should make possible a better classification, if it is demanded by theoretical study of the water molecule. Third, the lines measured represent, in more cases than in previous data, single absorption effects, so that more of the wave numbers are of actual physical significance.

THE DIFFUSION PROBLEM FOR A SOLID IN CONTACT WITH A STIRRED LIQUID

By T. E. W. Schumann
West Virginia University

(Received April 21, 1931)

Abstract

A cylindrical solid of length a in a direction x and of arbitrary cross-section normal to x is in contact on its plane face $x=a$ with a well-stirred liquid. The face $x=0$ of the solid and the lateral surface are impervious to heat. The liquid extends from $x=a$ to $x=a+b$. At $x=a+b$ the liquid is in contact with a source of heat at the constant temperature θ, the transfer of heat from this source being proportional to the difference in temperature between the outside source and the liquid. If the initial temperatures of solid and liquid are given, the problem of the temperature distribution at any subsequent time can be obtained by means of a modification of the well-known Fourier analysis.

IN STUDYING practical problems concerning the one-dimensional flow of heat in a solid, boundary conditions are sometimes met which are not directly amenable to the ordinary Fourier analysis. This is due to the fact that the characteristic solutions of the differential equation subject to the given boundary conditions do not form an orthogonal set of functions. This difficulty can be met in various ways. One method will be given in this paper.

The problem here considered is that of the one-dimensional flow of heat in a solid slab which, at its face $x=a$, is in contact with a well-stirred liquid extending from $x=a$ to $x=a+b$. The liquid receives heat at the face $x=a+b$ from an outside source kept at a constant temperature θ, the transfer of heat to the liquid being proportional to $\theta-v$, where v is the temperature of the liquid. The slab is impervious to heat at the face $x=0$. The lateral surfaces of the slab and the liquid are supposed to be impervious to heat so as to insure the one-dimensional flow of heat.[1] If the initial temperature of the liquid and the initial temperature distribution in the solid are known, then it is possible to determine the temperature distribution throughout the system at any subsequent instant.

Let $u(x, t)$ represent the temperature in the solid at any point x and at time t, and let $v(t)$ represent the temperature of the liquid at any time t. The function $v(t)$ must be continuous for all values of t.

Now, according to the well-known Fourier equation of heat conduction

$$\frac{\partial u}{\partial t} = \alpha^2 \frac{\partial^2 u}{\partial x^2}, \quad t > 0 \tag{1}$$

[1] These conditions are approximately realized when a slab of low thermal conductivity is heated between two similar parallel plates of high conductivity, metal plates for example, the outer plates being heated by a hot gas.

where α^2, the thermal diffusivity of the solid, is the quotient of its thermal conductivity k by the product of its density ρ and its specific heat c.

Also, since the face at $x=0$ is impervious to heat

$$\partial u/\partial x = 0, \quad x = 0, t > 0. \tag{2}$$

Furthermore, the heat gained by the liquid must be equal to the heat it acquires from the outer source minus the heat which is conducted across the solid-liquid boundary. If K is the heat capacity of a prism of the liquid of unit cross-section and γ is the coefficient of heat transfer from the outer source per unit cross-section, unit difference of temperature and unit time, then

$$K\frac{dv}{dt} = -k(\partial u/\partial x)_{x=a} + \gamma(\theta - v), \quad t > 0. \tag{3}$$

The thermal contact of the solid and the liquid at $x=a$ gives rise to the equation

$$u(a, t) = v(t), \quad t > 0. \tag{4}$$

If v_0 is the initial temperature of the liquid and $u_0(x)$ that of the solid, then we have

$$\lim_{t=0} v(t) = v_0 \tag{5}$$

and

$$\lim_{t=0} u(x, t) = u_0(x), \quad 0 \leqq x < a. \tag{6}$$

It will be noticed that we have restricted the validity of the last equation so as to exclude the point $x=a$ for the reason that it would be impossible to satisfy all the conditions imposed by Eqs. (1) to (6) if this point had been included, except for the special case when $u_0(a)=v_0$. The same difficulty, however, is met in any Fourier expansion. Fourier's theorem states that a function $f(x)$ which fulfills Dirichlet's conditions in a given interval can be represented by a series of sines and cosines except at points of discontinuity. If therefore we express u in terms of a Fourier series we shall expect it at time $t=0$, to satisfy the initial temperature distribution except at points of discontinuity including the point $x=a$, $\lim_{t=0} u(a, t)$ having some value different from $u_0(a)$. From physical consideration it is possible to determine the value of $\lim_{t=0} u(a, t)$.

Suppose that at any point $x=x_0$ there is a sudden change in the value of $u_0(x)$ from u_1 to u_2. This means that the temperature gradient is infinite at x_0. The heat conducted across unit area is proportional to the temperature gradient, and hence if the temperature gradient is still infinite after a small but finite time ϵ, then the heat transferred across unit area will be infinite, which is clearly impossible. From this it follows that the temperature discontinuity must have disappeared after the time ϵ, however small ϵ may be. These considerations also hold at the point $x=a$, where there is thermal contact between the solid and the liquid. Hence

$$u(a, \epsilon) = v(\epsilon) \tag{7}$$

however small ϵ may be.

Now let us consider the value of $v(\epsilon)$ when ϵ becomes very small. Since the liquid is kept stirred its temperature must be uniform at any instant of time. Therefore the change in temperature $v_0 - v(\epsilon)$ is proportional to the total heat conducted away from the liquid, and by choosing ϵ sufficiently small we may make this heat, and consequently $v_0 - v(\epsilon)$ as small as we please. Hence it follows that

$$\lim_{\epsilon=0} v(\epsilon) = v_0$$

and combining this result with Eq. (7) we have

$$\lim_{\epsilon=0} u(a, \epsilon) = v_0$$

or

$$\lim_{t=0} u(a, t) = v_0. \tag{8}$$

Eqs. (8) and (4) can now be combined into the single equation

$$u(a, t) = v(t) \tag{9}$$

for all time.

Accepting (9), we can rewrite the equations of condition, substituting $u(a, t)$ for $v(t)$

$$\frac{\partial u}{\partial t} = \alpha^2 \frac{\partial^2 u}{\partial x^2}, \quad t > 0 \tag{10}$$

$$\frac{\partial u}{\partial x} = 0, \quad x = 0, \quad t > 0 \tag{11}$$

$$K \frac{\partial u}{\partial t} = -k \frac{\partial u}{\partial x} + \gamma(\theta - u), \quad x = a, \quad t > 0 \tag{12}$$

$$\lim_{t=0} u(x, t) = u_0(x), \quad 0 \leqq x < a \tag{13}$$

$$\lim_{t=0} u(a, t) = v_0 \tag{14}$$

and our problem reduces to the determination of u so as to satisfy conditions (10) to (14).

On account of the rather unusual character of the analytical conditions it is perhaps advisable to demonstrate that this set of equations possesses a unique solution, and we proceed to show this briefly. If possible, let there be two independent solutions u_1 and u_2.

Let

$$V = u_1 - u_2. \tag{a}$$

Then V must satisfy the following set of conditions

$$\frac{\partial V}{\partial t} = \alpha^2 \frac{\partial^2 V}{\partial x^2} \tag{b}$$

$$\frac{\partial V}{\partial x} = 0, \quad x = 0 \tag{c}$$

$$K\frac{\partial V}{\partial t} = -k\frac{\partial V}{\partial x} - \gamma V, \quad x = 0 \tag{d}$$

$$V = 0, \quad t = 0, \quad 0 \leqq x \leqq a \tag{e}$$

Put

$$J = \frac{K\alpha^2}{2k} V_a^2 + \frac{1}{2}\int_0^a V^2 dx \tag{f}$$

where V_a is the value of V at $x=a$.

Then

$$\frac{\partial J}{\partial t} = \frac{K\alpha^2}{k} V_a \frac{\partial V_a}{\partial t} + \int_0^a V \frac{\partial V}{\partial t} dx$$

$$= \frac{K\alpha^2}{k} V_a \frac{\partial V_a}{\partial t} + \alpha^2 \int_0^a V \frac{\partial^2 V}{\partial x^2} dx$$

by virtue of (b).

$$= \frac{K\alpha^2}{k} V_a \frac{\partial V_a}{\partial t} + \alpha^2 \left[V \frac{\partial V}{\partial x}\right]_0^a - \alpha^2 \int_0^a \left(\frac{\partial V}{\partial x}\right)^2 dx$$

$$= -\frac{\gamma}{k} V_a^2 - \alpha^2 \int_0^a \left(\frac{\partial V}{\partial x}\right)^2 dx$$

by virtue of (c) and (d).

Therefore

$$\frac{\partial J}{\partial t} \leqq 0.$$

But since $J=0$ when $t=0$, it follows that

$$J \leqq 0.$$

Also, according to the definition as given by Eq. (f), J is essentially positive. Hence $J \equiv 0$, from which it follows that there can be only one solution to the problem.

We now proceed to find this solution.

Let us set

$$u = \theta + \sum_{n=0}^{\infty} E_n \cos \frac{z_n x}{a} e^{-z_n^2 \alpha^2 t / a^2} \tag{15}$$

which is the type of expression to which one is led by the ordinary Fourier analysis. If this series is convergent, then u attains the value θ when $t = \infty$, as

should be the case from physical considerations. Eqs. (10) and (11) are formally satisfied by this expression. Eq. (12) will also be satisfied provided the z's are the roots of

$$\tan z = -\lambda z + \frac{\gamma a}{kz} \tag{16}$$

where

$$\lambda = \frac{\alpha^2 K}{ak} = \frac{K}{a\rho c}. \tag{17}$$

There now remains the problem of determining the values of E so as to satisfy conditions (13) and (14), namely that

$$u(x, 0) = \theta + \sum E_n \cos \frac{z_n x}{a} = u_0(x), \quad 0 \leqq x < a \tag{18}$$

and

$$u(a, 0) = \theta + \sum E_n \cos z_n = v_0. \tag{19}$$

A difficulty is met here due to the fact that in (18) the characteristic functions are non-orthogonal.[2]

To overcome this difficulty we assume for the time being that (18) can be differentiated termwise, the result being

$$\frac{du(x, 0)}{dx} = -\sum \frac{E_n z_n}{a} \sin \frac{z_n x}{a}. \tag{20}$$

[2] The situation here encountered is entirely similar to that met by March and Weaver in connection with a problem which is a special case of the one here considered (see Phys. Rev. **31,** page 1072). A somewhat simpler device than the one here used is, however, sufficient to meet the situation of the former paper. In fact, one sought there to develop a function $u_0(x)$ in a series of non-orthogonal functions $\cos z_n x$ where z_n are the roots of $\tan z + \lambda z = 0$. This can be accomplished indirectly by expanding the integral of $u_0(x)$ in a series of the orthogonal functions $\sin z_n x$. This procedure leads at once to the solution:

$$u = \frac{\bar{u} + v_0\lambda}{1 + \lambda} + \sum_{n=0}^{\infty} E_n \cos \frac{z_n x}{a} e^{-\alpha^2 z_n^2 t/a^2}$$

where

$$\bar{u} = \frac{1}{a} \int_0^a u_0(x) dx$$

$$E_n = \frac{2}{1 + \lambda + \lambda^2 z_n^2}[(-1)^n(\bar{u} - v_0\lambda)(1 + \lambda^2 z_n^2)^{1/2} + 2(1 + \lambda^2 z_n^2)Q_n]$$

and

$$Q_n = \frac{z_n}{a} \int_0^a u_0(x) \cos \frac{z_n x}{a} dx$$

the notation being that of the paper referred to.

It will be shown that it is possible to obtain the values of E from (18) and (20) by the usual Fourier method. Multiply (18) by $\cos z_n x/a$ and (20) by $p_n \sin z_n x/a$, add and integrate with respect to x between o and a, and determine p_n such that the product terms vanish, i.e., such that

$$\int_0^a \cos\frac{z_n x}{a}\cos\frac{z_m x}{a}\,dx + \frac{p_n z_m}{a}\int \sin\frac{z_n x}{a}\sin\frac{z_m x}{a}\,dx = 0. \tag{21}$$

By making use of Eq. (16) it can readily be demonstrated that (21) is satisfied provided

$$p_n = \frac{\lambda k z_n}{\gamma} \tag{22}$$

The equation from which the value of E_n is to be determined is

$$E_n\int_0^a \cos^2\frac{z_n x}{a}\,dx - E_n\frac{k\lambda {z_n}^2}{\gamma a}\int_0^a \sin^2\frac{z_n x}{a}\,dx$$

$$= \int_0^a (u(x,0)-\theta)\cos\frac{z_n x}{a}dx + \frac{\lambda z_n k}{\gamma}\int_0^a \frac{du(x,0)}{dx}\sin\frac{z_n x}{a}\,dx. \tag{23}$$

All the integrals in the above expression are perfectly straightforward except the last one which can be integrated by parts:

$$\int_0^a \frac{du(x,0)}{dx}\sin\frac{z_n x}{a}\,dx = \left[u(x,0)\sin\frac{z_n x}{a}\right]_0^a - \int_0^a \frac{u_0(x)z_n}{a}\cos\frac{z_n x}{a}\,dx$$

$$= v_0\sin z_n - \frac{z_n}{a}\int_0^a u_0(x)\cos\frac{z_n x}{a}\,dx \tag{24}$$

by virtue of Eqs. (14) and (18). If the other integrations are performed it is found that

$$\frac{E_n}{2}\left\{1+\left(\frac{\gamma a}{k{z_n}^2}+\lambda\right)\cos^2 z_n\right\}$$

$$= \left(v_0\lambda - \frac{\theta a\gamma}{k{z_n}^2}\right)\cos z_n + \frac{1}{a}\int_0^a u_0(x)\cos\frac{z_n x}{a}\,dx \tag{25}$$

The problem has now been formally solved, the value of u being given by Eq. (15), where the values of z have to be determined from Eq. (16) and those of E from Eq. (25). The value of v, the temperature of the liquid, is the same as $u(a, t)$ according to Eq. (9). We know that the expression obtained for u will satisfy Eqs. (10) to (12) but it still has to be demonstrated that it also satisfies (13) and (14). If this can be proved, then we know that we have obtained the true and unique solution to the problem. A formal proof that (13) and (14) will also be satisfied would require a considerable amount of space and the inclusion of such a proof in a journal devoted entirely to physics could hardly be justified. It may be stated, however, that a satisfactory

proof has been obtained, the method employed involving the use of Green's functions and being essentially the same as that employed by Carslaw[3] in solving a similar type of problem. In brief, the procedure is first to find a solution due to a point source of heat at the point x', where $0<x'<a$, subject to the boundary conditions as expressed by Eqs. (11) and (12), with the restriction that θ is assumed to be zero. The result is expressed in the form of a complex integral. By complex integration over a suitably chosen path it is then an easy matter to show that the solution obtained satisfies the equations of condition and also the initial condition of a unit point source at $x=x'$

Now the sum of any number of such solutions will still be a solution. Hence, by choosing a suitable distribution of point sources we can build up the final solution corresponding to the initial temperature distribution as given by Eqs. (13) and (14). In building up this initial temperature distribution it must be borne in mind that the distribution must be of strength $u_0(x)\rho c$ per unit length of the solid, when we deal with unit cross-section. At the point $x=a$, however, there is concentrated a point source of total strength Kv_0, corresponding to the heat initially contained in the liquid. This holds for the case when $\theta=0$. The transition to the case when $\theta\neq 0$ is easy and need not be elaborated here. Since the validity of the solution for a single point source has been proved the solution thus obtained for any distribution of point sources must also be valid. The result, which is in the form of a complex integral can be transformed into an infinite series by integrating over a suitable path and applying Cauchy's theorem to the poles of the integrand. In carrying out this transformation the resulting infinite series was found to be entirely in agreement with that already obtained by the Fourier method. Our problem has therefore been finally and completely solved.

Numerical example.

We give a numerical example which was worked out in connection with the heat conduction into a slab of coal bounded by two plates of steel. The values adopted for the different constants are $K=2.23$; $k=0.01425$;$a=1.27$; $\gamma=0.0452$; $\rho=0.8$; $C=0.2775$; $\theta=1$; $v_0=0.8$; $u_0=0$. where the centimeter, gram, minute, and degree Fahrenheit are the fundamental units of length, mass, time and temperature respectively.
It follows that $\lambda=7.9$ and $\alpha^2=0.0645$, and Eq. (16) takes the form

$$\tan z = -7.9z + \frac{4.03}{z}. \tag{17}$$

The values of z as determined graphically from this equation were $z=0.666$, 1.663, 4.74, 7.85. These values of z were substituted in Eq. (16) and the values of the E's were found to be

$$E = -0.703,\ -0.428,\ 0.213,\ -0.181.$$

Furthermore the successive values of α^2z^2/a^2 were

[3] Carslaw, The Conduction of Heat, p. 180. MacMillan and Co.

$$\frac{\alpha^2 z^2}{a^2} = 0.0178, \quad 0.1105, \quad 0.899, \quad 2.464.$$

Therefore the final form that Eq. (7) takes in this case is

$$u = 1 - 0.703 \cos \frac{0.666x}{a} e^{-0.0178t} - 0.428 \cos \frac{1.663x}{a} e^{-0.1105t}$$

$$+ 0.213 \cos \frac{4.74x}{a} e^{-0.899t} + \text{etc.}$$

The temperature $u(o, t)$ at $x = 0$ and the temperature $u(a, t)$ or $v(t)$ were calculated from this equation and the values are given in Table I.

TABLE I.

Time, $t=$	*0*	*0.5*	*0.1*	*2.0*	*4.0*	*10.*	*20.*	*30.*	*80.*
$u(o, t)=$	0	0	0	0.013	0.104	0.360	0.582	0.753	0.883
$v(t)=$	0.8	0.685	0.683	0.683	0.685	0.701	0.739	0.813	0.908

From the table we see that the temperature $v(t)$ of the steel (or stirred liquid) sinks rapidly from its initial value of 0.8, stays practically constant for an appreciable time at about 0.685, and then begins to rise steadily attaining its asymptotic value of 1.0 after infinite time.

From this example it is evident that numerical calculation for any practical problem will in general not require an excessive amount of labor.

My thanks are due to Dr. S. P. Burke, Chairman of the Industrial Science Division of this University for his interest in this problem, and to the Combustion Utilities Corporation for permission to publish the results. I also wish to thank Professor Warren Weaver of the University of Wisconsin for a number of helpful suggestions concerning the form of presentation of the paper.

THE DIELECTRIC CONSTANT OF FORMIC, ACETIC, AND PROPIONIC ACIDS, AND THE ELECTRIC MOMENT OF COMPLEX MOLECULES

By C. T. Zahn
Palmer Physical Laboratory, Princeton University

(Received April 20, 1931)

Abstract

The *temperature and pressure variation of the dielectric constant of formic and propionic acid vapors* has been studied experimentally. The behavior is similar to that previously found for acetic acid. For formic acid it is possible to calculate from Coolidge's vapor density measurements the amount of association into double molecules, and to explain the apparent departures from Debye's theory in terms of such association. It is then seen that the apparently linear pressure curves can be explained by the compensation of several factors in the measurements. By assuming that the optical part of the polarization is doubled on association and taking this value from refractivity measurements, values for the electric moment of the single and double molecules of formic acid are obtained, 1.51×10^{-18} and 0.99×10^{-18} c.g.s.e.s.u., respectively. Although no reliable vapor density measurements exist for acetic acid it is assumed that the anomaly in this case also is due to association rather than to the previously suggested effect of vibrational quantization. The previous data are reinterpreted accordingly. By using the optical refractivity as before a value is obtained from the high temperature measurements for the *electric moment of the single molecule* of acetic acid, 1.73×10^{-18}; and similarly for propionic acid, 1.74×10^{-18} c.g.s.e.s.u. *The electric moment of complex molecules* is then discussed with reference to directed valence and to internal free rotation around single bonds. The possibility of the importance of interaction between external rotation and internal free rotation is suggested. The question of the interpretation of measured electric moments is raised for the case where free rotation causes a time variation of electric moment. In this connection the experimental values of electric moment are discussed. The values of the electric moment of these acids indicate that the OH group is tightly bound as supposed by Eucken and Meyer. A structure for the double molecule of formic acid is suggested, with the four oxygen molecules at the corners of a rectangle, the planes of the two constituent single molecules at an angle of about 120°, and the OH groups bound tightly in positions of minimum potential energy. This structure does not seem to be inconsistent with the observed electric moment.

IN A previous communication[1] measurements of the dielectric constant of acetic acid vapor were published. These measurements indicated that there is a change of the electric moment of the acetic acid molecule with temperature, and it was suggested as a possible explanation that the effect is due to a transition in vibrational quantum state of the OH group. The possibility that the apparent change in electric moment could be due to association was considered excluded by the fact that the variation of dielectric constant with pressure was linear within the limits of experimental error. The presence of association could not be further tested since there exist no

[1] C. T. Zahn, Phys. Rev. **35**, 1047 (1930).

reliable measurements of the vapor density of acetic acid. It was decided to make a further study of this effect by making measurements of the dielectric constant of formic acid and propionic acid vapors. In the case of formic acid excellent vapor density measurements have been made recently by Coolidge,[2] who has shown that his measurements can be explained by the existence of double molecules and has given satisfactory equations for the calculation of the degree of association. A study of these data shows that there is a considerable amount of association in the region of temperature and pressure available for convenient dielectric constant measurements. This suggests that the anomaly in the previous acetic acid measurements might be due to association in spite of the apparently linear pressure curves. For example, this might be possible if the shape of the vapor density curve were such as to effect the linearity of the pressure curve only very slightly throughout the measured range of pressure, and particularly if the molecular polarizations of the single and the double molecules were not greatly different.

Formic Acid

The present data on formic acid show the same general characteristics as those on acetic acid. The pressure curves are apparently linear and the electric moment apparently decreases with the temperature. This being a partial confirmation of the above suggestion of association, an attempt was made to explain the anomaly in formic acid quantitatively in terms of association and to calculate the electric moment of the single and double molecules. The percentage of associated molecules was calculated from Coolidge's equations for the points of maximum pressure on the curves and at the four different temperatures included by the data. At the highest temperature there was found 9 percent association and at the lowest temperature 58 percent. A

Table I. *Formic acid data.*

$T°K$	p cm Hg	$3(\epsilon-1)/(\epsilon+2)v$	$3(\epsilon-1)/(\epsilon+2)vT$	P
344.63	18.62	5547	1.912	41.43
386.91	28.32	5542	2.144	41.40
403.10	28.27	5536	2.231	41.34
423.43	28.36	5525	2.338	41.26

rough calculation from the data of Table I shows that if the effect is due to association the associated molecule cannot have zero electric moment as it would have in case the two associating moments were antiparallel. This also is in confirmation of the above suppositions.

In Table I the data were calculated from the readings at the highest pressures only. An example of a pressure curve is shown in Fig. 1. For economy in space the individual pressure data were not included in the table. In column 3 of Table I the value of the specific volume was calculated from the ideal gas equation and refers therefore to the normal ideal value. Therefore the values in column 3 represent the apparent polarization referred to a normal ideal

[2] A. S. Coolidge, Jour. Amer. Chem. Soc. **50**, 2166 (1928).

number of gas molecules. The values in column 5 represent the molecular polarization, or the polarization referred to a mol of the molecules. The values in column 4 plotted against the absolute temperature would give a Debye line if the molecules were of one kind only. The absolute values of ϵ used here are the values corrected as described later for the extrapolation to zero pressure under the assumption of association.

In order to determine the molecular polarization of the single and double molecules individually, it was assumed that the constant, or so-called optical, part of the polarization is doubled on association. This is probably justified by the well-known principle of the additivity of refractivity, particularly since the energy of association is not great. In any case the optical part is the smaller part of the electric polarization under the available experimental con-

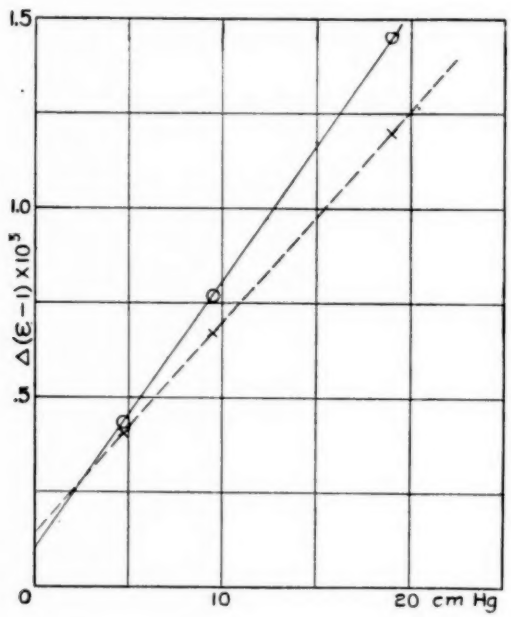

Fig. 1. Pressure Curve.

ditions. The two molecular polarizations are set respectively equal to $A + B_1/T$ and $2A + B_2/T$ according to the Debye theory. Hence the measured molecular polarization is

$$P = n_1(A + B_1/T) + n_2(2A + B_2/T)$$

where n_1 and n_2 are the respective mol fractions. B_1 and B_2 are proportional to the squares of the two electric moments. An approximate idea of the magnitude of the effect of association can be obtained by assuming that the association is negligible at the highest temperature, and then calculating $2A + B_2/T$ from the data at the lowest temperature and maximum pressure. If the pressure curves are then corrected so as to correspond to the single molecule alone, it is found that these curves are still apparently linear. This

can be seen in Fig. 1, where the uncorrected points are shown by crosses and the corrected points by circles.

It can therefore be stated that so far as the linearity of the pressure curves is concerned the assumption of association is justified. It remains only to see whether the constants can be chosen so as to fit all the data satisfactorily. The more accurate calculations are slightly complicated by the fact that it is never possible in a pressure curve to measure accurately the vacuum value of the experimental condenser capacity. This is true because inequalities in the temperature of the condenser plates arise on evacuation.[3] It is therefore necessary to extrapolate to zero pressure in order to obtain absolute values of the dielectric constant. Fig. 1 shows that the extrapolated value differs slightly for the corrected and the uncorrected curves. (This shows that the greatest departure from linearity exists at the very low pressures and partially explains why it was not originally detected.) These curves were first corrected roughly as above stated in order to locate the zero, and then new absolute values of the dielectric constant and molecular polarization were determined.

Because of the complicated nature of the calculations and the smallness of the association effect, no attempt was made to determine A, but it was taken from the molecular refractivity of formic acid in the liquid state as given in Landolt Börnstein, 8.53. This value is probably a little too small because of infrared terms in the refractivity, and the resulting calculations are subject therefore to a small error. Appropriate values of B_1 and B_2 were obtained by choosing the value of B_1 which gives on subsequent calculation the most nearly constant value for the ratio B_1/B_2. The value chosen for B_1 is 14160. Table II shows the corresponding values of B_1/B_2 with a weighted

TABLE II. *Formic acid: calculation of molecular constants.*

$B_1=14160$ $A=8.53$

$\mu_1=1.51\times10^{-18}$; $\mu_2=0.99\times10^{-18}$

$T°K$	cm Hg	Mol fraction association	P	B_1/B_2
344.63	18.62	0.580	41.43	0.45
386.91	28.32	0.275	41.40	0.40
403.10	28.27	0.171	41.34	0.37
423.43	28.36	0.092	41.26	0.50
				0.43 mean

mean of 0.43. From these values it can be seen that while the reduction in the electric moment is considerable the doubling of the optical term masks a considerable portion of the effect. Further, in order to show how nearly the data for the four different temperatures and maximum pressures are consistent with these constants A, B_1, and B_2, the values of the electric polarization were calculated and compared with the experimental values. This is shown in Fig. 2. The upper straight line is the Debye line for single molecules, and the lower line, for double molecules. The product of the polarization and the absolute temperature is plotted against the absolute temperature. For con-

[3] C. T. Zahn, Phys. Rev. **35**, 848 (1930).

venience the values of the polarization here refer not to a mol but to the ideal number of molecules per cc under normal conditions of a gas. The crosses represent the experimental values and the circles the calculated values for the maximum pressures. The deviations are seen to be of the order of one percent. This agreement is almost better than one could expect in view of the nature of the calculations and the possibility of small errors due to absorption on the condenser plates.

Finally it seems that the anomaly for formic acid can be satisfactorily explained by association and the values of the electric moment for the single

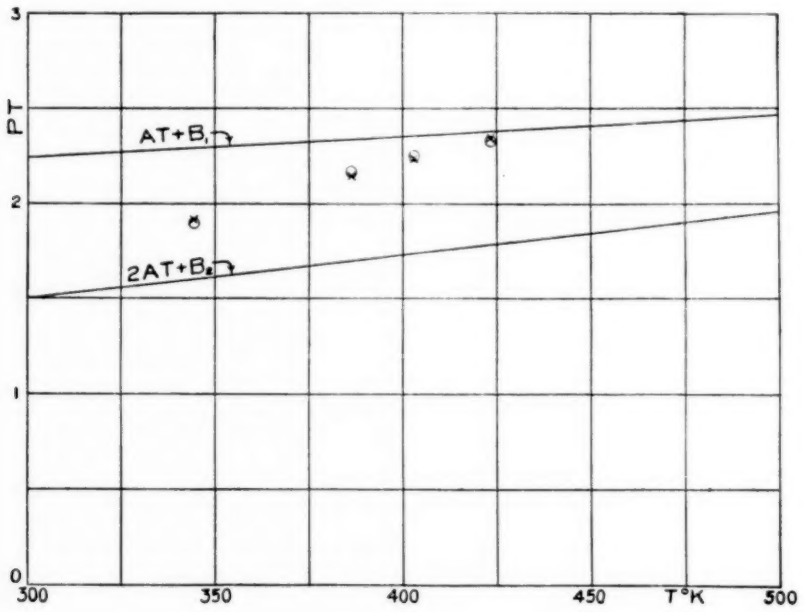

Fig. 2. Debye Lines.

and double molecules can be calculated. The above values of B_1 and B_2 correspond to electric moments of 1.51 and 0.99×10^{-18} c.g.s.e.s.u., respectively.

In order to obtain a good specimen of formic acid for these tests Kahlbaum formic acid was distilled at 0°C as described by Coolidge in the paper cited above.

Acetic and Propionic Acids

In view of the above results of the calculations for *formic* acid it seems more than probable that the previous data on *acetic* acid should also be interpreted in terms of association rather than the previously suggested temperature variation of electric moment. The same can be said for the data here presented on propionic acid, which shows a similar but somewhat smaller effect. The fact that the effect is smaller in propionic acid may be due to a greater masking of the moment reduction by the doubling of the optical term on association; or it may also be due to a smaller amount of association.

For these two acids the calculations cannot be carried out as in the case of formic acid since their vapor densities are unknown at present. Still if it is assumed that the effect is due to association the data can be used to obtain a fairly accurate value of the electric moment of the single molecules.

In Table III are shown the previously published data on acetic acid and also the present data on propionic acid together with calculated values of the apparent electric moment, μ. The values of apparent molecular polarization

TABLE III.

Acetic acid $A=12.9$ $\mu=1.73\times10^{-18}$			Propionic acid $A=17.4$ $\mu=1.74\times10^{-18}$		
$T°K$	P	μ	$T°K$	P	μ
297.51	55.0	1.42	356.12	61.4	1.59
320.85	50.7	1.40	373.42	59.7	1.60
341.13	50.8	1.45	374.41	59.8	1.61
357.78	51.2	1.49	389.86	59.8	1.63
360.37	51.6	1.50	404.64	59.1	1.65
389.64	53.7	1.60	418.44	59.4	1.69
410.84	53.5	1.64	429.57	60.3	1.73
450.09	53.3	1.72	455.37	58.4	1.74
471.42	52.3	1.73	485.81	56.0	1.74
491.44	50.2	1.72			
493.86	50.3	1.73			

are calculated from the uncorrected pressure curves and are subject to small errors due to incorrect extrapolation to zero pressure. At the higher temperatures this error is negligible since the association effect is very small. Values for A are taken as before from refractivity data. The values of μ should approach a constant value as the temperature is increased since the association then becomes negligible. From Table III it is seen that in both cases μ becomes practically constant above 440°K. The asymptotic values may be taken as 1.73 for acetic acid and 1.74×10^{-18} c.g.s.e.s.u. for propionic acid. Because of the danger of decomposition the highest safe temperature for formic acid was about 425°K and there was still 9 percent association. Fig. 2 shows, however, that the association should become negligible at approximately the same temperature as for the other two acids, at 440°K.

In the previous article[1] on acetic acid it was stated that there was evidence at high pressures indicating association in which the polarization is increased. This effect was noticed at pressure beyond the apparently linear portions of the pressure curves near to saturation, and is probably now to be considered as due to surface adsorption on the condenser plates.

The purified propionic acid was obtained by fractional distillation of a specimen from the Eastman Kodak Company.

ELECTRIC MOMENT OF COMPLEX MOLECULES

In recent years a number of authors, chiefly Eucken and Meyer, and Wolf,[4] have made attempts to calculate the electric moment of molecules,

[4] H. Sack, Ergebnisse der Exakten Naturwissenschaften, Band VIII, 337 (1930).

assuming that the total electric moment can be obtained by adding vectorially electric moments characteristic of each chemical bond and directed approximately along the valence directions given by the tetrahedral theory. These calculations have in some cases been complicated by the fact that whenever there is a single bond between two atoms there is a possibility of free rotation of two atomic groups relative to one another. In such cases the molecules cannot be regarded as rigid in the sense that the average relative positions of the nuclei are practically fixed. In fact, atomic groups having their own characteristic vector electric moments can rotate relatively to one another and cause a time variation of the electric moment. (Hojendahl first used this idea to explain difficulties which had arisen from the fact that certain molecules of the type CR_4 have an electric moment different from zero.) In these complicated molecules the question arises as to how one should regard such molecules in interpreting the apparent measured values of electric moment. Various attempts have been made in this direction. First attempts were made by assuming that the electrostatic interaction between the two rotating groups is negligible and that the rotation is therefore truly free. In this case it was assumed that the measured value of the square of the electric moment was the average square of the moment taken over a random distribution of the angle of free rotation. For example, two electric moments, μ, perpendicular to the axis of free rotation would give rise to an apparent or resultant moment $2^{1/2}\mu$.

Hojendahl has also pointed out that these internal rotations are never truly free but are hindered to some extent by electrostatic interaction; e.g., dipole interaction. In many cases this interaction may be considerable. Meyer[5] has made an extension of Debye's *classical* theory of the dipole polarization for certain non-rigid molecules, assuming dipole interaction. These calculations indicate an appreciable temperature variation of apparent electric moment when the innermolecular potential exceeds $(1/10)kT$; and that if the rotation is truly free the apparent moment is as if μ^2 were averaged over a random motion of the internal rotation as mentioned above. Certain objections may be raised to these conclusions. If the internal rotational energy were not too great the actual motions of the rotating parts would certainly be affected appreciably by centrifugal action due to the external rotations of the molecules as a whole and these rotating parts might be deformed by electrostatic interaction in varying degrees depending on the kinetic energies of the various parts of the molecule. Then the individual rotating parts of the molecule could not be considered as rigid and Meyer's calculations might be invalid. An idea of the importance of dipole deformation can be gotten from the electric moments of the substitution products of methane.

On the quantum theory it is found that deviations from the classical dipole theory are appreciable only at very low temperatures. Van Vleck has derived the classical formula of Debye to a close approximation from general quantum-mechanical considerations having to do chiefly with the relative values of possible energy transitions in the molecules and spectroscopic

[5] L. Meyer, Zeits. f. Phys. Chem. (B) **8**, 27 (1930).

principles. It is assumed that the energy levels of the molecule are such that $h\nu$ is never of the order of kT, but is either much larger or much smaller than kT. Then the dipole term in μ^2/T arises from possible transitions for which $h\nu \ll kT$; and the optical term from transitions for which $h\nu \gg kT$. There arises in the calculations a quantity μ^2 which is interpreted as being associated with the fixed electric moment of the molecule. The theory is developed for the case of rigid molecules and has not been explicitly stated so as to include the possibility of internal free rotation. It seems probable that in this latter case there will arise a quantity which is to be interpreted as an average μ^2 but just how this should be averaged would require further consideration of the theory. Whether this μ^2 appreciably depends on temperature or not will probably depend on the magnitude of the interaction between the rotating parts, and possibly not in the same way as it would on the classical theory.

Strictly speaking Van Vleck's theory applies to the cases where all the transitions in energy can be separated into the above two cases relative to kT. When $h\nu$ is of the order of kT difficulties may arise. Actually this condition may exist for some of the ordinary vibration states, but Van Vleck states that, under his assumptions of invariant fixed moment, these states, which correspond to linear oscillators would cause no temperature variation in the electric polarization. Now in complex molecules there may be certain other types of motion for which $h\nu$ is of the order of kT and a temperature variation does result. In this connection it is interesting to consider the internal rotation of the OH group in organic molecules. Since this group has a large electric moment there exists the possibility of strong electrostatic interaction, for example, with the C=O bond in the COOH group. The quantized motions of the OH group might be similar to those for the physical pendulum as described by Condon.[6] The lower states correspond to vibration and the higher states to non uniform rotation. The motions of the OH group might be considerable and the corresponding changes in electric moment quite large. Then the assumption of fixed electric moment would be invalid and some kind of average should be taken. This average might depend upon temperature, as was originally suggested to explain the data on acetic acid vapor.[7]

With regard to the interpretation of experimental values of μ three possibilities suggest themselves for the internal rotation here discussed. (1) If the interaction energy were sufficiently small the rotation could be regarded as truly free. Then the corresponding energy levels would be closely spaced and according to Meyer's classical derivation one would expect the apparent μ^2 to be an average over random internal rotational angle. (2) If the interaction energy were large, the lower states might correspond to oscillations of the rotator and have large energy separations. At ordinary temperatures practically all the molecules would be in the lowest state and this

[6] E. U. Condon, Phys. Rev. **31,** 891 (1928).

[7] It seems now that such a temperature variation is not necessary to explain the data on acetic acid; still the effect may exist to an appreciable extent but be undetectable as a departure from the linearity of a Debye line, for example if the deviations were approximately linear in temperature in the experimental interval.

oscillation would not contribute to the temperature variation of electric polarization, but would contribute a small amount to the atomic, or infrared, part of the constant polarization. In this ground state the corresponding motions of the oscillator would be fast compared to the external rotations and the apparent fixed electric moment μ should probably be regarded as a *vector* average over the oscillation as for the electronic motions, rather than a root mean square value as for the case of slow internal rotation. (3) The previous two cases are the extreme cases of Van Vleck's theory, for which the Debye equation holds. In the intermediate case where the energy separations are of the order of kT the temperature variation in electric polarization would be very complicated. This variation would now be due not only to the distribution of states of external rotation but also to the distribution in the states of internal rotation. Further because of the combined centrifugal and electrostatic interaction the perturbations of the individual states would no longer be like those of a simple dipole rotator. As regards the interpretation of experimental data, if such an effect exists in any actual molecules, it might be regarded as an apparent variation of electric moment with temperature. Such a variation with temperature will not necessarily be detectable as a deviation from the Debye equation $P=A+B/T$; for it is easily seen that a variation in apparent B which is linear with temperature is equivalent to a different but constant B together with a change in the constant A. If the effect is relatively small it may easily be such that the apparent B is approximately linear in the experimental interval. Then the experimental data would lead to a spurious value of the optical part A. For example, this possibility may be of interest in connection with Sänger's[8] abnormal value of A for ethylene chloride. Meyer[9] seems to think that a temperature variation in μ really exists in spite of the linearity of the Debye line.

There exists another serious difficulty in any quantitative treatment of free rotation in that the electrostatic interaction cannot be expressed accurately. Attempts have been made to consider this interaction as due to dipoles concentrated and located in various ways, but such models cannot give anything more than the roughest approximation to the facts, since the atoms are separated by distances comparable to atomic radii. The difficulties seem at present unsurmountable, whether one regards the interaction as a dipole effect, or as due to residual valence and van der Waals' forces as in London's theory.

Tetrahedral symmetry: The assumption of tetrahedral symmetry cannot be accurately true as is seen, for example, from the values of the electric moment of the chlorine substitution produces of methane. The discrepancies are usually explained by saying that the valence directions tend toward tetrahedral symmetry in the absence of dipole interaction and that this interaction produces a bending of the valence directions. This seems to be consistent with experimental data. A recent article by Slater[10] is especially interesting in this

[8] R. Sänger, Phys. Zeits. **32,** 21 (1931).
[9] L. Meyer, Phys. Zeits. **32,** 260 (1931).
[10] J. C. Slater, Phys. Rev. **37,** 481 (1931).

connection. On the basis of the quantum theory it is suggested that in the carbon atom the valence directions tend toward tetrahedral symmetry, while in the nitrogen and oxygen atoms they tend to be mutually perpendicular. The case of oxygen is of special interest here since it has been assumed by Eucken and Meyer that the undistorted valence angle for oxygen is the tetrahedral angle of about 110°. This is of importance in the original determination of the characteristic electric moments of the various chemical bonds.

Structure of the Carboxyl Group

From the previous calculations it is seen that the electric moments of acetic and propionic acids are of practically the same value, 1.73 and 1.74 $\times 10^{-18}$, but that of formic acid is smaller, 1.51×10^{-18}. It would be of interest to know whether this difference arises chiefly in the carboxyl group or in the alkyl group. If it arises in the alkyl group one could regard it as due to simple dipole induction which increases with the length of the carbon chain. Such an effect is well known in the series methyl, ethyl, propyl, to butyl chloride, where the moment increases by about 0.2×10^{-18}. This would indicate that the moment of the alkyl group changes from 0.4 to 0.6×10^{-18} by induction. Since the observed change in moment from formic to acetic acid is 0.22×10^{-18} it seems probable that this is also due to induction; particularly in view of the fact that the moment of COOH is not greatly different from that of C-Cl. The only observed difference in the two cases is that the transition is more abrupt in the fatty acid series.

It is, of course, possible that the transition may be at least in part due to a motion of the OH group of the type discussed under the above case (3) of relatively small interaction energy; but the values of the electric moment seem to indicate that the OH group is bound relatively tightly, either oscillating or rotating nonuniformly as in case (2). This is suggested by Meyer's calculated limiting values of the moment of the COOH group for the extreme positions of the OH group allowed by free rotation, 3.5 and 1.1×10^{-18}, corresponding to maximum and minimum potential energy, respectively. Because of the uncertainty in the calculations of electric moment, particularly in the valence directions, one cannot be certain whether these values indicate that the OH group has a considerable oscillation or not. The experimental values may be consistent with a very tightly bound OH group and a simultaneous bending of the valence directions, for example. We can, however, say with some degree of certainty that the motion of the OH group is not free since the expected moment would be much larger than the observed moment, about 3×10^{-18}. This is in agreement with the chemical evidence responsible for the supposition of the existence of a chelate ring in the carboxyl group.

The Double Molecule of Formic Acid

As regards the structure of the double molecule of formic acid, of moment 0.99×10^{-18}, this value of the electric moment excludes the possibility of the antiparallel type of association. Taking into consideration the relative sizes of the C and O atoms and assuming tetrahedral symmetry for the carbon

atoms, it is almost possible geometricaly to fit the molecules together in such a way that the four O atoms lie at the corners of a square and the C atoms on a line perpendicular to the square. The planes of the two associating HCOOH molecules would then be mutually perpendicular. If this is the approximate structure of the double molecule, the OH group of one of the original molecules of HCOOH would tend to be directed toward the doubly bound O atom of the other molecule and would be attracted toward it, distorting the square into the form of a rectangle. The OH group would then be quite near to the C=O group and the interaction woud probably bind the OH group relatively tightly in the ground state. It is, of course, impossible to make an accurate calculation of the electric moment of the double molecule, but a rough estimate after the manner of Eucken and Meyer is perhaps of some interest. The sizes of the atoms permit of a distortion of the square by interaction such that the planes of the two HCOOH atoms subtend an angle a little less than 120°. In the position of minimum potential energy the OH groups would lie approximately in the plane of the oxygen rectangle and at an angle of 60° relative to one another. Using the values of Eucken and Meyer for the characteristic moments one obtains a value of about 1.1×10^{-18} for the electric moment of the double molecule. Finally, one can say that the experimental value 0.99×10^{-18} does not seem to be inconsistent with the proposed type of structure so far as this rough estimate is concerned.

At present it is not possible to calculate the electric moment of the double molecule of acetic or propionic acid. These values would be particularly interesting in connection with the interpretation of the transition in electric moment from formic to acetic acid.

ON IMPURITIES IN METALS

By Francis Bitter
Westinghouse Research Laboratories, East Pittsburgh

(Received April 27, 1931)

Abstract

In order to arrive at a satisfactory understanding of many of the properties of metals, especially ferromagnetic metals, it is necessary to take into account the distorting effect of impurities and of other irregularities in the crystal lattice. The present paper is an attempt to describe some of the corrections that must be applied to the usual model of a perfect crystal before it can be expected to reproduce the properties of actual substances. Starting with the usual law of force between any two atoms—repulsion for small distances, attraction for large distances—the distortion of the lattice in the immediate neighborhood of an atom of impurity is discussed, with especial reference to the significance of the formation of molecules. Phase distributions in substances capable of allotropy are described, together with the influence of impurities on such distributions. The existence of diffusion makes it possible to apply statistical mechanics to solid solutions. It is shown that, in general, atoms of impurity in solids do not exert long range forces on each other by means of the distortions they produce in the lattice. This makes it possible to give simple formulae for the distribution of concentration of the impurities. These distributions are sometimes far from uniform, and a phenomenon similar to opalescence in gases may occur. Applications of the above concepts to ferromagnetic solutions are pointed out, and it is suggested that the ferromagnetism of austenite containing in the neighborhood of 0.8 percent carbon may be due to the presence of small granules of α-iron resulting from local fluctuations in the distribution of carbon atoms.

IT IS an old story that small amounts of impurities are sometimes of great importance in determining the physical properties of a substance, but in spite of this, the mechanism of such actions is very little understood. The magnetism of iron is a good example of the magnitude and importance of these effects. Yensen[1] has pointed out that in the interval between 1900 and 1928 the maximum permeability of iron has been increased from 2,000 to 61,000, chiefly by controlling small amounts of impurity. The most recent advance in this field is due to Cioffi,[2] who produced iron having a maximum permeability of 130,000 by annealing at high temperatures in a hydrogen atmosphere. There is little hope of understanding such phenomena until our theories of ferromagnetism and of other structure-sensitive properties are based on models of solids in which allowance is made for the chemical and mechanical effects of impurities. It is the purpose of this paper to describe such a model in some detail.

1. Pure Perfect Crystals

The substance to be investigated will be supposed made up of atoms between which the usual simple law of force acts—repulsion for small separa-

[1] T. D. Yensen, Journal of the Franklin Inst. **206,** 503 (1928).
[2] P. P. Cioffi, Nature **126,** 200 (1930).

tions, attraction for large separations, and only one position of equilibrium for finite separations. Out of this law of force may be calculated[3] the potential energy Φ of any given spacial arrangement of the atoms. Such calculations neglect a possible block structure as postulated by Zwicky,[4] but they may be thought of as being applicable to a single block and as an approximation to an aggregate of blocks. Since, however, a knowledge of the free energy is necessary for the interpretation of the properties of crystals with temperature aggitation, and since this free energy is not calculable from our present knowledge of atomic physics, it is impossible to make any quantitative theory of distorted lattices. A few qualitatively applicable observations can, however, be made, and for these we will confine ourselves in the main to the above simple model, the object being to find which of the properties of actual substances can be found in such a model, and which of the properties require the introduction of further assumptions regarding the atomic interactions.

Beyond the above definition of the substance with which the further discussion deals, there is only one point to be brought out before attacking the problem of the effect of impurities, and that concerns the mechanism of change of phase, and the associated problem of phase distribution throughout the volume of the substance. Let this substance be designated by A, and let it be assumed that A is capable of existing in two phases, α and β. Let the potential energy in each of these phases be designated by $\Phi_\alpha(p)$, $\Phi_\beta(p)$, where p represents those parameters on which the potential energy depends. For the sake of definiteness let us think of p as being the pressure, and as p is varied the lattice expands or contracts uniformly, remaining geometrically similar to itself. If Φ were thought of as the free energy, p might stand for the temperature. Φ_α and Φ_β satisfy the following conditions:

$$\Phi_\alpha < \Phi_\beta \text{ for } p < p_c$$

$$\Phi_\alpha = \Phi_\beta \text{ for } p = p_c$$

$$\Phi_\alpha > \Phi_\beta \text{ for } p > p_c.$$

As p increases from a value just less than p_c to one just greater than p_c, the whole substance *may* suddenly change from the α-phase to the β-phase. The intention is to bring out that this change *need* not take place all at once, because the substance may not be homogeneous, as is usually assumed. These inhomogeneities may be due to several causes. One such would be local spontaneous fluctuations in p (this, of course, only if there is temperature aggitation). Another would be the presence of an atom of some foreign substance B, or of an atom of A in an excited state. Such atoms would exert anomalous forces on their neighbors, which would really be equivalent to local pressures. Or the material might,without the interference of any of these factors, have its free energy a minimum for a mixture of the two phases.[5] For instance, suppose A is at a pressure $p_c - \delta p$, and that due to some unspecified cause a small region R is already in the β-phase. Suppose, further, that nor-

[3] Jones and Ingham, Proc. Roy. Soc. **A107,** 640 (1925) have done this for laws of force of the type $ar^m + br^n$ for various cubic lattices.

[4] F. Zwicky, Helevetica Physica Acta **3,** 269 (1930).

mally an expansion is associated with the $\alpha-\beta$ transition. It follows that the region R will be under compression due to its increase in volume while still surrounded by the unexpanded α-phase. In determining whether this local pressure is sufficient to maintain the region R in the β-phase, and how large R may be expected to be, it is necessary to consider the surface energy of R, the presence of other such regions, etc. A detailed discussion of these considerations cannot be given here, but the following points may be mentioned:

1. That in solid solutions such phase mixtures do occur.
2. That in some pure substances the transition from the crystalline to the liquid state probably involves such phase mixtures.
3. That phase mixtures of purely crystalline phases may exist in pure substances.[23]
4. That even under conditions far removed from the critical conditions, under which a phase change $\alpha-\beta$ takes place, small (ultramicroscopic) inclusions of one phase in the other may be present.
5. That such inclusions would have a considerable effect on structure sensitive properties.

2. One Atom of Impurity

An atom of a substance[6] B in the lattice of a substance A will in general produce very complex changes, especially if B is chemically very different

[5] A theoretical attack on this problem is possible following a procedure indicated by N. Rashevsky in an article on the size distribution of colloidal particles (Zeits. f. Physik **46,** 300, 1927). Instead of considering a substance B in another A, we can think of a phase β in another α, of the same substance. With this change of nomenclature, Rashevsky's results are

$$n(m) = e^{\lambda+\alpha m-K/K}$$

$n(m)$ being the number of regions in the β-phase having a mass m. K is the Boltzmann constant, $\lambda=\phi+k \log n_0$; $\phi=s-(u+pv)/T$, the entropy s being defined by $ds=(du+pdv)/T$. The constant α is chosen to satisfy the equation

$$\int_0^\infty me^{\lambda+\alpha m-K/K}dm = M$$

where M is the total mass of substance in the β-phase. Further progress can only be made when the function u is known. Rashevsky shows that with reasonable assumptions for u, the function $n(m)$ may have a maximum either for $m=0$ (a true solution), $m=m_0$ (a colloidal solution), or $m=\infty$ (two distinct and separate phases).

If such a phase distribution is wanted at temperatures which are not convenient for observation, the following procedure may be found useful as a basis for extrapolation. Instead of speaking of an inclusion of mass m, it will be convenient to refer to an inclusion of radius R. Then $u(R)=\int_T^{T'}\sigma_\beta dt+l+(3/2)KT+$constant. The first term represents the energy required per unit mass to heat the β-phase to the transformation temperature. l is the latent heat of transformation of a colloidal particle and may be written (G. Bakker, Handbuch der (Experimental) Physik **6,** page 210)

$$l = (v_\beta - v_\alpha)T\frac{d(p_\beta + p_\alpha)}{dT} - \frac{2(v_\beta + v_\alpha)}{R}T\frac{dH}{dT}$$

H is the surface tension. From this equation a reasonable form for $u(R, T)$ can be found, and hence the temperature dependence of the size distribution of the particles in the colloidal phase.

[6] B may be an excited atom of the substance A.

from A. For the sake of this qualitative discussion, however, it will suffice to assume that ϕ_{AB}, the potential energy between an atom of A and one of B, is the same sort of function as the function ϕ_{AA} which gives rise to the interatomic forces already specified in section 1. Typical curves are to be found in Fig. 1. In the simple case where B is a substitution atom, the effect of the substitution is to add to the undistorted lattice a potential $\phi_{AB}-\phi_{AA}$ resulting from the excess forces exerted by the atom of impurity on its neighbors. This curve may have a maximum for finite values of r, or it may have a minimum, or it may be of a much more complicated nature, the important point being that even with the above simple assumptions a curve of the type shown in Fig. 1 for $\phi_{AB}-\phi_{AA}$ is obtainable.

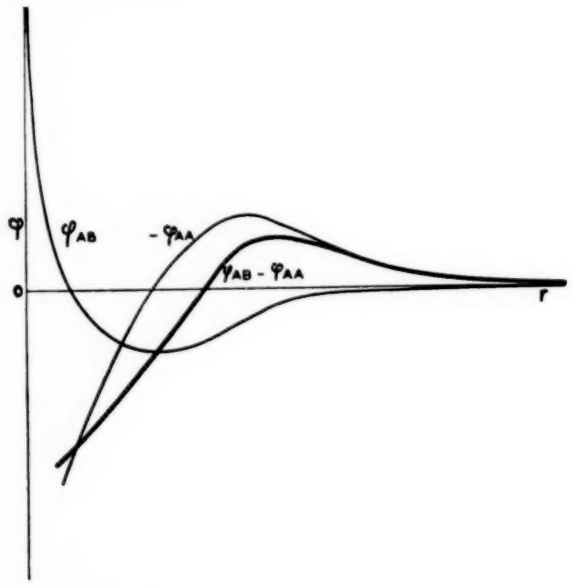

Fig. 1. The potential energy of two similar atoms $A-A$ and of two dissimilar atoms $A-B$ as a function of their distance apart, and finally the difference between these two functions, which is used in Fig. 3.

The most striking changes are brought about by the atom of impurity in its immediate neighborhood, but these are not of primary importance in this paper, and we shall discuss them only for the sake of their possible bearing on the phenomenon of thermal hysteresis. In Fig. 2 are shown two ways in which an atom of B may interact with its neighbors in accordance with the potential energy curve shown in Fig. 1. In both cases the impurity is in solution, but in order to distinguish between them, one might say that in case a, the atom B is in solution, whereas in case b, the molecule A_4B is in solution. The existence of a solution in two forms as described above is of interest in relation to temperature hysteresis. In Fig. 3 is shown a curve representing the potential energy of the atom A_1 adjoining the impurity as it approaches its neighbors, B and A_2, the latter being considered fixed. Curve 1 would represent the conditions if no impurity were present. The presence of the impurity necessitates

the addition of $\phi_{AB}-\phi_{AA}$, or curve 2, and the result is curve 3, which has two minima. As Rashevsky has pointed out,[7] it is just such curves as 3 Fig. 3 that give rise to hysteresis, and it is fairly obvious without further discussion that the relative concentration of atoms in the two minima will depend not

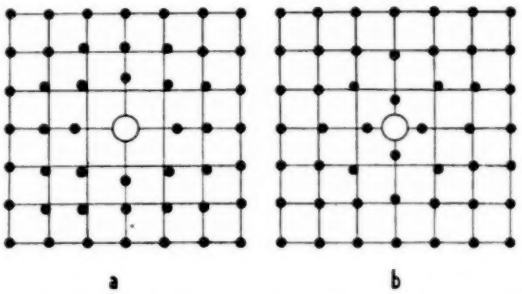

Fig. 2. Two possible distortions of a crystal around an atom of impurity compatible with the potential curves in Fig. 1 and Fig. 3.

only on the temperature and pressure, but also on the previous history of the sample. Since the physical properties of the substance $A+B$ will surely depend to some extent on whether B is in solution in the form A_4B or B, the

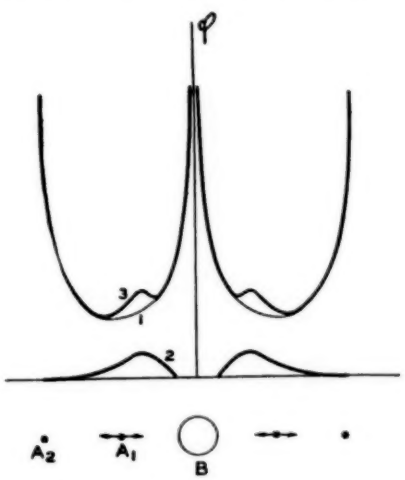

Fig. 3. The potential energy of A, as a function of displacement (1) when the atom B is identical with A_1 and A_2, and (3) when B is an atom of impurity giving rise to the additional energy (2), deduced from Fig. 1.

above described thermal hysteresis will give rise to a thermal hysteresis of other physical properties.

The only influence of the atom of impurity on distant parts of the lattice to be considered here will be the elastic deformation. In the calculation of this effect, it is assumed that the medium is isotropic, and that the distortion produced is spherically symmetrical. Under these conditions the strains in the

[7] N. Rashevsky, Zeits. f. Physik **53,** 102 (1929); **59,** 562 (1930); **61,** 511 (1930); **60,** 237 (1930).

lattice will diminish as some function of the distance from the impurity atom, and there will exist a sphere of radius R_0 (see Fig. 4) around this atom such that the strains outside it may be considered small, and proportional to the stresses. R_0 will, as a rule, be of the order of magnitude of a few atomic diameters. Unless the medium is very anisotropic the effect of the impurity at distant points may then be approximated by the strains set up in a homogeneous medium within which a pressure p is exerted normally to the surface of a sphere of radius R_0. Let E represent Young's modulus; ν Poisson's ratio, ρ the displacement of any given point, which will necessarily be radial; ϵ_r and ϵ_t

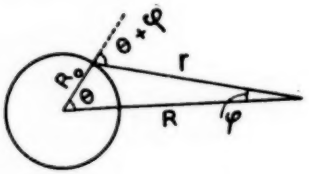

Fig. 4. Diagram to illustrate the symbols used in calculating distortions due to impurities in crystals.

the radial and tangential elongations; and σ_r and σ_t the radial and tangential stresses. It then follows that (see appendix A)

$$\epsilon_r = \frac{d\rho}{dr};\ \epsilon_t = \frac{\rho}{r}$$

$$E\frac{d\rho}{dr} = \sigma_r - 2\nu\sigma_t \tag{1}$$

$$E\frac{\rho}{r} = -\nu\sigma_r + (1-\nu)\sigma_t.$$

For equilibrium it is necessary that the radial forces acting on any volume element $(rd\theta)^2dr$ be cancelled by the radial component of the tangential forces, or $F_r = -4[F_t]_r$. But

$$F_r = \sigma_r(rd\theta)^2 - \left[\sigma_r + \frac{d\sigma_r}{dr}dr\right](r+dr)^2d\theta^2$$

$$[F_t]_r = \sigma_t r d\theta dr d\theta/2$$

which gives

$$r\frac{d\sigma_r}{dr} - 2(\sigma_t - \sigma_r) = 0. \tag{2}$$

Solving Eq. (1) for σ_r and σ_t and substituting the result in Eq. (2), we obtain

$$r^2\frac{d^2\rho}{dr^2} + 2r\frac{d\rho}{dr} - 2\rho = 0. \tag{3}$$

The general solution of this is easily found to be

$$\rho = c_1 r + \frac{c_2}{r^2} \tag{4}$$

and since we are interested in the problem for which one boundary condition is $\rho = 0$ for $r = \infty$, we may put $c_1 = 0$. Using for the other boundary condition that $\sigma_r = p$ for $r = R_0$ we find

$$c_2 = -\frac{(1 - \nu - 2\nu^2)}{2(1 - 2\nu)E} R_0^3 p \tag{5}$$

$$\sigma_r = p\frac{R_0^3}{r^3} \quad \sigma_t = -\frac{p}{2}\frac{R_0^3}{r^3} \tag{6}$$

and for the total energy of the distortion

$$E_n = \frac{1}{2}\frac{4\pi p^2 R_0^3}{E}\frac{1 - \nu - 2\nu^2}{2(1 - 2\nu)}. \tag{7}$$

These results[8] describe the distortion of the lattice at points more than a few atomic diameters removed from the atom causing the distortion and will be used in part 4 in discussing the possible existence of long range forces between atoms of impurity.

3. Diffusion

That diffusion and self-diffusion in solids exists has been known for some time, but the mechanism by which it proceeds is considerably in doubt. Frenkel[9] studied the phenomenon, first with the assumption that the atoms of a solid exchange places, and then[10] somewhat more elaborately with the assumption that some of the atoms occupy positions of "irregular equilibrium" in the interatomic spaces, and that diffusion proceeds by the movement of such atoms down the "aisles" of the lattice. Frenkel, and also Braunbeck[11] obtain expressions for the diffusion coefficients, of which the most interesting feature is that $D \sim e^{-b/T}$ where b is essentially a measure of the work required of an atom to break through its potential walls and so change places with a neighbor. The diffusion process is perhaps best described in terms of wave-mechanics. A particle surrounded by a potential wall will eventually appear on the other side no matter what its energy, the probability w of getting through at a single impact being[12] essentially $e^{-(4\pi/h)\int[2\mu(v-w)]^{1/2}dx}$. The diffusion coefficient for particles having an energy W is then proportional[11] to w. In the above expression $V(x)$ is the potential energy of the particle at a point x, and the integration extends between values of x that make $(V - W)$ vanish. These two formulae agree in predicting that D will increase rapidly with the temperature. Further, because b and V appear as exponents, it is to be ex-

[8] I am indebted to Dr. A. Nadai for his advice and help in handling this problem.
[9] J. Frenkel, Zeits. f. Physik **26,** 137 (1924).
[10] J. Frenkel, Zeits. f. Physik **35,** 652 (1926).
[11] W. Braunbeck, Zeits. f. Physik **44,** 690 (1927).
[12] R. W. Gurney and E. U. Condon, Phys. Rev. **33,** 132 (1929).

pected that the diffusion coefficients for different substances will vary greatly —even as to order of magnitude.

4. More Than One Atom of Impurity

The problem of impurities in solids is essentially that of studying the effects of inhomogeneities in a crystal.[13] But aside from the irregularities produced by the impurity because of its atomic character, there is a large scale effect if its atoms are not disposed at regular intervals. In ferromagnetic substances, for instance, the magnetic quality is determined not by the individual atoms alone, but by their relationship to each other in the lattice. This relationship involves groups of various sizes, such as the crystal grains; the Barkhausen[14] units; the individual blocks, if block structure, as has been suggested,[15] plays a part in ferromagnetic phenomena; and finally, each atom and its immediate[16] neighbors. Therefore, in discussing the effect of an impurity, it is necessary to know how its atoms are distributed among these various groups. Even in the case of a perfect single crystal, fluctuations in the concentration of impurities will in general have the effect of varying its physical properties from point to point, and the macroscopic sample will have to be treated as a heterogeneous medium.

The first case to be considered will be that in which the atoms are incapable of moving through the lattice. Here any distribution whatever will be stable, but the only repeatable distribution will be a random one. In the second case, where diffusion takes place, we shall limit ourselves to stable distributions, namely those which set in after the substance has been kept under constant physical conditions for a sufficiently long time. These distributions will depend on the existence of forces acting between the atoms of the impurity.

Case 1. (see appendix B)

Consider n cells or boxes in which N particles are arranged at random. We require the probability $f(a)$ that a cell chosen at random contain "a" particles. This will be the fraction of the total number of arrangements of the N particles among the n cells in which one particular cell contains "a" particles. The total number of arrangements possible is n^N. If we put "a" particular particles in a given cell, the number of arrangements possible is reduced to $(n-1)^{N-a}$. But the number of ways in which we can choose the "a" particles is $N!/a!(N-a)!$, so that the desired probability becomes

$$f(a) = \frac{N!(n-1)^{N-a}}{a!(N-a)!n^N}. \tag{8}$$

We shall be interested in the case where N and n, but not necessarily a, are large. Applying Stirling's formula for N and n we get

[13] Impurities along crystal boundaries and other surfaces are here neglected.

[14] J. Frenkel and J. Dorfman, Nature **126,** 274 (1930).

[15] F. Bitter, Phys. Rev. **37,** 91 (1931).

[16] F. C. Powell, Proc. Phys. Soc. **42,** 400 (1930) suggests that this last group may contain as many as 58 atoms in iron.

$$\lim_{N\to\infty,n\to\infty} f(a) = \left(\frac{N}{en}\right)^N \left(\frac{e(n-1)}{N-a}\right)^{N-a} \frac{1}{a!}$$

which, neglecting N^{-1} compared to unity, can be written

$$\lim_{N\to\infty,n\to\infty} f(a) = \frac{e^{-\xi}\xi^a}{a!} \tag{9}$$

where $\xi = N/n$, and is the average number of particles per cell. This formula is not convenient for computation when ξ is large, and for this case it is possible to derive[17]

$$\lim_{N\to\infty,n\to\infty,\xi\to\infty,a\sim\xi} f(a) = \frac{e^{-(\xi-a)^2/2\xi}}{(2\pi\xi)^{1/2}}. \tag{10}$$

Curves for various values of ξ are plotted in Figs. 5 and 6. Eq. (10) was used for $\xi = 1000$ only; the other curves represent Eq. (9).

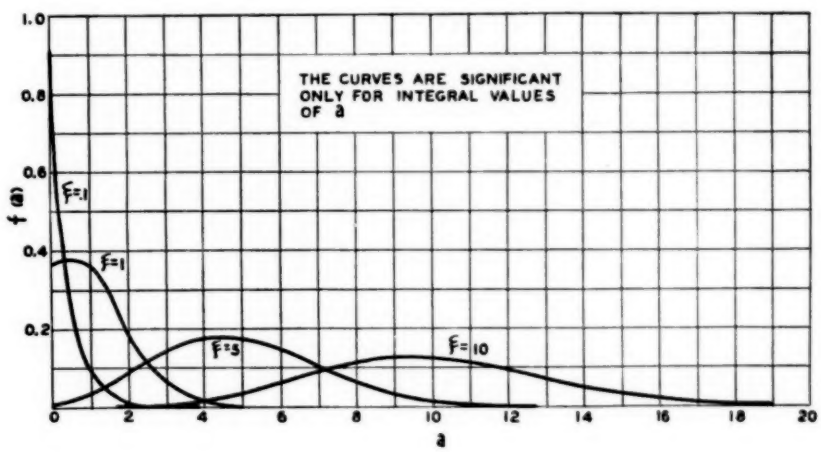

Fig. 5. N particles are randomly distributed among n cells, both N and n being $\gg 1$. $N/n = \xi$. $f(a)$ is the probability of finding "a" particles in a cell chosen at random. This figure shows $f(a)$ for small values of ξ.

Case 2. (See appendix B)

If the particles are capable of motion, they may be considered as a gas exerting a pressure, and the fluctuations will evidently depend on the equation of state. Fowler[18] shows that if v_0 is the volume normally occupied by ξ molecules at a pressure p_0, then writing $((a/\xi)-1)=\gamma$, the fluctuations are determined by

$$f(\gamma)d\gamma = \mu d\gamma \exp\cdot\left[\frac{1}{KT}\left\{\frac{v_0^2\gamma^2}{2!}\frac{\partial p_0}{\partial v_0} + \frac{v_0^3\gamma^3}{3!}\frac{\partial^2 p_0}{\partial v_0^2} + \frac{v_0^4\gamma^4}{4!}\frac{\partial^3 p_0}{\partial v_0^3} + \cdots\right\}\right]. \tag{11}$$

[17] See appendix B.

[18] Fowler, Statistical Mechanics, pp. 515–516.

For a perfect gas $\partial p_0/\partial v_0 = -n_0 KT/v_0$, the terms involving $\partial^2 p_0/\partial v_0^2$ etc. are negligible, and (11) reduces to (10).

The problem of finding the fluctuations in concentration of impurities in solids is now reduced to that of determining the forces acting between the impurity atoms, and hence the equation of state of the impurity. Two impurity atoms separated by only one or two atomic diameters may exert forces on each other arising from their electrons. But if they are separated by much greater distances, it seems reasonable to suppose that the only forces to be taken into consideration will be those resulting from the distortion of the lattice as given in Eqs. (4), (5) and (6). Thus it is necessary to determine the energy $E_n(R)$ of the distortion produced by two atoms of impurity a distance R apart, and then derive the forces by taking the gradient of $E_n(R)$.

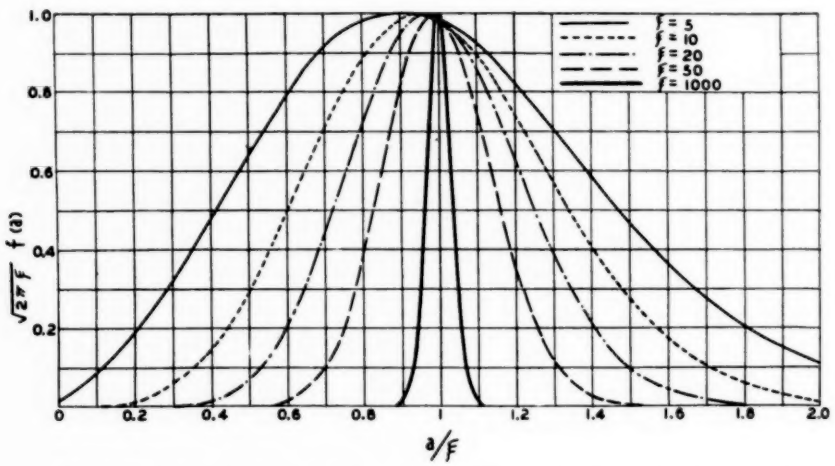

Fig. 6. For the meaning of the symbols see Fig. 5. In Fig. 6 $f(a)$ is plotted for large values of ξ.

Since the differential equations for small strains in an elastic solid are linear, we may add integrals provided the boundary conditions are still satisfied. Referring to the problem treated in part 2, this means that the small distortion of a continuous elastic medium produced by pressures on the surface of two spheres whose centers are a distance R apart are equal to the sum of the displacements ρ as given in Eqs. (4) and (5). The boundary conditions give rise to the added energy

$$\Delta E_n = \oint p\rho_a ds \tag{12}$$

where the integral is taken over the surface of both spheres, and ρ_a is the normal component of the distortion produced by the one sphere at a point on the surface of the other. As is evident from Fig. 4, $\rho_a = -\rho \cos(\theta+\phi)$, $r^2 = R^2 + R_0^2 - 2RR_0 \cos\theta$, and since $\cos(\theta+\phi) = \cos\theta\cos\phi - \sin\theta\sin\phi$, and $\cos\phi = (R - R_0\cos\theta)/r$, $\sin\phi = R_0 \sin\theta/R$, ΔE_n may be written

$$\Delta E_n = -2\int_0^{2\pi} d\phi \int_0^{\pi} R_0^2 \sin\theta d\theta p \frac{c_2}{r^2}\left[\frac{\cos\theta(R - R_0\cos\theta) - \sin\theta a \sin\theta}{r}\right]$$
$$= 4\pi p c_2 R_0^2 \int_{+1}^{-1} \frac{R_0 - R_x}{r^3} dx = 0. \tag{13}$$

In the above the substitution $x = \cos\theta$ has been made for simplicity in integration. This means that for dilute solutions to which alone the above considerations are applicable, the heat of solution per atom is independent of the concentration, and that the molecules of the solute or impurity exert no forces on each other over distances greater than a few atomic diameters. Thus the solute may be treated as a perfect gas and the fluctuations in concetration are correctly given by Eqs. (9) and (10) and Figs. 5 and 6.

There may, however, be short range forces between atoms of impurity, such as cause precipitation. Near a temperature at which precipitation occurs,

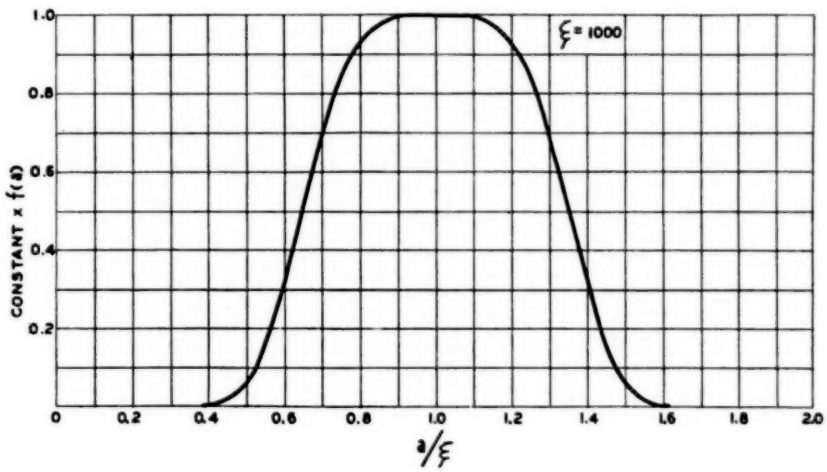

Fig. 7. A volume containing N gaseous molecules is divided into n regions, both N and n being $\gg 1$. $N/n = \xi$. $f(a)$ is the probability of finding "a" molecules in a cell chosen at random. If the gas is near the critical point and $\xi = 1000$ $f(a)$ is given by the curve above. This should be compared with the curve for $\xi = 1000$ in Fig. 6, which represents the corresponding conditions in a perfect gas.

these short range forces may cause very large density fluctuations, as they are in fact known to do in gases near the critical temperature, giving rise to the phenomenon of opalescence. As an example of the order of magnitude of the fluctuations to be expected under such circumstances, the fluctuations of a gas obeying Dietrici's equation of state

$$p(v - b) = NKTe^{-a/NKTV} \tag{14}$$

at the critical temperature are plotted in Fig. 7 for $\xi = 1000$. The formula for this curve may be derived by substituting Eq. (14) and Eq. (11), and the result[18] is

$$f(a) = \text{constant } e^{-(\xi - a)^4/22.2\xi^3}. \tag{15}$$

5. Applications

The above ideas may be applied to the effect of impurities on various properties of metals, but we shall in this paper only point out their bearing on a few ferromagnetic phenomena.

As a first example, consider platinum containing 1–10 percent cobalt, as has been studied by Constant.[19] One of the questions of primary importance in attempting to understand the properties of such solutions will be that of determining how many cobalt atoms are adjacent to 1, 2, 3, . . . etc. other cobalt atoms. In this particular case interatomic forces will be of importance, but it seems clear that unless they are strongly repulsive, one can hardly expect such solutions to be homogeneous. That is, the solution will consist of small regions which will behave like pure platinum, and small regions which will approximate pure cobalt, and all intermediate gradations. Since paramagnetism and diamagnetism are as a rule negligibly small compared to ferromagnetism, it may be a good approximation to treat the above solution as a group of ferromagnetic inclusions in non-magnetic material. In a future communication on block structure and ferromagnetism I hope to return to a more detailed discussion of the properties of such solutions.

One of the outstanding facts about ferromagnetism is its susceptibility to strains, and in the preceeding sections we have discussed the strains due to individual atoms of impurity. To these may be added strains due to fluctuations in concentration of impurities. Until more is known of the mechanism of magnetization it is useless to say anything about the effects of these strains on the hysteresis loop, magnetization curve, etc. beyond pointing out that strains do have large effects, that impurities do cause strains, and that consequently impurities may be expected to have large effects on magnetic properties by virtue of these strains.[20]

As has been mentioned, an impure metal may be expected to behave like an aggregate of regions whose physical properties are dissimilar. A phenomenon which would show the effect of these small regions would be the change of phase, if observed under suitable conditions. Suppose that some pure substance A undergoes a transformation at the temperature T, and that addition of some other substance B which dissolves in A lowers the transformation temperature. According to what has been said, B will distribute itself over A in such a way as to produce varying concentrations of B. It is to be expected that those regions containing small concentrations of B will undergo transformation at higher temperatures than those regions containing larger concentrations. The conclusion is that solutions undergo transformation *gradually* over a finite range of temperatures, a phenomenon which is often observed. So many other factors enter into the rate of transformation, however, that it is not practicable to attempt here a detailed comparison bebetween experimental facts and the above ideas.

[19] F. W. Constant, Phys. Rev. **36**, 1654 (1930).

[20] In this connection, see, for instance, an article by T. D. Yensen, Metals and Alloys **1**, 493 (1930).

Lastly, let us consider a peculiar feature of the iron-carbon diagram as it is usually drawn. This concerns the magnetic transformation A_2 in iron containing between 0.6 percent and 0.9 percent carbon, which, at the A_2 temperature of about 770°C is in the form of austenite, or γ-iron+carbon in solution. The significant point, as Honda and Takagi[21] have pointed out, is that the A_2 point in γ-iron+carbon is essentially the same as that of α-iron+carbon. This fact, for it has been observed so often as seemingly to leave no room for doubt, is not to be understood in the light of present concepts about the nature of ferromagnetism, and will necessitate fundamental changes, unless it is found that what has heretofore been called γ-iron+carbon actually contains small inclusions of α-iron which are responsible for the observed ferromagnetism of austenite. In the light of the previous discussion one would expect to find small regions having low carbon concentration, and it is these regions that might form inclusions of α-iron. Such regions should be capable of detection by means of x-rays, and an investigation is under way to determine whether or not they are actually present.[22]

Appendix A

Calculation of small strains due to impurities, and the resulting long range forces between atoms of impurity

Consider an infinite isotropic elastic medium in which a spherical hole has been excavated. A pressure p acts normally to the surface of the excavation, whose radius is R_0. What is the distortion and stress throughout the medium?

E = Youngs modulus; ν = Poisson's ratio; ρ = displacement—which is everywhere radial; ϵ_r = radial elongation; ϵ_t = tangential elongation; σ_r = radial stress; and σ_t = tangential stress.

Consider an element of volume bounded by two spherical surfaces $[rd\theta]^2$ and $[(r+dr)d\theta]^2$ and by the four plane surfaces $(r+dr/2)d\theta dr$

$$\epsilon_r = \frac{d\rho}{dr} \qquad \epsilon_t = \frac{\rho}{r}$$

$$\left.\begin{aligned} \epsilon_r &= \frac{1}{E}(\sigma_r - 2\nu\sigma_t) \\ \epsilon_t &= \frac{1}{E}(\sigma_t - \nu\sigma_t - \nu\sigma_r) \end{aligned}\right\} \text{ or } \left\{\begin{aligned} E\frac{d\rho}{dt} &= \sigma_r - 2\nu\sigma_t \\ E\frac{\rho}{r} &= -\nu\sigma_r + (1-\nu)\sigma_t \end{aligned}\right. \qquad \text{I}$$

[21] K. Honda and H. Takagi, Sci. Rep. Tohoku Univ. **2**, 203 (1914).

[22] See item 3 at the conclusion of the first section. Since completing this paper an article by F. M. Jaeger and J. E. Zanstra, Proc. Akad. Amsterdam **34**, 15, 1931 has come to my attention. Among other things, the authors investigate the crystal structure of rhodium as a function of temperature, and find (p. 19) that two phases co-exist as a mixture, one phase being present in the other in the form of very small particles containing $(33)^3$ or 36,000 atoms. Not only is the co-existence of the two phases of interest in connection with the previous discussion, but also the estimated size of the small inclusions, as having a possible bearing on the block theory of Zwicky.[4]

F_r and F_t are the forces acting on the various faces of the above volume element. For equilibrium

$$F_r = \sigma_r(rd\theta)^2 - \left[\sigma_r + \frac{d\sigma_r}{dr}dr\right](r + dr)^2d\theta^2$$

$$-F_r = \sigma_r 2rdrd\theta^2 + \frac{d\sigma_r}{dr}drr^2d\theta^2$$

$$[F_t]_r = \sigma_t rd\theta drd\theta/2$$

and using the equilibrium conditions

$$r\frac{d\sigma_r}{dr} - 2(\sigma_t - \sigma_r) = 0. \qquad \text{II}$$

From I eliminate σ_r

$$E(\rho/r + \nu\rho') = \sigma_t(1 - \nu - 2\nu^2).$$

Eliminate σ_t

$$\sigma_r = E\rho' + \frac{2\nu E}{1 - \nu - 2\nu^2}(\rho/r + \nu\rho')$$

or

$$\sigma_t = \frac{E}{1 - \nu - 2\nu^2}(\rho/r + \nu\rho')$$

$$\sigma_r = \frac{E}{1 - \nu - 2\nu^2}[2\nu\rho/r + (1 - \nu)\rho'] \qquad \text{III}$$

Substitute III in II and get

$$r^2\rho'' + 2r\rho' - z\rho = 0. \qquad \text{IV}$$

Substitute $\rho = r^n$, and it is seen that $n = 1$ or -2 and the solution of IV therefore is

$$\rho = c_1 r + \frac{c_2}{r^2}$$

which in our case becomes $\rho = c_2/r^2$ since $\rho = 0$ for $r = \infty$ and therefore $c_1 = 0$.

If the boundary conditions are put in the form

$$\sigma_r = p \text{ for } r = R_0, \text{ then}$$

$$c_2 = -\frac{(1 - \nu - 2\nu^2)}{2(1 - 2\nu)E}R_0^3 p$$

$$\sigma_r = pR_0^3/r^3$$

$$\sigma_t = -p/2a^3/r^3.$$

If the boundary conditions are given in terms of strains instead of stresses

$$\rho = \delta \text{ for } r = R_0,$$

then

$$c_2 = R_0^2\delta \qquad \rho = \delta R_0^2/2$$

$$\sigma_r = \frac{-2(1-2\nu)c_2E}{1-\nu-2\nu^2}\frac{1}{r^3}, \qquad \sigma_t = -\sigma_r/2.$$

The energy of the distortion can be calculated in two ways

$$E_n = \delta\tfrac{1}{2}\sigma_r\big]_{r=R_0}\cdot\rho\big]_{r=R_0}\cdot\text{area} = \tfrac{1}{2}p\cdot\frac{-(1-\nu-2\nu^2)}{2(1-2\nu)E}\frac{R_0^3p}{R_0^2}\cdot 4\pi R_0^2$$

$$= \frac{1}{2}\frac{4\pi p^2R_0^3}{E}\frac{1-\nu-2\nu^2}{2(1-2\nu)}$$

or

$$E_n = \tfrac{1}{2}\int_{r=a}^{r=\infty}(\epsilon_r\sigma_r + 2\epsilon_t\sigma_t)dv$$

$$= \tfrac{1}{2}4\pi\int_a^\infty\left(-2c_2pR_0^3 - \frac{2c_2pR_0^3}{2}\right)\frac{dr}{r^4}$$

$$= -\frac{4\pi}{2}\int_a^\infty\frac{dr}{r^4}3c_2pR_0^3 = 4\pi c_2pR_0^3\frac{3}{3R_0^3}$$

$$= \frac{1}{2}\frac{4\pi p^2R_0^3}{E}\frac{1-\nu-2\nu^2}{2(1-2\nu)}$$

in agreement with the above.

For two spheres whose centers are a distance R apart ($R \gg R_0$) the total energy becomes $2E_n + \Delta E_n$ where

$$\Delta E_n = -2\int_0^\pi a^2\sin\theta d\theta p\frac{\delta R_0^2}{r^2}\left[\frac{\cos\theta(R - a\cos\theta)}{r} - \frac{\sin\theta a\sin\theta}{r}\right]$$

see Eq. (13) of the text. Substituting $\cos\theta = x$, we have

$$\Delta E_n = -4\pi p\delta R_0^4\int_1^{-1}\frac{x(R - R_0x) - R_0(1-x^2)}{r^3}dx$$

$$= 4\pi p\delta R_0^4\int_1^{-1}\frac{R_0 - Rx}{r^3}dx = 4\pi p\delta R_0^4(R_0A - RB)$$

where

$$A = \int_1^{-1}\frac{dx}{r^3} \quad B = \int_1^{-1}\frac{xdx}{r^3}.$$

Let

$$r^3 = (\alpha + \beta x)^{3/2} \quad a = R^2 + R_0^2 \quad \beta = -2R_0R$$

$$A = \int_1^{-1} \frac{dx}{(\alpha + \beta x)^{3/2}} = \frac{2}{\beta}\left[\frac{(\alpha - \beta x)^{-1/2}}{-1}\right]_1^{-1} = -\frac{2}{\beta}\left[\frac{1}{(\alpha-\beta)^{1/2}} - \frac{1}{(\alpha-\beta)^{1/2}}\right]$$

$$B = \int_1^{-1} \frac{x dx}{(\alpha + \beta x)^{3/2}} = \frac{2}{\beta^2}\left[\frac{(\alpha + \beta x)^{1/2}}{1} + \frac{\alpha}{(\alpha + \beta x)^{1/2}}\right]_1^{-1}$$

$$= \frac{2}{\beta^2}\left[\frac{2\alpha + \beta x}{(\alpha + \beta x)^{1/2}}\right]_1^{-1}$$

$$B = \frac{2}{\beta^2}\left[\frac{2\alpha - \beta}{(\alpha - \beta)^{1/2}} - \frac{2\alpha + \beta}{(\alpha + \beta)^{1/2}}\right]$$

But

$$(\alpha + \beta)^{1/2} = (R^2 - 2RR_0 + R_0^2)^{1/2} = R - R_0$$

$$(\alpha - \beta)^{1/2} = R + R_0$$

$$A = -\frac{2}{R(R^2 - R_0^2)} \qquad B = \frac{2R_0}{R^2(R^2 - R_0^2)}$$

and therefore

$$\Delta E_n = 4\pi p \delta R_0^4 (R_0 A - RB) = 0.$$

Appendix B

Details of calculations of density fluctuations

The derivation of Eq. (8) in the text

$$f(a) = \frac{N!(n-1)^{N-a}}{a!(N-a)!n^N}$$

is perhaps given in sufficient detail to be quite clear. Assuming $N \to \infty$, $n \to \infty$, we may write, according to Stirling's theorem

$$\lim_{n\to\infty} p! = (2\pi p)^{1/2}\left(\frac{p}{e}\right)^p$$

$$\frac{N!}{(N-a)!} = \frac{N^{1/2}}{(N-a)^{1/2}} \frac{\left(\frac{N}{e}\right)^N}{\left(\frac{N-a}{e}\right)^{N-a}} = e^{-a}N^N(N-a)^{-(N-a)}$$

Here $\lim_{N\to\infty} N^{1/2}/(N-a)^{1/2}$ has been put equal to unity, and we get

$$\lim_{N\to\infty, n\to\infty} f(a) = \left(\frac{N}{eN}\right)^N \left(\frac{e(n-1)}{N-a}\right)^{N-a} \frac{1}{a!} \cdot$$

It is desired to put this in a form in which N and n appear only as a ratio, $N/n=\xi$. To this end we put

$$\frac{e(n-1)}{N-1}=\frac{e(n-1)}{N}\,\frac{1}{1-a/N}$$

and hence

$$\lim_{N\to\infty,n\to\infty} f(a) = \left(\frac{N}{en}\right)^N\left(\frac{e(n-1)}{N}\right)^N\frac{1}{(1-a/N)^N}\left(\frac{e(n-1)}{N-a}\right)^{-a}\frac{1}{a!}$$

$$=\left[\frac{1-\dfrac{1}{n}}{1-\dfrac{a}{N}}\right]^{N-a}\left(\frac{en}{N}\right)^{-a}\frac{1}{a!}$$

But, simplifying, we find

$$\left[\frac{1-\dfrac{1}{n}}{1-\dfrac{a}{N}}\right]^{N-a} = \left[\left(1-\frac{1}{n}\right)\left(1+\frac{a}{N}+\cdots\right)\right]^{N-a} = \left(1-\frac{1}{n}+\frac{a}{N}\right)^{N-a}$$

$$=\left[1+\frac{a-\xi}{N}\right]^N\left[1+\frac{a-\xi}{N}\right]^{-a}=\left[1+\frac{a-\xi}{N}\right]^N$$

since

$$\lim_{N\to\infty}\left[1+\frac{a-\xi}{N}\right]^{-a}=1.$$

Expanding $[1+a-\xi/N]^N$, and neglecting $1/N$ compared to unity, we get

$$1+a-\xi+\frac{1}{2!}(a-\xi)^2+\frac{1}{3!}(a-\xi)^3+\cdots=e^{a-\xi}$$

and finally

$$\lim_{N\to\infty,n\to\infty} f(a) = e^{a-\xi}\left(\frac{en}{N}\right)^{-a}\frac{1}{a!}=\frac{e^{-\xi}\xi^a}{a!} \qquad \text{I}$$

and

$$\lim_{N\to\infty,n\to\infty,\xi\to\infty,a\sim\xi} f(a) = \frac{e^{-\xi}\xi^a}{(2\pi a)^{1/2}}\left(\frac{e}{a}\right)^a. \qquad \text{II}$$

To find for what value of "a", say a_m $f(a)$ has a maximum, we require the formula

$$\frac{d}{da}\left(\frac{e}{a}\right)^a=\left(\frac{e}{a}\right)^{-a}\log_e\frac{1}{a}$$

We then find

$$\frac{df}{da} = \left\{ \frac{e^{\xi}\left(\frac{e\xi}{a}\right)^{a}}{(2\pi a)^{1/2}} \left[\log_e \frac{1}{a} + \log_e \xi - \frac{2\pi}{4\pi a} \right] \right\}_{a=a_m} = 0$$

or

$$\log_e a_m = \log_e \xi - \frac{1}{2a_m}$$

and for

$$a_m \gg 1, \quad a_m = \xi.$$

For large values of ξ these formulae are not very satisfactory for numerical computations, and the following procedure leads to a more desirable result.

Given n = number of cells, N = number of particles, $N/n = \xi$ is the average number of particles per cell, a_s = number of particles in cell s.

$$s\sum_1^n a_s = N \quad s\sum_1^n (a_s - N/n) = 0.$$

The fraction of the phase space occupied by this distribution is (see Jeans, Dynamical Theory of Gases, page 47)

$$\theta_a = n^{n/2}(2\pi N)^{-(n-1)/2} e^{-NK_a}$$

$$K_a = \frac{1}{N} s\sum_1^n (a_s + \tfrac{1}{2}) \log_e \frac{na_s}{N}.$$

This assumes the applicability of Stirling's formula. Substituting $\alpha_s = a_s - N/n$ in the expression for K_a, we get

$$K_a = \frac{1}{N} s\sum_1^n \left(\frac{N}{n} + \alpha_s + \frac{1}{2}\right) \log_e \left(1 + \frac{n\alpha_s}{N}\right).$$

Neglecting $1/2$ compared to N/n, we get

$$K_a = \frac{1}{n} s\sum_1^n \left(1 + \frac{\alpha_s}{\xi}\right) \log_e \left(1 + \frac{\alpha_s}{\xi}\right)$$

$$= \frac{1}{N}\left\{ \frac{1}{2}\,\frac{n}{N} s\sum_1^n \alpha_s^2 - \frac{1}{6}\left(\frac{n}{N}\right)^2 s\sum_1^n \alpha_s^3 + \cdots \right\}$$

Whenever we can write

$$s\sum_1^n \left(\frac{n\alpha_s}{N}\right)^2 \gg \frac{1}{3} s\sum_1^n \left(\frac{n\alpha_s}{N}\right)^3 \text{ and higher powers} \qquad \text{III}$$

then the expression for K_a is considerably simplified.

$$NK_a = \frac{1}{2}\frac{n}{N} s \sum_1^n \alpha_s^2.$$

Jeans shows (page 48) that the fraction of the phase space which represents distributions for which $K_0 < K < K_0 + dK$ is

$$\frac{N^{(n-1)/2}}{\Gamma\left(\frac{n-1}{2}\right)} e^{-NK_0} K_0^{(n-3)/2} dK.$$

In a similar way it can be shown that the fraction of the phase space for which $K_0 < K < K_0 + dK$ and in addition for which an α_p chosen at random is equal to some given number, say α, is

$$\theta_a n^{-1/2} \frac{dA}{dK} dK$$

where θ_a and K have the values above and

$$A = \frac{\pi^{(n-2)/2}}{\Gamma\left(\frac{n}{2}\right)} \left(\frac{2N^2 K_0}{n} - \alpha^2\right)^{(n-2)/2}.$$

Substituting $x = NK - n\alpha^2/2N$ we get

$$A = \frac{\pi^{(n-2)/2}}{\Gamma\left(\frac{n}{2}\right)} \left(\frac{2N}{n} x\right)^{(n-2)/2}$$

$$\frac{dA}{dK} dK = \frac{dA}{dx}\frac{dx}{dK} dK$$

or

$$\frac{dA}{dK} dK = \frac{\pi^{(n-2)/2}}{\Gamma\left(\frac{n}{2}\right)} \frac{1}{2}(n-2)\left(\frac{2N}{n} x\right)^{n/2-2} \frac{2N}{n} dx$$

$$= \frac{\pi^{n/2-1}}{\Gamma\left(\frac{n}{2}-1\right)} \left(\frac{2N}{n}\right)^{n/2-1} dx$$

and

$$\theta_a n^{-1/2} \frac{dA}{dK} dK = \left(\frac{2\pi N}{n}\right)^{-n/2+1/2} \left(\frac{2\pi N}{n}\right)^{n/2-1} \frac{e^{-n\alpha^2/2N}}{\Gamma\left(\frac{n}{2}-1\right)} e^{-x} x^{n/2-2} dx$$

or

$$\frac{e^{-\alpha^2/2\xi}}{(2\pi\xi)^{1/2}\Gamma\left(\frac{n}{2}-1\right)} e^{-x}x^{n/2-2}dx.$$

In order to find the fraction of the phase space for which $\alpha_p=\alpha$, the above expression must be integrated over all values of K from 0 to ∞, or of x from $-n\alpha^2/2N$ to ∞.

$$\int_{-n\alpha^2/2N}^{\infty} e^{-x}x^{n/2-2}dx = \int_0^{\infty} e^{-x}x^{n/2-2}dx + \int_0^{n\alpha^2/2N} e^{-x}x^{n/2-2}dx$$

$$= I + II$$

$$I = \Gamma\left(\frac{n}{2}-1\right)$$

and the result is that the fraction of the phase space for which a given cell contains α-particles is

$$f(a) = \frac{1}{(2\pi\xi)^{1/2}} e^{-a^2/2\xi}\left[1 + \frac{II}{\left(\frac{n}{2}-2\right)!}\right]$$

But

$$II = -\left[e^{-x}\left(\frac{n}{2}-1\right)!\left\{1 + p\sum_1^{n/2-2}\frac{x^p}{p!}\right\}\right]_0^{\alpha^2/2\xi}$$

and therefore

$$\lim_{n\to\infty} \frac{II}{\left(\frac{n}{2}-2\right)!} = -\left[e^{-x}e^{x}\right]_0^{\alpha^2/2\xi} = 0$$

and the complete result is

$$\lim_{N\to\infty,\, n\to\infty,\, \xi\to\infty,\, a\sim\xi} f(a) = \frac{1}{(2\pi\xi)^{1/2}} e^{-a^2/2\xi} \qquad \text{IV}$$

the condition $\xi\sim a$ being intended to indicate that the assumption in Eq. III must be satisfied.

It remains to be shown that Eq. II and IV are equivalent.

$$\lim_{N\to\infty,\, n\to\infty,\, \xi\to\infty,\, a\sim\xi} \frac{e^{-(\xi-a)^2/2\xi}}{(2\pi\xi)^{1/2}} = \frac{e^{-\xi}}{(2\pi a)^{1/2}}\left(\frac{e\xi}{a}\right)^a$$

Omitting the cumbersome limits, we may write

$$e^{\xi^2-a^2/2\xi} = \left(\frac{\xi}{a}\right)^{a+1/2}.$$

Omitting 1/2 compared to a and taking the logarithm of both sides this becomes

$$\frac{\xi^2}{a^2} - 1 = \frac{\xi}{a} \log \left(\frac{\xi}{a}\right)^2$$

and expanding the logarithm for values of the argument near unity this becomes

$$\frac{\xi^2}{a^2} - 1 = \frac{\xi}{a}\left(\frac{\xi^2}{a^2} - 1\right)$$

which is valid for $\xi \sim a$.

LETTERS TO THE EDITOR

Prompt publication of brief reports of important discoveries in physics may be secured by addressing them to this department. Closing dates for this department are, for the first issue of the month, the twenty-eighth of the preceding month; for the second issue, the thirteenth of the month. The Board of Editors does not hold itself responsible for the opinions expressed by the correspondents.

OH Bands and the Ultraviolet Line Spectrum of the Wehnelt Interrupter

With an improved form of Wehnelt interrupter, equipped with a cooling coil and an electrolyte circulator, the spectrum of the discharge at the positive platinum point electrode has been investigated in the region λ4000 to λ2230. Solutions of hydrochloric, sulphuric, and nitric acid were used.

The OH bands were particularly prominent. A continuous banding from head to head was present. The new lines observed have been analysed and rotational assignments made. Twenty-four new lines have been added to the analysis by Jack (Proc. Roy. Soc. **A115,** 373 (1927)) of the band λ2608, and 120 lines to the analysis by Watson (Astrophys. J. **60,** 145 (1924)) of the bands λλ2811 and 2875. A few rearrangements of previous assignments were made in the case of the latter bands—particularly in the *R* branch of λ2875. Seventy three new assignments were made in the analysis by Fortrat (J. de Physique **5,** 20 (1924)) of the bands λλ3064 and 3122. A preliminary comparison of wave-lengths of the new lines observed in these bands with values given in Rowland's table of solar lines showed good agreement with lines of unknown origin.

The band λ3428 is present on the plates but seems to present no new features.

A new band in the region λ3525 is being investigated in view of its possible relationship to the OH system.

Up to the present only lines arising from the platinum anode have been observed between λλ2608 and 2230.

R. WILLIAM SHAW

Department of Physics,
Cornell University.

May 6, 1931.

An Infrared Band System of Iodine Bromide

During an investigation of the absorption of iodine bromide in the visible, the writers recently observed an infrared band system due to this substance which, so far as they are aware, has not previously been reported. When an absorption cell 3 ft. in length was used, containing IBr at about 90 mm pressure at 50°, five band progressions of moderate intensity were observed in the region λλ6850–8060. Due to the fact that there is a rather sudden change in the slope of the ω_v v curve for the upper state at $v'=12$ it is not possible to represent the entire system satisfactorily by one simple formula. However, those bands for which v' is less than 12 are well represented by the equation:

$$\nu(\text{cm}^{-1}) = 13{,}251 + (105.9\, v' - 2.42\, v'^2) - (266.5\, v'' - 0.81\, v''^2).$$

The absolute numbering of the vibrational levels of the upper electronic state is still in some doubt as it has not as yet been possible to make use of the isotope effect which is not very readily measurable.

The upper electronic level of the infrared system is a state which yields normal atoms on dissociation. By means of a graphical extrapolation the energy of dissociation of the normal IBr molecule into normal atoms has been estimated to be 1.801 ± 0.007 volts ($41{,}520 \pm 150$ cal). The good agreement with the value 1.84 volts estimated by Cordes and Sponer[1] from fluorescence data of Loomis

[1] H. Cordes and H. Sponer, Zeits. f. Physik **63,** 334 (1930).

is possibly due to a compensation of errors in the latter case.

Recent studies in this laboratory[2] on the effect of temperature on the equilibrium between iodine, bromine, and iodine bromide have given an accurate value for the heat of formation of iodine bromide ($H_{298°}$) given in the following equation:

$I_2 + Br_2 = 2\ IBr + 2{,}540$ cal (0.110 volts).

Since the heat of this reaction is practically independent of temperature it may be compared directly with the energy change at the absolute zero, for the reaction, calculated from the spectroscopic determinations of the dissociation energies of iodine,[3] bromine, and iodine bromide. This spectroscopic value is 2,440 cal (0.106 volts), which checks with the thermal value well within the probable experimental error. This agreement is good evidence for the self consistency of the spectroscopic values of the dissociation energies of the three molecules in question.

RICHARD M. BADGER
DON M. YOST
Gates Chemical Laboratory,
California Institute of Technology,
May 7, 1931.

[2] D. M. Yost and J. McMorris, to appear shortly in the Journ. Am. Chem. Soc.

[3] We have used for the dissociation energy of iodine a value 1.535 volts received in a personal communication from Mr. W. G. Brown, at Berkeley, California.

Thermionic Emission in Caesium-Oxide Photo-cells at Room Temperatures

During an investigation of the suitability of some caesium oxide on silver photoelectric cells for astronomical photometric work at low intensities it was noticed that in some cases there was, in total darkness, a large, unidirectional leakage which increased rapidly as the cell was warmed and which could be decreased considerably by the application of a magnetic field. These facts indicated conclusively that the leakage was of thermionic origin. Subsequently more careful temperature measurements were made both above and below room temperatures which showed that the emissions were following the ordinary T^2 equation with thermionic work functions in different cells varying from about 0.40 to 0.80 volt.

The largest thermionic current which we have observed at 20°C and 22.5 volts is 8×10^{-9} amperes in a cell of about 88 cm² cathode area, which is approximately the current given photoelectrically by exposing the cell to an illumination of 3×10^{-4} lumens from tungsten light at 2848°K color temperature. Observations were made on this cell as low as −5°C and could undoubtedly have been continued lower if we had shifted from our high sensitivity galvanometer to the electrometer. The thermionic constants determined from a plot were $A=5\times10^{-3}$; $b_0=8550$. At 20°C an increase of one degree increases the thermionic current about 11.2 percent so that when such a cell is used for photoelectric measurements it might well be necessary to control its temperature. The value of b_0 for this particular cell is very close to that found by Koller (Phys. Rev. **33**, 1082 (1929)) for some caesium oxide on silver cells from 100° up to 170°C.

Another cell of somewhat lower photoelectric sensitivity gave the values, $A=3.7\times10^{-10}$; $b_0=4290$, the lowest that we have yet obtained. The cathode area of this cell was 19.4 cm², and the total current at 20°C was about 2.7×10^{-10} amperes, with only a 5.8 percent increase in a temperature rise of one degree. The largest thermionic current at room temperature was therefore not obtained with the cell of lowest work function due to the very great decrease in the value of A. The measurements made so far on different cells do not indicate any precise relation between $\log A$ and b_0 which would enable one to predict definitely the emission at room temperature from the thermionic work function. If there is a large decrease in b_0 as shown above, it is of course reasonable to expect a decrease in A otherwise the emission would increase enormously.

Measurements on some of the cells at constant illumination to tungsten light showed a decided drop in the photo current with considerable increase of temperature while on the other hand the effect of cooling did not seem to be nearly as great in producing an increase. This is opposite to what Koller found with cathodes much less sensitive photoelectrically than our own.

We have purposely selected for this work cells with clean walls and stems which gave negligible ohmic leakage. The two kinds of leakage are present in many cells and it is difficult to separate them with certainty. If

the caesium oxide on silver cell is to be used for measuring very small light intensities, the area of the cathode should not be any larger than is necessary to intercept the radiation; that is, the photoelectric emission should be made as large as possible relative to the thermionic emission.

E. F. KINGSBURY
G. R. STILWELL
Bell Telephone Laboratories,
New York, New York,
March 30, 1931.

A Case of Abnormal Molecular Rotation

In the fluorescence of mercury vapor with the addition of nitrogen and a trace of hydrogen, Gaviola and Wood[1] observed the band spectrum of the HgH molecule with an abnormal rotation corresponding to an apparent temperature of 3000°, although the gas was at room temperature. This observation has been interpreted[2] by the assumption of the following sequence of processes: formation of the HgH molecule, then excitation of this molecule with high oscillation and normal rotation according to the Franck-Condon rule, and finally change of oscillation into rotation during the life time of the excited state through collisions with N_2 molecules. In this interpretation, the high rotation observed in the band spectrum is therefore not directly excited but due to a secondary effect.

An interesting similar observation has recently been described by W. Lochte-Holtgreven.[3] He found in the electric discharge in acetylene the C_2 bands with an abnormal rotational energy corresponding to 4700° and the CH bands with 2000°.

By varying the conditions, he found that these "rotational temperatures," being much larger than the real temperatures, are not due to secondary effects such as collisions during the life time of the excited state. Instead he concluded they must arise from the elementary process of excitation itself. Thus the interpretation must differ from that of the rotation of the HgH molecule just described. The present letter deals with this new observation, thus supplementing the interpretation of the HgH bands given in a previous paper.

It seems possible to understand the high rotation of the C_2 and CH bands in the acetylene discharge on the basis of the Franck-Condon rule dealing originally with oscillations. According to Hedfeld and Mecke, the $HC \equiv CH$ molecule in its normal state forms a straight line.[4] Let us assume that in its excited state it forms a crooked line. Professor Slater has pointed out to me that such a pronounced change in the shape of the molecule is not all an arbitrary assumption, but should be expected, if in the excitation process the carbon atom goes over from the quadrivalent to the divalent state. The same change of valence by excitation has been found e.g. in the CN molecule.[5] According to Slater's new theory,[6] the straight line model of the normal state points to quadrivalent C atoms while the two valences of a divalent atom should always be at right angles, thereby forming a crooked molecule.

This pronounced change in the shape of the molecule lends itself to an application of Franck's idea. The change of electron configuration is fast compared with the motion of the nuclear masses. Immediately after the excitation process, the molecule in its new electronic state has still its old shape and therefore a large potential energy leading to intense vibration. Contrary to the vibration of the diatomic molecule, the motion is essentially transverse.[7] This vibration might produce dissociation, if the potential energy exceeds the dissociation energy. Any dissociation process brought about by absorption of light can be recognized experimentally by the continuous absorption spectrum. In the case of the HCCH molecule, mainly continuous absorption has been observed as reported by

[1] E. Gaviola and R. W. Wood, Phil. Mag. **6**, 1191 (1928).

[2] H. Beutler and E. Rabinowitsch, Zeits. f. physik. Chem. (B) **8**, 403 (1930); O. Oldenberg, Phys. Rev. **37**, 194 (1931).

[3] W. Lochte-Holtgreven, Zeits. f. Physik **67**, 590 (1931); G. B. Kistiakowsky, Phys. Rev. **37**, 276 (1931).

[4] K. Hedfeld and R. Mecke, Zeits. f. Physik **64**, 151 (1930).

[5] W. Heitler and G. Herzberg, Zeits. f. Physik **53**, 52 (1929).

[6] J. C. Slater, Phys. Rev. **37**, 481 (1931).

[7] Cf. R. Mecke, Zeits. f. Physik **64**, 173 (1930).

Lochte-Holtgreven and by Kistiakowsky. It might be assumed that this absorption corresponds partly to the described process.

This splitting up of the molecule by *transverse* vibration leads necessarily to strongly *rotating* molecules. (Fig. 1). The transverse vibration which splits up the centre bond of the HC≡CH molecule leads to two CH molecules strongly rotating in opposite direction,

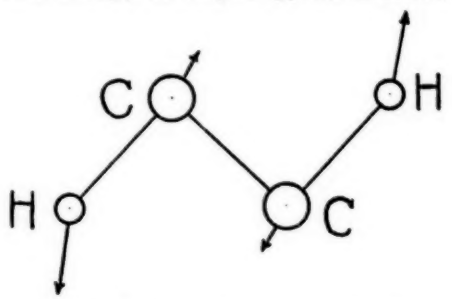

Fig. 1. Vibration of the excited HCCH molecule.

while the total moment of momentum of the system remains unchanged or changed only by unity. In the other dissociation process mentioned by Lochte-Holtgreven, the H atoms might fly away in the direction of the arrows (Fig. 1) leaving an excited C_2 molecule. This must have high rotation as indicated again by the arrows. Dissociation in steps might take place too.

In general any combination of increasing longitudinal and transverse vibration should lead to a dissociation resulting in a rotating and vibrating molecule, the energy of which is determined by the potential curves and not by the temperature of the gas. Thus we understand the observation reported by Lochte-Holtgreven, that the rotation of the excited molecules C_2 and CH is characteristic for this excitation process starting from HC≡CH and that its energy shows some deviation from a Boltzmann distribution.[8]

Has this argument a bearing on the diatomic molecule? This might be the case, considering the diatomic molecule in collision with an atom. When by impact of the second kind the HgH molecule takes over excitation energy from the Hg′, it is generally assumed, that the rotation of the HgH does not change considerably, but that the vibration might change on the basis of the Franck-Condon rule. It must be taken into account, however, that after the excitation process the H atom starts its fast vibration in the close neighbourhood of the colliding slow Hg atom. *In the same collision process*, therefore, this might turn over the motion of the H atom from *vibration* into *rotation*. No appreciable kinetic energy of *translation* is produced due to the heavy weights of the Hg atom and the HgH molecule. In other words, the H atom starts its motion in a modified field of force determined by the new electronic state of the HgH molecule and at the same time the presence of the colliding Hg atom. This motion might be rotation as well as vibration. (If in the case of good resonance the transfer of electronic energy by impact of the second kind takes place over an exceptionally large distance, this argument might fail, because in this case the HgH molecule would become excited without being disturbed in its vibration by the close neighbourhood of a colliding heavy body.)

The statement, therefore, that no appreciable rotation is produced by impact, holds for excitation by electron impact and for every thermal impact. However, it should not be supposed to hold for this type of impact of the second kind between heavy bodies.

This process in addition to the process discussed in the writer's recent paper[9] would be expected to play a part in Gaviola's and Wood flourescence experiment.

O. OLDENBERG

Jefferson Physical Laboratory,
Harvard University,
Cambridge, Massachusetts,
April, 1931.

[8] R. M. Badger and J. L. Binder (Phys. Rev. **37**, 800 (1931)). mention a certain difficulty in calculating dissociation energies of polyatomic molecules from band spectra, due to the fact the fragments might retain a considerable amount of energy in their *electronic* and *vibrational levels*. According to the present result, also the *rotation* is able to keep energy far exceeding the thermal value.

On the Effect of Resonance in the Exchange of Excitation Energy

I should like to add a few words to the letter recently sent to the Editor of the Physical Review, under the above title. The application of the Franck-Condon principle to this problem brings out another point which supplements those already considered and which

will be of importance if the two curves shown in Fig. 1 of the above mentioned article reach their asymptotic values at something like the same value of r, which may often be expected to be the case. Then it is seen that, unless the asymptotic values are the same within the order of magnitude of the average relative translational energy of two at the temperature considered, the intersection of the two curves will occur so high up that it will be out of reach of an average pair of colliding atoms even though the initial state be represented by the upper curve; of course if the initial state is represented by the lower curve, the transition cannot occur with an average pair of atoms unless the curves are close enough together so that the difference in energy can be made up by conversion of the limited translational energy available to electronic energy, but this consideration shows that transitions will often be prevented even when the conversion is in the other direction, from internal to translational energy. It is of interest to note that in the cases considered by Kallmann and London (Zeits. f. physik. Chem. **2B**, 226 ff. (1929)) the energy transferred from translational to internal or *vice versa* is, in the case of those transitions which occur with exceptional probability, of the order of magnitude of the translational energy of an atom at room temperature.

O. K. RICE

Chemical Laboratory,
Harvard University,
May 7, 1931.

Continuous Spectrum of Hydrogen Molecular Ion (H_2^+)

The negative glow is generally aceepted as a good source of ionized spectra, due to the probable high concentration of ions at this portion. In hydrogen, therefore, there may be some hope to obtain some spectrum at the negative glow, which had, if any, H_2^+ as an emitter. The hydrogen molecular ion has been dealt with theoretically by a number of investigators. Recently E. Teller[1] has calculated the excited states produced when the ion is separated step by step into a proton and a hydrogen atom in the ground state. According to him almost all the potential energy curves show no minima, except those corresponding to the $1s\sigma$ and the $3\ d\sigma$.

Following the interpretation of the ordinary hydrogen continuous spectrum, we can expect some continuous spectrum which can be explained by transitions to any one or all of the unstable states of the H_2^+ molecule. With such an expectation a spectroscopic examination of the negative glow in hydrogen, at a pressure of about 0.2 mm Hg was carried out. Although the ordinary continuous spectrum is absent in the negative glow, an indication of the continuous spectrum, even if not so intense, is observed between H_β and H_γ.

The probable high concentration of the H_2^+ molecule suggests that the above mentioned continuous spectrum may be due to the H_2^+ molecule. The energy involved in this region of spectrum is not inconsistent with such an explanation. As the spectrum was not observed at so extremely low pressures as in the cases of Herzberg[2] and Brasefield,[3] it is not in danger of being confused with that of the fluorescence light on the walls of the tube. So that it will not be inadequate to ascribe this continuous spectrum to the H_2^+ molecule. Details will be published with reproduction in the Science Reports of the Tôhoku Imperial University, **20** (1931).

Y. HUKUMOTO

The Physical Institute,
Imperial University, Sendai, Japan,
May 4, 1931.

[1] E. Teller, Zeits. f. Physik **61,** 458 (1930).
[2] G. Herzberg, Ann. d. Physik **84,** 560 (1927).
[3] C. J. Brasefield, Phys. Rev. **33,** 925 (1929).

New Covariant Relations Following from the Dirac Equations

1. In an article appearing in this issue of the Physical Review the authors derive by means of the spinor calculus four invariant relations between the four wave functions which are independent of the potentials. (Eq. (6), (11), (12), (13) of Ch. III.) The first of these is

$$\frac{\partial j^\lambda}{\partial x^\lambda} = 0 \qquad (1)$$

where j^l is the four-current. The second relation with which we shall concern ourselves in this letter, may be written, using ordinary tensor notation:

$$\frac{\partial k^\lambda}{\partial x^\lambda} = \frac{mc}{h} J \tag{2}$$

where k^l is also a four vector quadratic in the wave functions and defined by the equation preceding Eq. (17) of our article. In Eq. (14) two complex quadratic invariants Δ and $\bar{\Delta}$ were introduced; from these we form the two real combinations:

$$\begin{aligned} \tfrac{1}{2}(\Delta + \bar{\Delta}) &= I \\ \tfrac{1}{2}i(\Delta - \bar{\Delta}) &= J. \end{aligned} \tag{3}$$

These quantities are identical with the invariants I and J of Darwin. We also prove in our paper that

$$k^\lambda j_\lambda = 0;\ k^2 = -j^2. \tag{4}$$

Further we proved (Eq. (17)) that:

$$k^\alpha M_{\alpha l} = \frac{h}{mc} j_l \cdot J;\ j^\alpha M_{\alpha l} = \frac{h}{mc} k_l \cdot J. \tag{5}$$

Here M_{kl} is the antisymmetric tensor of the polarization (Darwin, Gordon), whose components are again quadratic in the wave functions.

2. For the sake of a possible physical interpretation and to facilitate comparison with recent work of Fock, it seems desirable to express the above relations in term of matrices. It is easily seen, however, that the original α matrices of Dirac are unsuited to express covariance relations. We use instead the form of the Dirac equations

$$(\Gamma^\lambda p_\lambda + mc)\psi = 0 \tag{6}$$

which is used by Weyl and Sommerfeld. (see our paper, Eq. (1), (2), (3), Introduction). The Γ^l matrices satisfy the well known relations:

$$\Gamma^k\Gamma^l + \Gamma^l\Gamma^k = 2g^{kl}. \tag{7}$$

We adopt now the first point of view mentioned in the introduction of our paper, and regard the ψ as invariant and the Γ^l as a matrix four-vector. Using this and the relations (7), we can now form the following covariant quantities.[1]

$$\begin{array}{ll} 1 & \backsim I \\ \Gamma^i & \backsim j^i \\ \Gamma^i\Gamma^k & \backsim M^{ik} \\ \Gamma^i\Gamma^k\Gamma^l & \backsim k_m \\ \Gamma^i\Gamma^k\Gamma^l\Gamma^m & \backsim J \end{array} \tag{8}$$

None of the indices are allowed to be equal. We assert that the quantities in the right column are obtained by multiplying the corresponding quantities in the left column with ψ' from the left and ψ from the right, (ψ' is the transposed ψ; see[2]). The relations (1) and (2) can now be derived independently from the Dirac equation (6); for (1) this is well known, whereas Eq. (2) becomes:

$$\frac{\partial}{\partial x_1}\psi'\Gamma^2\Gamma^3\Gamma^4\psi\ \pi - \frac{\partial}{\partial x_2}\psi'\Gamma^3\Gamma^4\Gamma^1\psi + \cdots = \frac{2imc}{h}\psi'\Gamma^1\Gamma^2\Gamma^3\Gamma^4\psi. \tag{9}$$

Relations (4) and (5) can now be derived immediately with the help of (7).

3. One can also easily, though not so symmetrically, express the quantities (8) in terms of the Dirac α and the Dirac-Darwin ψ. For j and M we refer to Gordon's[2] paper. For k, I and J one obtains the following expressions:

$$\begin{aligned} k^1 &= -i\alpha_2\alpha_3 & k^2 &= -i\alpha_3\alpha_1 \\ k^3 &= -i\alpha_1\alpha_2 & k^4 &= -i\alpha_1\alpha_2\alpha_3 \\ I &= \alpha_4 & J &= \alpha_1\alpha_2\alpha_3\alpha_4 \end{aligned}$$

We see therefore that the *spacial* components of k are identical with the three-vector σ as introduced by Dirac[3] and further used by Fock[4] and that the time component of k is equal to ρ_1 (Dirac) or ρ_a (Fock), whereas I is equal to ρ_3 (ρ_c) and J to $\rho_2(\rho_b)$. It thus appears that from the view point of covariance neither σ nor ρ are true vectors.

4. It follows from the equality of $k_{1,2,3}$ with σ_1, σ_2, σ_2 that the spacial components of the four-vector k are equal to the components of the magnetic moment of the electron. On the other hand it is well known that the spacial components of the tensor M^{ik} represent the magnetic moment of the electron also. When neglecting relativity (i.e. considering only the large ψ_3 and ψ_4) the k_1, k_2, k_3 become indeed equal to M_{yz}, M_{zx}, M_{xy} respectively. Thus it is seen that the

[1] For this systematization (without the above identifications) compare J. Schouten, Proc. Amsterdam **32,** 105 (1929); A. Proca, Journ. de Phys. **1,** 235 (1930). F. Sauter, Zeits. f. Physik **63,** 803 (1930) used it very profitably for the solution of special problems.

[2] Gordon, Zeits. f. Physik **50,** 630 (1928).

[3] P. A. M. Dirac, Principles of Quantum Mechanics, page 242.

[4] V. Fock, Zeits. f. Physik **68,** 522 (1931).

three-dimensional vector of the magnetic moment can be completed relativistically in two ways, either to a four-vector or to an antisymmetric tensor. In the corpuscular theory already L. H. Thomas[5] called attention to these two possibilities. What the exact physical meaning of this duplicity in character of the moment and especially of the fourth component of k is remains unclear to us. Perhaps it is connected with the two-fold interpretation of the spin as angular momentum or as magnetic moment.

G. E. UHLENBECK
OTTO LAPORTE

Department of Physics,
University of Michigan,
Ann Arbor, Michigan,
May 16, 1931.

[5] L. H. Thomas, Phil. Mag. **3**, 1 (1927).

On the Gas-Temperature in the Positive Column of an Arc

For the study of thermionization in the positive column of an arc the possibility of measuring exactly the gas temperature is of great importance. We have therefore developed a new method of ascertaining this temperature avoiding any errors of previous methods, which permits measuring the temperature by gas-density.

The density of the arc-gas in the axis of a stabilized (by whirling gas according to Schoenherr) straight d.c.-arc of 2 amp. in air and also nitrogen of atmospheric pressure were measured. This was done by testing the absorption of a soft x-ray (of about 6A) passing along the axis of arc. The intensity of the x-ray was observed by the Geiger-counter. In a comparative test without the arc, the gas density was diminished by evacuating the arc-space until the x-ray intensity became the same as with the arc. The intensity found thereby is also the average density of the arc-gas traversed by the x-ray. The disturbing spaces next to the electrodes were eliminated by measuring arcs of different lengths (5-20 cm).

With the ideal gas-law this density gives a temperature in the positive column of 5270 $\pm$300°K in the air-arc, and of 5460 $\pm$320°K in the nitrogen-arc. Considering the dissociation at these high temperatures, one gets a gas-temperature of 5000 $\pm$400°K in the air-arc and of 5200 $\pm$450°K in the nitrogen-arc. By pyrometric measurements a pure carbon (2 mm diameter) inserted in the arc axis had 3100°K in the air-arc and 2300°K in the nitrogen-arc. The temperature of the carbon is not identical with that of surrounding gas; clearly it depends on chemical reactions at its surface (oxidation!).

An extensive report on our investigations will be published in the next number of the "Wissenschaftliche Veröffenlichungen aus dem Siemens-Konzern."

ALFRED VON ENGEL
MAX STEENBECK

Wissenschaftliche Abteilung,
der Siemens-Schuckertwerke A.-G.,
Berlin,
April 28, 1931.